CHAPTER 1

INTRODUCTION

1.0 Overview

This chapter describes the need for carbon dioxide (CO_2) removal and prevalent processes used for that purpose. The most widely practiced amine based process for CO_2 capture and recently explored ionic liquids as green solvents for the said purpose have been discussed in detail. The justification for the present research has been deduced from the discussions. The aims and objectives of the present research have also been unfolded.

1.1 Research Background

1.1.1. Carbon Dioxide

Carbon dioxide (CO_2) is widely regarded as a major greenhouse gas, contributing to global warming. The prospect of worsening climatic situation due to global warming is a subject of widespread public concern. The world faces tremendous challenges associated with greenhouse gas emissions. The annual global emissions of CO_2 have been escalated by 80% between 1970 to 2004. The United Nations Intergovernmental Panel on Climate Change (IPCC) has studied these problems. The researchers, industry leaders and politicians have reached to the conclusion with consensus that dramatic reductions in greenhouse gas emissions must be achieved in order to stop and prevent these climatic changes. The increased CO_2 emissions are attributed to an increasing dependence on the combustion of fossil fuels (coal, petroleum and natural gas) which contribute 86% of anthropogenic greenhouse gas emissions, the remainder arising from land use change (primarily deforestation) and chemical processing. The current estimated worldwide annual emission of CO_2 due to fossil fuel usage are 9059 Mt/year (Bredesen et. al. 2004; Abu-Zahra et.al. 2009; D'Alessandro et. al. 2010; Ahmady et. al. 2011). Natural gas is regarded as cleanest among the other fossil fuels (coal, petroleum) due to the relatively lower amount of pollutants released during its burning. Therefore a major shift from conventional fossil fuels to natural gas has been observed in the past decades (Xiao et. al. 2009; Faiz et. al. 2011; Scholes et. al. 2012). Natural gas does not occur as pure mixture of hydrocarbons rather it is contaminated with CO_2, H_2S, N_2 *etc*. It has been reported that more than 50% of known gas reservoirs contained more than 2% CO_2, which is above the acceptable limits. The presence of CO_2 in natural gas reduces its calorific value. Therefore it is required to be removed, so that this relatively environment friendly fuel be utilized effectively (Darman and Harun 2006; Camper et. al. 2008; Rufford et. al. 2012). In the section ahead the prevalent processes used for CO_2 capture has been discussed in detail.

1.1.2 Current processes for CO_2 removal

There are many processes used for CO_2 capture. However each process has its own merits and demerits. Some important processes used for the said purpose are discussed below.

Adsorption is a surface phenomenon in which the molecules of a substance such as gas or liquid accumulate on the surface of the solid to form a thin film. The molecules are attracted by the surface but do not penetrate into the solid's void spaces as occurs in the absorption. Selective adsorption of gases depends upon the partial pressure, adsorbent pore size distribution and temperature. In this process, mixture of gases containing CO_2 is passed through a bed of solids that adsorbs CO_2 and let the other gases pass by. The process constitutes two steps namely; adsorption and regeneration of adsorbent. The solid bed when becomes fully loaded with CO_2 then the regeneration of bed is carried out by using technologies like PSA (Pressure swing adsorption) or by TSA (Temperature swing adsorption) or electric swing adsorption (ESA). The common adsorbents used for CO_2 capture include silica, zeolites, activated carbons and metal organic frame works. Even though adsorption process is considered cheaper however it is not feasible for large scale commercial processes due to its low CO_2 selectivity and limiting capacity (Gupta et. al. 2003; Cheung et. al. 2012).

Membrane technology for the removal of CO_2 emerged during 80’s after extensive research in the said field. This separation technique involves the principle of selective permeation. Membrane acts as a selective barrier between two phases and remains impermeable to specific molecules, substances, particles when exposed to the action of driving force. Some components are allowed to pass by whereas the others are retained and accumulate in the retentate stream. Membrane technology is extensively used for purification, concentration and fractionation of fluid mixtures. Many polymeric membranes are commercially available for the gas separation. However for bulk CO_2 removal the membrane technology has not yet proven fruitful. The presence of excessive CO_2 in the gas streams swells the pores of membrane thus hindering in selective removal of it. Furthermore membranes cannot withstand high operating conditions of temperature and pressure (Bredesen et. al. 2004; Simons 2010; Ambashta and Sillanpaa 2012).

Cryogenic technique for CO_2 removal is a unique separation method. In this process the components of mixture are separated by a series of compression, cooling and expansion steps, carried out on the basis of differences among the phase transition properties of the components. It involves the cooling of gases to a very low temperature so that CO_2 could be liquefied and hence separated from rest of the gases. In this process the water content in the feed stream to the cooling units should be minimal to prevent plugging by ice. The removal of water traces take additional steps before the original process of separation. These pre-treating steps make the cryogenic process more expensive which is already high in cost due to the installation of heavy refrigerant compressors and high energy requirements. The high cost of installation and operation are the major obstacles in the large scale industrial usage of cryogenic processes (Olajire 2010; Tuinier et. al. 2010; Xu et. al. 2012).

Absorption is a unit operation used in the chemical industry and extensively in environmental engineering. Absorption process is successfully used to separate gases by washing or scrubbing a gas mixture with a suitable solvent. One or more components of the gas mixtures are absorbed or dissolved in the liquid and subsequently removed from the mixture. In some cases the gaseous constituent is absorbed physically. In other cases, it experiences a chemical reaction with one or more components of the solvent (Gupta et. al. 2003; Kirk and Othmer 2008). Gas absorption is usually carried out in vertical counter current columns as shown in Figure 1.1.

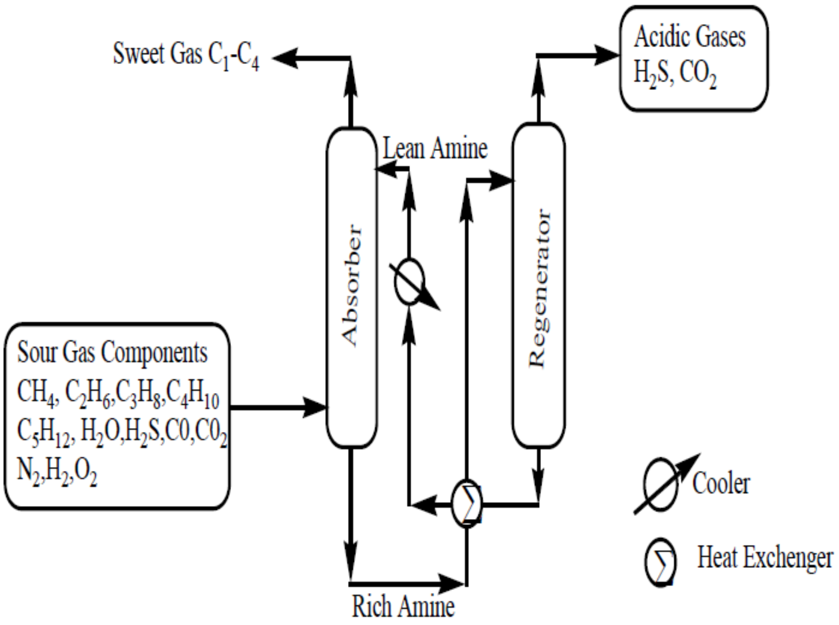

Figure 1.1. Gas absorption column with a regenerator (Islam et. al. 2010).

1.1.3 Common Solvents used for CO_2 capture

There are various solvents used for the CO_2 removal in industry and these have been classified into physical and chemical solvents.

Physical solvents are used for CO_2 removal when the partial pressure of the gas is quite high. The physical solvents combine less strongly with CO_2 as there is no chemical reaction taking place. The major advantage of using physical solvents is that the absorbed CO_2 could easily be stripped off by reducing pressure (in most cases or by the application of minimal heat in some cases) to regenerate the solvent. The maximum loading in physical solvents is proportional to the CO_2 partial pressure. Selexol and Rectisol are two common commercial CO_2 capture processes based on physical solvents. In Selexol, mixtures of dimethyl ether of polyethylene glycol and in Rectisol chilled methanol are used as solvents. In these processes the regeneration is endothermic and requires energy input. Another common CO_2 capture process based on physical solvent is Fluor process. In this process propylene carbonate is used as solvent. The weak bonding between CO_2 and this solvent allows the regeneration of solvent by simply reducing the total pressure in stripper. Many solvents have been explored by researchers as promising physical solvents for CO_2 capture. The CO_2 solubility in commercially available and promising physical solvents could be ranked as: diethylene glycol (DEG) < triethylene glycol (TEG) < methanol < ethanol < 1-propanol < 1-butanol < 1- pentanol < 1-octanol < 1,2,3,4- tetrahydronapthalene < sulfolane < *N*,*N*-dimethyl formamide < *N*-formyl morpholine (NFM) < propylene carbonate < TEGMME < dimethyl ether (DME) < diethyl polyethylene glycol (DEPEG) < genosorb 1753 (Rayer et. al. 2012). A list of commercially available physical solvents for CO_2 capture along with their licensor is given in Table 1.1.

Table 1.1: List of common CO_2 capture processes based on Physical Solvents (Gupta et. al. 2003)

Absorption Process	**Solvent**	**Process Conditions**	**Developer/Licensor**
Rectisol	Methanol	-10/-70ºC, >2 MPa	Lurgi and Linde Germany Lotepro Corporation, USA
Puisol	n-methyl-2-pyrolidone (NMP)	-20/+40ºC, >2 MPa	Lurgi, Germany
Selexol	Dimethyl ethers of polyethylene glycol	-40ºC, 2-3 MPa	Union Carbide, USA
Fluor Process	Propylene carbonate	Below ambient temperatures/ 3.1-6.9 MPa	Fluor, El Paso, USA

A significant problem associated with physical solvents is that their capacity is higher at lower temperature whereas at high temperatures they exhibit low solubility. Therefore the cooling of feed gas becomes necessary before CO_2 removal process which increases the cost of the operation (Gupta et. al. 2003; Burr and Lyddon 2000; Plasynski et. al. 2009).

Chemical solvents based CO_2 capture processes are most widely used in industries. Chemical absorption has established itself as a mature process for CO_2 removal. Chemical solvents can be divided into organic and inorganic categories with organic based solvents having the major market share. Chemical absorption process is suitable for low to moderate CO_2 partial pressures. Chemical absorption of CO_2 is based on the acid base neutralization reaction. CO_2 is an acid gas which is neutralized by using basic solvents. The resultant compound is weakly bonded bicarbonate. The compound formed is then broken by the application of heat, regenerating the original solvent and producing a pure CO_2 stream (David 2000; Yeh and Pennline 2004; Rochelle 2009).

Inorganic chemical solvents include potassium carbonate, sodium carbonate and aqueous ammonia. Among these solvents, potassium carbonate has the dominant market share. In Benfield process, CO_2 reacts with potassium carbonate and converts it to potassium bicarbonate. The process can be reversed by heating the bicarbonate formed and generating the reactants again. Most recently aqueous ammonia has been explored as a potential chemical solvent for CO_2 capture. It has been reported that aqueous ammonia solution could remove 99% of CO_2. This process exhibits high CO_2 loading capacity. However the usage of aqueous ammonia solution for CO_2 capture is not lucrative due to the high volatile nature of ammonia and the inability of the process to regenerate the solvent. The usage of inorganic chemical solvents for CO_2 sequestration has not yet proven fruitful for large scale industrial usage. The major drawback of these solvents are that they may release Na, K, and V (ions) in the product gas that could promote the deposition, corrosion and erosion in the gas turbines and plant equipments (Gupta et. al. 2003; Yeh and Pennline 2004; Plasynski et. al. 2009).

Organic chemical solvents or amines are derivatives of ammonia in which one or more of the hydrogen atoms has been replaced by an alkyl or aryl group. There are many amine solutions which are used for CO_2 capture. Some commonly used amine solutions include monoethanolamine (MEA), 2-amino-2-methyl-1-propanol (AMP), *N*-methyldiethanolamine (MDEA), piperazine (PZ), diglycolamine (DGA), diethanolamine (DEA) and di-isopropanolamine (DIPA) (Thitakamol et. al. 2007). Alkanolamines which are simple combination of alcohols and ammonia are most widely used category of amine solvents available for CO_2 capture. The aqueous alkanolamine based CO_2 absorption and stripping is a well understood, highly matured and most widely practiced CO_2 capture process on industrial scale since 1930. This technology can remove about 75-90% of the CO_2 and regenerate nearly pure (>99%) CO_2 product stream. Alkanolamines are classified into three categories; primary, secondary and tertiary, depending upon whether one, two or three of the hydrogen atoms of ammonia have been replaced by organic functional groups. Common examples of each type of alkanolamines are: primary – monoethanolamine (MEA), secondary – diethanolamine (DEA); and tertiary – methyldiethanolamine (MDEA) (Rao and Rubin 2002; Ebune 2008; Wu et. al. 2010; Bandyopadhyay 2011). Sterically hindered amines are usually reckoned as fourth class of alkanolamines. Sterically hindered alkanolamines have a bulky alkyl group attached to the amino group are reported to have good CO_2 solubility and less regeneration cost. However their slow reactivity and need for longer absorption columns to accomplish desired level of CO_2 removal are main hindrances in their usage (Abu-Zahra et. al. 2009; D'Alessandro et. al. 2010; Olajire 2010). The structures of primary, secondary, tertiary and sterically hindered amines are given in Figure 1.2. Primary *or* secondary alkanolamines react with CO_2 to form a carbamate species according to the reactions (Danckwerts 1979):

$$RNH_2 + CO_2 \leftrightarrow RNH_2^+COO^-$$

The intermediate product ($RNH_2^+COO^-$) then reacts with another mole of amine to form stable carbamate:

$$RNH_2^+COO^- + RNH_2 \leftrightarrow RNH_3 + RNHCOO^-$$

The above equations suggest that the CO_2 loading of the primary/secondary amines is limited to 0.5 mol_{CO2}/mol_{amine}, since 2 moles of amine are required to react with each mole of CO_2.

In tertiary alkanolmines the carbamate is not formed due to their inability to eliminate a hydrogen atom rather a hydrolysis catalyzed reaction takes place according to the following general form (Jou et. al. 1982):

$$R_2NCH_3 + CO_2 + H_2O \leftrightarrow R_2NHCH_3^+ + HCO_3^-$$

Among the available alkanolamines, monoethanolamine (MEA) shows the highest rate of reaction with carbon dioxide, whereas *N*-methyldiethanolamine (MDEA) has low reaction rate. However MDEA exhibits higher CO_2 loading capacity and less heat of regeneration. In addition to these solvents, mixtures of alkanolamines especially mixtures of primary *or* secondary alkanolamines with tertiary alkanolamine solvents are also used in industry.

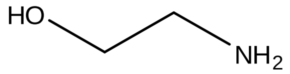

Monoethanolamine

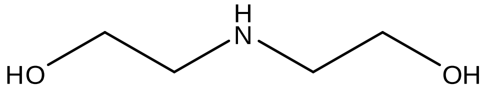

Diethanolamine

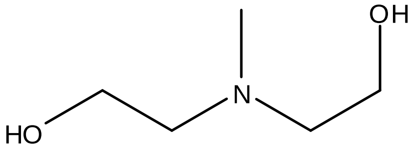

Methyldiethanolamine

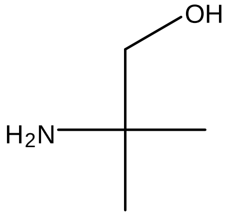

2-amino-2-methyl-1-propanol

Figure 1.2. Structures of the primary, secondary, tertiary and sterically hindred amines.

The mixture of primary and tertiary amine aims to couple the reactivity of primary amines with the low heat of regeneration requirements for tertiary amines. Even though the CO_2 removal by alkamolamines is an energy intensive process yet it is widely practiced in industries due to its effectiveness. In US, 95 % of CO_2 capture plants are based on amine scrubbing processes (Camper et. al. 2008; Derks 2006; Islam et. al. 2010; Taib et. al. 2012).

Recently ionic liquids have been reported by many researchers as potential environmental friendly solvents to capture CO_2 and these have been discussed below.

1.1.4 Ionic Liquids

Ionic liquids (ILs) are salts and contrary to other salts they remain liquid over a wide range of temperatures. Those ionic liquids which are liquid at room temperature are termed as room temperature ionic liquids (RTILs). Ionic liquids exhibit some unique properties such as; low melting point, stability at high temperatures, high solvency power for both polar and non polar (organic or inorganic) solvents, negligible vapor pressure, non flammability and non volatility. It is due to these unique and environmentally benign properties that ILs have garnered the focus of researchers to utilize these as replacement for many industrial solvents. One potential candidacy of ILs to be used as replacement solvents is their usage in gas separation technique based on absorption which currently employs environment unfriendly volatile organic solvents. ILs are comprised of bulky organic cation and polyatomic inorganic or organic anion. The common cations are *N*-alkylpyridinium, tetraalkylammonium, tetraalkylphosphonium, pyrrolidinium and imidazolium. The anions can be nitrate ($[NO_3]$), halide, dicyanamide ($[(CN)_2N]$), acetate ($[CH_3CO_3]$), triflate ($[CF_3SO_3]$), trifluoroacetate, alkylsulfate, hexafluorophosphate (PF_6), tetrafluoroborate (BF_4), trifluoromethylsulfonate ([OTf]), bis(trifluoromethylsulfonyl)imide ($[Tf_2N]$) and tris(pentafluoroethyl)trifluorophosphate ([FAP]). Designer solvents is also a term used for ILs, as by varying the combination of cations and anions plenty of feasible ILs could be prepared. The ILs tailored for specific task are thereby called as task specific ionic liquids (TSILs) (Kato et. al. 2004; Orchille's et. al. 2006; Han and Armstrong 2007; Twu et. al. 2012).

ILs could be used as alternative green solvents for numerous industrial applications in place of volatile organic compound. Recently many researchers have reported ILs as alternative green solvents to capture CO_2. It was observed that ILs showed greater tendency to dissolve CO_2 than other gasses like methane, ethane, oxygen, nitrogen and carbon monoxide (Baltus et. al. 2004; Scovazzo et. al. 2004; Camper et. al. 2004; Jacquemin et. al. 2006). The pioneering study to use RTILs as absorption media for CO_2 was carried out by Blanchard et. al. (2001). It was reported that CO_2 showed considerable solubility in the ionic liquid ($[bmim][PF_6]$) at all temperatures and pressures. Since then many researchers have started using various RTILs to investigate the CO_2 solubility and found that ILs possess considerable affinity for CO_2. Among the investigated RTILs for CO_2 it was observed that imidazolium based ionic liquids showed greater CO_2 solubility as compared to other classes of ILs. The ability of imidazolium based ILs to dissolve more CO_2 is attributed to the presence of acidic hydrogens on the imidazolium ring. Imidazolium based ILs can donate a hydrogen bond to the solute which results in enhanced CO_2 absorption (Cadena et. al. 2001; Camper et. al. 2008).

1.2 Problem Statement

The technology for CO_2 removal using alkanolamine solvents has some inherent drawbacks like; degradation, volatility of solvents, corrosion caused to the operating equipments and high energy requirements for regenerations. Solvents which posses the environmental friendly characteristics with efficient removal of CO_2 are need of the hour. Recently ionic liquids (ILs) have been reported as potential environmental friendly solvents for CO_2 removal. Though ILs are envisaged as environmentally benign solvents for efficient CO_2 removal however, their high viscosity and high cost of synthesis are the major obstacles in their large scale commercial usage for CO_2 removal. Furthermore their low CO_2 loading capacity in comparison to traditional alkanolamine solvents also limits their commercial usage (Feng et. al. 2010; Ahmady et. al. 2011; Sairi et. al. 2011; Aziz et. al. 2011). Therefore the need for efficient and environmental friendly solvents to effectively remove CO_2 prevails. This challenge could be met by using the hybrid solvents comprising of ionic liquids and amines. Both amines and ionic liquids have proven their capacity to absorb CO_2 individually. Therefore their hybrid mixtures are believed to offer better performance than the individual components. As it is aimed that such mixtures will combine the good characteristics of their parent solvents and offset the problems associated with these. The amines mixed with ionic liquids will open up a possibility of using a variety of tunable solvents for CO_2 capture. The addition of amines in the ionic liquids could prove fruitful for both the solvents. The addition of IL in the amine solvents could benefit the amine solvent by: 1) reducing the chemical reaction as less amine solvent would have been present in the mixture, 2) reduction in the vapor pressure and hence low volatility, 3) reduction in the thermal degradation as ILs have high stability at high temperatures. On the other hand, the addition of amine solvent in the IL would benefit the IL by: 1) reduction in the viscosity of IL, 2) resulting in augmentation of IL volume, 3) resulting in enhanced CO_2 solubility as amines exhibit higher CO_2 loadings than ILs. Therefore it can be inferred that the mixing of the amine solvents with ILs is beneficial for both the components. The drawbacks of ILs *i.e.* high viscosity, high price and low CO_2 loading could be overcome by the addition of low priced, low viscous and high CO_2 absorption capacity amine solvents. The drawback of amine solvents, *i.e.* volatility, degradation, thermal instability could be overcome by the addition of nonvolatile, and thermally stable ILs. The good solvency power of ILs is a proven fact, they can dissolve the commercially available inexpensive amine solvents to form a mixture. Hence in this work it is proposed to develop tunable hybrid solvents which are environmental friendly and capable for the efficient CO_2 removal. These hybrid solvents are aimed to bear the good characteristics of ILs and amines while offsetting the problems associated with these. Imidazolium based ILs (as these possess greater affinity for CO_2) have been mixed with amine solvent to make the hybrid solvents. The physical properties of these mixtures were established as they are important in terms of design, scale up and sizing of the equipments. CO_2 loading was measured in these mixtures and the results were correlated using thermodynamic models.

1.3 Research Objectives

The aim of the present research is to mix the targeted ILs with amine solution for their application towards CO_2 solubility. The objectives of the present research have been laid out stepwise as follows:

1. To investigate the CO_2 loading in pure liquids (ILs and amine) as well as in their hybrid mixtures (IL+amine) at different temperatures and pressures by using pressure drop method.

2. To analyze the effect of concentrations, anions, temperature and pressure on the solubility of CO_2.

3. To correlate the experimental CO_2 solubility data using thermodynamic models.

4. To investigate the regenerability of the pure solvents as well as of their binary mixtures towards recycling.

1.4 The scope of study

The scope of the present study is to systematically investigate the potential usage of hybrid solvents (comprising of ILs and amine) for CO_2 absorption. The development of fundamental understandings of physical properties of these solvents and their affinity towards CO_2 will be studied in the present work based on the experimental outcome. In this work the thermophysical properties namely; density, viscosity, refractive index and TGA of these solvents will be measured experimentally and correlated. Based on these the excess properties namely; excess molar volumes, viscosity deviations, refractive index deviations will be deduced to understand the interaction between the species present in the mixtures. The performance of these solvents for CO_2 removal will be examined by measuring the CO_2 solubility in these pure and binary mixtures at three different temperatures (298.15, 313.15, 323.15 K) and pressures up to ≤ 3000 kPa. Attempt will be made to correlate the CO_2 solubility data with the help of Peng Robinson (PR) and Soave Redlich Kwong (SRK) equation of state (EOS) models. Finally the possibility of regenerating the solvents will be made in order to identify their application for recycling operations. The information gathered through experimental CO_2 solubility results and thermodynamic modeling would help to suggest modification in the existing CO_2 removal processes and pave the way for the understanding of the potential usage of hybrid mixtures (IL + amine) for CO_2 removal.

1.5 Organization of the Thesis

Chapter 1 presents the background and the motivation behind this research. The prevalent processes used for CO_2 capture with their merits and demerits have been summarized. The objective and scope of the study are stated in this chapter also.

Chapter 2 presents the critical literature review pertaining to the MDEA, [hmim][Tf_2N], [hmim][BF_4] and [hmim][FAP]. The details of their physical properties and the CO_2 solubility data in these solvents measured by numerous researchers have been summarized. Common solvents (alkanolamines and ILs other than those mentioned above) used for the CO_2 solubility have also been described. In addition to this the mixtures of ILs with amine used for CO_2 capture have been analyzed in terms of operating parameters *i.e.* temperature and pressures. The research gap has been identified in these hybrid solvents. Chapter 3 describes the purities of the chemicals and the gases used in the present study. The details pertaining to the equipments and the methodologies used to measure the basic physical properties and the CO_2 solubility are the focus of this chapter.

Chapter 4 presents the results of the thermophysical properties (density, viscosity, refractive index and thermal stability) and the CO_2 solubility in the pure solvents and their mixtures. The empirical relation to correlate the physical properties data has been presented. The effects of temperatures, pressures, concentrations and anions on CO_2 solubility and Henry's constant, enthalpy and entropy are part of this chapter also. Thermodynamic models (Peng Robinson EOS and Soave Redlich Kwong EOS) are presented in this chapter to correlate the experimentally obtained CO_2 solubility data.

Finally Chapter 5 presents the conclusions of the study in line with the objectives as well as recommendations for the future study.

CHAPTER 2

LITERATURE REVIEW

2.0 Introduction

In industries pure alkanolamine solvents are not used for the CO_2 capture rather mixtures of amine with water are being used. Many researchers have reported the CO_2 solubility in the binary mixtures of *N*-methyldiethanolamine (MDEA) with water (Jou et. al. 1982; Chakma and Meisen 1987; Austgen et. al. 1991; Shen et. al. 1992; Dawodu et. al. 1994; Kuranov et. al. 1996; Mathonat et. al. 1997; Rho et. al. 1997; Xu et. al. 1998; Lemoine et. al. 2000; Park and Sandall 2001; Kamps et. al. 2001; Boumedine et. al. 2004; Ma'mun et. al. 2005; Ermatchkov et. al. 2006; Huttenhuis et. al. 2007). In addition to these, aqueous mixtures of *N*-methyldiethanolamine with other amines solvents (MEA *or* DEA *or* AMP *or* PZ) have also been extensively used by many researchers (Li and Lee 1996; Silkenbaumer et. al. 1998; Zhang et. al. 2002; Robolledo-Libreros and Trejo 2004; Mandal et. al. 2005; Kundu and Bandyopadhyay 2006; Choi et. al. 2007; Lin et. al. 2009; Vahidi et. al. 2009; Bottger et. al. 2009; Derks et. al. 2010; Speyer et. al. 2010; Samanta and Bandyopadhyay 2011; Kumar et. al. 2012; Zoghi et. al. 2012).

Recently a group of researchers from the University of Colorado, USA, put forward the idea of using the mixtures of (Ionic Liquids + Amine) for the removal of CO_2. They claimed that the IL-amine mixtures behave similar to aqueous amine solutions and may offer significant advantage over these especially in terms of energy consumed to process a given amount of CO_2 (as the heat capacities of ILs are less than that of water). The CO_2 absorption in these mixtures occurred rapidly and could be readily reversed. The mixtures also exhibited 20 times higher CO_2 loading capacity from the lean ILs. They proposed that IL-amine mixture offer a new and promising approach towards efficient CO_2 capture. Furthermore they concluded that these are advantageous over the existing energy extensive technologies (Camper et. al. 2008). The usage of IL-amine mixtures for CO_2 capture is relatively a new process and no such prolific data has been reported in the open literature. However some reports featuring IL-amine mixtures used for CO_2 solubility could be found in literature. Feng et. al. (2010) used the mixtures of aqueous MDEA with four tetramethylammonium based ILs for CO_2 absorption. The solubility was measured at temperature (298-318) K and at CO_2 partial pressure range of (4-400) kPa. A wide range of concentrations of ILs (5-100%) with amines was used in the study. They found that the presence of tetramethylammonium IL in the aqueous mixtures of MDEA greatly enhanced the CO_2 solubility and increased the absorption rate. On the other hand, Ahmady et. al. (2010) measured the CO_2 solubility in the mixtures of IL + aqueous MDEA solution at temperatures (303-333) K and pressure below 110 kPa. The IL mixed with aqueous MDEA solutions was 1-butyl-3-methylimidazolium tetrafluoroborate ([bmim][BF_4]). The results indicated that the IL present in the aqueous MDEA solutions increased the initial rate of absorption. However it was found that the rise in concentration of IL in the mixture significantly decreased the absorption capacity of aqueous MDEA solutions. In the same manner Sairi et. al. (2011) used the mixtures of aqueous MDEA with IL (guanidinium trifluoromethanesulfonate) to study the CO_2 solubility. The solubility was reported at three different temperatures (303.2, 323.2, 333.2) K and at a pressure range of (500-3000) kPa. The reported results indicated that the addition of IL to the aqueous MDEA solutions resulted in slight decrease in the solubility of the former. Ahmady et. al. (2011) used the mixtures of three different imidazolium based ILs (1-butyl-3-methylimidazolium tetrafluoroborate, 1-butyl-3-methylimidazolium acetate, 1-hexyl-3-methylimidazolium dicyanamide) with aqueous MDEA solution to study the CO_2 solubility. The experimental solubility was measured at temperatures (303-333) K and at pressure range of (100-700) kPa for different concentrations. They also reported that the increase in concentration of IL in aqueous MDEA mixtures significantly decreased the CO_2 solubility. Similarly Aziz et. al. (2012) utilized the mixtures of aqueous MDEA + IL (guanidium tris(pentafluoroethyl)trifluorophosphate) to study the CO_2 absorption in these. The absorption was carried out at three different temperatures (313.15, 333.15, 353.15) K and at pressures up to 3MPa. They also reported that the absorption capacity of aqueous MDEA solutions decreased with the addition of IL in the mixtures. On the other hand, Taib et. al. (2012) used two ILs namely bis(2-hydroxyethyl)ammonium acetate [bheea] and 1-butyl-3-metylimidazolium tetrafluoroborate [bmim][BF_4] mixed with aqueous MEA solutions to observe the CO_2 solubility in these. The CO_2 absorption was studied at temperatures (298.15, 303.15, 313.15) K and at pressure range of 100 to ≤1600 kPa and reported that the CO_2 solubility was higher in the mixtures of [bheaa]+aqueous MEA as compared with the mixtures of [bmim][BF_4]+aqueous MEA. They further concluded that the mixtures exhibited lower CO_2 absorption in comparison to pure ionic liquids.

There is plenty of scope available for the research in the area of IL-amine mixtures due to the availability of such a huge number of ILs. It is noteworthy to mention that the usage of IL-amine mixtures is not confined to the laboratory scale experiments only. ION engineering has recently commercialized the CO_2 removal process based on IL-amine mixtures. They showed that the IL mixtures are beneficial in terms of capital and processing cost, increasing gas output and shrinking the unit footprints. They claim that the IL-amine mixtures are not only cost effective but also environment friendly. The environmentally benign characteristics of ILs can successfully be incorporated in the high volatile amine solvents. On the other hand, the high cost and high viscosity of ILs can be reduced by successfully mixing these with less priced and less viscous amine solvents to result in a number of workable hybrid solvents. These hybrid solvents can be used for the effective removal of CO_2 (www.ion-engineering.com).

2.1 Thermophysical properties of the solvents used

The knowledge of thermophysical properties of the solvents used in gas absorption processes is essential. The understanding of basic thermophysical properties like densities, viscosities, refractive indices and thermal decomposition temperature is vital for engineering design and scaling up of gas treating units. These properties are helpful in analyzing and predicting the experimental absorption rate and the enhancement factors involved in gas absorption process. In gas absorption/desorption process, in thermodynamic modeling and in simulation processes the knowledge of physical properties is inevitable. In industrial processes the physical properties of a solvent are indispensable tool for the process engineers, as these enable to calculate the transfer coefficients and pressure drop (Hawrylak et. al. 2000; Fredlake et. al. 2004; Letourneux et. al. 2007).

For the calculation and correlation of data on CO_2 solubility in solvents the physical properties of solvents are required. It is known that in these binary mixtures, the solvents interact physically but not chemically. The physical properties of mixtures thereby differ from their parent solvents. The variation in concentration of either constituent in the mixture changes the physical properties of the mixture. Therefore it is important to measure the physical properties of the mixtures as these cannot be evaluated from the properties of the constituents comprising the mixture. Moreover each mixture is an individual solvent with its own indigenous properties, the properties of parent solvents have either diminished or dominating. The physical properties of binary mixtures are studied for many reasons. The most important of these is to provide necessary information pertaining to the molecular interactions between the solvents present in the mixture. The experimental data of physical properties namely density, viscosity, refractive index and thermal stability are required for the complete comprehension of thermodynamic properties of mixtures as well as for practical chemical engineering application. The analysis of excess thermodynamic properties of the binary mixtures is also of considerable interest as these are important for solving the problems concerning mass transport and fluid flow (Vural et. al. 2011). Many researchers have reported the physical properties data for the common solvents used for CO_2 absorption. Abundant data of physical properties for the pure alkanolamines and their mixtures is available in the literature. Physical properties data pertaining to IL-amine mixtures in the open literature is very scarce.

2.1.1 Density

Density is an important physical property of substances; it is defined as the mass per unit volume. The SI units of density are $kg \cdot m^{-3}$. The density data of the solvents used for CO_2 capture is of utmost importance as it benefits in many ways. The knowledge of density is used to improve the modeling and interpret the fluid dependent parameters. Density helps to derive some other important properties of solvents like, excess molar volumes, partial molar volumes and coefficients of thermal expansion.

In addition to these density is a key parameter in chemical engineering design and calculations like conversion of kinematic viscosity to dynamic viscosity and estimating the pressure head of solvents (Hernandez et. al. 2001; Cullinane 2005; Wallace 2005).

Many investigators using different types of pycnometers have reported the density of pure MDEA as well as its mixtures with water and other solvents. The density data of pure MDEA at different temperatures has been reported by many researchers (Li and Shen 1992; Wang et. al. 1992; Diguillo et. al. 1992; Hernandez et. al. 2001). The density data of pure MDEA as well as its binary mixtures with water (aqueous MDEA) at different temperatures and over a wide concentration range have been reported by many researchers (Hawrylak et. al. 2000; Al-Ghawas et. al. 1989; Li and Lie 1994; Rinker et. al. 1994; Maham et. al. 1995; Welsh et. al. 1995; Weiland et. al. 1998; Mandal et. al. 2003; Bernal-Garcia et. al. 2003; Paul and Mandal 2006; Robolledo-Libreros and Trejo 2006; Muhammad et. al. 2008; Han et. al. 2012). The densities of binary or tertiary mixtures of MDEA with other amine solvents have been reported by many researchers (Hsu et. al. 1997; Liao and Li 2002; Ko et. al. 2008; Derks et. al. 2008; Muhammad et. al. 2009; Alvarez et. al. 2010). An extensive literature review for the determination of densities of pure and aqueous MDEA solution has been summarized in Table 2.1 along with the concentration range (in the case of aqueous solutions) and details of the densitometer used and densities range.

The density data for the mixtures of MDEA with common solvents (other than amines) have also been reported by many researchers (Henni et. al. 2000; Amararene et. al. 203; Alvarez et. al. 2006; Garcia-Abuin et. al. 2009). The literature review pertaining to the determination of density of MDEA mixtures (other than amines) along with the details of the equipments and density ranges are listed in Table 2.2.

The density of ionic liquids depends upon their ionic components. The alkyl chain length of the cations and the molar mass of anions affect the density of the ionic liquids. Huddleston et. al. (2001) synthesized ionic liquids having 1-butyl-3-methylimidazolium ([C_4mim]) cation and different anions ([Cl], [I], [BF_4], [PF_6] and [Tf_2N]). They studied the physical properties of the ionic liquids and as part of it they

Table 2.1. Literature review for the determination of densities of pure MDEA as well as its aqueous solutions

Reference	Composition	Temperature (K)	Apparatus	Density Range ($g.cm^{-3}$)
Li and Shen 1992	Pure MDEA	303.15 to 353.15	Gay-Lussac Pycnometer	1.0315 to 0.9946
Wang et. al. 1992	Pure MDEA	292.85 to 361.35	Calibrated 25 ml Pycnometer bottles	1.0401 to 0.9875
Diguillo et. al. 1992	Pure MDEA	296.3 to 470.9	High Pressure Pycnometer	1.0371 to 0.8966
Hernandez et. al. 2001	Pure MDEA	313.15 to 333.15	Anton Paar DMA 45	1.0250 to 1.0096
Al-Ghawas et. al. 1989	Pure MDEA and w_{MDEA} = (0.1,0.2,0.3,0.4,0.5)	288.15 to 333.15	Gay-Lussac Pycnometer	1.0445 to 1.0123
Li and Lie 1994	Pure MDEA and w_{MDEA} = (0.2, 0.3)	303.15 to 333.15	Gay-Lussac Pycnometer	1.0133 to 0.9983
Rinker et. al. 1994	w_{MDEA} = (0.1, 0.2, 0.3, 0.4, 0.5)	293.15 to 373.15	Gay-Lussac Pycnometer	1.0185 to 0.9702
Maham et. al. 1995	Pure MDEA and x_{MDEA} = 0.0079 to 0.9475	298.15 to 353.15	Anton Paar DMA 45	1.0359 to 0.9936
Welsh and Davis 1995	w_{MDEA} = 0.5	283.15 to 353.15	Gay-Lussac Pycnometer	1.0514 to 0.0012
Weiland et. al. 1998	w_{MDEA} = (0.3, 0.4, 0.5, 0.6)	298.15	Hydrometer	1.1480 to 1.0270
Hawrylak et. al. 2000	Pure MDEA and x_{MDEA} = (0.0050 to 0.9800)	298.15, 308.15 318.15	Anton Paar DMA 45	1.0368 to 1.0226
Mandal et. al. 2003	Pure MDEA and w_{MDEA} = (0.3)	293.15 to 323.15	Gay-Lussac Pycnometer	1.0397 to 1.0194
Bernal Garcia et. al. 2003	Pure MDEA and x_{MDEA} = (0.0168 to 0.7430)	283.15 to 363.15	Anton Paar DMA 5000	1.0475 to 0.9873
Paul and Mandal 2006	Pure MDEA and w_{MDEA} = (0.1, 0.2, 0.3)	288 to 333	Gay-Lussac Pycnometer	1.0441 to 1.0126
Rebolledo Libreros et. al. 2006	Pure MDEA and w_{MDEA} = (0.3)	313.15, 323.15, 333.15	Sodev 03 D vibrating tube density meter	1.0250 to 1.0096
Muhammad et. al. 2008	Pure MDEA and x_{MDEA} = (0.3228, 0.4880)	298.15 to 338.15	Anton Paar DMA 5000	1.0382 to 1.0079
Han et. al. 2012	Pure and x_{MDEA} = (0.0609 to 0.5764)	298.15 to 328.15	Anton Paar DMA 5000	1.0360 to 1.0133

Table 2.2. Literature review on the determination of density of the mixtures of MDEA with solvents (other than amines)

Reference	Composition	Temperature (K)	Apparatus	Density Range ($g.cm^{-3}$)
Henni et. al.2000	MDEA+TEGMME (x_{MDEA} = 0.1082 to 0.8860) MDEA+ethanol (x_{MDEA} = 0.0079 to 0.2986)	298.15 to 343.15 for MDEA +TEGMME 313.15 for MDEA+ethanol	Anton Paar DMA 45	1.0430 to 1.0012 (MDEA+TEGMME) and 1.0251 to 0.77157 (MDEA+ethanol)
Amararene et. al. 2003	MDEA+water+methanol (w_{MDEA} = 0.200 to 0.399)	293.15 to 352.15	Anton Paar DMA 45 DMA 512 and Anton Paar DMA 5000	0.851 to 0.990
Alvarez et. al. 2006	MDEA+2-(Methylamino)ethanol+water (MAE/MDEA mass ratio 0/50 to 50/0) MDEA+2-(ethylamino)ethanol +water (EAE/MDEA mass ration 0/50 to 50/0)	298.15 to 323.15	Anton Paar DSA 5000	1.04246 to 0.9775 (EAE+MDEA) and 1.04246 to 0.9893 (MAE+MDEA)
Garcia-Abuin et. al. 2009	MDEA+water+ethanol (x_{MDEA} = 0.0677 to 0.9368)	288.15 to 323.15	Anton Paar DSA 5000	1.04432 to 0.90432

analyzed the effect of anion on the density of ionic liquids. It was found that the density of ionic liquids (having same cation but different anions) increased as the molar mass of anion increased. The same effect was reported by Fredlake et. al. (2004). They reported the density data of thirteen imidazolium based ionic liquids. Eight ionic liquids having the same cation ([bmim]) coupled with different anions ([BF_4], [PF_6], [Cl], [Br], [dca], [triflate], [methide], [Tf_2]) whereas another two also having the cation ([bmmim]) with different anions ([PF_6], [BF_4]) and the rest having the same anion ([Tf_2N]) with different cations ([emim], [emmim], [pmmim]). They also found that increase in the molar mass of anion resulted in increasing density of the ILs having the same cations. In addition they reported that as the alkyl chain length of cation increased (for the ILs having same anion but different cations) the density of the ILs decreased. Pereiro et. al. (2007) reported the density data for the ionic liquids having same anion ([PF_6]) coupled with different cations ([bmim], [hmim], [omim]) at T = (278.15 to 343.15) K. The estimated density values indicated that the alkyl chain length of cation have negative impact on density. To study the effect of cation and anion on the density of ionic liquids, Sanchez et. al. (2009) investigated thirteen ionic liquids formed by pairing imidazolium, pyridinium and pyrrolidinium cations with [dca], [BF_4], [SCN], [$MeSO_4$], and [TFA] anions. It was reported that the measured density values decreased as the temperature increased. Their systematic study on the effect of cation and anion on the density indicated that the density of ILs (having same cation) increased as the molar mass of anion increased, whereas the density of ILs (having same anion) decreased as the alkyl chain length of cations increased.

The literature review on the determination of densities of the pure [hmim][BF_4], [hmim][Tf_2N] and [hmim][FAP] as well as their mixtures (if any) with other molecular solvents at atmospheric pressure is presented in Table 2.3. From the available literature (Table 2.3) pertaining to the densities of ILs, it can be concluded that abundant data for the density of pure ILs is available. Only a few researchers have reported the density data of the mixtures of these ILs with other solvents. Density data of the mixtures of these ILs with alkanolamine has not been reported in the open literature. Based on the foregoing literature review, it is observed that there

Table 2.3. Literature review on the determination of densities of ILs namely; [hmim][BF_4], [hmim][Tf_2N], [hmim][FAP] and their mixtures (if any) with other solvents at atomospheric pressure.

Reference	Composition	Temp. (K)	Apparatus	Density Range (g.cm^{-3})
	[hmim][BF_4]			
Letcher et. al. 2004	Pure [hmim][BF_4]	298.15	Anton Paar DMA 5000	1.14838
Navia et. al. 2007	Pure [hmim][BF_4] and binary mixtures with [emim][BF_4] *or* [bmim][BF_4] $x_{[hmim][BF4]}$ = (0.0978 to 0.9455) for mixture with [emim][BF_4] and $x_{[hmim][BF4]}$ = (0.1083 to 0.9460) for mixtures with [bmim][BF_4]	298.15 to 308.15	Anton Paar DMA 602	1.1450 to 1.1388
Muhammad et. al. 2008a	Pure [hmim][BF_4]	298.15 to 358.15	Anton Paar DMA 5000	1.14532 to 1.10484
Garcia-Miajia et. al. 2009	Pure [hmim][BF_4]	293.15 to 318.15	Anton Paar DMA 5000	1.14880 to 1.13160
Zhu et. al. 2011	Pure [hmim][BF_4] and binary mixtures with butanone or butylamine or ethyl acetate or tetrahedrofuran; $x_{[hmim][BF4]}$ = (0.0492 to 0.8931) for mixtures with butanone; $x_{[hmim][BF4]}$ = (0.0492 to 0.8787) for mixtures with butylamine; $x_{[hmim][BF4]}$ = (0.0498 to 0.8908) for mixtures with ethyl acetate; $x_{[hmim][BF4]}$ = (0.0498 to 0.8925) for mixtures with tetrahedrofuran	298.15	Anton Paar DMA60/602	1.14670
Kermanpour et. al. 2012	Pure [hmim][BF_4] and binary mixtures with 1-propanol; $x_{[hmim][BF4]}$ = 0.1006 to 0.8894) for mixtures with 1-propanol.	293.15 to 333.15	Anton Paar DMA 4500	1.14924 to 1.12237
Vakili-Nezhaad et. al. 2012	Pure [hmim][BF_4]	278.15 to 363.15	Anton Paar DMA 4500	1.15910 to 1.10102
Hui et. al. 2012	Pure [hmim][BF_4] and binary mixtures with [hmim][Cl]; $x_{[hmim][BF4]}$ = (0.2 to 0.8)	303.15 to 333.15	Anton Paar DMA 5000	1.14220 to 1.12180
	[hmim][Tf_2N]			
Tokuda et. al. 2005	Pure [hmim][Tf_2N]	303.15	Kyoto thermoregulated density meter DA- 100	1.0350

contd…

		[hmim][Tf$_2$N]		
Lachwa et. al. 2006	Pure [hmim][Tf$_2$N]	293 to 303	Anton Paar DMA 5000	1.3726 to 1.3634
Widegren et. al. 2007	Pure [hmim][Tf$_2$N] and with different water contents (3×10^{-5} to 7.22×10^{-3})	293.15 to 373.15	Anton Paar Stabinger viscometer	1.4076 to 1.3048
Muhammad et. al. 2008a	Pure [hmim][Tf$_2$N]	298.15 to 358.15	Anton Paar DMA 5000	1.37213 to 1.31816
Jacquemin et. al. 2008	Pure [hmim][Tf$_2$N]	293.15 to 263.15	Anton Paar DMA 4500	1.37510 to 1.31190
Marsh et. al. 2009	Pure [hmim][Tf$_2$N]	293.15 to 363.15	Anton Paar 4500	1.37650 to 1.31330
Tariq et. al. 2009	Pure [hmim][Tf$_2$N]	293.15 to 333.15	Anton Paar DMA 5000	1.43155 to 1.42050
Ahosseini et. al. 2010	Pure [hmim][Tf$_2$N] and binary mixtures with 1-Octene $x_{[hmim][Tf2N]}$ = (0.72 to 0.95)	283.15 to 348.15	Anton Paar DMA 4500	1.3854 to 1.3240
		[hmim][FAP]		
Ignat'ev et. al. 2005	Pure [hmim][FAP]	293.15	Anton Paar viscosimeter SVM 3000	1.5600
Jacquemin et. al. 2008	Pure [hmim][FAP]	293.15 to 363.15	Anton Paar DMA 4500	1.5571 to 1.4824
Yao et. al. 2009	Pure [hmim][FAP]	293.15	Anton Paar SVM 3000 stabinger viscometer	1.5570
Guang Li et. al. 2011	Pure [hmim][FAP]	293.15 to 343.15	KEM oscillating-tube digital densimeter (DA-505)	1.5556 to 1.5018

are different types of pycnometers used to measure the density with wide range of uncertainties. The density values measured with an instrument having high accuracy and less uncertainty are preferable as in many processes density acts as a controlling parameter. The vibrating U tube density meter shows good accuracy and precision in readings. Furthermore it is equipped with good temperature controlling mechanism. Such properties of U tube density meter make it a choice of many researchers to accurately measure the density values. Many other researchers by using similar type of density meter (Anton Paar DMA-5000 oscillating U tube) have reported the densities of many pure solvents (other than amine and ILs) and in some cases their mixtures also (Peralta et. al. 2002; Wisnaik et. al. 2005; Kijevcanin et. al. 2007; Smiljanic et. al. 2008; Bald et. al. 2011; Tafat-Igoudjilene et. al. 2012).

2.1.2. Viscosity

Viscosity (η) is the property of the material that defines the quantitative relation between the applied shear stress and the shear deformation rate in a fluid. The viscosity indicates the thickness or the resistance to flow of a fluid. It is the property of a fluid by virtue it offers resistance to shear force. There are two broad classes of fluids with respect to viscosity; Newtonian and non-Newtonian. In Newtonian fluids there exists a linear relation between the magnitude of the applied shear stress and the resulting rate of deformation. The Newtonian fluids have constant viscosity regardless of strain rate (provided other conditions and parameters remain the same). The viscosity of a Newtonian fluid is independent of the rate of deformation at any given temperature and pressure. In non-Newtonian fluids the viscosity will change with the variation in the rate of deformation.

Ionic liquids (ILs) are considered as Newtonian fluids with some exceptions. ILs with shorter alkyl chain ($n<12$) exhibit Newtonian behavior where as those derivatives which exhibit liquid crystalline phases show non-Newtonian behavior. The van der waal forces and hydrogen bonding play a vital role in determining the viscosity of ILs. For the case of imidazolium based ILs the viscosity is dependent on the alkyl chain length of the cations as well as on the nature of anions. The viscosity of ILs increases with increasing alkyl chain length, due to the increased possibility of van der Waal interaction between the cations. The amines like many other organic solvents are Newtonian fluids also (Wasserschied and Welton 2008; Arshad 2009; Venkatachalam and Kandasamy 2010).

In the gas absorption processes the viscosity of solvent plays a vital role. The significance of liquid viscosity in chemical process design makes it as one of the most important measured physical property. The liquid viscosity has a direct effect on heat transfer coefficients. The viscosity data is essential for pump and piping calculations and also helps in estimating pressure drop. The solvent viscosity has a profound impact on the CO_2 absorption. It has been reported that viscosity is an important factor in the absorber performance and the lower values of it are advantageous in terms of absorption. The lower the viscosity of solvent the higher is the CO_2 diffusivity in the solvent and faster the absorption. The solvents with lower viscosity not only exhibit high CO_2 loadings but also fast absorption rates (Smith et. al. 2003; Feng et. al. 2010; Alvis et. al. 2012). ILs are generally 2 to 3 times more viscous than the conventional organic solvents. For example, at room temperature viscosity of toluene is 0.7 mPa.s., whereas [hmim][Tf_2N] has a value of 70 mPa.s. and [NHH,$(C_2OH)_2$][OAc] has a value as high as 5647 mPa.s. The viscosity range for a variety of ionic liquids is 66 mPa.s. to 1110 mPa.s. The viscosity of IL is significantly affected by the impurities water content, halides *etc*. present in it (Huddleston et. al. 2001; Yu et. al. 2012). The alkyl chain length also affect the viscosity of ILs. Tokuda et. al. (2005, 2006) carried out experimental work to study the viscosity of ILs (having a singular anion paired with a number of cations) and reported that with the increase in chain length of cation the viscosity of the ILs increased. They further reported that the viscosity of imidazolium based ILs is lower as compared to pyridinium, pyrrolidinium, and ammonium based ILs. The literature review for the viscosities of the pure ILs namely [hmim][Tf_2N], [hmim][BF_4], [hmim][FAP] has been summarized in Table 2.4. The literature review for the viscosities of the mixtures of non aqueous solutions of MDEA and the mixtures of IL ([hmim][BF_4]) with other solvents is presented in Table 2.5. From the literature review on the data for the viscosities of the MDEA and ILs ([hmim][BF_4], [hmim][Tf_2N] and [hmim][FAP]) as well as their mixtures (if any), it can be concluded that prolific data pertaining to the viscosities of the pure liquids is available in the literature, whereas very limited data pertaining to the non aqueous mixtures of MDEA and for the mixtures of said ILs

Table 2.4. Literature review on the determination of viscosities of MDEA, [hmim][BF_4], [hmim][Tf_2N] and [hmim][FAP] at the atmospheric pressure.

Reference	**Compsotion**	**Temp. (K)**	**Apparatus**	**Viscosity Range (mPa.s)**
		MDEA		
Al-Ghawas et. al. 1989	Pure MDEA and w_{MDEA} = (0.1,0.2,0.3,0.4,0.5)	288.15 to 333.15	Cannon Fenske Viscometer	141.90 to 14.15
Diguillo et. al. 1992	Pure MDEA	293.15 to 424.15	Cannon Ubbelohde Viscometer	102.7 to 1.4
Li and Lie 1994	Pure MDEA and w_{MDEA} = (0.2, 0.3)	303.15 to 353.15	Cannon Fenske Viscometer	57.15 to 7.08
Teng et. al. 1994	Pure MDEA and x_{MDEA} = 0.0079 to 0.8989	298.15 to 7.11	Cannon Fenske Viscometer	77.19 to 7.11
Baek et. al. 2000	Pure MDEA	303.15 to 343.15	Ubbelohde Viscometer	57.15 to 9.90
Henni et. al. 2000	Pure MDEA	298.15 to 343.15	Ubbelohde Viscometer	77.19 to 9.85
Bernal-Garcia et. al. 2004	Pure MDEA and x_{MDEA} = 0.0604 t0 0.7430	313.15 to 363.15	Cannon Fenske Viscometer	34.61 to 5.27
Paul and Mandal 2006	Pure MDEA and w_{MDEA} = (0.1, 0.2, 0.3)	288 to 333	Ostwald’s Viscometer	142 to 14.66
Muhammad et. al. 2008b	Pure MDEA and w_{MDEA} = 0.3228, 0.4880	298.15 to 338.15	Ubbelohde Viscometer	77.85 to 12.34
Chowdhury et. al. 2010	Pure MDEA and x_{MDEA} = 0.050 to 0.901	303.15 to 323.15	Ostwald’s Viscometer	57.14 to 21.53
		[hmim][BF_4]		
Sanmamed et. al. 2007	Pure [hmim][BF_4]	288.15 to 323.15	Anton Paar AMV Viscometer	315.7 to 53.9
Muhammad et. al. 2008a	Pure [hmim][BF_4]	288.15 to 338.15	Brookfield Viscometer	141 to 21
Zhu et. al. 2011	Pure [hmim][BF_4]	298.15	Ubbelohde Viscometer	195.36
Kermanpour et. al. 2012	Pure [hmim][BF_4] as well as mixtures with 1-propanol ($x_{[hmim][BF4]}$ = 0.1006 to 0.8894)	293.15 to 333.15	Ubbelohde Viscometer	232.65 to 34.02
Hui et. al. 2012	Pure [hmim][BF4] as well as mixtures with [hmim][Cl] ($x_{[hmim][BF4]}$ = 0.2 to 0.8	303.15 to 333.15	Anton Paar AMV Viscometer	189.1 to 49.4

contd…….

		[hmim][BF$_4$]		
Vakili-Nezhaad et. al. 2012	Pure [hmim][BF$_4$]	298.15 to 363.15	Rheometer double gap Gemini	383.01 to 10.60
		[hmim][Tf$_2$N]		
Dzyuba et. al. 2002	Pure [hmim][Tf$_2$N]	298.15	Ostwald’s Viscometer	79
Fitchett et. al. 2004	Pure [hmim][Tf$_2$N]	298.15	Zeitfuchs cross arm viscometer	78
Tokuda et. al. 2005	Pure [hmim][Tf$_2$N]	283.15 to 353.15	Toki RE 80 Viscometer	69 to 10.6
Widegren et. al. 2007	Pure [hmim][Tf$_2$N]	258.15 to 373.15	Stabinger Viscometer	941.8 to 7.463
Muhammad et. al. 2008a	Pure [hmim][Tf$_2$N]	288.15 to 328.15	Brookfield Viscometer	97 to 24
Marsh et. al. 2009	Pure [hmim][Tf$_2$N]	293.15 to 363.15	Brookfield Viscometer	80.7 to 8.33
Santos et. al. 2010	Pure [hmim][Tf$_2$N]	298.15 to 343.15	Ostwald’s Viscometer	69.43 to 14.10
		[hmim][FAP]		
Ignat’ev et. al. 2005	Pure [hmim][FAP]	293.15	Viscosimeter SVM Anton Paar	115.44
Yao et. al. 2009	Pure [hmim][FAP]	293.15	Stabinger Viscometer	119
Guang Li et. al. 2011	Pure [hmim][FAP]	293.15 to 343.15	Brookfield Viscometer	114.3 to 14.8
Ahmad et. al. 2011	Pure [hmim][FAP]	293.15	Brookfield Viscometer	116
Almantariotis et. al. 2012	Pure [hmim][FAP]	293.15 to 373.15	Anton Paar AMV Viscometer	118.8 to 7.87

Table 2.5. Literature review on the determination of viscosity of the non aqueous solutions of MDEA and mixtures of IL ([hmim][BF_4]) with other solvents.

Reference	Composition	Temp. (K)	Apparatus	Viscosity Range (mPa.s)
	Non aqueous MDEA solutions			
Weinland et. al. 1998	MDEA + MEA (MEA mass%: MDEA mass %: 5:45, 10:40, 20:30) MDEA + DEA (DEA mass%: MDEA mass %, 5:45, 10:40, 20:30)	298 K	Canon-Fenske viscometer	(13.3 to 7.36) & (13.3 to 2.2)
Henni et. al. 2000	MDEA + TEGMME (x_{MDEA} = 0.1004 to 0.9002) MDEA + ethanol (x_{MDEA} = 0.0079 to 0.2986)	298.15 to 343.15 for MDEA + TEGMME 313.15 for MDEA + ethanol	Ubbelohde viscometer No. 10 and Cannon-Ubbelohde viscometer Cole Parmer	(77.1 to 2.1) & (0.8 to 34.1)
	[hmim][BF_4]			
Rilo et. al. 2010	Pure and binary mixtures with water ($x_{[hmim][BF4]}$ = 0.28 to 0.8899)	288.15 to 318.15	Anton Paar SVM 3000	357.5 to 5.8
Zhu et. al. 2011	Pure and binary mixtures with butanone or butylamine or ethyl acetate or tetrahedrofuran; $x_{[hmim][BF4]}$ = (0.0492 to 0.8931) for mixtures with butanone; $x_{[hmim][BF4]}$ = (0.0492 to 0.8787) for mixtures with butylamine; $x_{[hmim][BF4]}$ = (0.0498 to 0.8908) for mixtures with ethyl acetate; $x_{[hmim][BF4]}$ = (0.0498 to 0.8925) for mixtures with tetrahedrofuran	298.15	Ubbelohde viscometer	195.3 to 0.38
Kermanpour et. al. 2012	Pure and binary mixtures with 1-propanol; $x_{[hmim][BF4]}$ = 0.1006 to 0.8894) for mixtures with 1-propanol.	293.15 to 333.15	Ubbelohde viscometer	232.6 to 0.6
Hui et. al.2012	Pure and binary mixtures with [hmim][Cl]; $x_{[hmim][BF4]}$ = (0.2 to 0.8)	303.15 to 333.15	Anton Paar AMVn	1879 to 189.1

with other molecular solvents is available. It has been discussed that many researchers, by using variety of viscometers have reported the viscosity of amine solvents and ionic liquids. Among these quite a number of researchers have used different models of Brookfield viscometers due to their better performance coupled with high precision and accuracy. It is also well known that the viscosity of ILs is higher than the conventional organic solvent. The industrial application of ILs becomes prohibitive as the pumping costs increase many folds. For the absorption of gases the solvent should possess lower viscosity to enable efficient diffusivity of gas through it. The viscosity of ILs is a limiting factor in their large scale commercial usage. Therefore in many real systems the IL would be mixed with other liquid components namely molecular solvents, water *etc.* to lower its viscosity and make it viable for the industrial usage (Croswaite et. al. 2005).

2.1.3 Refractive Index

Refractive index is defined as the ratio of the speed of light in vacuum to that in a given medium. It describes about the ability of a substance to refract light as it moves from one medium to another. The higher the refractive index of a substance the more light is refracted. The substances having higher density exhibit higher values of refractive index. The reason for higher values of refractive index for a substance having higher density is that it has in abundance of the loosely bound electrons A high refractive index is generally considered to be a value higher than 1.6 (above the range of most of the organic solvents) (Deetlefs et. al. 2006). The refractive index is one of the most important optical properties and is frequently used to characterize substances. It has been used as an indicator for the purity of the compounds. In material sciences and in chemical engineering refractive index is widely used to evaluate the purity of the materials and solvents. Refractive index values provide a satisfactory analytical method to determine the composition of solvents. These values are also used to evaluate molar refractions which describe the molecular interactions between the solutes present in a mixture. The refractive index is connected to many other physical properties. The relationship of refractive index with critical temperature, polarizability, density and boiling point along with other important properties has been reviewed by Partington (1953) and other researchers (Katritzky et. al. 1998). The literature pertaining to the refractive indices of MDEA, [hmim][BF_4]

and [hmim][Tf_2N] as well as for their mixtures (if any) with other solvents is presented in Table 2.6. From the literature review, it is clear that quite a number of researchers have reported the refractive indices values for these solvents. On the other hand, no data for the refractive indices of pure [hmim][FAP] and for the non aqueous mixtures of MDEA has been reported in the open literature.

Table 2.6 Literature review on the determination of refractive index of pure and aqueous MDEA and the ILs namely; [hmim][BF_4] and [hmim][Tf_2N].

Reference	Composition	Temp. (K)	Apparatus	RI Range
		MDEA		
Lagalante et. al. 2000	Pure MDEA	298.15, 323.15, 348.15	Abbe's prism refractometer	1.449 to 1.467
Muhammad et. al. 2008b	Pure MDEA as well as aqueous solutions (w_{MDEA} = 0.3228, 0.4880)	303.15 to 333.15	ATAGO (RX-5000) alpha refractometer	1.452 to 1.465
		[hmim][Tf_2N]		
Muhammad et. al. 2008a	Pure [hmim][Tf_2N]	302.95 to 332.95	ATAGO (RX-5000) alpha refractometer	1.423 to 1.429
Tariq et. al. 2009	Pure [hmim][Tf_2N]	293.15 to 333.15	Carl Zeiss Abbe refractometer	1.420 to 1.431
Seoane et. al. 2012	Pure [hmim][Tf_2N]	298.15	ABBEMAT Dr. Kernchen refractometer	1.430
Corderi et. al. 2012	Pure [hmim][Tf_2N]	298.15	ABBEMAT Dr. Kernchen refractomter	1.430
Gonzalez et. al. 2012	Pure [hmim][Tf_2N]	298.15	ABBEMAT-HP Dr. Kernchen refractomter	1.429
		[hmim][BF_4]		
Muhammad et. al. 2008a	Pure [hmim][BF_4]	302.95 to 332.95	ATAGO (RX-5000) alpha refractometer	1.421 to 1.426
Vakili-Nezhaad et. al. 2012	Pure [hmim][BF_4]	293.15 to 343.15	KEM (RA-620) refractometer	1.426 to 1.427

2.1.4 Thermal Stability

Thermogravimetric analysis (TGA) is a method of thermal analysis in which changes in physical and chemical properties of materials are measured as a function of increasing temperature (with constant heating rate), or as a function of time (with constant temperature or mass loss). Qualitative understanding of changes of properties of materials with temperature has existed since long (Coats and Redfern 1953; Bilyeu et. al. 2000). The thermogravimetric analysis of the solvents used for CO_2 capture is of utmost importance. This provides information about the decomposition of the solvents. The solvent which is being used for CO_2 absorption should be thermally stable over a wide range of absorption temperatures for its effective usage. Many researchers have performed TGA for numerous solvents used for CO_2 removal ranging from common alkanolamines to the promising ILs. Kim et. al. (2011) reported the TGA for various aqueous solutions of alkanolamine solvents (MEA, AMP, MDEA) and 1,8-diamino-p-menthane (KIER-C3). The reported results indicated that the order of thermal stability was as follows: AMP>MEA>KIER>MDEA. The MEA and AMP were decomposed rapidly with rise in temperatures. On the other hand, MDEA and KIER-3 showed opposite results. They concluded that MEA and AMP have the risk of solvent loss and degradation. Muhammad et. al. (2008b) evaluated the thermal stability of pure MDEA as well as for its aqueous mixtures (32.28 to 48.8 mass %) by using Perkin-Elmer thermogravimetric analyzer. The reported results indicated that the binary mixtures of MDEA with water showed low temperature values at the start of decomposition in comparison to the pure MDEA. It indicated that initially free water molecules were decomposed followed by the degradation of MDEA molecules. The final decomposition temperatures of aqueous MDEA solutions were found to be higher than the pure MDEA which they attributed to the strong hydrogen bonding. Similar kind of trend was observed by Murshid et. al. (2011) who reported the thermal stability of pure AMP as well as its mixtures with water. They reported that the binary mixtures of AMP with water showed lower onset values in comparison with pure AMP. On the other hand, the final decomposition temperatures of binary mixtures were higher than the pure AMP. They also attributed this with the strong hydrogen bonding within the binary mixtures. Ionic liquids (ILs) have high thermal stability, often beginning to decompose around 400 ^oC. The thermal decomposition of ILs heavily depends upon the salt structure. The themal stability of ILs increases as the molar mass of anion increases. Whereas the thermal stability of ILs decreasesd with increase in hydrophilicity of anions. The ILs with halide anion show less thermal stability in comparison to the one with non halide anions. One of the proposed mechanisms for ILs decomposition involves the proton abstraction to produce both volatile acids from the anion and carbene derivatives of the cation (Huddleston et. al.

2001). The thermal stability of ILs by means of TGA has also been reported by many researchers. Ngo et. al. (2000) reported the thermal stability of 35 imidazolium based ILs. The reported results indicated that ILs had minimal vapor pressure up to their thermal decomposition temperature (>400^{o}C). They concluded that halide contents in ILs drastically reduced their thermal stability. Furthermore, imidazolium ILs were more thermally stable than their tetra-alkyl ammonium counter parts. In the same manner Fredlake et. al. (2004) reported the thermal stability of 13 imidazolium based ILs, and concluded that the thermal stability of ILs increased with increasing size of anions. On the other hand, Stoppa et. al. (2010) studied the effect of cation on the thermal stability of ILs. The experimental results indicated that with increasing alkyl chain length of cation the thermal stability of ILs decreased, a trend which is opposite to that for anion size. Muhammad et. al. (2008a) studied the thermal stability of three imidazolium based ILs with a single cation (1-hexyl-3-methylimidazolium ([hmim])) coupled with different anions ([PF_6], [BF_4], [Tf_2N]) and found that all ILs had lower start decomposition temperature at heating rate of 20^{o}C·min^{-1} as compared to 10^{o}C·min^{-1}. The IL with [Tf_2N] anion displayed highest thermal stability followed by [PF_6] and [BF_4] respectively.

2.2. Excess Properties

The studies on the excess thermodynamic properties of mixtures are of considerable interest as these help in understanding the intermolecular interactions in binary liquid mixtures. Excess and deviation properties of binary mixtures are important as they are not only dependent on solute-solute, solvent-solvent, and solute-solvent interaction but also on the structural effects arising from interstitial accommodation. The knowledge of these properties at different temperatures is required for engineering design and for subsequent operations. Furthermore these help in understanding about the interparticle interactions between components. These properties are used extensively as qualitative and quantitative guide to predict the extent of complex formation in mixtures. These properties are important in many practical problems concerning mass transport and fluid flow and also used for testing molecular theories and models of solutions (Ivanov and Kustov 2010; Almasi and Iloukhani 2010; Vural et. al. 2011).

The excess and deviation properties of mixtures can be derived by using the experimental values of physical properties. These properties like excess molar volumes, viscosity deviations and refractive index deviations are helpful in understanding the molecular interaction between the components present in the mixtures and also describe the structural packing within the mixtures. Excess molar volume (V^E) is the result of several opposing factors. They can arbitrarily be divided into three types namely, physical, chemical and structural. Physical contributions which are non specific interaction between the components present in the mixture result in a positive value of V^E. On the other hand, the presence of chemical or specific intermolecular interactions decreases the volume, and they include charge transfer type of forces and other complex forming interactions which result in a negative value of V^E. Structural contributions are those in which geometrical fittings (interstitially accommodated) of one component into the other occur due to the difference in free volume and molar volume between components. Structural contributions mostly contribute to the negative values of V^E (Sovilj and Barjaktarovic 2000; Vural et. al. 2011).

Many researchers have studied the excess molar volumes for the mixtures of MDEA with different solvents to investigate the intermolecular interaction between the components present in the system (Maham et. al. 1995; Hawrylak et. al. 2000; Henni et. al. 2000; Bernal-Garcia et. al. 2003; Robolledo-Libreros and Trejo 2006; Muhammad et. al. 2008; Garcia-Abuin et. al. 2009; Alvarez et. al. 2010; Han et. al. 2012). On the other hand, the excess molar volumes of the mixtures involving various types of ionic liquids also been reported by many investigators (Canongia Lopes et. al. 2005; Lachwa et. al. 2006; Navia et. al. 2007; Garcia-Miaja et. al. 2009; Ahosseini et. al. 2010; Zhu et. al. 2011; Deng et. al. 2011; Gonzalez et. al. 2012; Hui et. al. 2012; Kermanpour et. al. 2012). The literature review pertaining to the excess molar volumes of the aqueous and non aqueous solutions of MDEA and for the mixtures of ILs with other solvents is summarized in Table 2.7. The binary mixture exhibits different viscosity values from that for pure components present in the mixture. These changes in viscosity further help in understanding the nature of the mixture and the types of the intermolecular interactions present between the unlike molecules. The viscosity deviation is defined as the deviation in viscosity of a mixture from ideality (ideal viscosity which a mixture should exhibit, ideal viscosity is considered as the sum of the viscosities of the components of whose the mixture is composed of). The viscosity deviations are a function of molecular interactions as well as size and shape of molecules (Iloukhani et. al. 2009; Clara et. al. 2010). The viscosity deviations are calculated from the experimental viscosity values of pure components comprising a mixture. The viscosity deviations are due to the function of molecular interactions, the size and shape of components, size of intermolecular complexes and dispersion forces also play an equal and important role. The viscosity deviations of multi component systems constitute a reliable criterion for assessing or for excluding the presence of any kind of interactions between the dissimilar molecules. Therefore the magnitude of these deviations from ideality of system can be positive, negative or zero, which could be explained as a balance between positive contributions (dispersive interactions

Table 2.7 The excess molar volumes for the aqueous and non aqueous solutions of MDEA and for the mixtures of the ILs ([hmim][BF$_4$], [hmim][Tf$_2$N]) with other solvents.

References	**System**	**Temp. (K)**	**V^E Range**
Maham et. al. 1995	MDEA + water	298.15 to 353.15	-0.044 to -1.154
Hawrylak et. al. 2000	MDEA + water	298.15	-0.022 to -1.241
Henni et. al. 2000	MDEA + TEGMME	298.15 to 343.15	0.050 to 0.250
Bernal-Garcia et. al. 2003	MDEA + water	283.15 to 363.15	-0.373 to -1.254
Rebolledo Libreros et. al. 2006	MDEA+DEA+water	303.15 to 343.15	-0.059 to -0.071
Muhammad et. al. 2008	MDEA +water	298.15 to 338.15	- 0.071 to -1.125
Alvarez et. al. 2010	MDEA + MEA	293.15 to 323.15	-0.100 to -0.500
Han et. al. 2012	MDEA + water	298.15 to 423.15	- 0.222 to -1.032
Canongia Lopes et. al. 2005	[hmim][Tf$_2$N]+[C$_{10}$mim][Tf$_2$N]	298.15 , 333.15	0.053 to 0.110
Navia et. al. 2007	[hmim][BF$_4$]+[C$_2$mim][BF$_4$], [hmim][BF$_4$]+[C$_4$mim][BF$_4$]	303.15	-0.050 to 0.250 -0.010 to -0.025
Garcia-Miaja et. al. 2009	[hmim][BF$_4$]+nitromethane	298.15 308.15 318.15	-0.010 to -0.800
Ahosseini et. al. 2010	[hmim][Tf$_2$N]+1-Octene	283.15 to 348.15	-0.010 to 0.040
Deng et. al. 2011	[hmim][Tf$_2$N]+methanol	298.15	-0.083 to -0.216
Zhu et. al. 2011	[hmim][BF$_4$]+butanone, [hmim][BF$_4$]+butylamine, [hmim][BF$_4$]+ethyl acetate, [hmim][BF$_4$]+tetrahydrofuran	298.15	-0.326 to -1.853 -0.341 to -1.374 -0.371 to -1.678 -0.423 to -2.075
Gonzalez et. al. 2012	[hmim][Tf$_2$N]+acetone, [hmim][Tf$_2$N]+dichloromethane	288.15	-0.126 to -1.009 -0.044 to -0.405

between unlike molecules and hydrogen bond rupture) and negative contributions (geometrical fitting between components and intermolecular interactions). In other words it could be inferred that the negative values of viscosity deviations occur when dispersion forces are dominant particularly for the systems having different molecular sizes. On the other hand, the positive values of viscosity deviations occur in the mixtures where the association forces are predominant (Iloukhani and Rakhshi 2009; Clara et. al. 2010; Doghaei et. al. 2010; Cwiklinska and Kinart 2011).

The viscosity deviation for the mixtures involving amine solvents have been reported by many researchers (Henni et. al. 2000; Maham et. al. 2002; Bernal-Garcia et. al. 2004; Geng et. al. 2008; Rayer et. al. 2010; Yasmin et. al. 2011). In the same manner the viscosity deviations for the mixtures involving various ILs have been reported by many investigators (Geng et. al. 2008; Wu et. al. 2011; Ahosseini et. al. 2011; Kavita et. al. 2012; Kermanpour et. al. 2012). The literature review for the estimated viscosity deviation ($\Delta\eta$) values for various systems involving alkanolamines and ILs is presented in Table 2.8.

Table 2.8: Viscosity deviation values for the different mixtures of solvents involving amines *or* ILs

References	**System**	**Temp. (K)**	**Values of $\Delta\eta$**
Henni et. al. 2000	MDEA+TEGMME	298.15 to 343.15	-0.05 to -35.00
Maham et. al. 2002	DEEA + water, MEEA + water, MEA + water	298.15	0.10 to 2.5 0.10 to 2.2 0.10 to 1.4
Bernal-Garcia et. al. 2004	MDEA + water	313.15 to 363.15	-0.767 to 10.028
Geng et. al. 2008	[bmim][PF$_6$]+MEA, [bmim][PF$_6$]+DMEA	288.15 to 323.15	-5.00 to -120.00 -4.00 to -122.00
Rayer et. al. 2010	1-AP+water, MEA +water, DEA+water, AEEA+water, DGA+water, MDEA+water	313.15	20.00 to -35.00 for all the sytems
Wu et. al. 2011	[MPI][PF$_6$]+ poly(ethyleneglycol)	293.15 to 353.15	-0.3527 to -128.045
Ahosseini et. al. 2011	[hmim][Tf$_2$N]+1-octene	283.15 to 348.15	-0.01 to -23.00
Kermanpour et. al. 2012	[hmim][BF$_4$]+AP, [hmim][BF$_4$]+isobutanol	303.15 to 338.15	-1.60 to -34.80 -2.80 to -35.10

Refractive index deviations like other excess properties (excess molar volumes and viscosity deviations) are also an important property. The refractive index deviations for a mixture are calculated from the experimental refractive index values of the components comprising the mixture. The refractive index deviations, similar to viscosity deviation not only depend upon the molecular interactions between the species present in the mixture but also on the size and shape of the molecules (Iloukhani and Rakhshi 2009). Refractive index deviations for the mixtures of solvents involving different amine solutions have been reported by many researchers (Gu et. al. 2000; Chen et. al. 2002; Iloukhani and Rakhshi 2009; Saravanakumar et. al. 2011; Narayanaswamy et. al. 2012). The RI deviations for the mixtures of solvents involving different ionic liquids have also been reported by many researchers (Pal et. al. 2010; Vercher et. al. 2010; Taib et. al. 2012; Wu et. al. 2012; Navarro et. al. 2012; Yu et. al. 2012; Larriba et. al. 2012). The RI deviations for the systems featuring various alkanolamine systems (alkanolamine+other solvents) and ionic liquids systems (IL + other solvents) are listed in Table 2.9.

Table 2.9. Refractive index deviations for the different mixtures of solvents involving ILs *or* amines.

References	**System**	**Temp. (K)**	**Values of Δn_D**
Gu et. al. 2000	*N*-ethylpiperazine +water	298.15	0.0065 to 0.0825
Chen et. al. 2002	*N*-ethylpiperazine+ methanol *or* ethanol *or* *n*-propanol *or* *n*-butalnol *or* isobutanol	298.15	0.0019 to 0.0429
Iloukhani and Rakhshi 2009	Cyclohexanone + *N*,*N*-dimethylacetamide *or* *N*,*N*-diethaylethanolamine, *N*,*N*-dimethylacetamide + *N*,*N*-diethaylethanolamine	298.15	-0.0003 to -0.0058
Saravanakumar et. al. 2011	Acetophenone + *N*,*N*-dimethylethanolamine, Acetophenone + *N*-*N*-diethylethanolamine	303.15, 313.15, 323.15	-0.0012 to -0.0034
Pal et. al. 2010	[bmim][PF_6] + DEGMME *or* PGMME *or* PGMEE	298.15	0.001 to 0.0045
Vercher et. al. 2010	[emim][triflate] + methanol *or* ethanol *or* 1-propanol *or* 2-propanol	288.15 to 338.15	0.001 to 0.05
Taib et. al. 2012a	[C_2CNHim][Br]+ethanol	293.15 to 323.15	0.0073 to 0.0620
Wu et. al. 2012	[MPI][BF_4]+MPEG	293.15	0.001 to 0.008
Navarro et. al. 2012	[bmim][BF_4]+water, [bmim][BF_4]+2-propanol	298.15, 323.15	0.0060 to 0.0249
Yu et. al. 2012	[bmim][Gly]+methanol, [bmim][Glu]+methanol	298.15 to 313.15	0.0183 to 0.0812
Larriba et. al. 2012	[bpy][BF_4]+[bpy][Tf_2N]	303.15 to 353.15	-0.0001 to -0.0018

2.3 Carbon Dioxide Solubility

2.3.1 Introduction

Carbon dioxide (CO_2) is a primary green house gas emitted through human activities. In 2010, CO_2 contributed 84% of US greenhouse gas emissions. CO_2 is naturally present in the atmosphere as the carbon cycle. The human activities are altering the carbon cycle by adding more CO_2 to the atmosphere and by influencing the ability of natural sinks like forests to remove CO_2. At present most of the world's energy supply comes from the fossil fuels. The main difficulty with the fossil fuels is that their burning produces CO_2; natural gas the least and coal the most. The increase of CO_2 emission in the atmosphere are mainly due to the combustion of fossil fuels for human needs. The burning of the fossil fuels is the dominant factor in the increased emission of CO_2. The upper limit for atmospheric CO_2 is 350 ppm. It means that a concentration lower than this value is not harmful to humans and the environment. According to Mauna Loa Observatory, in Hawaii, the average atmospheric CO_2 concentrations were higher than 350 ppm since 1988 and were 392.41ppm in August 2012. For the past decade (2002-2011) the annual increase in the concentration of atmospheric CO_2 is 2.07 ppm per year. The direct and indirect impacts of these increase in greenhouse concentration will result in increasing temperatures, acidification, changes to the density structure of upper ocean which will alter vertical mixing of water, weakening/intensification of upwelling winds, and changes to the timing and volume of freshwater runoff into marine waters. It is really an alarming situation and some of the mentioned changes are already underway. Therefore serious efforts are required for the efficient removal of CO_2 from the atmosphere.

The environmental impacts of CO_2 has been discussed above. It is known that natural gas is the cleanest of all the fossils fuels. The natural gas does not come in the purest form, from the well rather it is contaminated with some impurities like CO_2 *etc*. The presence of CO_2 in natural gas lowers its calorific value and also hinders its efficient burning. The presence of CO_2 in natural gas is the main obstacle for the production of LNG which is the most efficient mean of transportations and export of natural gas to the places where it is not found in abundance. For the countries, which are the major producer and exporters of LNG (Malaysia is ranked 3rd) the removal of

CO_2 from the natural gas is necessary. The present sweet sources of natural gas are depleting due to the increased demand of this clean fuel. The sour sources of natural gas (the sources which possess larger quantities of CO_2 as impurity) could be fully utilized by effectively and efficiently removing the unwanted CO_2. The captured CO_2 is used in the well for the enhanced oil recovery. It effectively reduces the surface tension of the oil and thus results in the enhanced yield of crude oil (Dresselhaus and Thomas 2001; Bates et. al. 2002; Moore et. al. 2008; LNG Report 2010).

There are many processes used for the removal of CO_2. Review of the current processes used for CO_2 capture has been discussed in section 1.1.2 of Chapter 1. Among the available processes the most common method is the absorption of CO_2 in a solvent. CO_2 removal through absorption and stripping by using aqueous solutions of amine is an established process. These aqueous solutions react rapidly with CO_2 (based on the classical acid base reaction) to form a corresponding carbamate. The carbamate formed is later subjected to less pressure and heat and hence the captured CO_2 is removed. These solvents are extensively used in most of the industrial CO_2 capture processes (in US 95% gas sweetening process are based on amine based scrubbing). The amine solvents have some inherent drawbacks associated with these like degradation, loss of solutions and high energy consumption. Despite all odds the amine solutions are still widely practiced due to their effectiveness in CO_2 capture technology. However the need for energy intensive and environmental friendly solvent to efficiently remove CO_2 prevails. In the following section the different amine solutions used for CO_2 capture will be discussed in detail.

2.3.2 Solubility of CO_2 in alkanolamine solvents

The alkanolamines commonly used for CO_2 removal by absorption are; monoethanolamine (MEA), diethanolamine (DEA), *N*-methyldiethanolamine (MDEA), di-2-propanolamine (DIPA) and 2-amino-2-methyl-1-propanol (AMP). The basic process patented in 1930 is one in which CO_2 is absorbed (in an absorber) from natural gas or flue gas near ambient temperature into the aqueous solution of amine. The amine is regenerated by stripping with steam at 100 to 120^oC (in a stripper) and the CO_2 is released. The key feature of the amine system is that large amount of heat is required to regenerate the solvent. The heat is typically drawn from the steam cycle and significantly reduces the efficiency of the plant. Flour Daniel Inc., Dow Chemicals Co., Kerr-McGee chemical Corp and ABB Lummus Crest Inc., were some of the initial developer of amine based technology for CO_2 removal. Typically about 80 to 90% of CO_2 is captured using this technology producing nearly pure (>99%) CO_2 product stream (Rayer et. al. 2012; Mandal et. al. 2005; Rubin and Rao 2002).

Abundant research reports pertaining to the usage of alkanolamine solvents for CO_2 capture have been published since the commercialization of this process. For instance, Jones et. al. (1959) reported the CO_2 solubility in the aqueous MEA solutions (15.3 weight % MEA) over a temperature range of (313.15 to 413.15) K and for CO_2 partial pressures up to 7000 mmHg. The reported results indicated that the CO_2 solubility decreased with increase in temperature. On the other hand, the solubility increased with increase in partial pressure of CO_2 (while keeping the temperature as constant). In a similar manner Isaacs et. al. (1980) measured the CO_2 solubility in the aqueous solutions of monoethanolamine at temperatures (353.15, 373.15) K and for partial pressures of CO_2 up to 1.75 kPa. The results indicated a similar trend that greater CO_2 solubility was observed at lower temperatures and at higher partial pressures. The CO_2 solubility data in all types of alkanolamine (primary, secondary, tertiary) have been reported in open literature. The secondary alkanolamine solvents like diethanolamine has also been the focus of researchers. Lawson et. al. (1979) reported the CO_2 solubility in the aqueous diethanolamine (25 weight %) over a temperature range of (310.92 to 394.261) K and for the CO_2 partial pressures up to 44 bar. The maximum solubility occurred at 338 K for CO_2 partial pressure of 40 bar and a similar trend that at lower temperatures and higher pressures greater CO_2 solubility occurred. Primary and secondary alkanolamines react rapidly with CO_2 to form a carbamate with a stoichiometric loading of 0.5 mol of CO_2 per mole of amine solvent. However, due to a relatively high heat of absorption is associated with the formation of carbamate ion the cost of regenerating primary and secondary amines is high. Primary and secondary amines also have the disadvantage of requiring 2.0 mol of amine to react with 1.0 mole of CO_2. Therefore their loadings are limited to 0.5 mol of CO_2 per mole of amine. Table 2.10 shows the common alkanolamines (other than MDEA) used for CO_2 capture. Figure 2.1 shows the comparison of CO_2 solubility data in aqueous (4.2 M) MEA, DEA, and MDEA. It can

Table 2.10. List of common alkanolamine (other than MDEA) used for CO_2 absorption

Alkanolamines	References
Monoethanolamine (MEA)	Jones et. al. 1959; Lawson et. al. 1979; Isaacs et. al. 1980; Austgen et. al. 1991; Shen et. al. 1992; Dawodu et. al. 1994; Song et. al. 1996; Jane and Li 1997; Mathonat et. al. 1998; Ma'mun et. al. 2005; Arcis et. al. 2011, Mandal et. al. 2006
Diethanolamine (DEA)	Lee et. al. 1972; Lawson et. al. 1976; Kennard and Meisen 1984; Dawodu et. al. 1994
2-amino-2-methyl-1-propanol (AMP)	Bosch et. al. 1990; Xu et. al. 1991; Saha et. al. 1993; Jane and Li 1997; Choi et. al. 2009

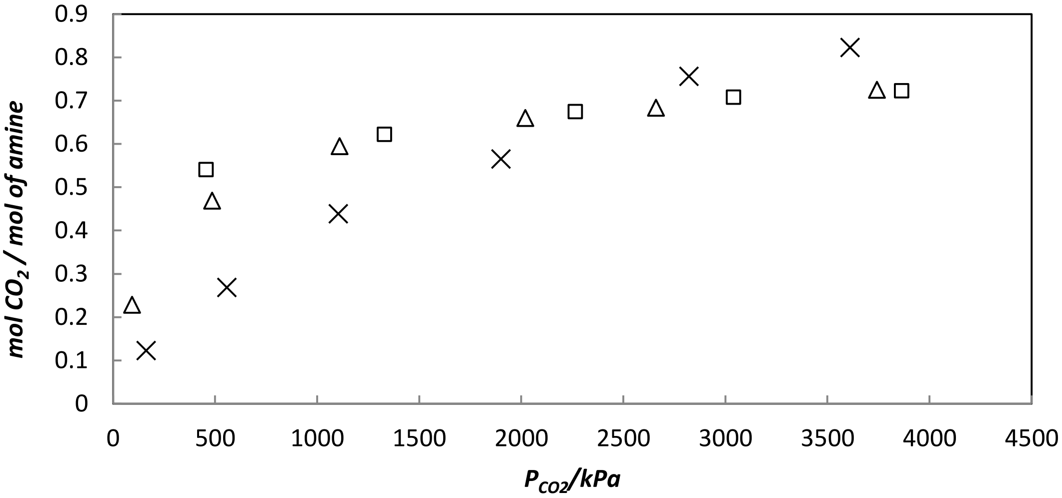

Figure 2.1. Comparison of CO_2 solubility 4.2 M aqueous amine solvents at $T = 373.15$ K. ×; MDEA, □, MEA; Δ, DEA (Dawodu et. al. 1994).

be seen that MEA and DEA has shown fast absorption rate in comparison to MDEA. However MDEA has shown higher CO_2 loadings at higher pressures indicating its stability. The advantage of tertiary amine (MDEA) over primary and secondary amine includes its high equilibrium loading capacity (1.0 mol of CO_2 per 1 mole of MDEA as compared to 0.5 mol of CO_2 per 1 mole of MEA *or* DEA) and its lower heat of reaction with CO_2, which results in lower energy requirements for regeneration purpose (which is about 70% of the operating cost). In addition to be advantageous in terms of less energy requirements for regenerations. MDEA is prominent among the available alkanolamines due to many other favorable properties also. It has low vapor pressure, hence no evaporative loss. It has favorable thermal and chemical stability. It shows low corrosive behavior (hence could be employed at a high concentration in the absorption process). The use of highly concentrated MDEA solutions can lead to significant savings in electrical energy, in comparison to the conventional absorbents due to lower circulation demands in the absorption process. Since MDEA does not react directly with CO_2 during the absorption process the stripping can easily be achieved by a simple pressure reduction rather to heat the solutions at elevated temperatures (Rho et. al. 1997; Kundu and Bandyopadhyay 2006; Mandal and Bandyopadhyay 2006). Therefore in the present study MDEA has been chosen as the amine counterpart for the ILs to be mixed with them to form hybrid mixtures. MDEA has been the focus of many investigators for the CO_2 removal. Table 2.11 shows the list of the aq. MDEA solutions used by researchers for CO_2 absorption along with the operating conditions. Jou et. al. (1982) reported the CO_2 solubility in aqueous MDEA

Table 2.11. List of aqueous MDEA solutions used by the researchers for CO_2 absorption.

Reference	MDEA conc. (wt %)	Temperature (K)	Pressure (kPa)
Jou et. al. 1982	11.8, 23.4, 48.9	298, 313, 343, 373, 393	0.001-6570
Chakma et. al. 1987	16.8, 33.8	373, 413, 433, 453, 473	103-4930
Austgen et. al. 1991	23.4, 48.9	313	0.006-93.6
Shen et. al. 1992	30	313, 333, 353, 373	1-2000
Dawodu et. al. 1994	33.8	373, 393	162-3832
Karnov et. al. 1996	19.2, 32.1	313,333,373,393,413	70-5000
Mathonat et. al. 1997	30	313,353,393	2000-10000
Rho et. al. 1997	5, 20, 50, 75	323,348,373	0.8-140
Xu et. al. 1998	35.1, 39.8, 48.9	313,323,343,353,363,373	0.9-1013
Lemoine et. al. 2000	11.8, 23.6	298,313	0.02-1.64
Park et. al. 2001	50	298,323,348,373	0.8-140
Kamps et. al. 2001	32, 48.8	313,353,393	228-7565
Boumedine et. al. 2004	25.73, 46.88	298, 313, 348	2.84-4386.8
Ma’mun et. al. 2005	50	328, 343, 358	65.75-813.4
Ermatchkov et. al. 2006	19.24,32.27,48.80	313, 353, 393	0.1-70
Huttenhuis et. al. 2007	35, 50	283, 298	0.054-986.80

(1.0, 2.0, 4.28 kmol/m^3) solutions at temperatures (313.15 to 393.15) K and at CO_2 partial pressures ranging from 0.001 to 6600 kPa. They correlated the solubility data with the help of Kent Eisenberg model. The results indicated that lower temperatures and higher pressures lead to greater solubility. On the other hand, the aqueous solutions having low concentrations of MDEA showed higher CO_2 loading capacities in comparison with the aq. solutions having higher MDEA concentration. It indicated that with increase in concentration of MDEA in aqueous solution the CO_2 loading decreased. Chakma and Meisen (1987) reported the CO_2 solubility data in aqueous MDEA (1.69 and 4.28 M) solutions, for a temperature and pressure range of 373.15 to 473.15 K and 172 to 4929 kPa respectively and correlated the experimental solubility results with their own proposed thermodynamic model. The correlated results agreed well with the experimental results. The experimental results indicated that CO_2 reacted more rapidly with aq. MDEA at higher temperatures however the loading were not higher at elevated temperatures. The highest CO_2 loadings were observed at lower temperatures and at elevated CO_2 partial pressures (a trend common in all aq. alkanolamine solvents). In a similar manner Kuranov et. al. (1996) measured the CO_2 solubility data in aqueous MDEA solutions (two molalities ≈ 2 and 4 mol/kg) in the temperature range of (T = 313 to 413 K) and at elevated pressures (up to 5 MPa) and correlated the data using their own model and also validated their thermodynamic model by correlating the available literature data on CO_2 solubility in aqueous MDEA solutions. The model showed a fair degree of agreement with the experimental results of their study as well as with the previous studies. The trend was similar that at lower temperature and at higher pressures, the CO_2 loading were found to be higher in the solvents. In addition to the aqueous MDEA solution the mixtures of aqueous MDEA with other amines have also been explored by many researchers for CO_2 solubility. These are ternary mixtures comprising of MDEA, other alkanolamine solution and water. The addition of some primary and secondary alkanolamine solvents to the aqueous MDEA solution have proven fruitful in terms of reaction rate and CO_2 loading. The CO_2 solubility in the aqueous mixtures of MDEA with MEA *or* DEA *or* PZ *or* AMP has been reported by many investigators also (Austgen et. al. 1991; Silkenbaumer et. al. 1998; Mandal et. al. 2005; Lin et. al. 2009; Bottger et. al. 2009; Zoghi et. al. 2012). For the aqueous MDEA solutions and their mixtures with other amines, prolific data has been reported in the literature as discussed. However, the

CO_2 solubility data for non aqueous MDEA solutions is very scarce in the literature. Versteeg and Swaaij (1988) reported the CO_2 solubility in the non aqueous solutions of MDEA in ethanol and found that only physical absorption occurred in non aqueous tertiary alkanolamines solutions. From the results they deduced that in non aqueous MDEA solutions neither any chemical reaction nor the alkyl carbonate formation took place between CO_2 and tertiary(alkanol)amines. Beside primary, secondary and tertiary amines, sterically hindered amines (which are usually reckoned as the fourth class of alkanolamines) have also been used by many investigators for CO_2 solubility. Sterically hindered alkanolamines have a bulky alkyl group attached to the amino group. These are reported to have good CO_2 solubility and less regeneration cost.

2.3.3. CO_2 solubility in Ionic Liquids

Ionic Liquids (ILs) have garnered considerable attention in the recent years as potential green replacement solvents for the conventional organic solvents used in many industrial operations. ILs are finding extensive applications in many industrial processes. Over the last few years many ILs have been experimentally demonstrated as effective solvents for CO_2 capture. ILs constitute an alternative solvent system for CO_2 removal. Researchers have found that ILs offer many advantages over the conventional organic solvents used for CO_2 removal (Twu et. al. 2012; Maiti 2009). ILs posses some unique properties like low melting point, negligible vapour pressure, non-volatility, non-flammability, stability at high temperature and good solvency power for both organic and in-organic substances (polar and non polar). The demerits of the traditional organic solvents and the favourable properties of the ILs make later as lucrative solvents for CO_2 capture. Typically ILs are composed of bulky cations and polyatomic anions. Since there are large numbers of cations and anions, which could be combined in a number of ways, there is virtually no limit in number of feasible ionic liquids. The estimated number of feasible ILs is of the order of 1 billion. ILs are also termed as designer solvent as by combining various cations and anions these can be tailored according to the needs for specific applications. This unique property coupled with the environmental friendly characteristics of ILs make them favourable candidate for variety of industrial applications (Kato et.al. 2004; Marsh 2004). Room temperature ionic liquids (RTILs) have been proposed as alternative or next generation CO_2 selective separation media. RTILs could be used in pressure swing configuration where CO_2 is preferentially absorbed, while CH_4 *or* N_2 and other gasses are swept away. As ILs are non volatile (due to low vapor pressure) the absorbed CO_2 could be desorbed without the loss of solvent. Such a scheme is similar to CO_2 solubility in Selexol and Rectisol. The CO_2 solubility in ILs is primarily a physical phenomenon, with no chemical reaction taking place. Ideal (single gas) CO_2 solubility in ILs at ambient temperature and at low pressures is comparable with some of the lower values for conventional organic solvents. The ideal selectivities of CO_2 solubility relative to N_2 and CH_4 in ILs is also at par with traditional organic solvents. However unlike conventional organic solvents both the solubility and selectivity of CO_2 in the ILs can readily be tuned by tailoring the structure of ILs (by combination of different cations and anions). ILs offer an unprecedented solvent range and control over solvent composition and functionality. There are many classes of ILs which have been used by many investigators for CO_2 capture. However among all the available classes (like phosphonium, ammonium, and pyridinium) imidazolium based ILs dominate the literature pertaining to CO_2 solubility. Imidazolium based ILs have shown greater CO_2 solubility compared to the other ILs (Cadena et. al. 2004; Bara et. al. 2009).

There are many factors involved for the selection of an IL for CO_2 solubility. The viscosity of the solvent used for CO_2 solubility is an important factor. It is well known that higher viscosity solvent increases the pumping cost and also viscous solvents don't exhibit greater CO_2 solubility. The ILs are generally more viscous than the conventional organic solvents. The viscosity of ILs is 2 to 3 times higher than the viscosity of common solvents. Therefore for enhanced CO_2 absorption and to reduce the operation cost less viscous ILs are preferred. It has been reported in the literature that imidazolium based ILs exhibit less viscosity than the other classes of ILs (Smith et. al. 2003; Crosthwaite et. al. 2005; Feng et. al. 2010; Alvis et. al. 2010).

The choice of the suitable cations and anions is crucial for the IL which is to be used for CO_2 solubility. It has been reported that the ILs with imidazolium cations show greater affinity for CO_2 capture. On the other hand, ILs with triflate [OTf], dicyanamide [dca], tetrafluoroborate [BF_4], bis(trifluoromethylsulfonyl)imide [Tf_2N] and tris(pentafluoroethyl)trifluorophosphate [FAP] anions exhibit higher CO_2 loadings compared to the ILs with other anions (Bara et. al. 2009).

The CO_2 absorption capacity of ILs depends on the molecular structure of these. The anion plays a vital role for the CO_2 solubility in the ILs. Blanchard et. al. (2001) studied the CO_2 solubility in six different ILs. They reported that the nature of anion dominates the CO_2 solubility in the ILs. They also found that ILs with fluorinated anions showed greater CO_2 solubility (particularly ILs with PF_6 anions). A change in anion (from [PF_6] to [BF_4]) with a ([C_8mim]) cation resulted in 8% decrease in CO_2 solubility at 40 ^oC over the studied pressure range. Cadena et. al. (2004) investigated the underlying principle of CO_2 solubility in imidazolium based ILs. They studied the CO_2 solubility data in six different ILs (formed by pairing three different anions with two cations). They also concluded that anion plays the major role in CO_2 solubility. ILs with Tf_2N showed greater CO_2 solubility as compared to ILs with BF_4 and PF_6. Aki et. al. (2004) presented the CO_2 solubility data for ten different ILs at temperature and pressure range of 25-60 ^oC and 150 bar respectively. They also reported that CO_2 absorption depends upon the nature of anion. The anions with fluoroalkyl group ([Tf_2N], [methide]) showed greater CO_2 affinity as compared to the others. They observed very marginal increase in CO_2 solubility with increase in alkyl chain length of cation. Carvalho et. al. (2009) studied the CO_2 solubility in two different ILs ([C_4mim][DCA], [C_4mim][Tf_2N]) and the results showed that [C_4mim][Tf_2N] exhibited greater CO_2 solubility than the other IL. The experimental results were correlated using Peng Robinson EOS model, which showed a fair degree of agreement with the experimental results. They concluded that it’s the anion which plays the vital role in interaction with CO_2. On the other hand, Chen et. al. (2006) experimentally measured the CO_2 solubility in the imidazolium based ILs with ([BF_4]) anion paired with different cations ([bmim], [hmim], [omim]) at temperatures (305 to 325 K) and at pressures from 1 to 9 MPa. They investigated the effect of alkyl chain length on the CO_2 loading capacity of ILs. The experimental results indicated that with increase in chain length of cation the solubility increased substantially. They further reported that with increase in temperature the solubility decreased where as for the case of pressure the trend was reverse. This observed trend is similar to the common organic solvents used for CO_2 capture. Muldoon et. al. (2007) investigated the effect of fluorination of anion and cation on the CO_2 solubility in ILs. The CO_2 solubility in different ILs was experimentally determined. The experimental results indicated that the anion fluorination resulted in enhanced CO_2 solubility. They observed that ILs with [FAP] anion showed higher CO_2 solubility in comparison to the ILs with [PF_6] and [Tf_2N] anions. The [FAP] anion is analogous to [PF_6] anion, where the replacement of three fluorine atoms with fluoroethyl group considerably increased the CO_2 solubility. On the other hand, the results indicated that the fluorination of cation did not considerably alter the CO_2 solubility in ILs. Table 2.12 shows some common ILs used for CO_2 absorption along with the operating conditions.

Table 2.12. Common Ionic Liquids (ILs) used for CO_2 absorption.

Reference	**Pressure Range**	**Temp. Range**	**Maximum CO_2 Solubility**
1-butyl-3-methylimidazolium hexafluorophosphate ([bmim][PF_6])			
Blanchard et. al. 2001	Up to 93 bar	(313.15, 323.15, 333.15) K	x_{CO2} = 0.75, at T = 313.15 K and P = 90 bar
Anthony et. al. 2002	Up to 13 bar	(283.15, 298.15, 323.15) K	x_{CO2} = 0.28at T = 283.15 K and P = 13 bar
Kamps et. al. 2003	Up to 97 bar	(293 to 393) K	x_{CO2} = 0.87at T = 313 K and P = 95 bar
Scovazzo et. al. 2004	> 1 bar	(303.15) K	x_{CO2} = 0.027 at T = 303.15 K
Aki et. al. 2004	Up to 140 bar	(298.15, 313.15) K	x_{CO2} = 0.56 at T = 298.15 K and P = 55 bar
Shariati et. al. 2005	Up to 90 bar	(280 to 380) K	x_{CO2} = 0.665at T = 350 K and P = 80 bar
1-butyl-3-methylimidazolium hexafluorophosphate ([bmim][PF_6])			
Shiflett et. al. 2005	< 20 bar	(283.15 to 348.15) K	x_{CO2} = 0.35 at T = 283.15 K and P = 20 bar
Kanakubo et. al. 2005	(40, 150) bar	298.15 K	x_{CO2} = 0.7 at T = 298.15 K and P = 150 bar
Zhang et. al. 2005	Up to 110 bar	(297 to 328) K	x_{CO2} = 0.56 at T = 297 K and P = 108 bar
Kim et. al. 2005	Up to 10 bar	298.15 K	x_{CO2} = 0.167 at T = 298.15 K and P = 9.27 bar
Urukova et. al. 2005	Up to 25 bar	(293 to 393) K	x_{CO2} = 0.32 at T = 313 K and P = 24 bar
Fu et. al. 2006	Up to 250 bar	(313.15 to 333.15)K	x_{CO2} = 0.65 at T = 313.15 K and P = 250 bar
Yokozeki et. al. 2008	Up to 19.9 bar	298 K	x_{CO2} = 0.286 at T = 298.15 K at P = 19.9 bar

Contd……

1-butyl-3-methylimidazolium tetrafluoroborate ([bmim][BF$_4$])			
Borg et. al. 2003	Approx. 1 bar	(303 to 343) K	x_{CO2} = 0.0133 at T = 303.15 K
Cadena et. al. 2004	Up to 14 bar	(283.15, 298.15, 323.15) K	x_{CO2} = 0.23 at T = 283.15 K and P = 13 bar
Aki et. al. 2004	Up to 120 bar	(298.15, 313.15, 333.15) K	x_{CO2} = 0.52 at T = 298.15 K and P = 52 bar
Kroon et. al. 2005	Up to 670 bar	(278 to 368) K	x_{CO2} = 0.6017 at T = 313.15 K and P = 365.8 bar
Shiflett et. al. 2005	< 2 bar	(283 to 348) K	x_{CO2} = 0.346 at T = 283.15 K and P = 1.98 bar
Jacquemin et. al. 2006	≥ 1 bar	(283, 343) K	x_{CO2} = 0.09 at T = 283 K
Sanchez et. al. 2007	Up to 10 bar	(298, 343) K	x_{CO2} = 0.16 at T = 298.15 K and P = 10 bar
Hou et. al. 2007	< 2 bar	(283 to 323) K	x_{CO2} = 0.32 at T = 283 K and P = 1.96 bar
Yokozeki et. al. 2008	Up to 20 bar	298 K	x_{CO2} = 0.277 at P = 20 bar
1-hexyl-3-methylimidazolium bis (trifluoromethylsulfonyl)imide ([hmim][Tf$_2$N])			
Aki et. al. 2004	Up to 120 bar	(298.15, 313.15, 333.15) K	x_{CO2} = 0.76 at T = 298.15 K and P = 120 bar
Kim et. al. 2005	Up to 8 bar	298.15 K	x_{CO2} = 0.236 at P = 8.59 bar
Kumelan et. al. 2007	Up to 100 bar	(293 to 413) K	x_{CO2} = 0.67 at T = 298.15 and P = 95 bar
Kim et. al. 2007	Up to 10 bar	298.15 K	x_{CO2} = 0.215 at P = 8.40 bar
Muldoon et. al. 2007	Up to 14 bar	(298.15, 333.15) K	x_{CO2} = 0.28 at T = 298.15 K and P = 13 bar
Shiflett et. al. 2007	Up to 20 bar	(282 to 348) K	x_{CO2} = 0.539 at T = 282.0 K and P = 19.8 bar
Yokozeki et. al. 2008	Up to 19.7 bar	298 K	x_{CO2} = 0.433 at P = 19.74 bar
Shin et. al. 2008	Up to 450 bar	(298.15 to 343.15)K	x_{CO2} = 0.8333 at T = 303.85 K and P = 204 bar
Ren et. al. 2010	Up to 250 bar	(298.15, 323.15, 343.15) K	x_{CO2} = 0.823 at T = 298.15 K and P = 140 bar

Contd…….

1-hexyl-3-methylimidazolium bis (trifluoromethylsulfonyl)imide ([hmim][Tf$_2$N])			
Raeissi et. al. 2010	Up to 240 bar	(280 to 370) K	x_{CO2} = 0.6485 at T = 278.15 K and P = 27.75 bar
Kumelan et. al. 2011	Up to 92 bar	(293 to 373) K	x_{CO2} = 0.59 bar at T = 298 K and P = 90 bar
Yazdizadeh et. al. 2011	Up to 200 bar	(303.15, 313.15) K	x_{CO2} = 0.86 at T = 303.15 K and P = 200 bar
1-hexyl-3-methylimidazolium tetrafluoroborate ([hmim][BF$_4$])			
Kim et. al. 2005	Up to 8.9 bar	298.15 K	x_{CO2} = 0.163 at P = 8.99 bar
Constantini et. al. 2005	Up to 870 bar	(293 to 368) K	x_{CO2} = 0.703 at T = 313.15 K and P = 567.4 bar
Chen et. al. 2006	Up to 90 bar	(307 to 322) K	x_{CO2} = 0.301 at T = 307 and P = 88 bar
1-hexyl-3-methylimidazolium hexafluorophosphate ([hmim][PF$_6$])			
Shariati et. al. 2005	Up to 90 bar	(280 to 380) K	x_{CO2} = 0.727 at T = 315. 15 K and 80 bar
Kim et. al. 2005	Up to 9.2 bar	298.15 K	x_{CO2} = 0.167 at P = 9.27 bar
Muldoon et. al. 2007	Up to 90 bar	(298.15, 333.15) K	x_{CO2} = 0.691 at T = 298.15 K and P = 78 MPa
1-hexyl-3-methylimidazolium tris(pentafluoroethyl) trifluorophosphate ([hmim][FAP])			
Muldoon et. al. 2007	Up to 90 bar	(298.15, 333.15) K	x_{CO2} = 0.782 at T = 298.15 K and P = 45 bar
Yokozeki et. al. 2008	Up to 19.9 bar	298 K	x_{CO2} = 0.494 at P = 19.98 bar
Zhang et. al. 2008	Up to 17.9 bar	(283, 298, 323) K	x_{CO2} = 0.361 at P = 17 bar
1-octyl-3-methylimidazolium tetrafluoroborate ([omim][BF$_4$])			
Blanchard et. al. 2001	Up to 93 bar	(313.15, 323.15, 333.15) K	x_{CO2} = 0.708 at T = 313.15 K and P = 92.90 bar
Gutkowski et. al. 2006	Up to 1000 bar	(303 to 363) K	x_{CO2} = 0.7523 at T =312.98 K and P = 676 bar
1-ethyl-3 methylimidazolium bis (trifluoromethylsulfonyl) imide ([emim][Tf$_2$N])			
Scovazzo et. al. 2004	< 1 bar	303.15 K	x_{CO2} = 0.027
Yokozeki et. al. 2008	Up to 19.9 bar	298	x_{CO2} = 0.390 at P = 19.998 MPa

The literature review on the CO_2 solubility in the ILs (Table 2.12) suggests that ILs with with BF_4, Tf_2N, PF_6, FAP anions were extensively used by many investigators for CO_2 capture. The ILs with these anions also exhibited higher CO_2 loadings in contrast to the one with other type of anions. Imidazolium based ILs with [BF_4], [Tf_2N], [FAP] anions have been selected for the present study. These were selected as; these have been extensively used by researchers for CO_2 absoroption (Table 2.12), these were found miscible with MDEA (where as ILs with other anions were not). The ILs ([hmim][BF_4], [hmim][FAP], [hmim][Tf_2N]) showed higher CO_2 loadings among their family (Table 2.13). The ILs with other cations ([emim],[bmim], [omim]) coupled with the same anions ([BF_4], [Tf_2N], [FAP]) showed lesser CO_2 loadings in comparison to the ILs having ([hmim]) cation at the same conditions of temperatures and pressures.

Table 2.13. CO_2 solubility comparison among the ILs having the same anion but different cations.

	Temp. (K)	**Pressure (MPa)**	**CO_2 solubility (x_{CO2})**	**Reference**
		ILs with [BF_4] anion		
[emim][BF_4]	298.2	6.35	0.8040	Hwang et. al. 2011
[bmim][BF_4]	298.15	5.70	0.5200	Aki et. al. 2004
[hmim][BF_4]	298.49	6.49	0.9750	Hwang et. al. 2011
[omim][BF_4]	298.15	6.29	0.9007	Hwang et. al. 2011
		ILs with [Tf_2N] anion		
[emim][Tf_2N]	298.1	1.29	0.287	Yokozeki et. al. 2008
[bmim][Tf_2N]	298.2	1.16	0.271	Aki et. al. 2004
[hmim][Tf_2N]	297.4	1.28	0.326	Yokozeki et. al. 2008
[omim][Tf_2N]	298.2	1.32	0.302	Aki et. al. 2004
		ILs with [FAP] anion		
[emim][FAP]	313	4.55	0.6	Althuluth et. al. 2012
[bmim][FAP]	N/A	N/A	N/A	N/A
[hmim][FAP]	313	4.53	0.686	Muldoon et. al. 2007
[omim][FAP]	N/A	N/A	N/A	N/A

2.4 Thermodynamic Modeling

Most of the available thermodynamic models are correlative in nature and quite a few are predictive. The experimentally obtained results are then validated by comparing these with theoretically obtained results, which are obtained by using the thermodynamic properties of the species involved in the system. The properties of the chemicals involved in the CO_2 capture help to understand the system in an elaborative way when supported and supplemented by a thermodynamic model. Each system has its own dynamics, therefore each system requires different kind of thermodynamic model to correlate its results. The thermodynamic model helps in understanding the underlying principle in a certain system as it effectively utilizes the thermodynamic properties of the species involved. Many scientists have proposed several models for the systems used for CO_2 solubility. The most widely used alkanolamine systems have been the focus of many researchers and hence abundant models are available to correlate the experimental data obtained for these systems. Many researchers proposed their indigenous models for their systems or generalized models (to cater any system within the scope) and others followed their proposed model. On the other hand, some researchers proposed models which were workable for their own systems but for other systems they did not fit. Initial attempts to model vapor-liquid equilibrium in CO_2-H_2S-amine-water system was proposed by Klyamer et. al. (1973). This model used an activity coefficient approach to the excess Gibbs free energy and was based on chemical reaction equilibrium in the liquid phase. The activity coefficients of all the species were taken equal to each other and the total ionic strength was considered by Debye Huckel limiting law. The interactions between the species were not taken into account and the activity and fugacity coefficients of free acid gases were taken as unity. This simple model was immediately followed by even more simpler approach of Kent and Eisenberg (1976). This model became popular among the practitioners due to its simple approach and better ability to correlate the solubility data. This model also takes all the activity and fugacity coefficients to unity (ideal solutions and ideal gases) and forces agreement with experimental results by regressing the reaction equilibrium constants for the amine protonation reaction and the carbamate formation reaction to give apparent equilibrium constants. The Kent-Eisenberg model has several deficiencies namely, the fit is good only in the narrow loading range (0.2 to 0.7 mol of acid gas/mol of amine), the model's performance was poor for the case of mixtures of gases. Furthermore the model was not applicable for tertiary amines because these do not form carbamate at all so no free parameters are available for fitting (Weiland et. al. 1993). Deshmukh and Mathur (1981) proposed a thermodynamic model for the solubility of acid gases (H_2S and CO_2) in the aqueous alkanolamine solutions. The model was based on extended Debye Huckel theory of electrolyte solutions. The predicted partial pressures of the acid gases over monoethanolamine solutions were in good agreement with the experimental data.

That model was later extensively used for many aqueous alkanolamine and CO_2 system and yielded fairly good results. Chen and Evan (1986) also proposed an electrolyte NRTL model to represent the acid gases solubility in aqueous alkanolamine solutions. The proposed models of Chen and Evan and Deshmukh and Mather were developed based on fundamental thermodynamic principles. Non idealities of solutions were taken into consideration by allowing long and short range interactions between the different species present in the system. The Chen and Even model used a combination of Debye Huckel theory and the electrolye–NRTL equation to calculate the activity coefficients. On the other hand, Deshmukh and Mathur model employed the Guggenheim equation to represent activity coefficients where interaction parameter are regressed to fit the experimental results. The Deshmukh model is simpler than Chen and Evan and requires less computational efforts (Benamor and Aroua 2005). Both of these models have been successfully used to correlate the data for all types of aqueous alkanolamine (pure and mixtures of amines) solutions. Ionic Liquids (ILs) are relatively new and promising solvents for CO_2 solubility. The measured experimental CO_2 solubility data in ILs have also been modeled by researchers utilizing the existing models and equations of states (EOS). Different approaches were proposed for modeling the phase behavior of IL + CO_2 systems. At the molecular level, CO_2 solubilities were predicted by using Monte Carlo simulation technique. Molecular simulations allow the elucidation of microscopic phenomena which controls macroscopic physical properties. In this technique it was shown that CO_2 occupies the cavities in the pure ILs phase. Lee (2005) and Carda-Broch et. al. (2003) used a linear salvation energy relationship in solute parameters in order to analyze the CO_2 solubility in ILs. The irregular ionic lattice model was used to correlate CO_2 solubility in ILs by Ally et. al. (2004). Scovazzo et. al. (2004) used regular solution theory for that purpose. Equations of State (EOS) have also been used successfully for the modeling of IL + CO_2 systems. Shiflett et. al. (2005) resorted to Redlich-Kwong EOS for modeling of CO_2 solubility in 1-butyl-3-methylimidazolium tetrafluoroborate ([bmim][BF_4]) and 1-butyl-3-methylimidazolium hexafluorophosphate ([bmim][PF_6]), the predicted results fairly agreed with the experimental data. On the other hand, Shariati et. al. (2003) used Peng Robinson EOS to model the fluoroform (CHF_3) solubility in 1-ethyl-3-methylimidazolium hexafluorophosphate ([emim][PF_6]), and the predicted results fairly agreed with the experimental data. The equations of state have also been used for ternary systems of ILs (IL+ another solvent + CO_2) in addition to binary system (IL + CO_2) (Kroon et. al. 2006). Lukasik et. al. (2010) successfully correlated the experimental results of ternary mixtures of different ILs (IL + 1-propanol + CO_2) by using Peng Robinson and Soave Redlich Kwong equations of the state. It was found that both the equations successfully correlated the experimental results with estimated deviations of (< 0.047) for all cases of ternary mixtures.

2.5. Summary

Based on the foregoing literature review it can be inferred that abundant physical properties data for the pure; MDEA, [hmim][BF_4], [hmim][Tf_2N] and [hmim][FAP] solvents over a wide range of temperatures have been reported by many researchers (except the n_D values for [hmim][FAP], which were not found in the literature). On the other hand, the physical properties data pertaining to the mixtures of these ILs with other molecular solvents is very limited. The CO_2 removal by using conventional alkanolamines solvents and promising alternative green solvents (ionic liquids) has been reported by many researchers. The literature pertaining to the usage of IL+amine solvents for CO_2 removal suggest that only a limited number of IL+amine solutions have been used for CO_2 absorption and there is a plenty of room available in this field. The usage of the mixtures of the ionic liquids namely; [hmim][BF_4], [hmim][Tf_2N] and [hmim][FAP] with other solvents (especially alkanolamines) for CO_2 absorption has not been reported in the literature. These ILs were experimentally found to be miscible with alkanolamine solvents like MDEA (which is prominent among the alkanolamine due to its unique properties such as low vapor pressure and less energy requirements for regeneration *etc.*).

CHAPTER 3

MATERIALS AND METHODS

3.0 Overview

This chapter describes the details of the materials, apparatus, experimental setup, and the experimental methods/methodology used in the present study. The details of the materials used are presented in section 3.1. The preparations of binary and ternary mixtures and the experimental details for the measurement of thermophysical properties namely, density, viscosity, refractive index, thermogravimetric analysis (TGA) are presented in section 3.2. The details pertaining to the CO_2 solubility experiments have been discussed in the sections 3.3 and 3.4.

3.1 Materials

In the present study eight imidazolium based ionic liquids (ILs) and one hydroxyl ammonium based IL were used. The imidazolium based ILs used are: 1-hexyl-3-methylimidazolium tetrafluoroborate ([hmim][BF_4]), 1-hexyl-3-methylimidazolium bis(trifluromethylsulfonyl)imide ([hmim][Tf_2N]), 1-hexyl-3-methylimidazolium tris(pentafluoroethyl) triflurophosphate ([hmim][FAP]), 1-butyl-3-methylimidazolium tetrafluoroborate ([bmim][BF_4]), 1-butyl-3-methylimidazolium tris(pentafluoroethyl)trifluorophosphate ([bmim][FAP]), 1-butyl-3-methylimidazolium bis(trifluoromethylsulfonyl)imide ([bmim][Tf_2N]), 1-ethyl-3-methylimidazolium tris(pentafluoroethyl)trifluorophosphate ([emim][FAP]), 1-ethyl-3-methylimidazolium bis(trifluoromethylsulfonyl)imide ([emim][Tf_2N]). The hydroxyl ammonium based IL was bis(2-hydroxyethyl)ammonium acetate ([bheaa]). The alkanolamine used are *N*-methyldiethanolamine (MDEA), monoethanolamine

(MEA) and diethanolamine (DEA). The details of the materials, supplier information, purities of the chemicals have been stated in this section. Furthermore the purification of chemicals, estimation of impurities and the preparations of the samples (binary and ternary mixtures) have also been described in this section. The structures of the ILs ([hmim][BF_4], [hmim][Tf_2N], [hmim][FAP], [bheaa]) and MDEA are shown in Figure. 3.1.

3.1.1 Ionic Liquids

The ionic liquids used in this present study namely 1-hexyl-3-methylimidazolium tetrafluoroborate ([hmim][BF_4]), 1-hexyl-3-methylimidazolium bis(trifluormethylsulfonyl)imide ([hmim][Tf_2N]), 1-hexyl-3-methylimidazolium tris(pentafluroethyl) trifluorphosphate ([hmim][FAP]), 1-butyl-3-methylimidazolium tetrafluoroborate ([bmim][BF_4]), 1-butyl-3-methylimidazolium tris(pentafluoroethyl)trifluorophosphate ([bmim][FAP]), 1-butyl-3-methylimidazolium bis(trifluoromethylsulfonyl)imide ([bmim][Tf_2N]), 1-ethyl-3-methylimidazolium tris(pentafluoroethyl)trifluorophosphate ([emim][FAP]) and 1-ethyl-3-methylimidazolium bis(trifluoromethylsulfonyl)imide ([emim][Tf_2N]) were purchased from Merck Chemicals Sdn. Bhd. Malaysia with a stated purity of > 99 % (determined by HPLC). The IL bis(2-hydroxyethyl)ammonium acetate ([bheaa]) was generously provided by the Petronas Ionic Liquid Centre, Universiti Teknologi PETRONAS with a stated purity of > 99 %. The ILs were dried under vacuum at 353.15 K for 48 hrs to remove any possible traces of water and impurities. The water content of dried ILs was determined by using Karl Fischer coulometric titrator (Mettler Toledo DL-39) with hydranal-coulomat AG (Riedel-de-Haen) reagent. The estimated water contents for [hmim][Tf_2N], [hmim][BF_4], [hmim][FAP], [bmim][BF_4], [bmim][FAP], [bmim][Tf_2N], [emim][Tf_2N], [emim][FAP], [bheaa] were 230ppm, 280ppm, 289ppm, 272ppm, 287ppm, 267ppm, 287ppm, 245ppm, 259ppm respectively. The chloride contents of all the ILs used were determined by using DL-55 autotitrator (Mettler Toledo) with 0.005 M $AgNO_3$ as the titrant. The estimated chloride content for [hmim][Tf_2N], [hmim][BF_4], [hmim][FAP], [bmim][BF_4], [bmim][FAP], [bmim][Tf_2N], [emim][Tf_2N], [emim][FAP], [bheaa] were 39ppm, 30ppm, 36ppm, 38ppm, 36ppm, 32ppm, 33ppm, 37ppm and 35ppm

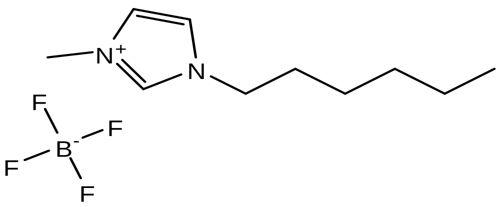

1-hexyl-3-methylimidazolium tetrafluoroborate

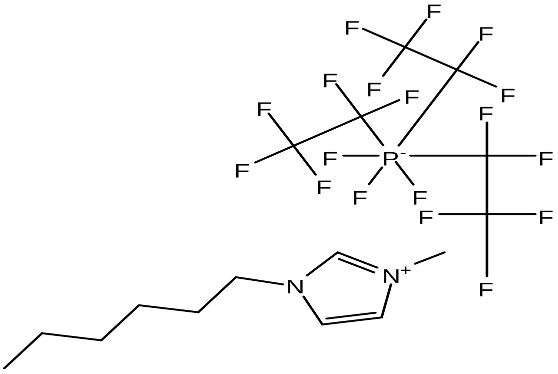

1-hexyl-3-methylimidazolium tris(pentafluoroethyl)trifluorophosphate

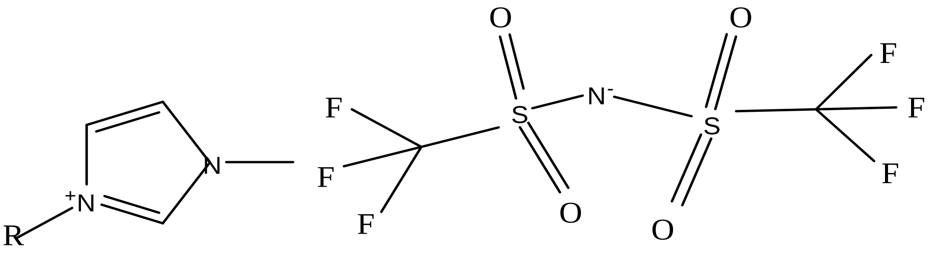

1-hexyl-3-methylimidazolium bis(trifluoroborate)imide

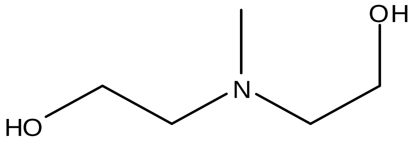

Methyldiethanolamine

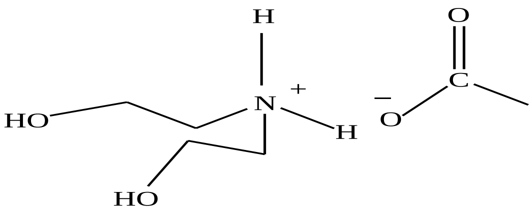

Bis(2-hydroxyethyl)ammonium acetate

Figure 3.1. Structures of the ILs ([hmim][BF_4],[hmim][Tf_2N],[hmim][FAP], [bheaa]) and MDEA.

respectively. All the measurements were made in triplicate and the values are reported as an average with an accuracy of ± 5%.

3.1.2 Alkanolamines

The alkanolamines namely *N*-methyldiethanolamine (MDEA), monoethanolamine (MEA), diethanolamine (DEA) used in this study were obtained from Merck Chemicals Sdn. Bhd. Malaysia with a stated purity of > 99.5% (GC, area %). The alkanolamines were used as received. The water content of MDEA, MEA, DEA, used in this study was determined by Karl Fischer titrator (Mettler-Toledo, DL-39) using hydranol-coulomat E (Riedel-de-Haen) reagent with benzoic acid (90 mL anolyte + 5 g benzoic acid) as standard procedure described for amines in Mettler-Toledo (DL-39) operating manual. The estimated water contents for MEA, DEA, MDEA were 2861ppm, 2790ppm and 2756ppm respectively.

3.1.3 Gasses

Purified gases which have been used in this study namely carbon dioxide (CO_2) and nitrogen (N_2) were purchased from Malaysian Oxygen Berhad. The carbon dioxide used was supplied with a stated purity of > 99.9 % and other contents included moisture < 10vpm and hydrocarbons < 1vpm. The nitrogen (N_2) used in the present study was supplied with a stated purity of >99.999%.

3.2 Methods

This section includes: i) the preparation of the binary and ternary mixtures, ii) steps involved and description of apparatus used for measuring thermophysical properties of solvents.

3.2.1 Preparation of Binary Mixtures

All the binary mixtures were freshly prepared and retained at room temperature for 24hrs to ensure complete miscibility. The binary mixtures thus prepared were kept in glass vials with PTFE septum. The samples were prepared on mass basis by using an analytical balance (Mettler Toledo, model AS 120S) and later converted to mole fractions. The estimated uncertainty in the mole fraction prepared was around ± 0.001. The binary mixtures used in the present study included ([hmim][Tf_2N]+MDEA), ([hmim][BF_4]+MDEA), ([hmim][FAP]+MDEA), ([bheaa] + MDEA), ([bmim][BF_4]+MDEA), ([bmim][FAP]+MDEA), ([bmim][Tf_2N]+MDEA). The range of the mole fraction prepared varies from 0.1 to 0.9 for the

[hmim][BF_4]+MDEA, [hmim][Tf_2N]+MDEA and [hmim][FAP]+MDEA binary systems. The mole fractions prepared for the binary mixtures [bheaa]+MDEA, [bmim][BF_4]+MDEA, [bmim][FAP]+MDEA, [bmim][Tf_2N]+MDEA were 0.2, 0.5 and 0.8. The physical properties namely density, viscosity and refractive index measurements were made for pure liquids namely; MDEA, [hmim][BF_4], [hmim][Tf_2N], [hmim][FAP] as well as for the full range of the mole fractions (0.1 to 0.9) of their binary mixtures ([hmim][Tf_2N]+MDEA), ([hmim][BF_4]+MDEA), ([hmim][FAP]+MDEA). The TGA analysis was also performed for these pure liquids as well as their binary mixtures (0.2, 0.5, 0.8 mole fractions). CO_2 solubility measurements were made for all the pure liquids and mole fractions (0.2, 0.5, 0.8) of all the binary mixtures prepared. The molar fractions 0.2, 0.5 and 0.8 are (1:4), (1:1), (4:1) molar ratios of each IL to amine respectively.

3.2.2 Preparation of Ternary Mixtures

The acqueous IL mixtures with monoethanolamine (MEA) or (DEA) were prepared on mass basis. Doubled distilled deionized water was used to prepare the mixtures. The detail of the ternary mixtures prepared is listed in Table 3.1.

Table 3.1. Detail of the acqueous IL mixtures prepared.

([emim][FAP] *or* [emim][Tf_2N])(wt%)	MEA(wt%)	Water(wt%)
5%	15%	80%
10%	15%	75%
15%	15%	70%
	DEA	
5%	25%	70%
10%	25%	65%
15%	25%	60%

3.2.3 Density

The densities of pure liquids as well as their binary mixtures were measured by using Anton Paar density meter (model DMA-5000) at temperatures (298.15 to 323.15) K with an uncertainty of 0.01 K. The density meter contains a U shaped oscillating tube made of borosilicate. The U-tube cell (the sample container) is encompassed by a thermostated jacket. The density meter is based on the principle of oscillations (the U tube oscillates). The viscosity of the sample influences its density by damping effect. The errors in the measurements caused by this damping effect are automatically offsetted by the software of the density meter. The density meter was precise within $\pm$ 1×10^{-5} g.cm^{-3}. The overall uncertainty of all the measurements was better than $\pm$ 3×10^{-5} g.cm^{-3}. The density meter was calibrated frequently by measuring the density of Millipore water and dry air as per instructions of the supplier. The calibrated meter was validated by using pure solvents of known/established density. Samples were taken out from the vials with the help of syringe and a defined volume (approx 2mL) was injected into the density meter. The inserted sample was viewed carefully so as to ensure that there were no air bubbles inside it. All the density measurements were made in triplicate and the average values were considered for further analysis.

3.2.4 Viscosity

The viscosities of the pure liquids as well as their binary mixtures were measured by using Brookfield cone and plate type (CAP 2000, L-series) viscometer at temperatures (298.15 to 323.15) K with a temperature control accuracy of 0.02 K. The viscometer was calibrated according to the procedure provided by the supplier by using the standard solutions. The calibrated viscometer was validated by using many pure organic and ionic liquids of known/established viscosity. The viscometer was placed in a dry atmosphere to avoid humid effects of atmosphere. The samples were taken out of the glass vials with the help of syringe and placed on the viscometer plate, the cone was closed immediately to avoid humidity effects. All the viscosity measurements for samples were performed at a rotational speed of 900 rpm. Different cones (from 1 to 4) were used for different viscosity range (20 to 1667) mPa.s. All the measurements were made in triplicate and the average values were taken for further consideration. The estimated uncertainty of the measured viscosity values was better than 3%.

3.2.5 Refractive Index

The refractive indices of the pure liquids as well as their binary mixtures were measured by using digital refractometer (ATAGO model RX-5000) at temperatures (298.15 to 323.15) K with a temperature control accuracy of 0.05 K. The overall accuracy of the measured values was better than ± 4×10^{-5}. The apparatus was calibrated frequently by using Millipore water and the calibrated meter was validated by using several pure organic and ionic liquids of known/established refractive indices. All the refractive index measurements were performed in triplicate and the average have been considered for further analysis.

3.2.6 TGA (Thermogravimetric Analysis)

The thermal stability of the pure liquids as well as their binary mixtures (for 0.2, 0.5, 0.8 mole fractions) was determined by thermogravimetric analysis (TGA). Thermogravimetric analysis (TGA) was performed using Perkin-Elmer (Model STA 6000) under nitrogen atmosphere. The TGA thermograms were recorded for 5mg of sample at a heating rate of 10 ^{o}C min^{-1} in the temperature range of 30-800 ^{o}C. The weight loss with respect to temperature increase was recorded accordingly.

3.3 Carbon Dioxide Solubility Measurement

The solubility of carbon dioxide in solvents was measured by using a high pressure solubility cell. The SOLTEQ (Model BP 22) high pressure solubility cell has been used in this study to carry out the solubility experiments. The schematic diagram of the apparatus is shown in Figure 3.2. The major components of SOLTEQ high pressure solubility cell include the storage vessel for gas and the absorption cell. The storage vessel and absorption cells were jacketed for maintaining the temperature at a desired value. A water circulation system (JULABO thermostatic bath) was used to maintain the temperature within ± 0.1 K by circulating water through the jackets. The air driven gas booster pump (Haskel, model AG 15) was used to send in the gas to storage vessel and to build a desired pressure in it. The absorption cell was connected with storage vessel, from which the gas at desired pressure was transferred into the absorption cell. The gas evacuation system was attached with the absorption cell which establishes vacuum in the absorption cell prior to the dosing of sample. The evacuation system consists of turbo molecular vacuum pump (Pfeiffer, model TSH 071 E). The reciprocating metering pump (Eldex Laboratories Inc. USA) was used to pump in the sample in the absorption cell. Before each experiment the absorption cell was cleaned by using solvents like methanol *etc*. and after that the cell was purged with N_2 gas to make it dry and ready for the desired experiment. The N_2 present thereafter was evacuated by turbo vacuum pump.

3.4 Procedure to Measure CO_2 Solubility in Solvents

The CO_2 solubilities in pure liquids as well as their binary mixtures were measured by using SOLTEQ high pressure solubility cell. The principle for the measurement of solubility is the pressure drop method. In this method the solvent in which the desired gas is to be absorbed are kept in a closed vessel. The initial pressure of the gas is recorded. As the gas begins to dissolve/absorb in the solvent the pressure of the gas reduces. The reduction in the pressure is recorded at different time intervals and after certain time (it can vary from solvent to solvent) the pressure of the gas no longer reduces and become constant indicating the equilibrium. This is the point where no further absorption of the gas takes place in the solvent. The volume of the solvents was kept constant where as the pressure drop in the absorption cell was monitored during the process of absorption. Pressure drop method is a synthetic technique and widely practiced for CO_2 absorption. It is also known as isochoric method of absorption. The volume of the solvent is kept constant and the pressure drop is

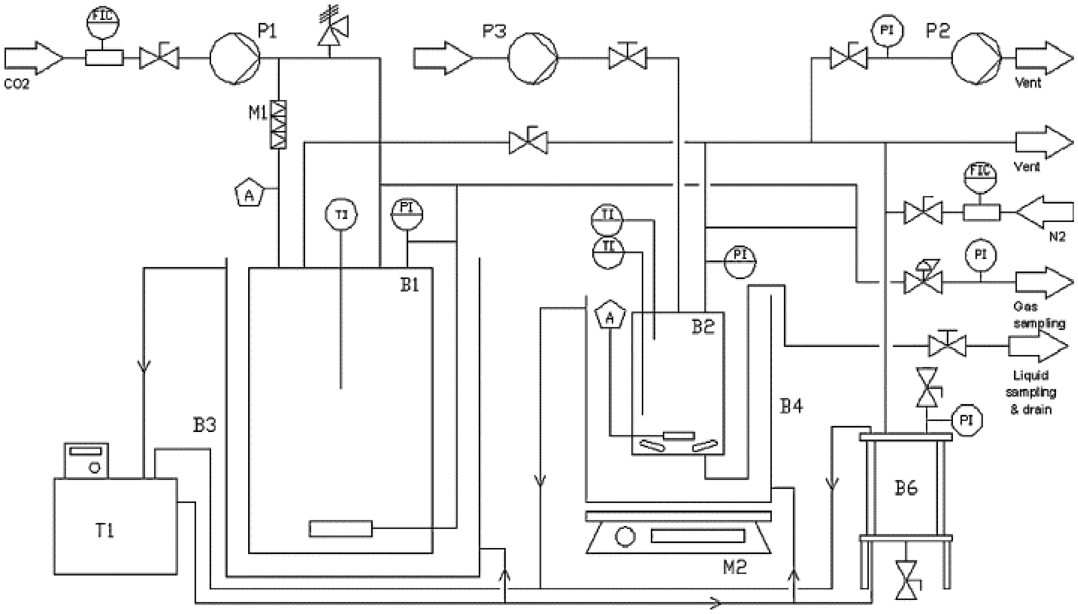

Figure. 3.2. Schematic diagram of SOLTEQ-BP22 high pressure solubility cell used in the present study. B1, mixing cell; B2, equilibrium cell; B3, heating jacket for B1; B4, heating jacket for B2; B6, liquid degassing unit; M1, static mixer; M2, magnetic stirrer; T1, thermostat heating bath; P1, gas booster; P2, vacuum pump; P3, liquid pump.

monitored. The solvent like ILs have negligible vapor pressure, therefore the assumption could be made that the gaseous phase remains pure. Pressure drop method has been successfully employed by many researchers (Dawodu et. al. 1994; Karnov et. al. 1996; Mathonat et. al. 1997; Rho et. al. 1997) to accurately report CO_2 solubility in a variety of solvents over wide ranges of temperatures and pressures. Pressure drop method is simple, precise, and requires less computational effort to report accurate absorption. The other methods (e.g. gravimetric sorption method, which measures the solubility by measuring the mass gain in the solvent) require more parameters (e.g. density of gas, buoyancy effect on sample and dilation of the sample with blowing agent uptake) to accurately estimate solubility (Aionicesei et. al. 2008; Mahmood 2012). Therefore in the present study pressure drop method has been selected to measure CO_2 solubility. The experiments on solubility measurements were carried out by following the steps described below:

1. Prior to the start of the experiment, the absorption cell was cleaned by using solvent (methanol *or* acetone) to remove any residues of previous sample or any contaminations present in it. The cleaning solvent was pumped in by the metering pump and after some time it was drained out. The procedure was repeated several times to ensure that all the contaminants have been removed. The absorption cell was then purged with pure N_2 for 20 minutes to clean and dry the cell. The dried equilibrium/absorption cell was evacuated by vacuum pump to attain the desired level of vacuum (< 5 kPa). The gas storage/mixing vessel was purged with pure N_2 to ensure that all the previous feed gases or mixtures of gasses have been removed. After that the mixing vessel was evacuated by using vacuum pump and the same level of vacuum was achieved as was in absorption cell.
2. The CO_2 gas supply was opened from the cylinder. The air driven gas booster pump was turned on and the gas started to fill in the mixing vessel (3 Litre capacity). The gas booster pump helps to build up the pressure of gas in the mixing vessel. As the desired pressure (different in each set of experiments ranging from 300kPa to 6000kPa) was attained in mixing vessel the gas booster pump was turned off. Digital pressure transducers (Druck, DPI-150)

displayed the pressure inside the mixing vessel and absorption cell with an accuracy of + 0.01 bar.

3. A desired temperature was set (298.15, 313.15, 323.15 K) by circulating water through the Jackets by using the water circulation system (JULABO thermostatic bath). The temperature of the mixing vessel and absorption cell was measured with the help of digital thermometers (YOKOGAWA 7653) with an accuracy of ± 0.01 K.
4. Once the desired temperature was attained then a known/weighed amount of solvent (Approx 5mL in volume) was dosed inside the absorption cell (50mL capacity) with the help of reciprocating metering pump. The pressure inside the absorption cell was noted.
5. The CO_2 gas was transferred from the mixing vessel to the absorption cell. The pressure of mixing vessel before and after gas transfer was recorded. After gas transfer the initial pressure of the gas in the absorption/equilibrium cell was recorded. The magnetic stirrer (inside the mixing vessel) was turned on to enhance the contact between the two phases resulting in efficient solubility of gas in the solvent.
6. The pressure inside the absorption cell start to decrease as the CO_2 started to dissolve in the liquid sample. The pressure drop inside the absorption cell was recorded for every minute by auto logging LABVIEW software installed in the computer/data logging system.
7. The pressure inside the absorption cell continued to decrease until it reached a steady state. After this point there was no such pressure decrease in the absorption cell. This constant value of pressure was retained for at least 2 hrs, after that time the equilibrium was assumed and the final values were recorded. In the case of samples studied in this present study the time taken to reach equilibrium was 20-30 hrs, depending on the nature of solvents used.
8. After that the sample was withdrawn from the equilibrium cell.
9. It is noteworthy to mention that before starting the experiments using the present samples, the solubility measurements were validated by conducting the CO_2 solubility experiments in pure solvents and aqueous solvents with established/known solubilities.

The amount of CO_2 absorbed in the liquid samples was calculated by using the following set of equations (Park and Sandal 2005)

The amount (moles) of CO_2 transferred from the mixing vessel to the absorption cell was calculated by using the equation:

$$n_{CO_2} = \frac{V_T}{RT}\left(\frac{P_1}{z_1} - \frac{P_2}{z_2}\right) \tag{3.1}$$

where V_T is the volume of the mixing vessel and z_1 and z_2 are the compressibility factors corresponding to the initial (P_1) and final (P_2) pressure of the mixing vessel before and after transferring CO_2 and T is the temperature of the mixing vessel.

The equilibrium pressure was calculated by using the equation:

$$Pco_2 = P_T - P_v \tag{3.2}$$

where P_T denotes the total pressure (equilibrium pressure), P_v represents the vapor pressure of the liquid samples which can be neglected in the case of pure IL and amine and subsequently of their mixtures also as pure ILs and MDEA exist under negligible vapor pressure for the studied temperature range (Kuranov et. al. 1996; Blanchard et. al. 2001; Kamps et. al. 2003). The moles of the remaining (unabsorbed) CO_2 in the gas phase were calculated by using the following equation:

$$n^g co_2 = \frac{V_g P_{CO2}}{z_{CO2} RT} \tag{3.3}$$

where V_g is the gas-phase volume of the equilibrium cell, z_{CO2} is the compressibility factor at P_{CO2}, T is the temperature inside the cell.

The moles of the CO_2 dissolved in the liquid phase were then determined by using the equation:

$$n^1_{CO2} = n_{CO2} - n^g_{CO2} \tag{3.4}$$

The CO_2 absorbed was expressed in terms of molar fraction by using Eq. 3.5 (for the case of pure liquids), Eq. 3.6 (for the case of binary mixtures) and Eq. 3.7 (for the case of ternary mixtures)

$$x_{CO2} = \frac{n^1_{CO2}}{n_{liq} + n^1_{CO2}} \tag{3.5}$$

$$x_{CO2} = \frac{n^1_{CO2}}{n_{IL} + n_{MDEA} + n^1_{CO2}} \tag{3.6}$$

$$x_{CO2} = \frac{n^1_{CO2}}{n_{IL} + n_{amine} + n^1_{CO2} + n_{water}} \tag{3.7}$$

The compressibility factors were calculated by using several equations of state (EOS) including van der Waals, Redlich Kwong (RK), Soave Redlich Kwong (SRK), Peng Robinson (PR). A computer program written by chemSOF was used for this study to estimate compressibility factors by using different EOS.

CHAPTER 4

RESULTS AND DISCUSSIONS

4.0. Introduction

The aim of the present study is to systematically study the potential use of hybrid solvents (comprising of IL and amine) for CO_2 absorption. The targeted ILs were mixed with MDEA solvent. These hybrid mixtures were then used for CO_2 absorption. Prior to use these hybrid solvents for absorption, their basic physical properties were established. The knowledge of basic thermophysical properties like densities (ρ), viscosities (η), refractive indices (n_D) and thermal stability (TGA) of the solvents used in gas absorption processes is essential for the engineering design and scaling up of gas treating units (Huddleston et. al. 2001). These properties are important tools for the estimation of transfer coefficients (Schmidt number *etc.*) velocities and pressure drop and hence for the design and scale up of the process. These properties are further used to derive the excess and deviation properties of the mixtures like; excess molar volumes (V^E), viscosity deviations ($\Delta\eta$) and refractive index deviations (Δn_D). A study on these excess thermodynamic properties are of considerable interest as they help in understanding the intermolecular interactions in the liquids mixtures. The pure liquids used in the present study were namely; 1-hexyl-3-methylimidazolium tetrafluoroborate ([hmim][BF_4]), 1-hexyl-3-methylimidazolium bis(trifluormethylsulfonyl)imide ([hmim][Tf_2N]), 1-hexyl-3-methylimidazolium tris(pentafluroethyl) trifluorphosphate ([hmim][FAP]), 1-butyl-3-methylimidazolium tetrafluoroborate ([bmim][BF_4]), 1-butyl-3-methylimidazolium tris(pentafluoroethyl)trifluorophosphate ([bmim][FAP]), 1-butyl-3-methylimidazolium bis(trifluoromethylsulfonyl)imide ([bmim][Tf_2N]), 1-ethyl-3-

methylimidazolium tris(pentafluoroethyl)trifluorophosphate ([emim][FAP]), 1-ethyl-3-methylimidazolium bis(trifluoromethylsulfonyl)imide ([emim][Tf_2N]), bis(2-hydroxyethyl)ammonium acetate ([bheaa]), monoethanolamine (MEA), diethanolamine (DEA) and methyldiethanolamine (MDEA). Thermophysical properties estimations and TGA analysis were performed for pure solvents: [hmim][FAP], [hmim][BF_4], [hmim][FAP], MDEA and their binary mixtures. CO_2 absorsption were also initially measured in these pure solvents and their binary mixtures. The measured thermophysical properties of the solvents are presented in Appendix A and B. The details pertaining to the effects of temperature, concentration on the physical properties along with the deduced excess and deviation properties are discussed in this chapter. This chapter also presents the data on the CO_2 solubility data in the pure liquids as well as in their respective hybrid mixture. The effects of temperatures, pressures, concentrations and anions on the CO_2 solubility in the pure as well as in the binary mixtures have been discussed in detail. The estimated Henry's constant and the evaluated entropy and enthalpy changes have also been discussed in this chapter. The thermodynamic models used to correlate the experimental CO_2 solubility data has also been presented and discussed in this chapter.

4.1 Density

The densities of pure liquids as well as their binary mixtures were measured by using Anton Paar density meter (model DMA-5000) at temperatures (298.15 to 323.15) K. The detailed description for the measurement of densities is described in section 3.2.2. of chapter 3. The measured densities of the pure liquids used in the present study are illustrated in Figure 4.1. It can be seen from the Figure 4.1 that among the pure chemicals MDEA has least density where as [hmim][FAP] has highest, indicating that the MDEA molecule is lighter than the other pure chemicals. All the ILs showed higher density values than MDEA. The IL [hmim][BF_4] showed 1.104 times higher density values than MDEA, where as [hmim][Tf_2N] and [hmim][FAP] respectively showed 1.321 and 1.492 times higher density values than MDEA. The pure ILs in terms of density could be arranged as; [hmim][FAP]>[hmim][Tf_2N]>[hmim][BF_4]. The density of IL increased as the molar mass of anion increased. This observed behaviour of ILs is in accordance with the trend reported in the open literature (Muhammad et. al. 2008; Jacquemin et. al. 2008). Huddleston *et. al.* (2001) reported

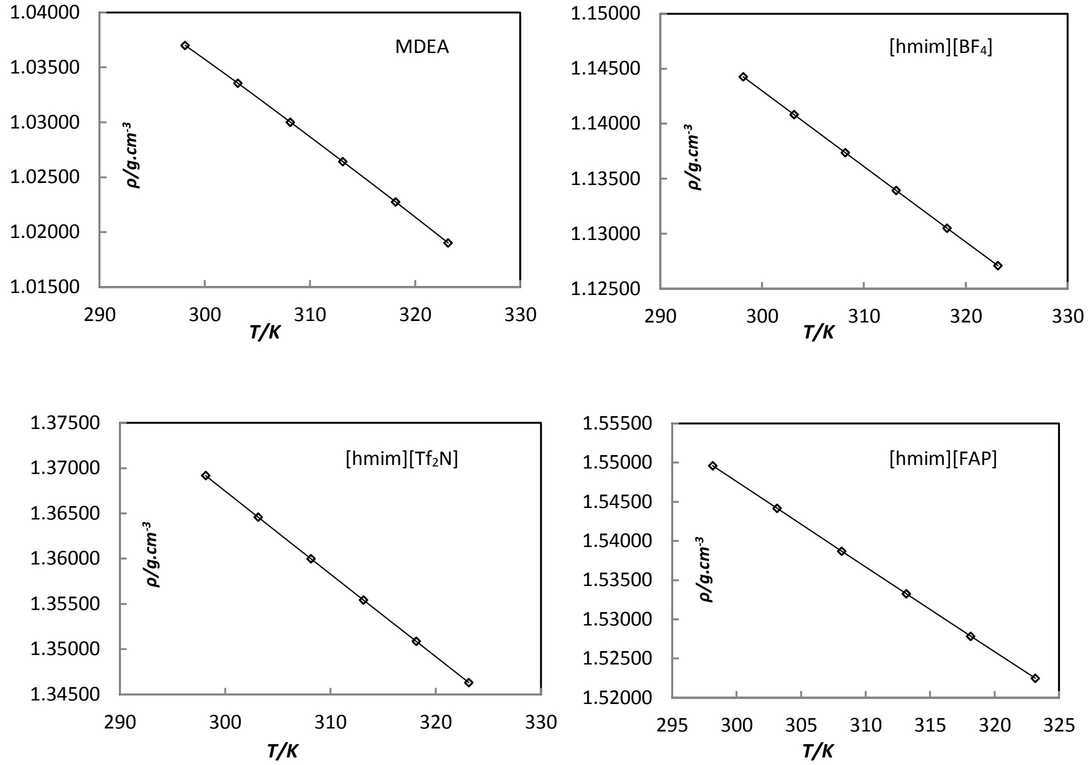

Figure 4.1. Plot of experimental densities for the pure liquids [hmim][BF$_4$],[hmim][Tf$_2$N],[hmim][FAP], MDEA against temperatures.

the density of several ILs having the same cation ([bmim]) paired with different anions and concluded that the density of ILs increased as the molar mass of anion increased. Similarly Fredlake et. al. (2004) observed the same behaviour when they measured the density of different ILs; that density of the given ILs (having same cation paired with different anions) increased as the molar mass of anion increased. The comparisons of the measured density values for the pure liquids with the reported literature values for those are illustrated in Figures 4.2 to 4.5. The measured density values for pure MDEA showed a fair agreement (calculated deviation ≤ 0.12) with the reported literature density values over the entire temperature range (Figure 4.2). The measured density values of pure [hmim][BF$_4$] (Figure 4.3), [hmim][Tf$_2$N] (Figure 4.4) and [hmim][FAP](Figure 4.5) also showed satisfactory agreement with the reported literatures value. The calculated deviations were < 0.21% for [hmim][BF$_4$]), < 0.30 % for [hmim][Tf$_2$N] and ≤ 0.2 % for [hmim][FAP]. The minor differences in the measured density values for pure ILs could be attributed to the difference in water content and halide contents of the sample. The density of ILs is greatly affected by

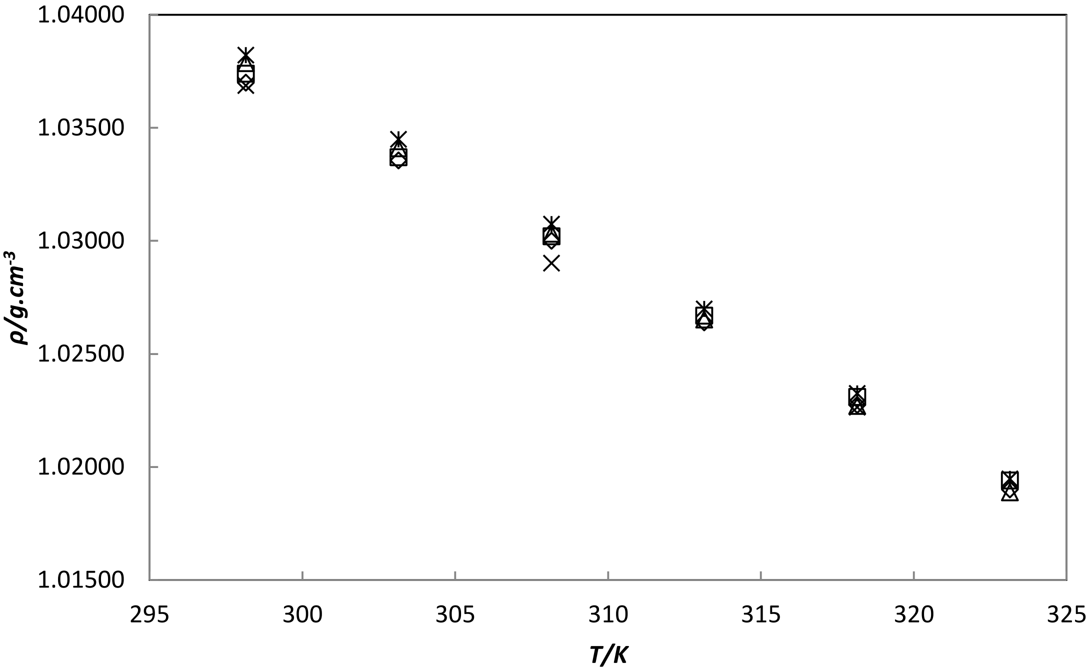

Figure 4.2. Comparison of the experimental density data for pure MDEA with literature: ◊, this work; □, Al-Ghawas et. al. (1989); ×, Maham et. al. (1995); Δ, Bernal-Garcia et. al. (2003); *, Muhammad et. al. (2008).

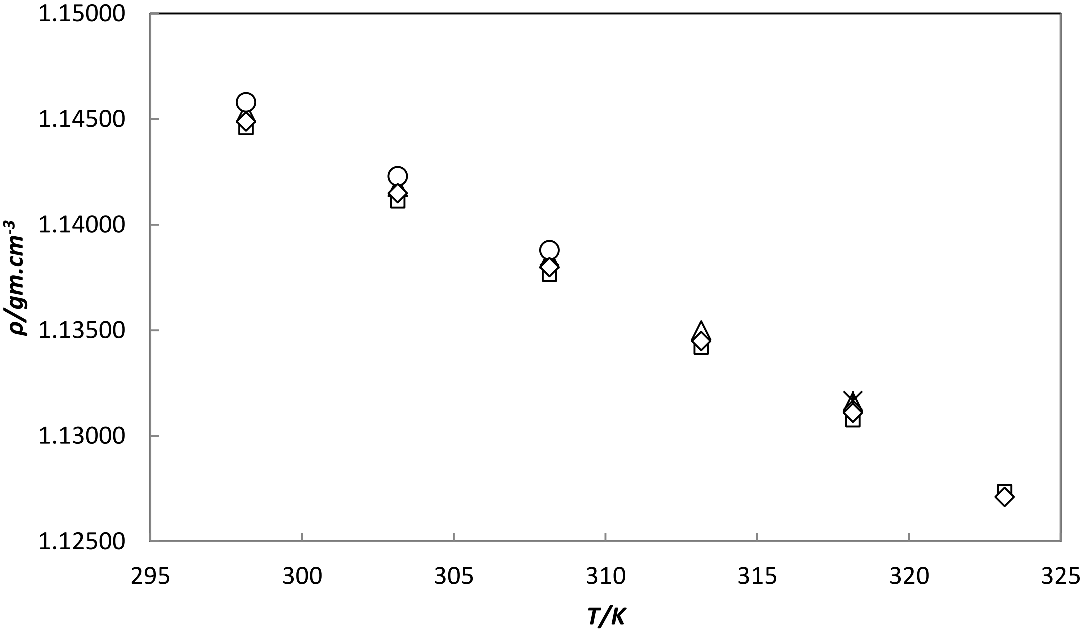

Figure 4.3. Comparison of the experimental density data for pure [hmim][BF_4] with literature: ◊, this work; □, Vakili-Nezhaad et. al. 2012; Δ, Garcia-Miaja et. al. 2009; *, Muhammad et. al. 2008; ○, Navia et. al. 2007.

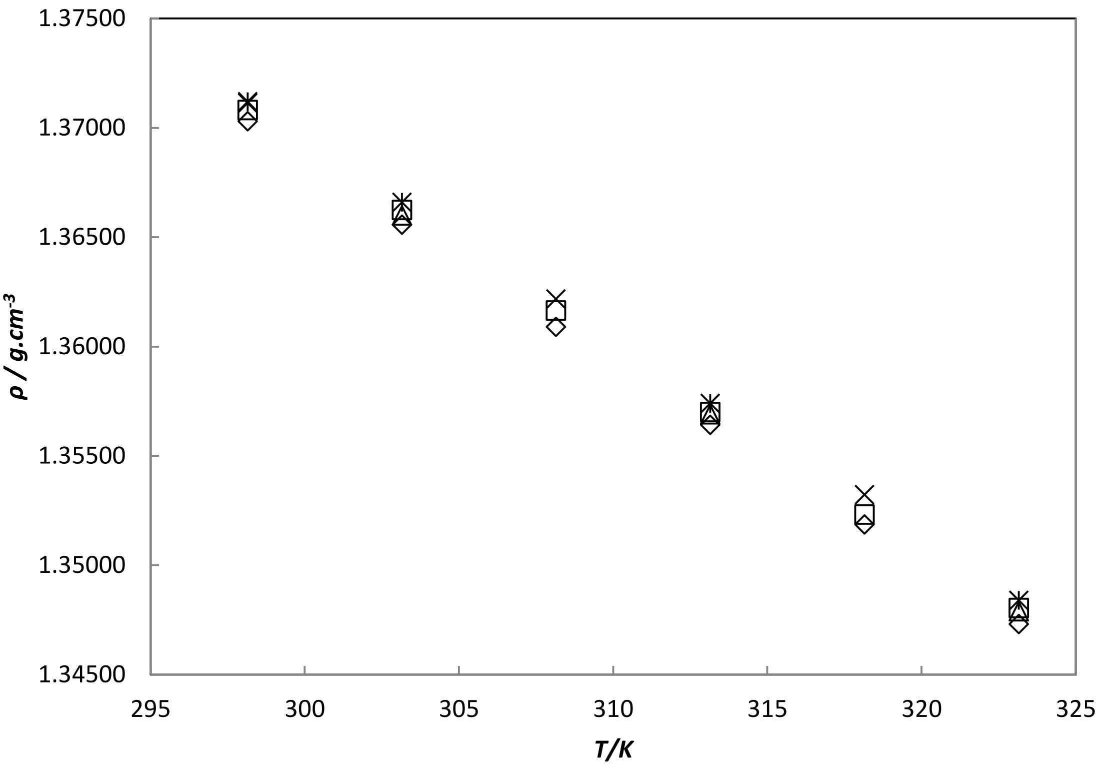

Figure 4.4. Comparison of the experimental density data for pure [hmim][Tf_2N] with literature: ◊, this work; □, Azevedo et. al. 2005; *, Widegren et. al. 2007; Δ, Jacquemin et. al. 2008; ×, Muhammad et. al. 2008.

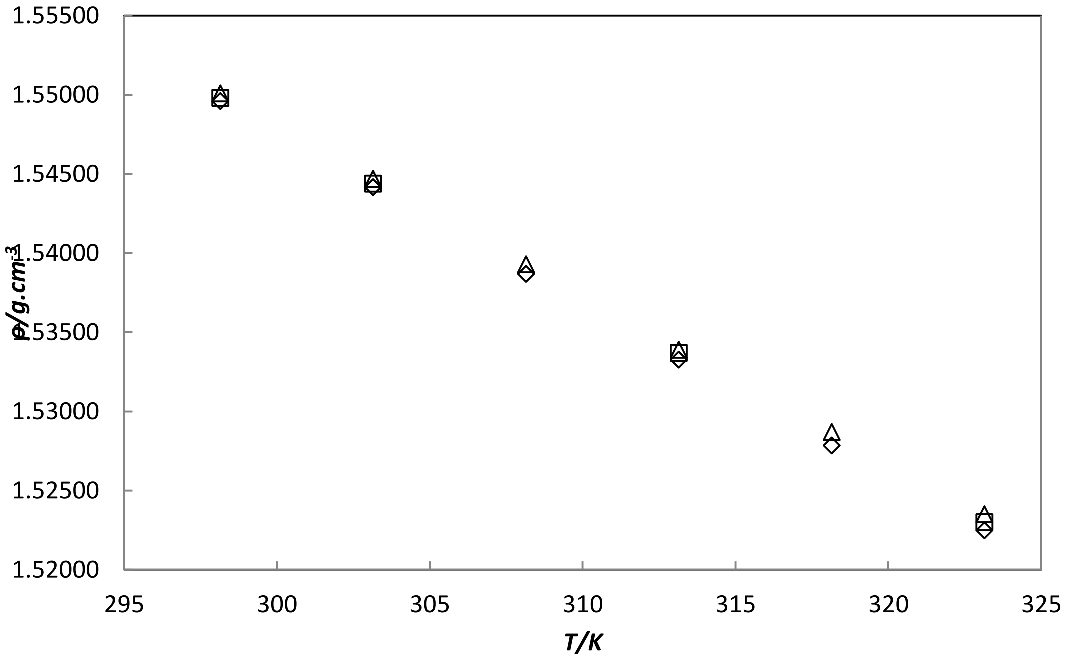

Figure 4.5. Comparison of the experimental density data for pure [hmim][FAP] with literature: ◊, this work; □, Jacquemin et. al. 2008; Δ, Guang Li et. al. 2011.

these factors. The experimental water contents for [hmim][Tf_2N], [hmim][BF_4] and [hmim][FAP] were 230, 280, 289 ppm and chloride contents were 39, 30 and 36 ppm respectively. Seddon et. al. (2000) carried out systematic study to probe the effect of impurities and additives (*e.g.* water and chloride contents) on the physical properties of ionic liquids and confirmed that these impurities remarkably altered the physical properties of ILs. The reported results indicated that the presence of high amount of chloride and water content decreased the density of the ILs. The density of all the pure liquids decreased linearly (Figure 4.1) with increase in temperature as expected. The measured density values for the pure liquids as well as their binary mixtures are listed in Table A-1 to A-3 of the Appendix A.

4.1.1. Binary Mixtures

[hmim][BF_4] + MDEA System

The measured density values for the binary system [hmim][BF_4]+MDEA are illustrated in Figure 4.6. From the analysis of data it was found that by increasing the mole fraction of [hmim][BF_4] in the mixtures density values increased. Similar trends were also observed by Zhu et. al. (2011), who reported the density values for the binary mixtures of [hmim][BF_4] with different organic solvents (butanone, butylamine, ethyl acetate and tetrahedrofuran). They observed that in the binary mixtures as the mole fraction of [hmim][BF_4] increased the density values increased significantly. Similarly Kermanpour et. al. (2012) also reported a similar trend for the binary mixtures of [hmim][BF_4] with 1-propanol.

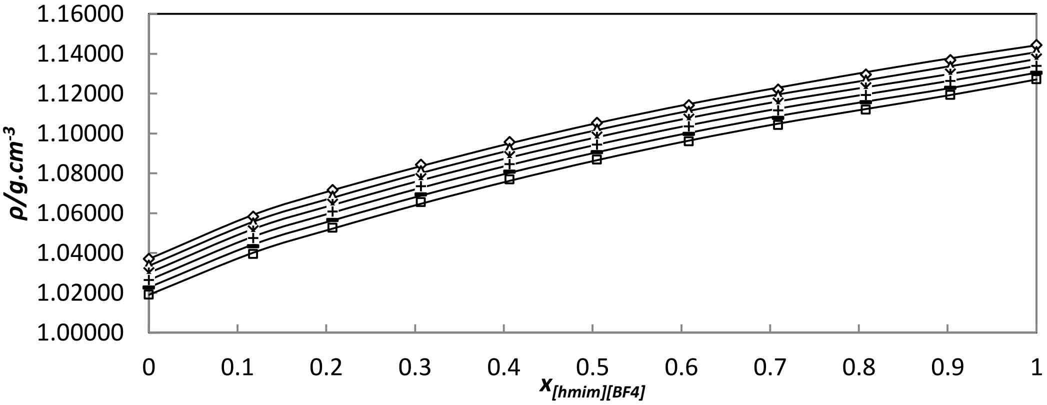

Figure 4.6. Plot of experimental values of density *ρ,* vs mole fraction of IL, for the system [hmim][BF_4] (1) + MDEA (2), at several temperatures. ◊, 298.15K; Δ, 303.15 K; *, 308.15 K, +, 313.15 K, -, 318.15 K, □, 323.15 K. The solid curves were calculated by using Eq.4.1.

The density values of all the binary mixtures were higher than the pure MDEA and lower than the pure [hmim][BF_4]. In other words the density values of binary mixtures were in between the density values of pure MDEA and [hmim][BF_4]. As [hmim][BF_4] has higher density values than MDEA therefore the addition of it to MDEA resulted in enhanced density values. The density values of all the binary mixtures decreased with increase in temperature as expected.

[hmim][Tf$_2$N] + MDEA System

The density values for the binary mixtures ([hmim][Tf_2N]+MDEA) increased with increase in mole fraction of [hmim][Tf_2N] and decreased with increase in concentration of MDEA, over the entire range of temperatures (Figure 4.7). A similar trend was observed by Ahosseini et. al. (2010) for the binary mixtures of [hmim][Tf_2N] with 1-octene. They reported that in these mixtures, the density values increased as the concentration of [hmim][Tf_2N] increased.

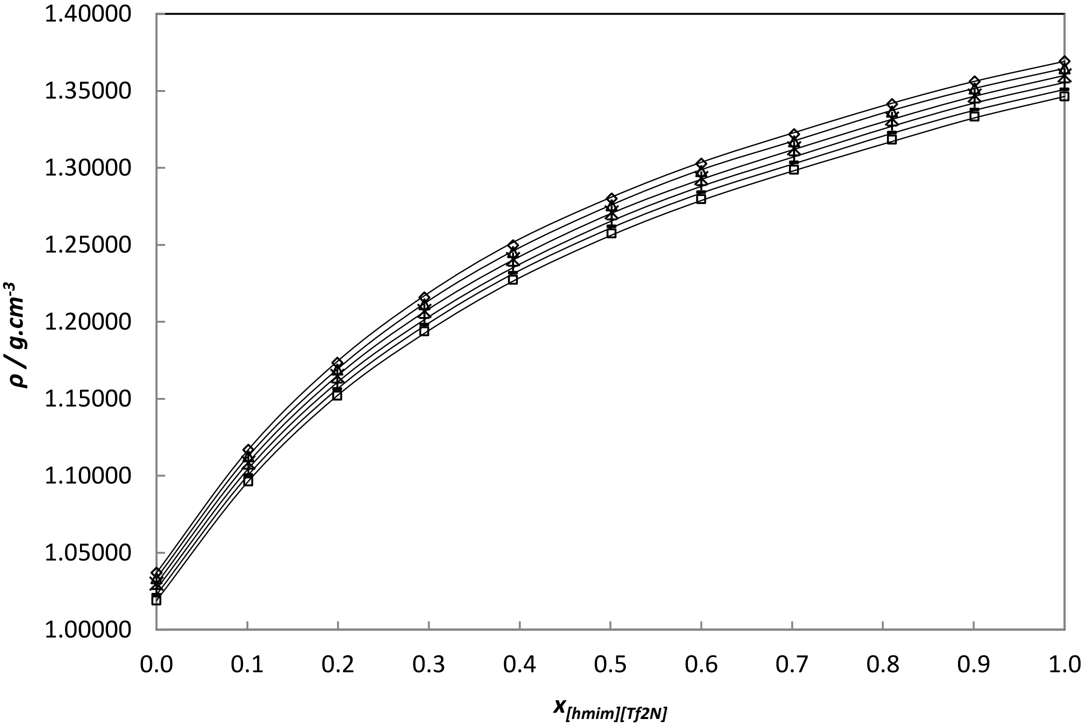

Figure 4.7. Plot of experimental values of density ρ, vs mole fraction of IL, for the system [hmim][Tf_2N] (1) + MDEA (2), at several temperatures. ◊, 298.15K; Δ, 303.15 K; *, 308.15 K, +, 313.15 K, -, 318.15 K, □, 323.15 K. The solid curves were calculated by using Eq. 4.1.

The density values for the binary mixtures of [hmim][Tf_2N] with MDEA are higher than the binary mixtures of [hmim][BF_4] with MDEA (Table A-1, A-2). The density values for the binary mixtures followed the general pattern and decreased with increase in temperature. The variation in the density values of the mixtures with the temperature was not as significant as was with the change in the concentration of [hmim][Tf_2N].

[hmim][FAP] + MDEA System

The variations in the densities for the binary mixtures of [hmim][FAP] with MDEA at different temperatures and with mole fraction of ([hmim][FAP]) are illustrated in Figure 4.8. The density of the binary mixtures increased with increase in mole fraction of [hmim][FAP].

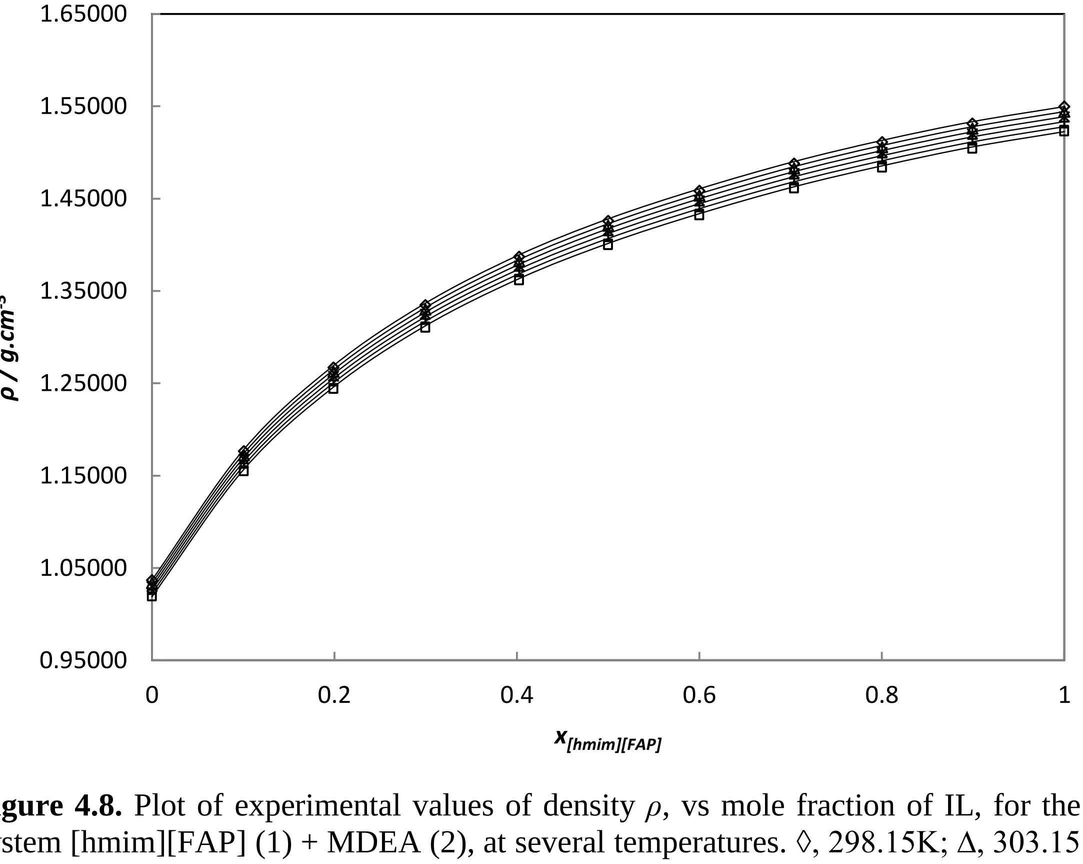

Figure 4.8. Plot of experimental values of density ρ, vs mole fraction of IL, for the system [hmim][FAP] (1) + MDEA (2), at several temperatures. ◊, 298.15K; Δ, 303.15 K; *, 308.15 K, +, 313.15 K, -, 318.15 K, □, 323.15 K. The solid curves were calculated by using Eq. 4.1.

The density values of the binary mixtures ([hmim][FAP]+MDEA) were higher than the values for the binary mixtures of [hmim][BF_4] *or* [hmim][Tf_2N] with MDEA over the entire range of temperatures (Figures 4.6 - 4.8). The density values of the binary mixtures varied with the change in concentration of [hmim][FAP] and temperature. However the variations occurred with the change in temperature were not as significant as were with the variations in concentration of [hmim][FAP].

4.2 Viscosity

The viscosities of the pure liquids as well as their binary mixtures were measured by using Brookfield cone and plate type (CAP 2000, L-series) viscometer at temperatures (298.15 to 323.15) K with a temperature control accuracy of + 0.02 K. The detailed methods for the measurements of viscosities are listed in section 3.2.3 of chapter 3. The measured viscosity values of the pure liquids used in the present study are illustrated in Figure 4.9. It can be seen from the figure that [hmim][BF_4] has highest viscosity among the pure chemicals and MDEA has lowest viscosity (except at T = 298.15 K where [hmim][Tf_2N] has lowest viscosity). The pure ILs in terms of viscosity could be arranged as; [hmim][BF_4]>[hmim][FAP]>[hmim][Tf_2N]. Ahosseini and Scurto (2008) studied the effect of anion on the viscosity of ILs (having [hmim] cation; paired with different anions; [BF_4], [PF_6], [Tf_2N]). They concluded that the 'hole theory' applied by Abbot et. al. (2004;2005;2006) to the ILs, which states that the viscosity of the IL is inversely proportional to the size of anion molecule, was not applicable to all ILs. According to this theory the viscosity of their studied ILs should have the order [hmim][BF_4]>[hmim][PF_6]>[hmim][Tf_2N]. On the contrary, the experimental viscosity of the ILs showed the mixed trend as; [hmim][PF_6]>[hmim][BF_4]>[hmim][Tf_2N]. According to 'hole theory' the viscosity of the ILs studied in the present study should have the order; [hmim][BF_4]>[hmim][Tf_2N]>[hmim][FAP], whereas the actual experimental viscosities of ILs have shown the mixed trend; [hmim][BF_4]>[hmim][FAP]>[hmim][Tf_2N]. Therefore it could be concluded that the 'hole theory' is not applicable to all set of ILs (having similar cation paired with different anions) as observed by Ahosseini and Scurto (2008). The experimental viscosity trends obtained for ILs ([BF_4]>[FAP]>[Tf_2N]) are in accordance to the one reported in the literature (Muhammad et. al. 2008a; Guang Li et. al. 2011) for these. It has been reported in the literature that the viscosity of IL is inversely proportional to its ionic conductivity (Wu et. al. 2011a). The ILs studied in the present work follow this general principle. The ionic conductivities of ILs [hmim][BF_4], [hmim][Tf_2N], [hmim][FAP] are 1.26 mS.cm^{-1}, 2.18 mS.cm^{-1} and 1.66mS.cm^{-1} (T = 298.15 K) respectively (Widegren et. al. 2007; Rilo et. al. 2010; Guang Li et. al. 2011). The IL [hmim][BF_4] shows the least value of ionic conductivity therefore principally showed highest viscosity. [Hmim][FAP] showed lower values of viscosities than [hmim][BF_4] as it's ionic conductivity is greater than [hmim][BF_4]. Similary [hmim][Tf_2N] showed less viscosity values than [hmim][BF_4] and [hmim][FAP] as it has highest ionic conductivity value than these two ILs. The viscosity of pure [hmim][BF_4] was found to be 1.5 times higher than the viscosity of pure MDEA. Similarly the viscosities of pure IL ([hmim][FAP]) were 1.24 times higher than those for pure MDEA. MDEA has higher viscosity than [hmim][Tf_2N] at T = 298.15 K where as for rest of the temperatures (303.15 to 323.15) K, it showed lower viscosity than the IL. [hmim][Tf_2N] showed 1.18 times higher viscosities than the pure MDEA at (T = 303.15 to 323.15) K (Figure 4.9). This difference is not as much significant. It could be said that [hmim][Tf_2N] had slightly higher values of viscosities than the amine at higher temperatures (303.15 to 323.15 K). The higher viscosity of MDEA at lower temperature (T = 298.15 K) is contrary to the common understanding that ILs are more viscous than the other organic solvents (Yu et. al. 2012). It could be inferred that some organic solvents are more viscous (at certain conditions) than the ILs. This is a favourable property of [hmim][Tf_2N] that it has lower viscosity than MDEA at T = 298.15 K.

The comparisons of the measured viscosity values for pure MDEA and [hmim][BF_4] with the literature values are shown in Figure 4.10. The calculated deviations were found to be $\leq$1.98 % (for pure MDEA) and $\leq$ 2.0 % (for pure [hmim][BF_4]) showing a good agreement with the literature values. Similarly the comparisons of the measured viscosity values of pure [hmim][Tf_2N] and [hmim][FAP] with the reported literature values are illustrated in Figures 4.11 and 4.12 respectively. The measured values showed a good agreement with the reported literature values (calculated deviations $\leq$ 1.75 % for [hmim][Tf_2N] and $\leq$ 1.6 % for [hmim][FAP]). The minor differences in the viscosity of the ILs could be attributed to

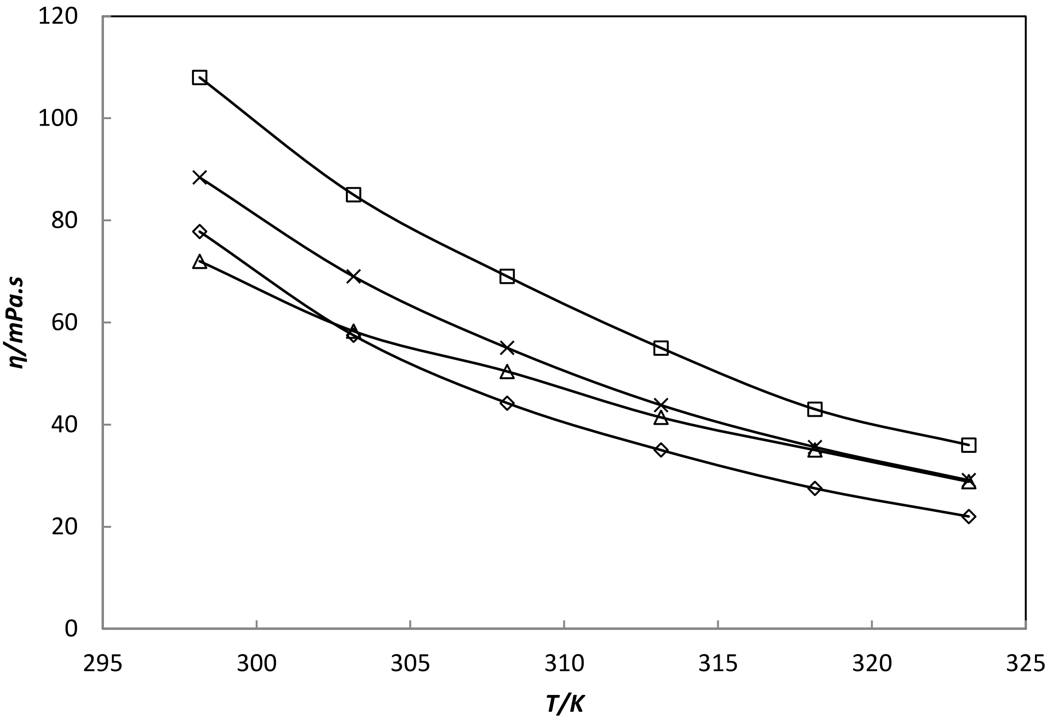

Figure 4.9. Plot of experimental viscosites for the pure liquids against temperatures. ◊, MDEA; □, [hmim][BF$_4$]; Δ, [hmim][Tf$_2$N]; ×, [hmim][FAP].

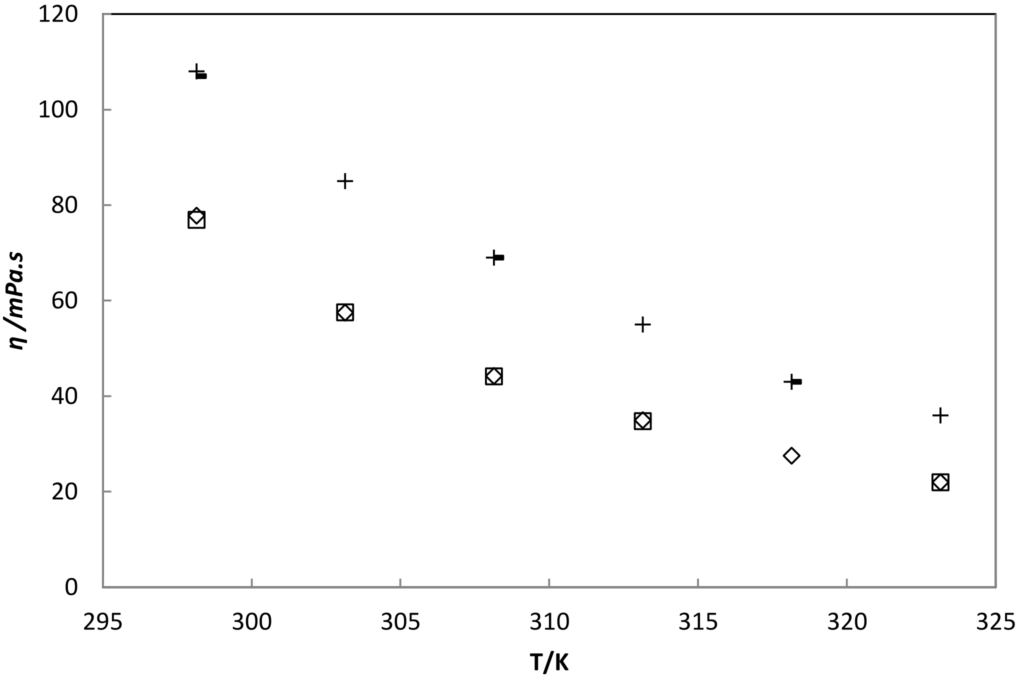

Figure 4.10. Comparison of the experimental viscosity data for pure MDEA and [hmim][BF$_4$] with literature: ◊, MDEA this work; □, Al-Ghawas et. al. 1989; +, [hmim][BF$_4$] this work; -, Muhammad et. al. 2008.

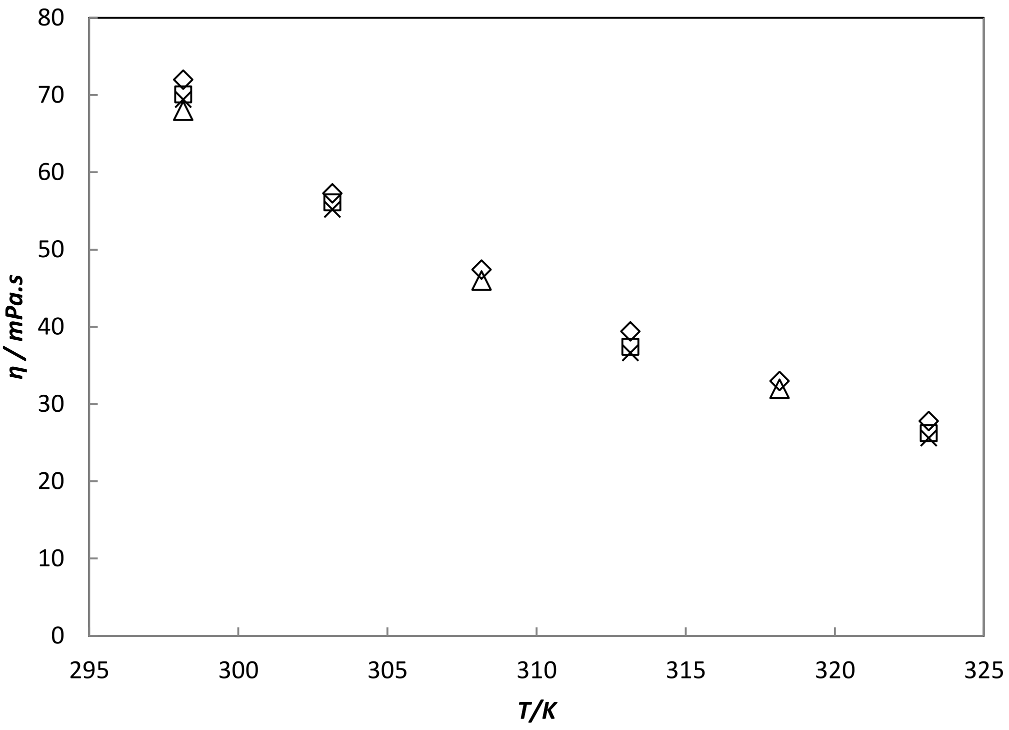

Figure 4.11. Comparison of the experimental viscosity data for pure [hmim][Tf$_2$N] with literature: ◊, this work; □, Widegren et. al. 2007; Δ, Muhammad et. al. 2008; ×, Santos et. al. 2010.

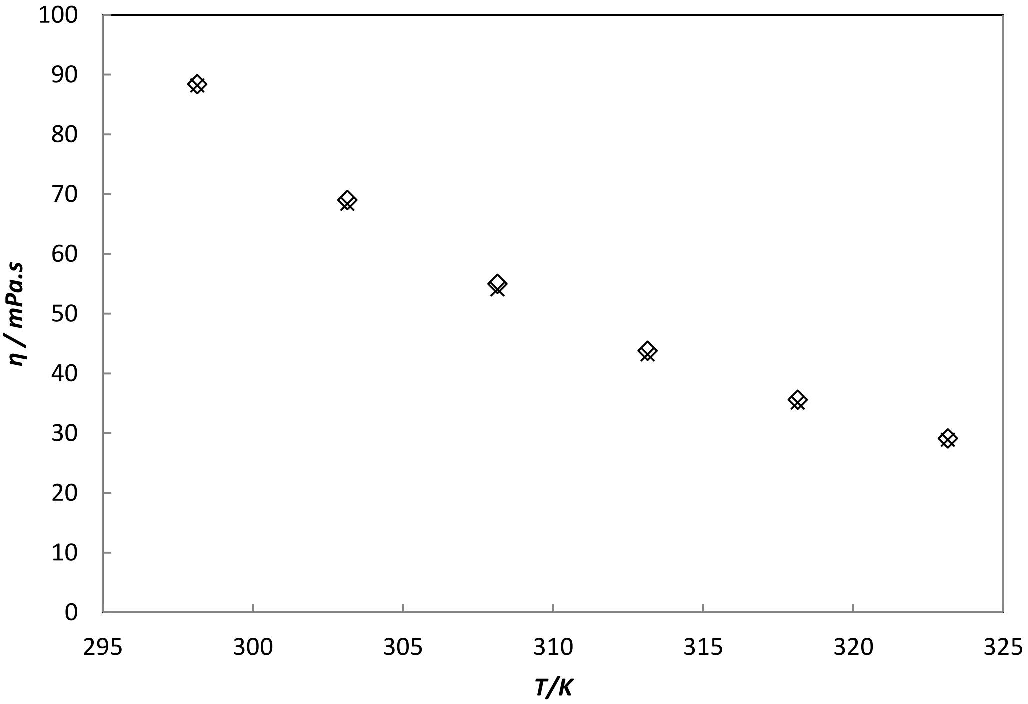

Figure 4.12. Comparison of the experimental viscosity data for pure [hmim][FAP] with literature: ◊, this work; ×, Guang Li et. al. 2011.

the differences in the amount of impurities present (samples used in the present study and the one with which the comparisons have been made). The viscosity of the ILs is affected by the impurities (water content, halide content etc.) present in these (Huddleston et. al. 2001; Yu et. al. 2012). Seddon et. al. (2000) carried out systematic study to investigate the effect of impurities like chloride contents and water contents on the viscosity of ionic liquids and concluded that the presence of excess chloride contents dramatically increased and excess water contents decreased the viscosity of ionic liquids. The measured viscosity values for the pure liquids as well as for the binary mixtures are listed in Tables A-4 to A-6 of Appendix A.

4.2.1 Binary Mixtures

[hmim][BF$_4$] + MDEA System

The addition of MDEA to pure [hmim][BF$_4$] decreased the viscosity of the former (Table A-4). The viscosities of the binary mixtures ([hmim][BF$_4$]+MDEA) increased as the mole fraction of [hmim][BF$_4$] increased (Figure 4.13). Similar trends were also observed by Zhu et. al. (2011) for the binary mixtures comprising of [hmim][BF$_4$] with different organic solvents (butanone, ethyl acetate, butylamine, tetrahydrofuran).

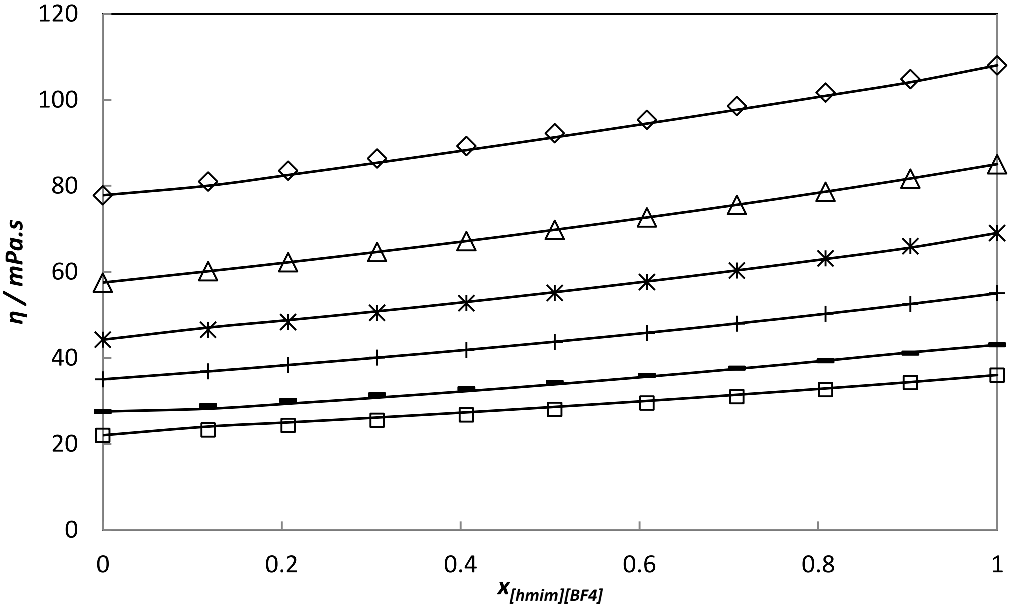

Figure 4.13. Plot of experimental values of viscosity η , vs mole fraction of IL, for the system [hmim][BF$_4$] (1) + MDEA (2), at several temperatures. ◊, 298.15K; Δ, 303.15 K; *, 308.15 K, +, 313.15 K, -, 318.15 K, □, 323.15 K. The solid curves were calculated by using Eq.4.1.

The viscosities of the binary mixtures followed the general trend and decreased significantly with increase in temperature. The viscosities of the binary mixtures varied with a change in concentration and temperature.

[hmim][Tf$_2$N] + MDEA System

The variations in the viscosity values for the binary mixture ([hmim][Tf$_2$N]+MDEA) with temperature and concentration of [hmim][Tf$_2$N] are illustrated in Figure 4.14. The viscosity of the binary mixtures decreased with increasing mole fraction of [hmim][Tf$_2$N] at T = 298.15 where as at T = (303.15 to 323.15) K the viscosity of binary mixtures increased with increase in mole fraction of [hmim][Tf$_2$N].

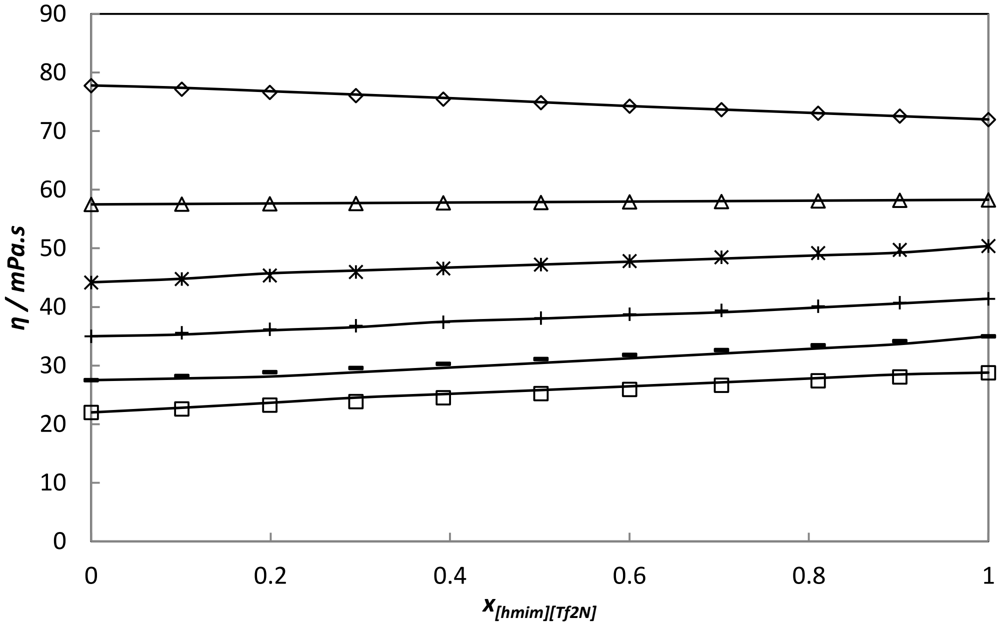

Figure 4.14. Plot of experimental values of viscosity η , vs mole fraction of IL, for the system [hmim][Tf$_2$N] (1) + MDEA (2), at several temperatures. ◊, 298.15K; Δ, 303.15 K; *, 308.15 K, +, 313.15 K, -, 318.15 K, □, 323.15 K. The solid curves were calculated by using Eq.4.1.

The increments in the viscosities of the binary mixture were not significant with the addition of [hmim][Tf$_2$N]. On the other hand, viscosities of the binary mixtures decreased significantly with increase in temperature. The addition of MDEA to the IL has decreased its viscosity (except at T = 298.15 K) though the decrement was not a significant one, yet it cannot be neglected.

[hmim][FAP] + MDEA System

The viscosities of the binary mixtures of [hmim][FAP] with MDEA increased as the mole fraction of [hmim][FAP] increased (over the entire temperature range). The viscosities of pure liquids as well as their binary mixtures decreased with increase in temperature (Figure 4.15).

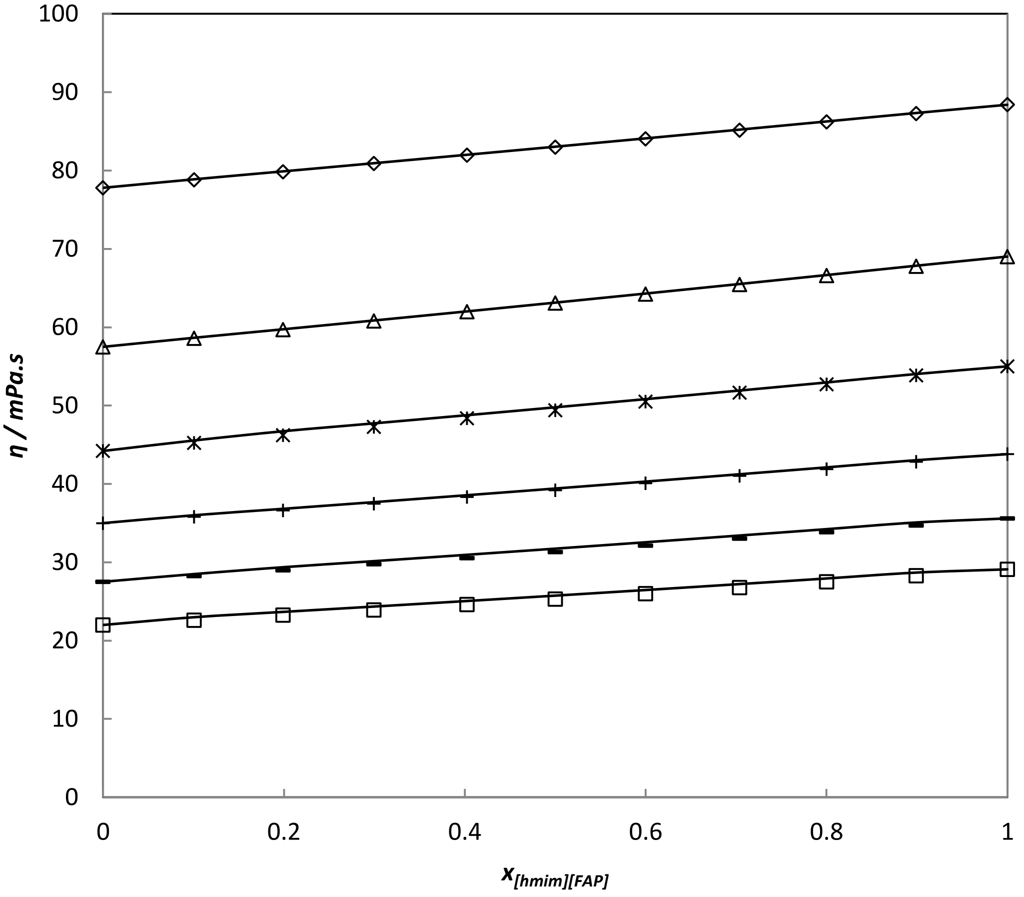

Figure 4.15. Plot of experimental values of viscosity η , vs mole fraction of IL, for the system [hmim][FAP] (1) + MDEA (2), at several temperatures. ◊, 298.15K; Δ, 303.15 K; *, 308.15 K, +, 313.15 K, -, 318.15 K, □, 323.15 K. The solid curves were calculated by using Eq.4.1.

The addition of MDEA to pure [hmim][FAP] resulted in a decrease in viscosity of the mixture. The variation in the viscosities with change in concentrations of [hmim][FAP] were not as significant as were with the change in temperatures.

4.3 Refractive Index

The refractive indices of the pure liquids as well as their binary mixtures were measured by using digital refractometer (ATAGO model RX-5000) at temperatures (298.15 to 323.15) K with a temperature control accuracy of 0.05 K. The detail of the measurement of refractive indices were presented in Section 3.2.4. The refractive indices of the pure liquids used in the present study are illustrated in Figure 4.16. It can be seen from the Figure that the values of the refractive indices for pure MDEA (MW: 119.16 g.mol^{-1}) are higher than the values of refractive indices for pure [hmim][BF_4] (MW: 254.08 g.mol^{-1}), pure [hmim][Tf_2N] (MW: 447.42 g.mol^{-1}) and pure [hmim][FAP] (MW: 612.29 g.mol^{-1}) over the entire range of temperatures. Generally it is believed that the refractive index values increase as the density of the substances increase (Deetlefs et. al. 2006). On the contrary, reverse trend was observed for the case of the solvents studied in the present study. [Hmim][FAP] has the highest density (among all the solvents) (Figure 4.1) but it shows the lowest value of refractive index. On the other hand, MDEA has the lowest density, whereas it shows the highest values of refractive index. MDEA showed 1.0234 times higher refractive index values than pure [hmim][Tf_2N] and 1.0244, 1.0577 times higher RI values than [hmim][BF_4] and [hmim][FAP] respectively. [Hmim][Tf_2N] and [hmim][BF_4] showed almost similar values of refractive index with [hmim][Tf_2N] showing a slightly higher values. The solvents in the present study did not follow the general trend (*i.e.* RI increases linearly with density). This RI display by the solvents tells that this general principle is either incorrect or limited to a set of substances. Liu et. al. (2008) probed into this principle by analyzing the RI and density data of 4000 pure materials. They concluded that this principle only holds good when the density of the substance is much less than 1 g/cm^3. The solvents in the present study therefore were not following this trend as these have higher values of density (>1g/cm^3). The comparison of the measured values of refractive indices for pure [hmim][BF_4] with the literatures values is illustrated in Figure 4.17. A fair agreement was found between the measured values and the literature data (calculated deviations $\leq$ 1.20%). Similarly the comparison of the measured values of the refractive indices for pure [hmim][Tf_2N] and MDEA with the literature values are illustrated in Figures 4.18 and 4.19 respectively. The measured values showed a fair degree of agreement (calculated deviation are: $\leq$ 1.52 % for [hmim][Tf_2N] and $\leq$ 1.01 % for pure MDEA)

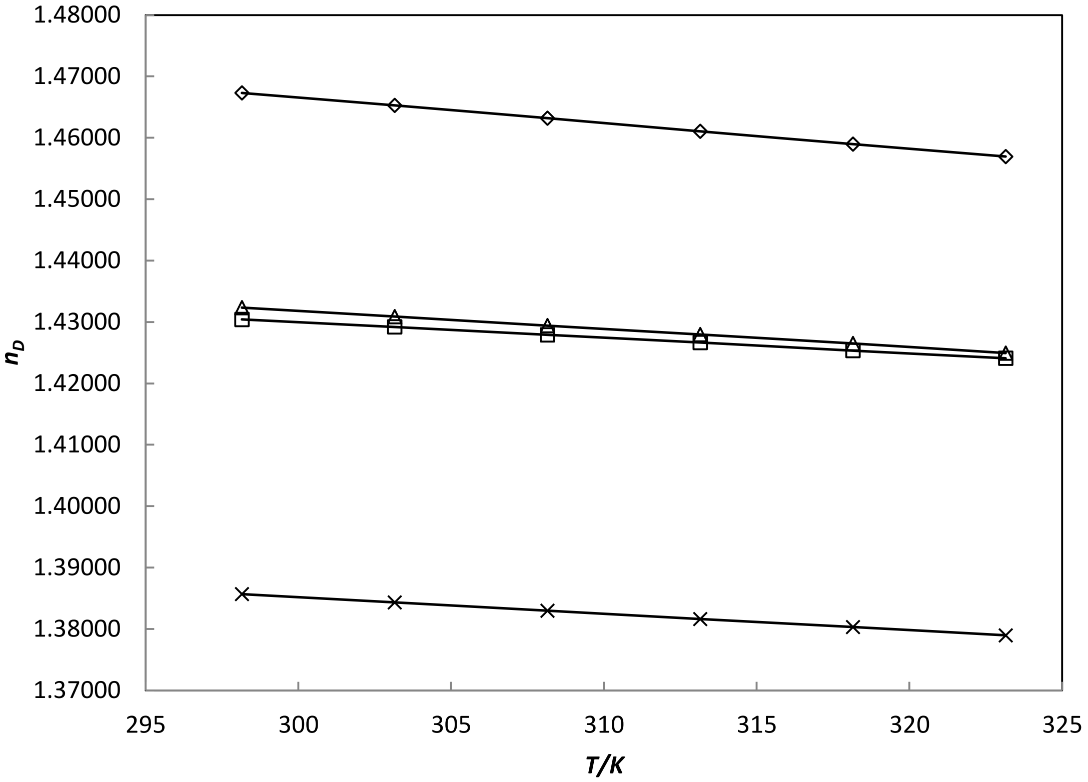

Figure 4.16. Plot of experimental refractive index for the pure liquids against temperatures. ◊, MDEA; □, [hmim][BF_4]; Δ, [hmim][Tf_2N]; ×, [hmim][FAP].

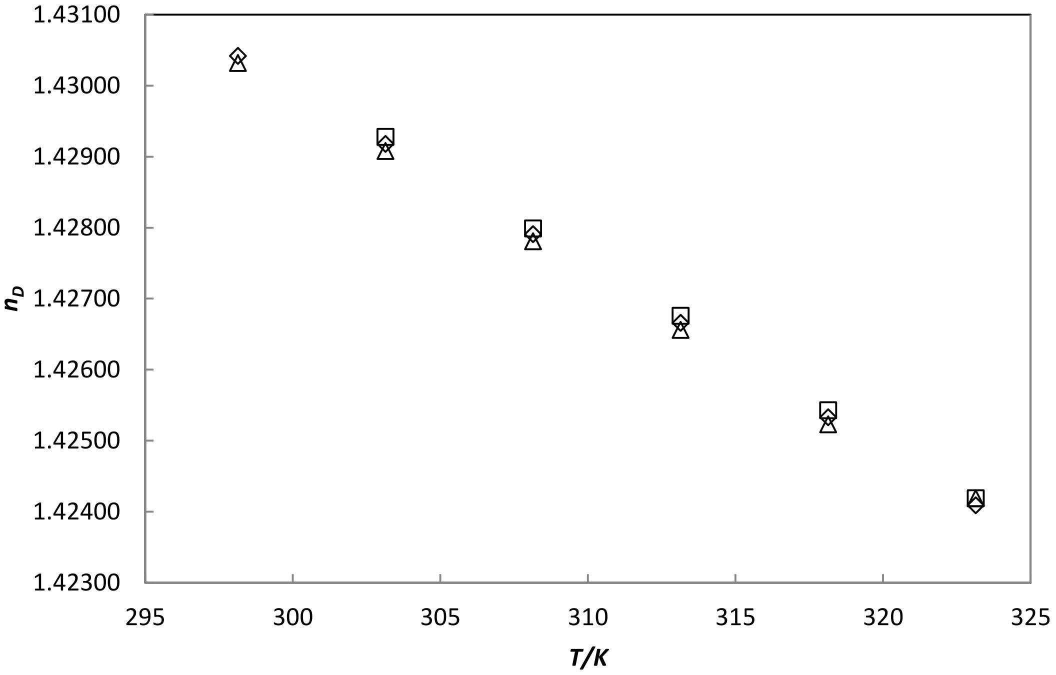

Figure 4.17. Comparison of the experimental refractive index data for pure [hmim][BF_4] with literature: ◊, this work; □, Muhammad et. al. 2008; Δ, Vakili-Nezhaad et. al. 2012.

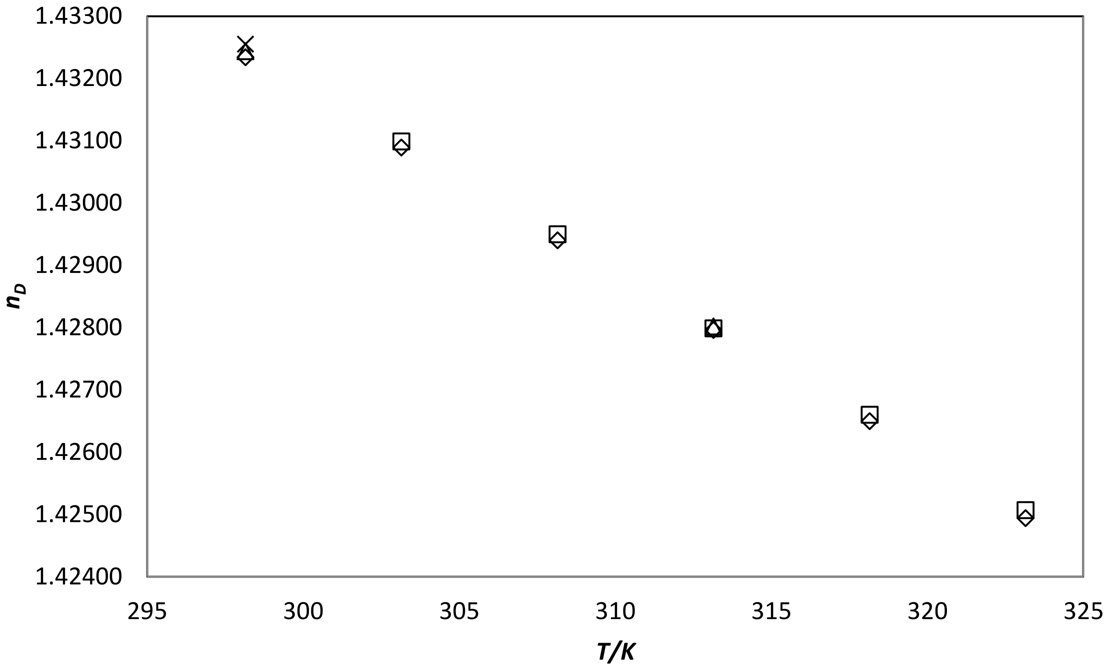

Figure 4.18. Comparison of the experimental refractive index data for pure [hmim][Tf_2N] with literature: ◊, this work; □, Muhammad et. al. 2008; Δ, Tariq et. al. 2009; ×, Corderi et. al. 2012.

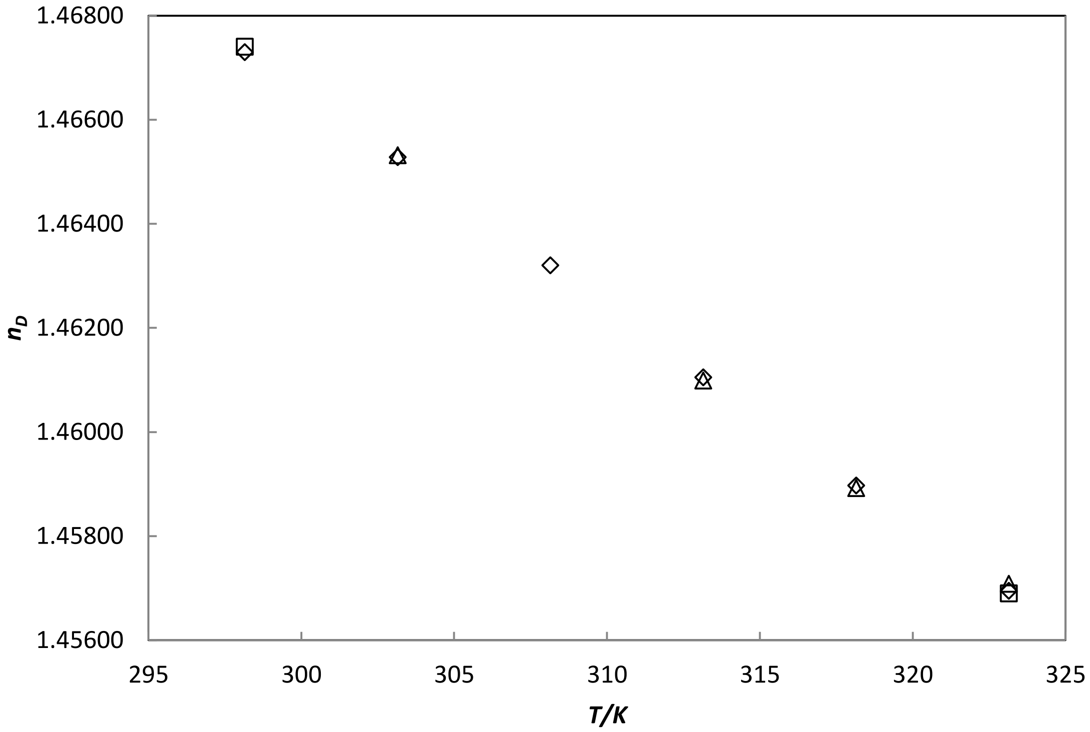

Figure 4.19. Comparison of the experimental refractive index data for pure MDEA with literature: ◊, this work; □, Lagalante et. al. 2000; Δ, Muhammad et. al. 2008.

with the literature values. The refractive index values for pure [hmim][FAP] have not been reported in open literature till date. For the first time the refractive index values for pure [hmim][FAP] are reported in the present work. The refractive index values for the pure liquids as well as their binary mixtures are listed in Table A-7 to A-9 of Appendix A.

4.3.1 Binary Mixtures

[hmim][BF$_4$] + MDEA System

The refractive index values for the binary mixtures of [hmim][BF$_4$] with MDEA decreased with increasing mole fraction of [hmim][BF$_4$] and also with an increase in temperature (Figure 4.20). The same trend was observed over the entire range of temperatures.

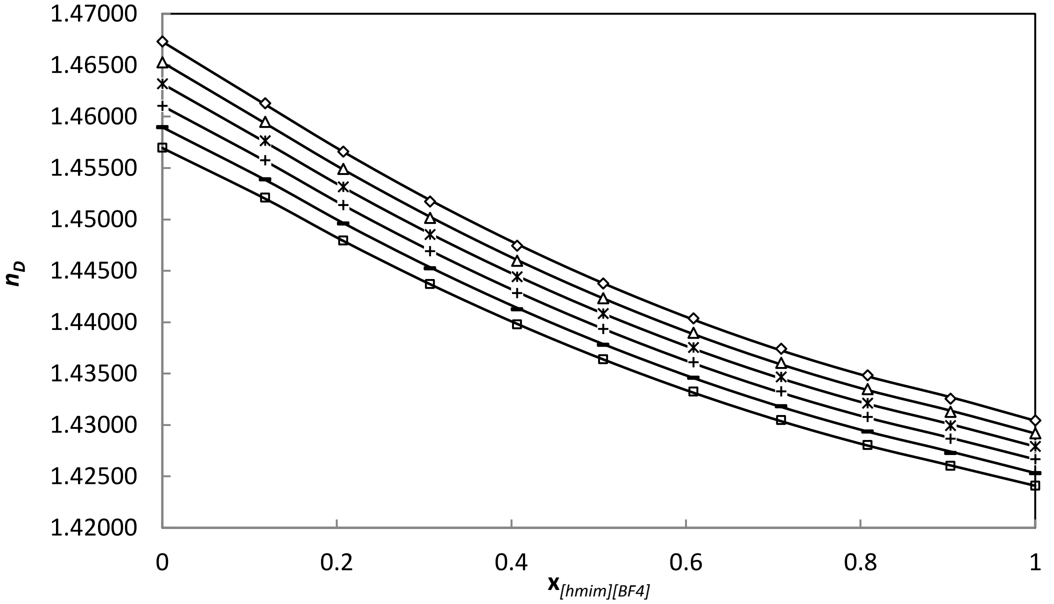

Figure 4.20. Refractive index n_D vs mole fraction of IL, for the system [hmim][BF$_4$] (1) + MDEA (2), at several temperatures. ◊, 298.15 K; Δ, 303.15 K; *, 308.15 K; +, 313.15 K; -, 318.15 K; □, 323.15 K. The solid curves were calculated by using Eq.4.1.

It could be seen from the Figure 4.20 that the change in refractive index values with respect to temperature was not as significant as with change in concentration of IL was. The values depend on both factors. However the variation with respect to change in mole fraction of [hmim][BF$_4$] is greater as compared to the variation with respect to temperature.

[hmim][Tf$_2$N] + MDEA System

The variations in the refractive index values for the binary mixtures of [hmim][Tf$_2$N] with MDEA with respect to temperature and mole fraction of [hmim][Tf$_2$N] are illustrated in Figure 4.21. It can be seen that the refractive index values for the binary mixtures decreased with increasing mole fraction of pure [hmim][Tf$_2$N]. This is due to the fact that pure MDEA has higher refractive index values than the pure [hmim][Tf$_2$N]. Therefore in the mixtures when the concentration of [hmim][Tf$_2$N] increased then the refractive index values decreased gradually.

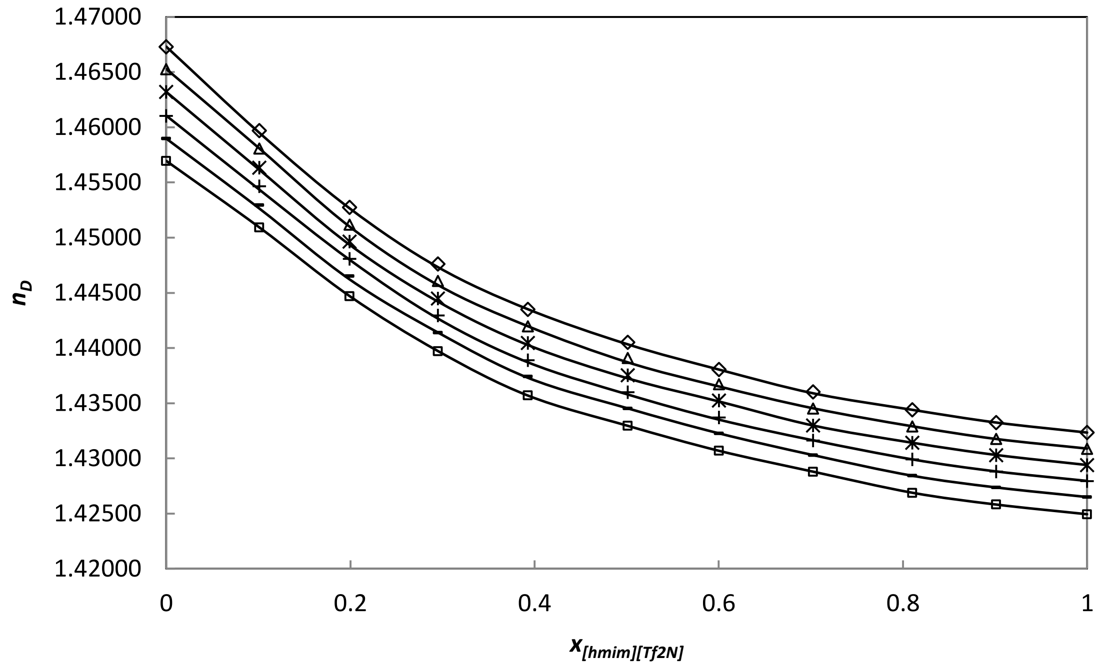

Figure 4.21. Refractive index n_D vs mole fraction of IL, for the system [hmim][Tf$_2$N] (1) + MDEA (2), at several temperatures. ◊, 298.15 K; Δ, 303.15 K; *, 308.15 K; +, 313.15 K; -, 318.15 K; □, 323.15 K. The solid curves were calculated by using Eq.4.1.

The refractive index values for binary mixtures decreased with an increase in temperature following the general pattern. The refractive index values of the binary mixtures varied significantly with a change in mole fraction of [hmim][Tf$_2$N] and temperatures.

[hmim][FAP] + MDEA System

The measured refractive index values for the binary mixtures of ([hmim][FAP]+MDEA) at temperatures 298.15 to 323.15 K, vs mole fraction of [hmim][FAP] are illustrated in Figure 4.22. It can be seen that the values of the refractive indices for the binary mixtures decrease with an increase in mole fraction of [hmim][FAP]. Similar to the observations made for the binary mixtures of [hmim][Tf$_2$N] with MDEA. MDEA has higher refractive index value than [hmim][FAP]. The refractive index values of binary mixtures followed general trend and decreased with increase in temperature as expected.

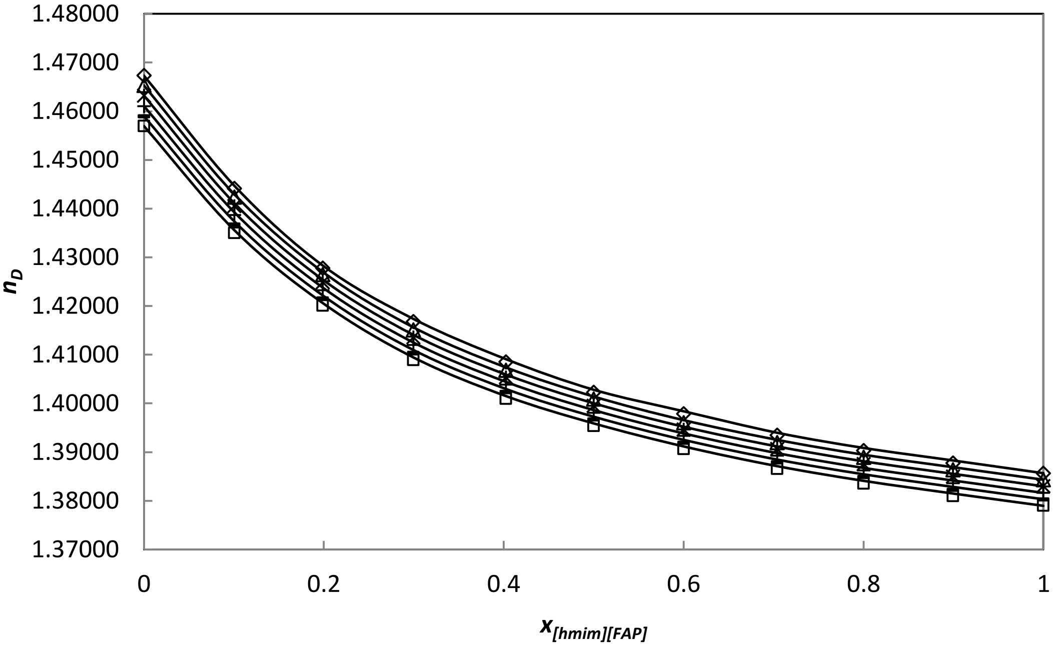

Figure 4.22. Refractive index n_D vs mole fraction of IL, for the system [hmim][FAP] (1) + MDEA (2), at several temperatures. ◊, 298.15 K; Δ, 303.15 K; *, 308.15 K; +, 313.15 K; -, 318.15 K; □, 323.15 K. The solid curves were calculated by using Eq.4.1.

It could be seen (Figure 4.22) that significant variation in the refractive index values of the binary mixtures occurred with respect to the change in concentration of [hmim][FAP]. On the other hand, variations with respect to temperature were not significant.

Correlation of density, viscosity and refractive index data for binary system

The density, viscosity and refractive index data for all the binary systems used in the present study has been presented and the variations are discussed in the earlier sections. It was observed that density, viscosity and refractive index data of the binary mixtures varied with change in concentration (mole fraction of respective IL) and temperature. Hence, the density, viscosity and refractive indices data of all the systems ([hmim][BF$_4$]+MDEA, [hmim][Tf$_2$N]+MDEA and [hmim][FAP]+MDEA) under study has been correlated as a function of temperature and concentration simultaneously by the using following form of relation:

$$\rho/g.cm^{-3} \ \boldsymbol{or} \ \eta/mPa.s \ \boldsymbol{or} \ n_D = \sum_{i=0}^{2}\left[A_i x^i + B_i x^i (T/K) + C_i x^i (T/K)^2\right] \quad (4.1)$$

where *x* is the mole fraction of IL in the binary mixture, *T* is the temperature in Kelvin and A_i, B_i and C_i are correlation coefficients obtained by regression and are listed in Table 4.1 along with the values of the standard deviations (σ) calculated by using the following relation:

$$\sigma = \left[\frac{\sum\left(Z_{exp} - Z_{calc}\right)^2}{n}\right]^{\frac{1}{2}} \quad (4.2)$$

where *n* is the number of experimental points, Z_{exp} and Z_{calc} are the experimental and calculated values respectively. It can seen from Table 4.1 that Eq. 4.1 successfully correlated the experimental results as the maximum standard deviation values were ≤ 0.008 for the case of viscosity and ≤ 0.007, ≤ 0.001 for the cases of density and refractive index values respectively among all the systems. Similar forms of Eq. 4.1 have been used by many researchers to correlate their experimental density, viscosity and RI data (as function of temperature and concentration simultaneously) for the binary (Park et. al. 2002; Yoon et. al. 2002; Paul et. al. 2009) ternary (Kim et. al. 1996) and tertiary (Koo et. al. 1998) mixtures of solvents. Sample calculations for the estimation of density values are listed in Section 4A of Appendix A.

Table 4.1: Fitting parameters of Eq. (4.1) for the correlation of density *or* viscosity *or* refractive index as a function of temperature and concentration, for the binary systems ([hmim][BF$_4$] *or* [hmim][Tf$_2$N] *or* [hmim][FAP] (1) + MDEA (2)) along with the values of standard deviations (σ).

[hmim][BF$_4$] + MDEA System				
		A_i	B_i	C_i
ρ / g.cm^{-3}	$i = 0$	0.92934	0.00142742	-3.5198×10^{-06}
	$i = 1$	0.30869	-9.9415×10^{-04}	1.5712×10^{-06}
	$i = 2$	-0.03118	-2.3108×10^{-04}	5.2726×10^{-07}
	σ		6.4770×10^{-04}	
η / mPa.s	$i = 0$	7361.7	-44.984	0.068927
	$i = 1$	1757.3	-10.537	0.015870
	$i = 2$	-1504.6	9.7492	-0.015728
	σ		6.7480×10^{-04}	
n_D	$i = 0$	1.584424	-3.8682×10^{-04}	-1.4930×10^{-08}
	$i = 1$	-0.15222	3.6047×10^{-04}	-1.5399×10^{-07}
	$i = 2$	0.059774	-1.2241×10^{-04}	-1.7517×10^{-08}
	σ		6.5662×10^{-05}	
[hmim][Tf$_2$N] + MDEA System				
ρ / g.cm^{-3}	$i = 0$	1.2854	-6.6765×10^{-04}	-1.8960×10^{-07}
	$i = 1$	0.58739	1.6075×10^{-04}	-8.7294×10^{-07}
	$i = 2$	-0.19690	-7.2968×10^{-04}	1.6041×10^{-06}
	σ		4.2204×10^{-03}	
η / mPa.s	$i = 0$	7407.0	-45.276	0.069394
	$i = 1$	-3879.5	24.564	-0.038809
	$i = 2$	39.724	-0.27772	4.8542×10^{-04}
	σ		8.4574×10^{-03}	
n_D	$i = 0$	1.4128	6.7223×10^{-04}	-1.6615×10^{-06}
	$i = 1$	0.25191	-2.2436×10^{-03}	3.9096×10^{-06}
	$i = 2$	-0.15740	1.3798×10^{-03}	-2.4290×10^{-06}
	σ		5.4697×10^{-04}	
[hmim][FAP] + MDEA System				
ρ / g.cm^{-3}	$i = 0$	1.3914	-1.1212×10^{-03}	5.2402×10^{-07}
	$i = 1$	0.81853	1.0782×10^{-03}	-2.9727×10^{-06}
	$i = 2$	-0.31235	-1.3660×10^{-03}	2.9829×10^{-06}
	σ		7.0451×10^{-03}	
η / mPa.s	$i = 0$	7406.7	-45.274	0.069391
	$i = 1$	-480.58	3.3289	-5.6404×10^{-03}
	$i = 2$	-111.70	0.71875	-1.1486×10^{-03}
	σ		8.7870×10^{-04}	
n_D	$i = 0$	1.4362	4.8117×10^{-04}	-1.3893×10^{-06}
	$i = 1$	0.52234	-4.6088×10^{-03}	7.8867×10^{-06}
	$i = 2$	-0.52340	4.0972×10^{-03}	-6.8998×10^{-06}
	σ		1.3783×10^{-03}	

4.4. Thermal Stability

The thermal stability of the pure liquids as well as their binary mixtures (which were used for CO_2 solubility) was determined by thermogravimetric analysis (TGA). Thermogravimetric analysis (TGA) was performed with Perkin-Elmer (Model STA 6000) with dynamic nitrogen (atmosphere). The TGA thermograms were recorded using 5mg of sample at a heating rate of 10 ^{o}C min^{-1} in the temperature range of 30-800 ^{o}C. The over all accuracy of temperature control was found to be ± 0.03^{o}C. The weight loss with respect to temperature rise was recorded accordingly. The thermal stability is an important parameter for the solvents when used for CO_2 absorption. It provides with information about the extent of temperature a solvent can withstand. Thereby help in setting the optimum operating conditions for absorption (Fredlake et. al. 2004). Therefore the solvents used for CO_2 solubility in the present study were analysed for their thermal stability. The start temperature (T_{start}) at which the decomposition starts; and the onset temperature (T_{onset}) which indicate the upper range for the liquids to decompose were reported. T_{onset} is the point of intersection of the baseline weight and the tangent of the weight vs temperature curve as the decomposition occurs. To report the thermal stability in terms of ‘onset temperature’ has the advantage of its well defined reproducibility and ease of measurement (Muhammad et. al. 2008; Muhammad 2009). The T_{start} and T_{onset} for the solvents used in the present study are listed in Table 4.2 along with the comparisons with the literature values for the pure liquids. It could be seen that a fair agreement was found between measured T_{start} and T_{onset} temperatures for the pure liquids and the reported literature (Muhammad et. al. 2008; Ignat’ev et. al. 2005; Muhammad et. al. 2008) data. The thermograms for the pure liquids are illustrated in Figure 4.23. It can be seen that the pure ILs show greater thermal stability in comparison to pure MDEA. The pure liquids could be arranged in terms of thermal stability as: [hmim][Tf_2N] > [hmim][FAP] > [hmim][BF_4] > MDEA. The ILs studied in the present research did not follow the general trend that thermal stability increases as the molar mass of anion increases. On the other hand, IL with [Tf_2N] anion showed the highest thermal stability. The experimental thermal stabilities of ILs ([Tf_2N]>[FAP]>[BF_4]) are in accordance to the literatue values (Muhammad et. al. 2008a; Ignat’ev et. al. 2005; Muhammad et. al. 2008b) reported for these. However the ILs [hmim][BF_4],

[hmim][FAP], [hmim][Tf_2N] did not follow the general principle that the thermal stability of IL increases as the molar mass of anion increases. It has been reported in the literature that molar size of anion is not the only factor influencing the thermal stability of ILs. Thermal stability of IL increases with increase in charge density of both cation and anion (Khupse et. al. 2010; Faridbod et. al. 2011). The thermal stability of the ILs corresponds well with this principle that with increased charge density thermal stability increases. The charge density of [hmim][Tf_2N] is higher (ionic conductivity = 2.18mS.cm^{-1}) than [hmim][FAP] (ionic conductivity = 1.66mS.cm^{-1}) and [hmim][BF_4] (ionic conductivity = 1.26mS.cm^{-1}) (Widegren et. al. 2007; Rilo et. al. 2010; Guang Li et. al. 2011). Therefore [hmim][Tf_2N] shows highest thermal stability followed by [hmim][FAP] and [hmim][BF_4] respectively. The binary mixtures (MDEA + IL) show higher T_{start} values in comparison to pure MDEA and lower T_{start} values in comparison to pure ILs. The addition of IL in pure MDEA enhanced its thermal stability (as IL is more thermally stable than MDEA). Whereas, the addition of MDEA in IL decreased its thermally stability (as MDEA is less thermally stable than IL). The higher T_{onset} values in both steps (in the first step these values were higher in comparison to pure MDEA and in the second step these values were higher in comparison to pure ILs) are due to the forces of attraction (hydrogen bonding etc.) between the two molecules present in the mixtures. The same trends have also been reported in the literature that when two solvents (one having high thermal stability and one showing less thermal stability) are mixed together their mixtures show higher T_{onset} values than both the pure solvents present in the mixture at each step of degradation. This behaviour was attributed to the presence of forces of attraction between molecules by researchers (Muhammad et. al. 2008b; Murshid et. al. 2011). The same has been observed in the case of binary mixtures of IL + MDEA. The thermograms for the binary mixtures are presented in Appendix A (Figure A-1 to A-9). The onset temperature and the two-step degradation of all binary mixtures indicate that initially MDEA molecules were decomposed followed by the degradation of ionic liquid molecules (in each case of binary mixture). The binary mixtures showed high temperature values at the start of decomposition than pure MDEA (Table 4.2) as expected.

Table 4.2: T_{start} and T_{onset} for the pure and binary mixtures

Solvents		$T_{\text{(Start)}}$ ^{o}C	$T_{\text{(Onset)}}$ ^{o}C
Pure			
[hmim][BF$_4$]		263.92 (262^{a})	426.48 (425^{a})
[hmim][Tf$_2$N]		300.59 (302^{a})	462.9 (461^{a})
[hmim][FAP]		291.87(290^{b})	373.28
MDEA		58.83 (58^{c})	169.48 (169^{c})
Binary	Molar Ratio (IL to MDEA)		
[hmim][BF$_4$]+MDEA	(1:4)	70.49	174.51 *and* 453.33
	(1:1)	72.34	175.24 *and* 452.89
	(4:1)	73.97	176.52 *and* 458.32
[hmim][Tf$_2$N]+MDEA	(1:4)	84.87	174.54 *and* 469.34
	(1:1)	105.02	174.28 *and* 470.02
	(4:1)	118.73	177.86 *and* 473.18
[hmim][FAP]+MDEA	(1:4)	123.05	178.20 *and* 383.67
	(1:1)	70.09	176.87 *and* 382.18
	(4:1)	127.71	174.24 *and* 386.23

^{a}Muhammad et. al. 2008a, ^{b} Ignat'ev et. al. 2005, ^{c} Muhammad et. al. 2008b

4.5 Excess Properties

The excess properties of the mixtures supplement useful information about the interactions present within the molecules comprising the mixture. The molecules present in the mixtures interact with each other. These interactions are outlined by these excess properties. Furthermore the structural packing effects arising due to the interstitial accommodations of molecules and the complex formations within the mixtures are also inferred from these excess properties. The excess properties for the mixtures are derived from the experimental physical properties data of the pure solvents and mixtures, by using standard equations (Vural et. al. 2011; Ivanov and Kustov 2010; Almasi and Iloukhani 2010).

a)

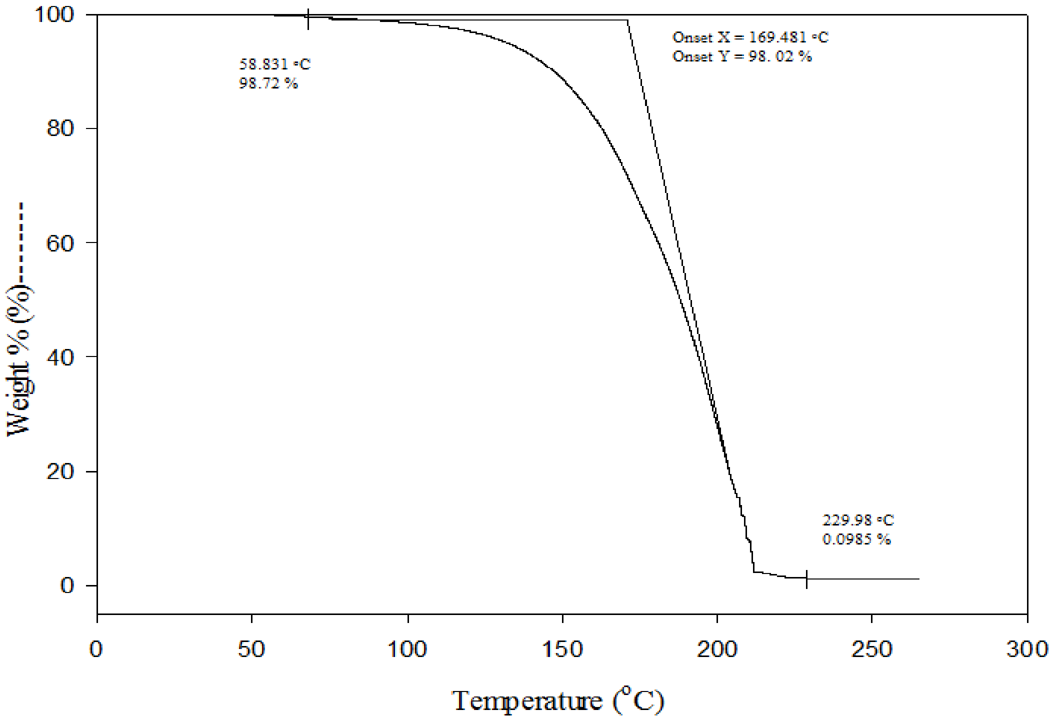
Weight % (%)
Temperature (°C)
100
80
60
40
20
0
0
50
100
150
200
250
300
58.831 °C
98.72 %
Onset X = 169.481 °C
Onset Y = 98. 02 %
229.98 °C
0.0985 %

b)

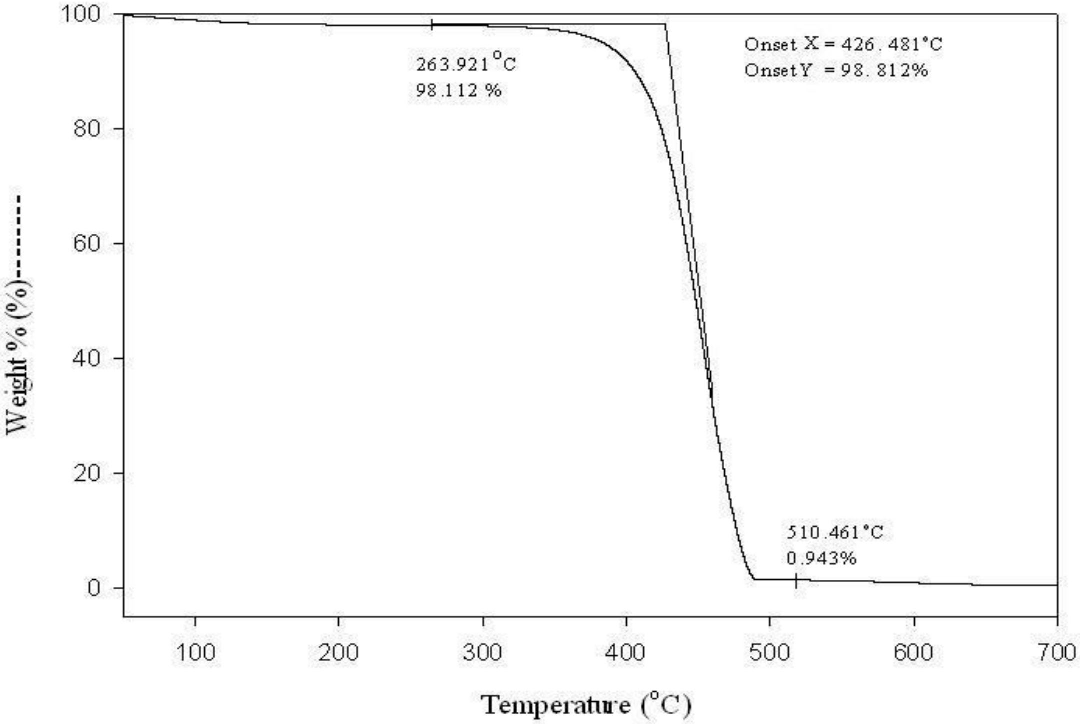
Weight % (%)
Temperature (°C)
100
80
60
40
20
0
100
200
300
400
500
600
700
263.921 °C
98.112 %
Onset X = 426. 481°C
Onset Y = 98. 812%
510.461°C
0.943%

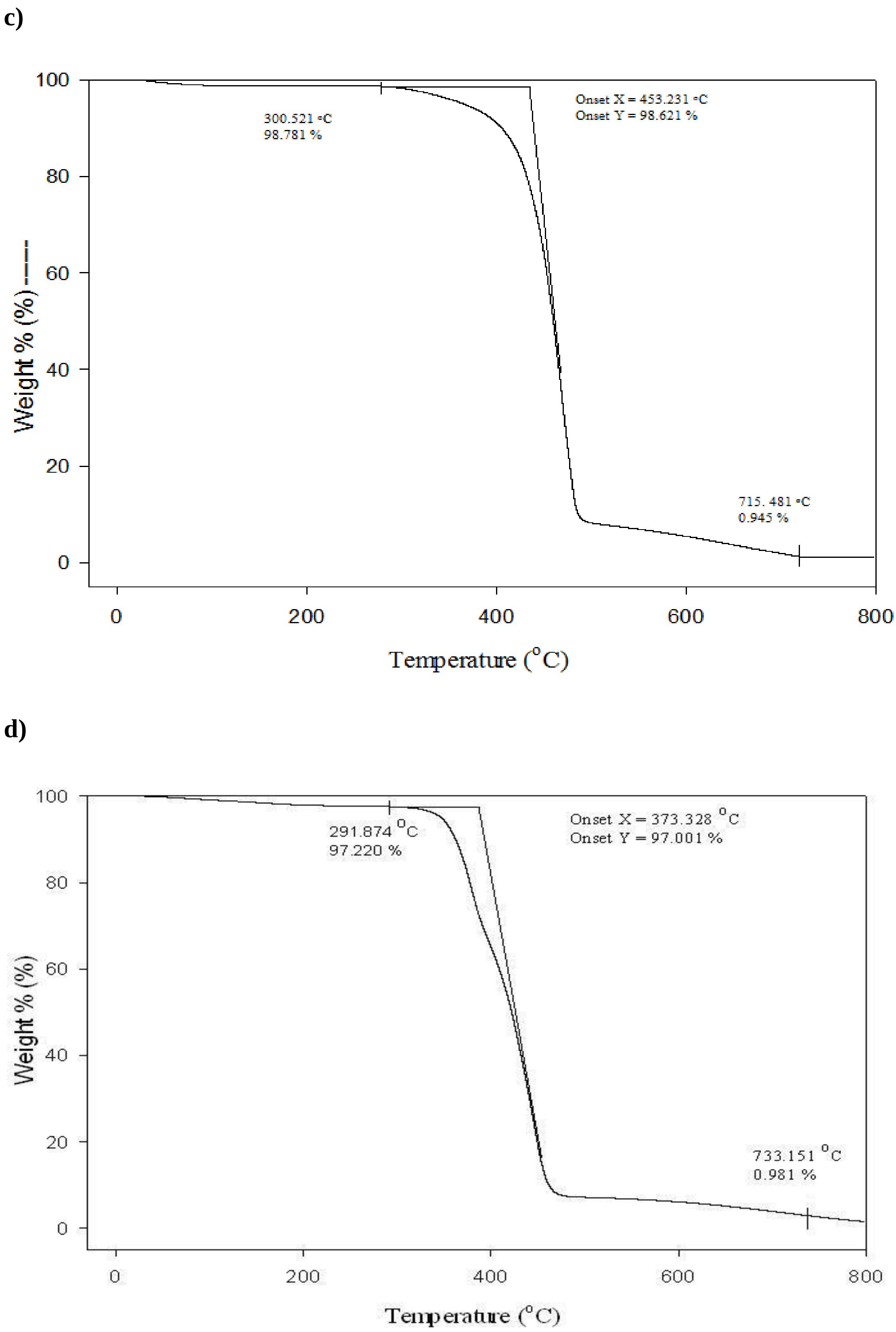

Figure 4.23: Plot of thermal decomposition of a) MDEA; b) [hmim][BF_4]; c) [hmim][Tf_2N]; d) [hmim][FAP] at a heating rate of 10 ^{o}C.min^{-1}.

4.5.1 Excess Molar Volumes

Volume of a mixture is not the sum of the volumes of the constituents (comprising it) as it is generally assumed. The volume of the mixture could either be higher or lower than the sum of the volumes of the constituents. This is due to the intermolecular forces present between the molecules of the constituents present in the mixture. These intermolecular forces could be more or less stronger causing the contraction or expansion in the volume of the mixture. This change in volume is represented by excess molar volume (V^E). The excess molar volume represents the difference between the molar volume of the real solution and the molar volume of the ideal solution (Deenadayalu et. al. 2010). The values of excess molar volumes could either be positive or negative. The positive values indicate the breakdown of the self associated molecules and the presence of non specific interaction between the components present in the mixture. On the other hand, the negative values of V^E indicate the presence of the strong intermolecular interaction (hydrogen bonding, packing effect and ion-dipole forces) between the associated molecules (Sovilj 2000; Vural et. al. 2011; Deenadayalu et. al. 2008). The excess molar volume (for binary mixture) could be calculated by the experimental densities of the pure components and mixture by using the following relation (Taib et. al. 2011):

$$V^E = \frac{x_1 M_1 + x_2 M_2}{\rho} - \frac{x_1 M_1}{\rho_1} - \frac{x_2 M_2}{\rho_2} \tag{4.3}$$

where ρ is the density of the mixture, x_1 and x_2 are the mole fractions of the pure components 1 and 2, respectively; and M_1 and M_2 are the molar masses of the pure components 1 and 2, respectively. The estimated excess molar volumes for the binary mixtures studied in the present work are listed in Table B-1 to B-3 of Appendix B.

4.5.1.1. Binary Mixtures

[hmim][Tf$_2$N] + MDEA System

The estimated excess molar volumes for the binary mixtures ([hmim][Tf$_2$N] (1) + MDEA (2)) are illustrated in Figure 4.24. The excess molar volumes showed positive deviations from ideality over the entire range of temperatures and concentrations.

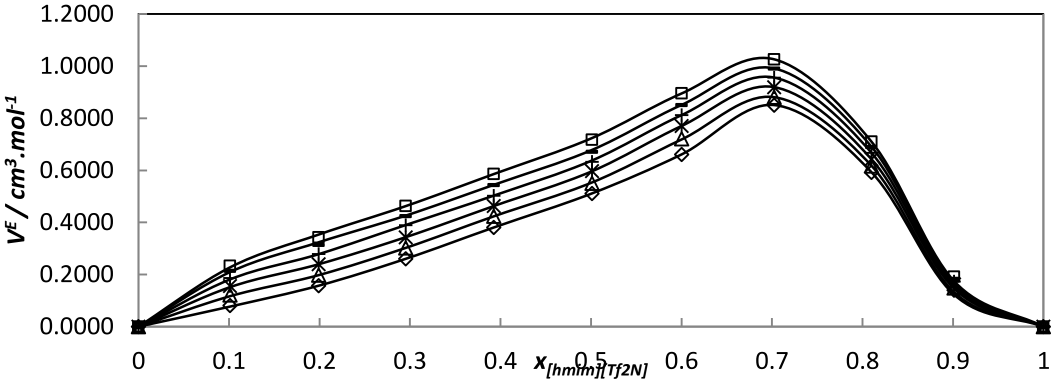

Figure 4.24. Excess Molar Volume V^E vs mole fraction of IL, for the system [hmim][Tf$_2$N] (1) + MDEA (2), at several temperatures: ◊, 298.15K; Δ, 303.15 K; *, 308.15 K, +, 313.15 K, -, 318.15 K, □, 323.15 K. The solid curves were calculated by using $\rho_{(cal)}$ (which was obtained by using Eq. 4.1).

It indicated that the interaction between [hmim][Tf$_2$N] and MDEA was not a strong one. Excess molar volumes depend on the concentration of components (either [hmim][Tf$_2$N] or MDEA) involved. However the excess molar volumes changed predominantly with a change in concentration of [hmim][Tf$_2$N]. The positive values of excess molar volumes increased with an increase in mole fraction of [hmim][Tf$_2$N], reaching a maximum at $x_{[hmim][Tf2N]}$ = 0.7023. After that point with increase in mole fraction of [hmim][Tf$_2$N] the positive values decreased sharply. It can be seen that in [hmim][Tf$_2$N] rich areas; $x_{[hmim][Tf2N]}$ = (0.8101, 0.9011) the positive values showed a sharp decrease as compared to the gradual decrease in MDEA rich areas. It could be inferred that as long as the concentration of MDEA *or* [hmim][Tf$_2$N] were significant (in MDEA rich area also, $x_{[hmim][Tf2N]}$ = (0.1010, 0.1990)) the positive values of V^E were less. It is well known that the positive values of V^E occur when the components present in the mixture experience structural breaking effects (Vural et. al. 2011). Hence as long as the concentration of either component was significant, they suppressed structural breaking effects. The V^E values increased gradually until $x_{[hmim][Tf2N]}$ = 0.7023 but after that point there is a sudden decrease in these. It could be inferred that in mixtures when the concentration of MDEA is very low ($x_{[hmim][Tf2N]}$ = 0.8101, 0.9011) [hmim][Tf$_2$N] strongly and sharply overcame the structural breaking effects. Excess molar volume values showed more positive behavior at higher temperatures. It showed that the weak forces of interaction present between [hmim][Tf$_2$N] and MDEA were further weakened by an increase in temperature as expected.

[hmim][BF$_4$] + MDEA System

The excess molar volumes for the system ([hmim][BF$_4$] +MDEA) showed positive behaviour over the entire range of temperatures and concentrations (Figure 4.25). The positive values of excess molar volumes arise from the weak dipole-dipole interaction or dispersion forces present between unlike molecules due to the rupture of hydrogen bond. The positive values suggest that structural breaking effects of the components are dominant in these mixtures (Sovilj et. al. 2000). The positive values of V^E for the binary mixtures increased with an increase in mole fraction of [hmim][BF$_4$], reaching a maximum at $x_{[hmim][BF4]}$ = 0.7091. After that point with increase in concentration of [hmim][BF$_4$] the V^E values decreased. At higher temperatures the V^E values showed more positive behaviour. It indicated that with increase in temperature the weak forces of interaction between [hmim][BF$_4$] and MDEA were further weakened as expected.

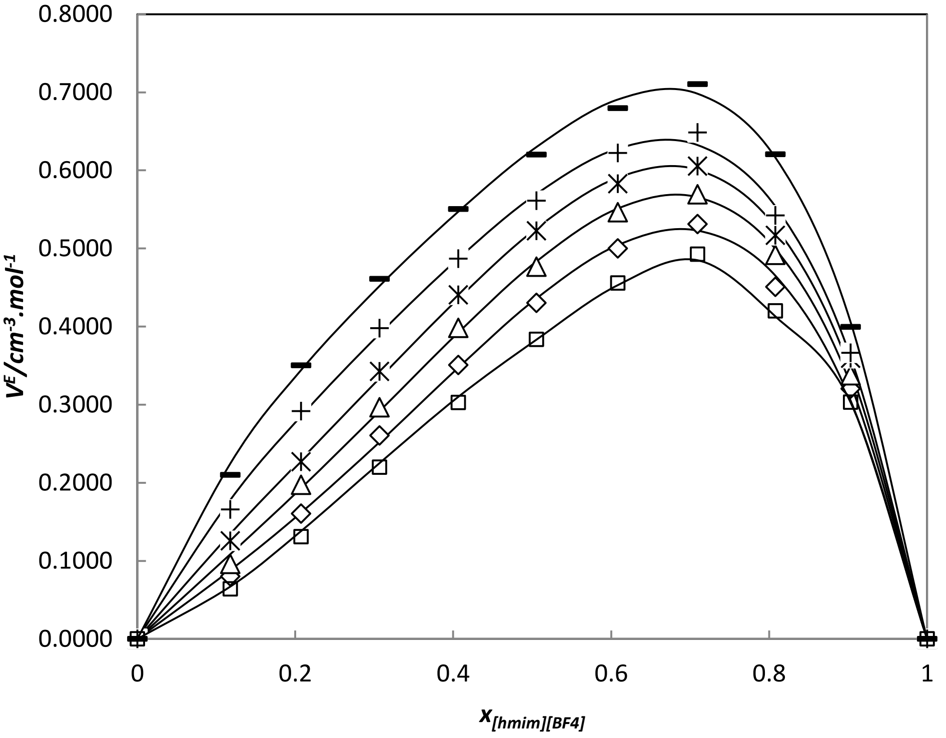

Figure 4.25. Excess Molar Volume V^E vs mole fraction of IL, for the system [hmim][BF$_4$] (1) + MDEA (2), at several temperatures: □, 298.15 K; ◊, 303.15 K; Δ, 308.15 K; *, 313.15 K; +, 318.15 K; -, 323.15 K. The solid curves were calculated by using $\rho_{(cal)}$ (which was obtained by using Eq. 4.1).

[hmim][FAP] + MDEA System

The excess molar volumes for the system ([hmim][FAP]+MDEA) are illustrated in Figure 4.26. The excess molar volumes showed positive behaviour over the entire range of concentrations and temperatures. The positive values of excess molar volumes indicate that the non-specific forces of interaction are present between [hmim][FAP] and MDEA molecules. The [hmim][FAP] and MDEA molecules present in the mixture have undergone the structural breaking effect (Vural et. al. 2011). The positive values of excess molar volumes increased with an increase in mole fraction of [hmim][FAP] and reached a maximum value at $x_{[hmim][FAP]}$ = 0.5999. After that point with increase in mole fraction of [hmim][FAP] the positive values of excess molar volumes decreased. The positive values of excess molar volumes increased with an increase in temperature. It could be inferred that the weak forces of interactions present between the molecules were further weakened due to a rise in temperature.

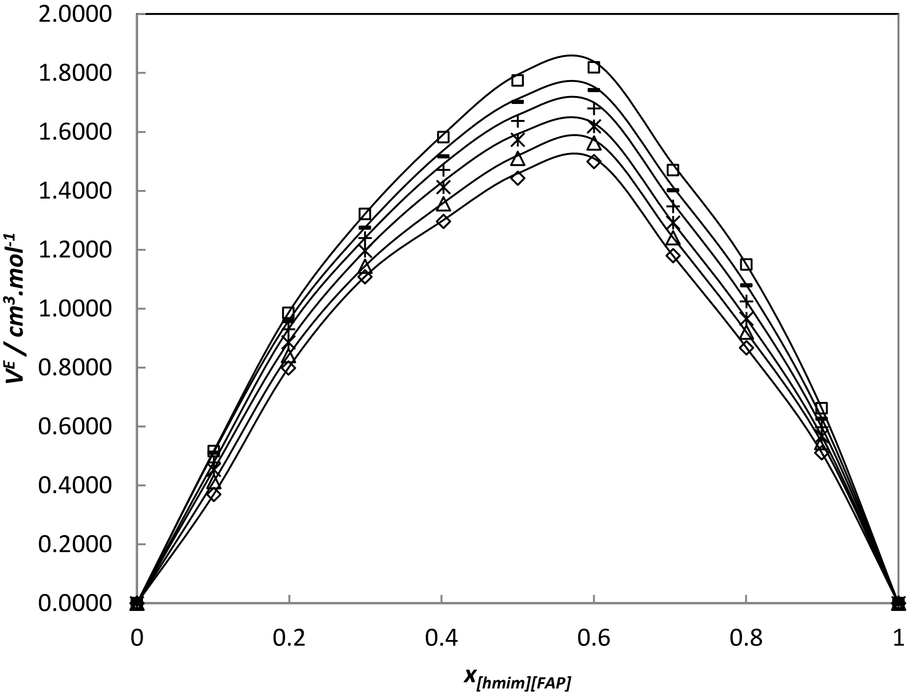

Figure 4.26. Excess Molar Volume V^E vs mole fraction of IL, for the system [hmim][FAP] (1) + MDEA (2), at several temperatures: ◊, 298.15K; Δ, 303.15 K; *, 308.15 K, +, 313.15 K, -, 318.15 K, □, 323.15 K. The solid curves were calculated by using $\rho_{(cal)}$ (which was obtained by using Eq. 4.1).

The values of excess molar volumes changed predominantly with variation in concentration of either pure component ([hmim][FAP] *or* MDEA). In [hmim][FAP] rich areas ($x_{[hmim][FAP]}$ = 0.8003, 0.8993) or in MDEA rich areas ($x_{[hmim][FAP]}$ = 0.1007, 0.1989) excess mole volume values were less positive indicating the ability of the pure solvents to oppose the structural breaking effects while one is in high concentration as compared to the other constituent comprising the mixture.

4.5.2 Viscosity Deviations

The mixture exhibits different viscosity values from the corresponding pure components. These changes in viscosity help to assess the type of intermolecular interactions present between the molecules of the pure components comprising the mixture. These changes in viscosity values are termed as viscosity deviations ($\Delta\eta$). The viscosity deviations for a mixture are deduced from the experimental viscosity of the mixture and pure components. The magnitude of $\Delta\eta$ values from the ideality of the system could be zero, negative or positive. According to Fort and Moore (1966) negative values of viscosity deviation occur in the mixtures of components having unequal size and in which dispersion forces are present (Sinha 2010). On the other hand, the positive values of viscosity deviations are attributed to the presence of specific interaction (self association of molecules via inter and intra molecular hydrogen bonding) between the molecules of the constituents comprising the mixtures (Diwedi and Singh 2007; Li et. al. 2009).

The viscosity deviations for the binary mixtures could be estimated by using the following relation (Iloukhani and Rakhshi 2009):

$$\Delta\eta = \eta - x_1\eta_1 - x_2\eta_2 \tag{4.4}$$

where η, η_1 and η_2 are the dynamic viscosities of the mixture, pure component 1, and pure component 2, respectively. x_1 and x_2 are the mole fractions of the pure component 1 and 2, respectively. The estimated viscosity deviations for the binary mixtures ([hmim][BF_4]+MDEA, [hmim][Tf_2N]+MDEA and [hmim][FAP]+MDEA) are listed in Table B-4 to B-6 of the Appendix B.

4.5.2.1. Binary Mixtures

[hmim][BF$_4$] + MDEA System

The viscosity deviations for the binary mixtures of [hmim][BF$_4$] with MDEA showed negative values over the entire range of temperatures and concentrations. The viscosity deviation values increased with increase in the mole fraction of [hmim][BF$_4$] and reached the maximum at $x_{[hmim][BF4]}$ = 0.5051 (Figure 4.27). After that point with increase in mole fraction of [hmim][BF$_4$] the viscosity deviation values decreased. The viscosity deviation values showed more negative behaviour at higher temperatures as expected. The negative values of viscosity deviations indicate the presence of dispersion forces between the molecules of the constituents comprising the mixture. Furthermore negative values of viscosity deviations occur when the viscosities of the associates formed between unlike molecules are relatively less than those for the pure components (Cwiklinska and Kinart 2011).

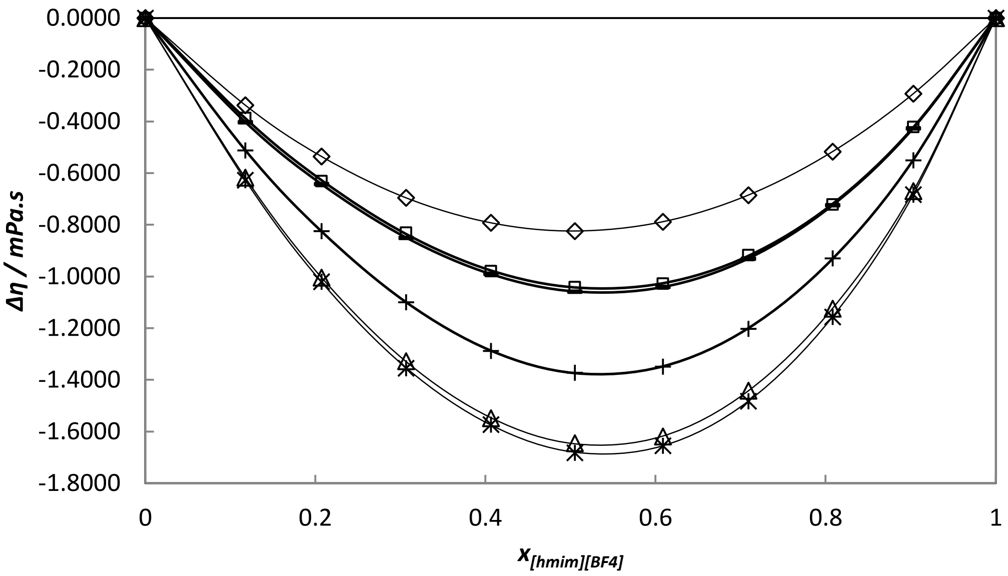

Figure 4.27. Viscosity deviation $\Delta\eta$ vs mole fraction of IL, for the system [hmim][BF$_4$] (1) + MDEA (2), at several temperatures ,◊ 298.15K; □, 303.15 K; -, 308.15 K, +, 313.15 K, Δ, 318.15 K, *, 323.15 K. The solid curves were calculated by using $\eta_{(cal)}$ (which was obtained by using Eq. 4.1).

[hmim][Tf_2N] + MDEA System

The viscosity deviations for the system ([hmim][Tf_2N]+MDEA) showed negative behaviour over the entire range of temperatures and concentrations similar to those of ([hmim][BF_4]+MDEA) system. The values of viscosity deviations increased with increase in mole fraction of [hmim][Tf_2N] and reached a maximum at ($x_{[hmim][Tf2N]}$ = 0.5012) (Figure 4.28).

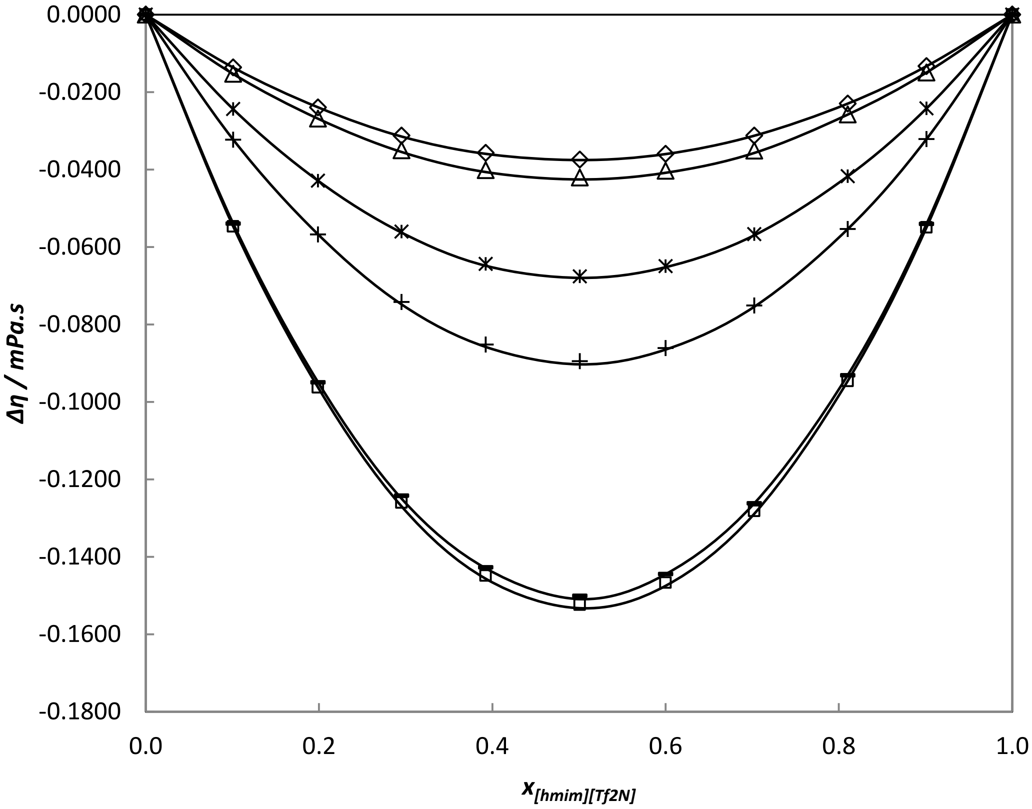

Figure 4.28. Viscosity deviation $\Delta\eta$ vs mole fraction of IL, for the system [hmim][Tf_2N] (1) + MDEA (2), at several temperatures , ◊, 298.15K; Δ, 303.15 K; *, 308.15 K, +, 313.15 K, -, 318.15 K, □, 323.15 K. The solid curves were calculated by using $\eta_{(cal)}$ (which was obtained by using Eq. 4.1).

After that point with increase in mole fraction of [hmim][Tf_2N] the viscosity deviation values decreased. The viscosity deviation values showed more negative values at higher temperatures. The negative values of viscosity deviation occur when the constituents of the mixture have different molecular sizes and the dispersion forces are present between the molecules (Doghaei et. al. 2010).

[hmim][FAP] + MDEA System

The viscosity deviations values for the binary mixtures of [hmim][FAP] with MDEA increased with increase in mole fraction of [hmim][FAP] and reached the maximum value at $x_{[hmim][FAP]}$ = 0.5001. After that point with an increase in mole fraction of [hmim][FAP] the viscosity deviation values decreased (Figure 4.29).

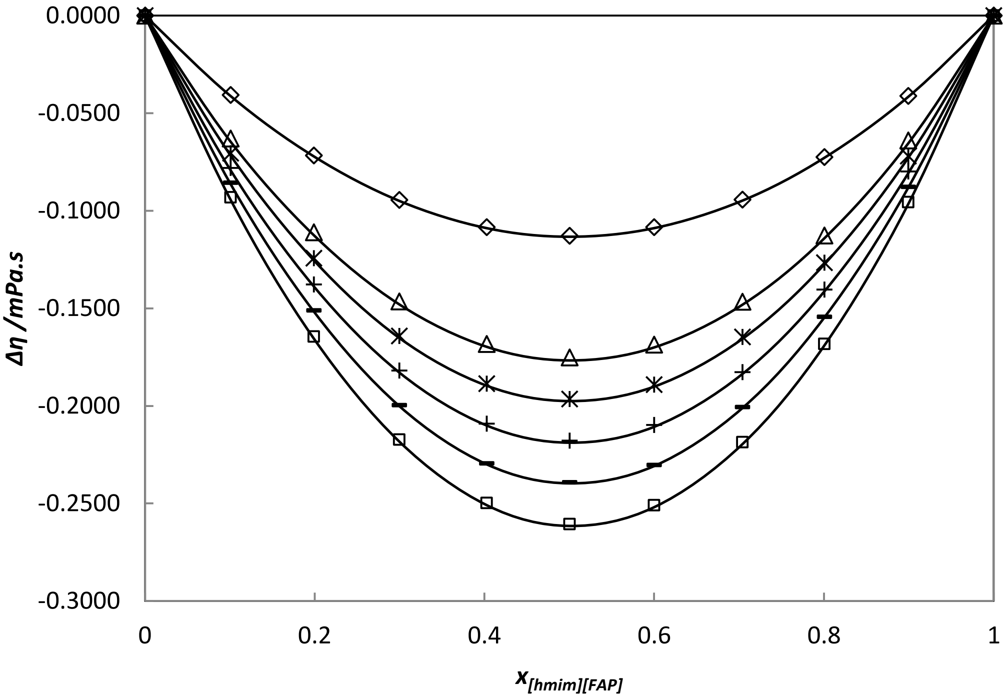

Figure 4.29. Viscosity deviation $\Delta\eta$ vs mole fraction of IL, for the system [hmim][FAP] (1) + MDEA (2), at several temperatures , ◊, 298.15K; Δ, 303.15 K; *, 308.15 K, +, 313.15 K, -, 318.15 K, □, 323.15 K. The solid curves were calculated by using $\eta_{(cal)}$ (which was obtained by using Eq. 4.1).

The viscosity deviations for the system ([hmim][FAP]+MDEA) showed negative trend over the entire range of temperatures and concentration, similar to the $\Delta\eta$ values for the ([hmim][Tf_2N]+MDEA) and ([hmim][BF_4]+MDEA) systems. The negative values of viscosity deviations increased with increase in temperature (Figure 4.29). The negative values of viscosity deviations indicate the presence of dispersion forces between the [hmim][FAP] and MDEA molecules, comprising the mixtures (Iloukhani and Rakhshi 2009).

4.5.3 Refractive Index Deviations

Refractive index deviation like other excess properties (excess molar volumes and viscosity deviations) is also an important property. The refractive index deviations for a mixture are calculated from the experimental refractive index values of the components comprising the mixture. The refractive index deviations depend not only upon the molecular interactions between the species present in the mixture but also on the size and shape of the molecules. The refractive index deviations (for a binary mixture) can be calculated by using the following relation (Iloukhani and Rakhshi 2009):

$$\Delta n_D = n_D - x_1 n_{D1} - x_2 n_{D2} \tag{4.5}$$

where n_D, n_{D1} and n_{D2} are the refractive index of the mixture, pure component 1 and pure component 2 respectively. x_1 and x_2 are the mole fractions of the pure component 1 and 2 respectively. The estimated refractive index deviations for the binary mixtures under study are listed in Table B-7 to B-9 of Appendix B.

4.5.3.1. Binary Mixtures

[hmim][BF$_4$] + MDEA System

The estimated refractive index deviations for the system ([hmim][BF$_4$]+MDEA are graphically represented as a function of mole fraction of [hmim][BF$_4$] (Figure 4.30). The refractive index deviations showed negative values over the entire range of temperatures and concentrations studied. The negative values of refractive index deviations increased with an increase in mole fraction of [hmim][BF$_4$] and reached a maximum at $x_{[hmim][BF4]}$ = 0.5051. After that with increase in mole fraction of [hmim][BF$_4$] the refractive index deviation values decreased. The refractive index deviations decreased with increasing temperature. Negative values of refractive index deviation indicate that the strength of specific interaction is not the only influencing factor in refractive index deviations, whereas molecular size and shape of [hmim][BF$_4$] and MDEA molecules also played an important role (Bhatia et. al. 2011).

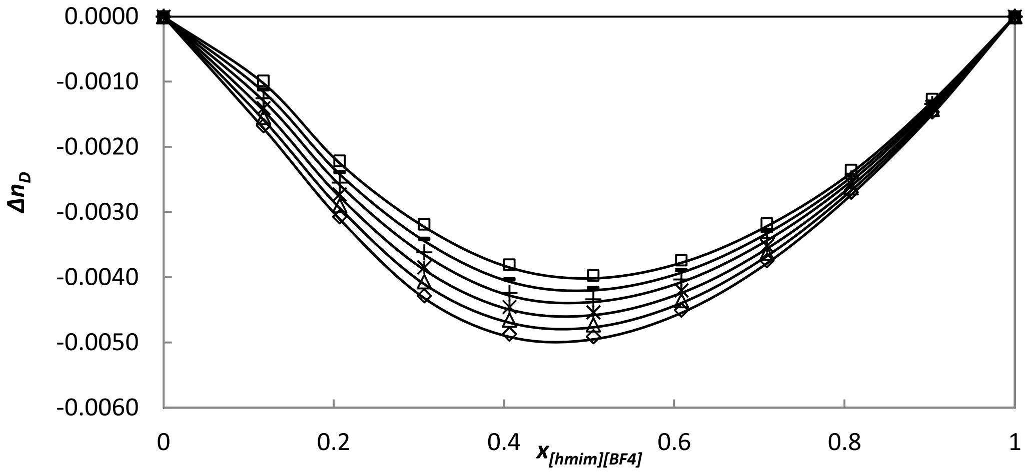

Figure 4.30. Refractive index deviations Δn_D vs mole fraction of IL, for the system [hmim][BF$_4$] (1) + MDEA (2) at several temperatures. ◊, 298.15 K; Δ, 303.15 K; *, 308.15 K; +, 313.15 K; -, 318.15 K; □, 323.15 K. The solid curves were calculated by using $n_{D(calc)}$ (which was obtained by using Eq. 4.1).

[hmim][Tf$_2$N] + MDEA System

The refractive index deviations for the binary mixtures of [hmim][Tf$_2$N] with MDEA showed negative behaviour over the entire range of temperatures and concentrations (Figure 4.31).

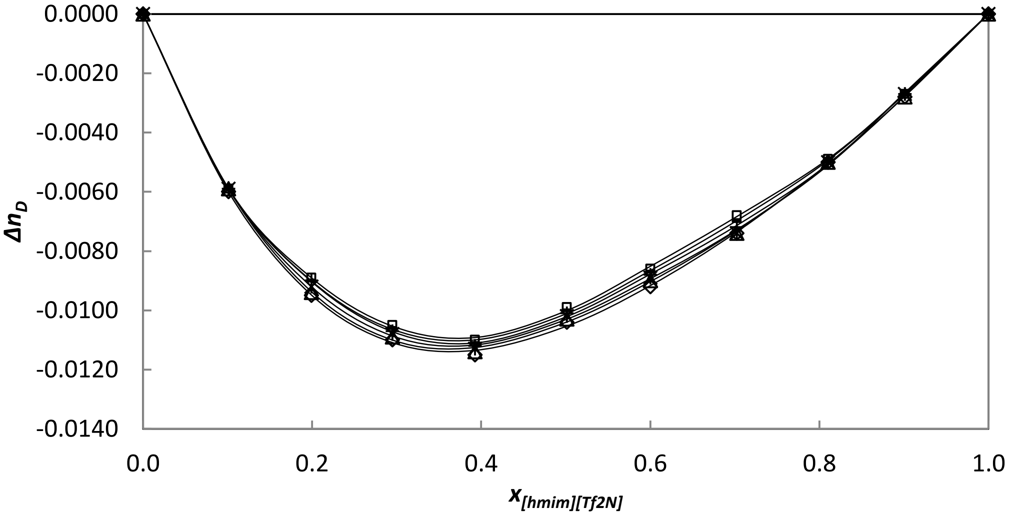

Figure 4.31. Refractive index deviations Δn_D vs mole fraction of IL, for the system [hmim][Tf$_2$N] (1) + MDEA (2) at several temperatures. ◊, 298.15 K; Δ, 303.15 K; *, 308.15 K; +, 313.15 K; -, 318.15 K; □, 323.15 K. The solid curves were calculated by using $n_{D(calc)}$ (which was obtained by using Eq. 4.1).

The negative values of refractive index deviations increased with increasing in mole fraction of [hmim][Tf$_2$N] and reached a maximum at $x_{[hmim][Tf2N]} = 0.3925$. After that point with increase in mole fraction of [hmim][Tf$_2$N] the refractive index deviations decreased.The values of refractive index deviations decreased with increasing temperature. The negative values of refractive index deviations indicate the presence of dispersion forces between the [hmim][Tf$_2$N] and MDEA molecules present in the mixture (Iloukhani and Rakhshi 2009).

[hmim][FAP] + MDEA System

The refractive index deviation values for the binary system [hmim][FAP]+MDEA showed negative trend similar to the Δn_D values for the [hmim][BF$_4$]+MDEA and [hmim][Tf$_2$N]+MDEA systems and the same trend was observed over the entire range of temperatures and concentrations studied (Figure 4.32).

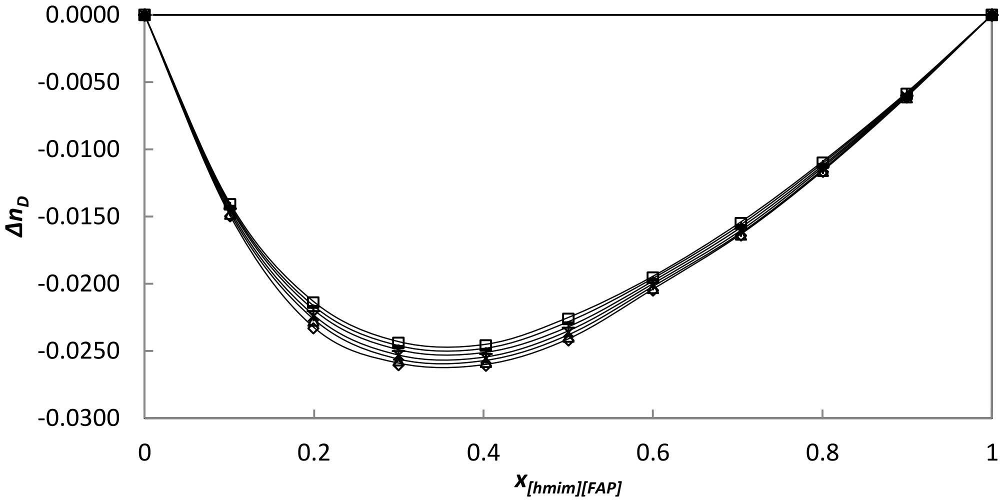

Figure 4.32. Refractive index deviations Δn_D vs mole fraction x_1 for the system [hmim][FAP] (1) + MDEA (2) at several temperatures. ◊, 298.15 K; Δ, 303.15 K; *, 308.15 K; +, 313.15 K; -, 318.15 K; □, 323.15 K. The solid curves were calculated by using $n_{D(calc)}$ (which was obtained by using Eq. 4.1).

The refractive index deviation values increased with increase in mole fraction of [hmim][FAP] and reached a maximum at $x_{[hmim][FAP]}$ = 0.4026. After that point with increase in mole fraction of [hmim][FAP] the refractive index deviations decreased. The refractive index deviation values showed less negative behaviour at higher temperatures. The negative values of refractive index deviations indicate that the strength of specific interaction is not the only factor contributing to these rather the shape and size of the MDEA and [hmim][FAP] also played an equal and important part (Bhatia et. al. 2011). It was observed that refractive index deviations (Δn_D) were negative for all the studied binary systems ([hmim][BF$_4$]+MDEA,

[hmim][Tf_2N]+MDEA and [hmim][FAP]+MDEA). The Δn_D values for the [hmim][FAP]+MDEA system were higher in comparison to those for [hmim][Tf_2N]+MDEA and [hmim][BF_4]+MDEA systems (Figures 4.30 to 4.32). According to Nakata and Sakurai (1987) the sign of Δn_D is opposite to that of V^E (excess molar volumes) if the refractive index behaviour is not too non linear between n_{D1} and n_{D2} (refractive index of the pure component 1 and 2 respectively, comprising the binary mixture). The Δn_D values of the binary mixtures under study show a similar trend with opposite sign as their corresponding V^E values. Since the V^E are positive (Figures 4.24 to 4.26) and Δn_D values are negative, according to Brocos et. al. (2003), the refractive index deviations could be interpreted as sign reversed measure of the deviation of reduced free volume from ideality and consequently of changes in intermolecular interaction (Bhatia et. al. 2011). The negative values of refractive index deviations for the systems under study follow the order: [hmim][FAP]>[hmim][Tf_2N]>[hmim][BF_4]. These results correlate well with the V^E data for these systems.

Correlation of Excess Molar Volumes, Refractive Index and Viscosity deviations

The excess molar volumes (V^E), viscosity deviations ($\Delta\eta$) and refractive index deviations (Δn_D) were calculated with the experimental values of density, viscosity and refractive index, respectively. These excess and deviation properties were later estimated with the help of the calculated densities (ρ_{calc}), viscosities (η_{calc}) and refractive indices (n_{Dcalc}) values (which were obtained with the help of Eq. 4.1). Eq. (4.1) represents the estimation of these properties as a function of both mole fraction and temperature simultaneously. The experimental and calculated (dependencies on Eq. 4.1) were later drawn side by side (Figurues 4.24 to 4.32) to compare these. The estimated V^E, $\Delta\eta$ and Δn_D (obtained with the help of ρ_{calc}, η_{calc} and n_{Dcalc}) fairly agreed with the experimental data. The estimated deviations (obtained with the help of Eq. 4.2) were 6.5578×10^{-04}, 6.6517×10^{-04} and 6.4529×10^{-04} for V^E, $\Delta\eta$ and Δn_D respectively.

4.6 Solubility of CO_2

In the present study CO_2 solubilities were measured in seven pure ionic liquids namely; 1-hexyl-3-methylimidazolium tetrafluoroborate ([hmim][BF_4]), 1-hexyl-3-methylimidazolium bis(trifluromethylsulfonyl)imide ([hmim][Tf_2N]), 1-hexyl-3-methylimidazolium tris(pentafluoroethyl) triflurophosphate ([hmim][FAP]), 1-butyl-3-methylimidazolium tetrafluoroborate ([bmim][BF_4]), 1-butyl-3-methylimidazolium tris(pentafluoroethyl)trifluorophosphate ([bmim][FAP]), 1-butyl-3-methylimidazolium bis(trifluoromethylsulfonyl)imide ([bmim][Tf_2N]), bis(2-hydroxyethyl)ammonium acetate ([bheaa]) and one pure alkanolamine namely; MDEA. The binary mixtures used for CO_2 solubility were [hmim][BF_4]+MDEA, [hmim][Tf_2N]+MDEA, [hmim][FAP]+MDEA, [bmim][BF_4]+MDEA, [bmim][Tf_2N]+MDEA, [bmim][FAP]+MDEA and [bheaa]+MDEA. The CO_2 solubility experiments were performed in three phases. In the first phase, CO_2 absorption was measured in pure liquid namely; [hmim][BF_4], [hmim][Tf_2N], [hmim][FAP], MDEA as well as for their binary mixtures ([hmim][FAP]+MDEA, [hmim][TF_2N]+MDEA, [hmim][BF_4]+MDEA at eight different pressures between (100 to 3000) kPa and at three different temperatures (298.15, 313.15, 323.15) K. In the second phase pure ILs; [bmim][FAP], [bmim][Tf_2N], [bmim][BF_4], [bheaa] and their binary mixtures with MDEA were examined for CO_2 absorption. In the third phase aqueous IL mixtures comprising of ILs, 1-ethyl-3-methylimidazolium tris(pentafluoroethyl)trifluorophosphate ([emim][FAP]) or 1-ethyl-3-methylimidazolium bis(trifluoromethylsulfonyl)imide ([emim][Tf_2N]) with MEA or DEA were utilized for CO_2 absorption. The CO_2 solubility experiments for second and third phases were carried out at T=298.15 K and eight different pressures between (100 to 3000) kPa. The CO_2 solubility was measured by using SOLTEQ high pressure solubility cell and employing pressure drop method, CO_2 pressure commenced to decrease as it was enclosed with the solvent, due to the start of solubility. The pressure drops in the pure solvents ([hmim][FAP], [hmim][Tf_2N], [hmim][BF_4]) as well as in their binary mixtures at T = 298.15 K and for the pressure range of ≤ 3000 kPa are illustrated in Figure C-1 to C-7 of Appendix C. Prior to measure CO_2 solubilites in the solvents used in the present study the apparatus was validated by measuring the CO_2 solubility in the solvents of known/established CO_2 solubility. The comparisons of the measured CO_2 solubilities in pure [hmim][BF_4], [hmim][Tf_2N], [hmim][FAP] and 50% aqueous MDEA solution with the available literature values are shown in Figures 4.33 to 4.36. The measured CO_2 solubility values for pure [hmim][BF_4] (calculated deviations $<$ 2.3 %) and 50% aqueous MDEA (calculated deviation $<$ 2.1 %) showed a fair agreement with the available literature values. The minor differences could be attributed to the presence of the impurities in the liquids. Aki et. al. (2004) reported that the presence of impurities like water content, halide content in the ILs greatly influence their CO_2 absorption capability.

4.6.1. CO_2 solubility in pure liquids

The CO_2 solubility data of the pure liquids ([hmim][BF_4], [hmim][Tf_2N], [hmim][FAP], MDEA) at temperatures T = (298.15, 313.15, 323.15) K is listed in Table C-1 of the Appendix C and illustrated in Figure 4.37. It can be seen that among the pure liquids [hmim][FAP] shows highest CO_2 solubility. The CO_2 solubility in pure liquids followed the order; [hmim][FAP]>[hmim][Tf_2N]>MDEA>[hmim][BF_4]. The same trend was observed over the entire temperature range. The CO_2 solubility in the pure ILs ([hmim][FAP]>[hmim][Tf_2N]>[hmim][BF_4]) is in accordance with the available literature data. Cadena et. al. 2004 concluded that ILs with [Tf_2N] anions exhibited higher CO_2 solubility in comparison with the ILs with [BF_4] anions. Similarly, Muldoon et. al. 2007 concluded that ILs with [FAP] anions showed greater CO_2 solubility in comparison with the ILs with [Tf_2N] anions. The pure MDEA also showed fairly good absorption by finding a position among the available ILs and even showing higher CO_2 solubility than pure [hmim][BF_4]. The ILs used in the present study have the same cation ([hmim]) coupled with different anions. The IL with [FAP] anion showed highest CO_2 solubility in comparison to those with [BF_4] and [Tf_2N] anions. This observed trend validates the major role of anion in CO_2 absorption. Blanchard et. al. 2001 conducted experiments to study the effect of anion on the solubility of CO_2 in ILs. They concluded that it is the anion which dominates the CO_2 solubility. They further reported that the ILs with fluorinated anions showed greater CO_2 solubility in comparison to the ILs with non fluorinated anions. The similar trend was also reported by Cadena et. al. (2004) while studying the CO_2 solubility in ILs with different anions. They also verified the pivotal role of anion in CO_2 absorption in ILs. The detailed discussion on the effects of anions on CO_2

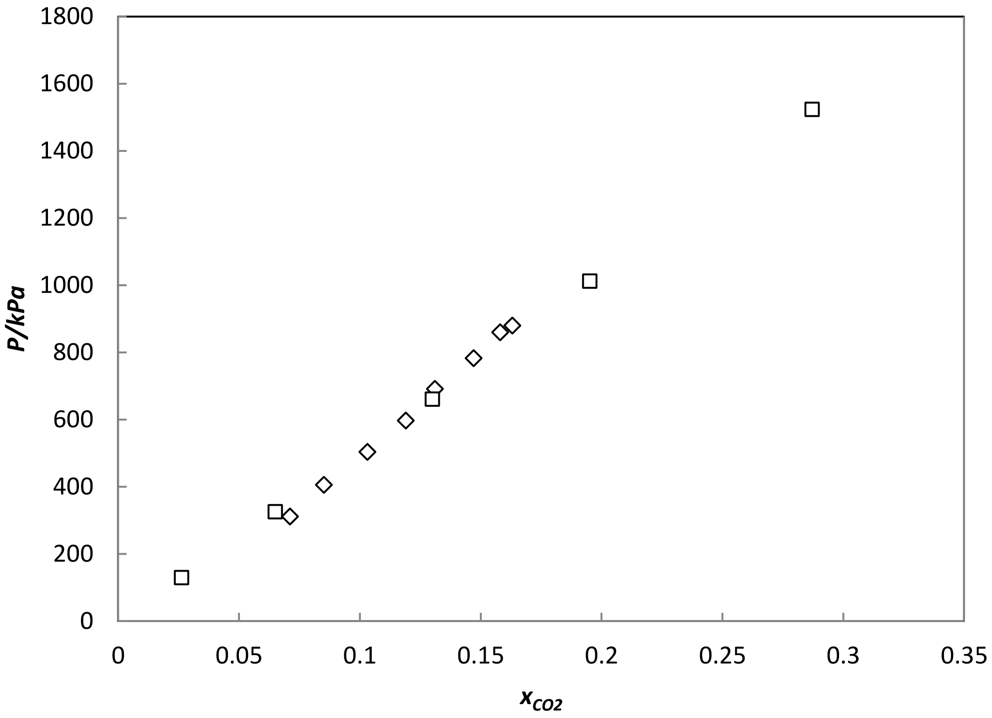

Figure 4.33. CO_2 solubility in [hmim][BF_4] at *T* = 298.15 K. □, This work; ◊, values from Kim et. al. 2005.

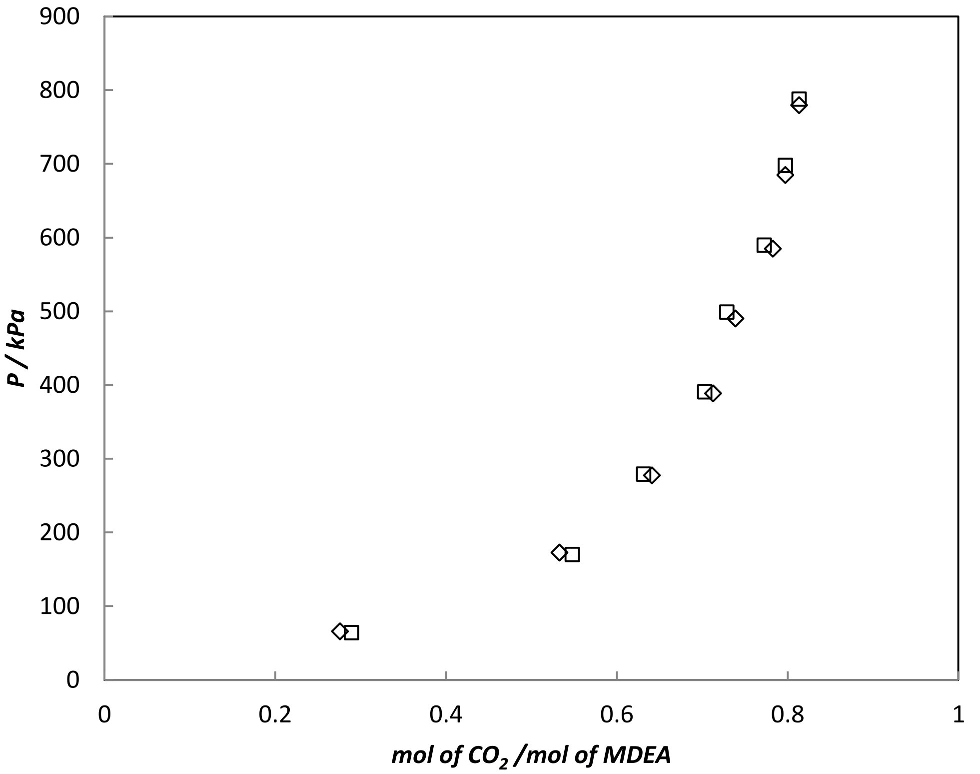

Figure 4.34. CO_2 solubility in 50% aq.MDEA solution at *T* = 328.15 K. □, This work; ◊, values from Ma'mun et. al. 2005.

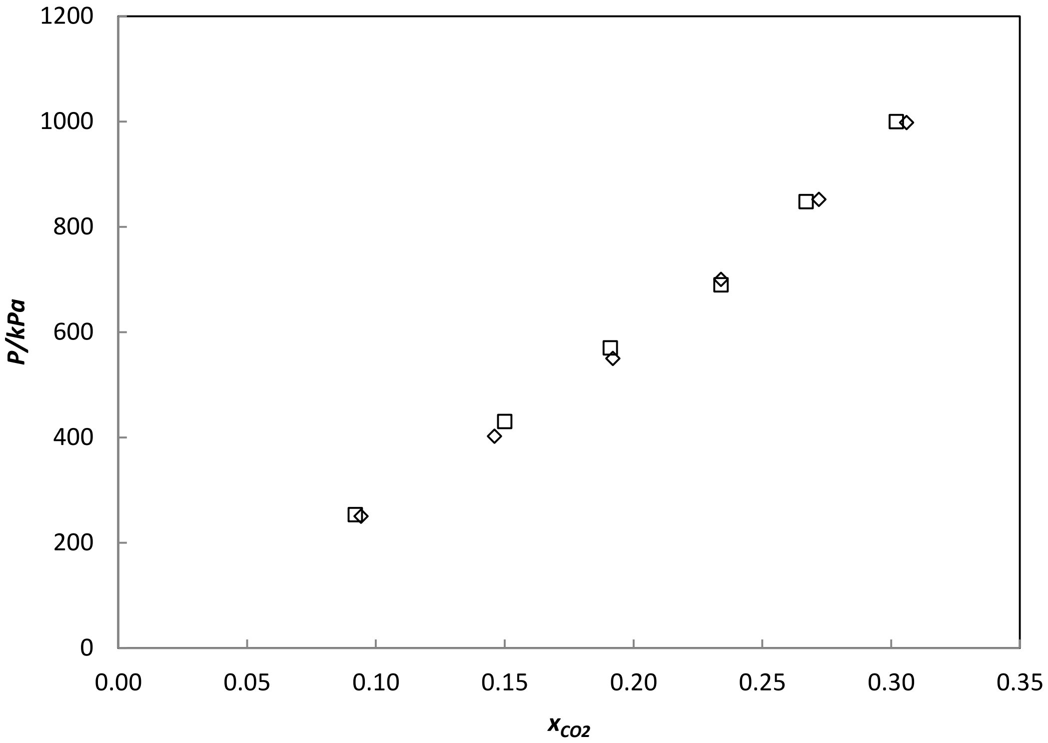

Figure 4.35. CO_2 solubiility in pure [hmim][FAP] at T = 298.15 K. □, This work; ◊, values from Muldoon et. al. 2007.

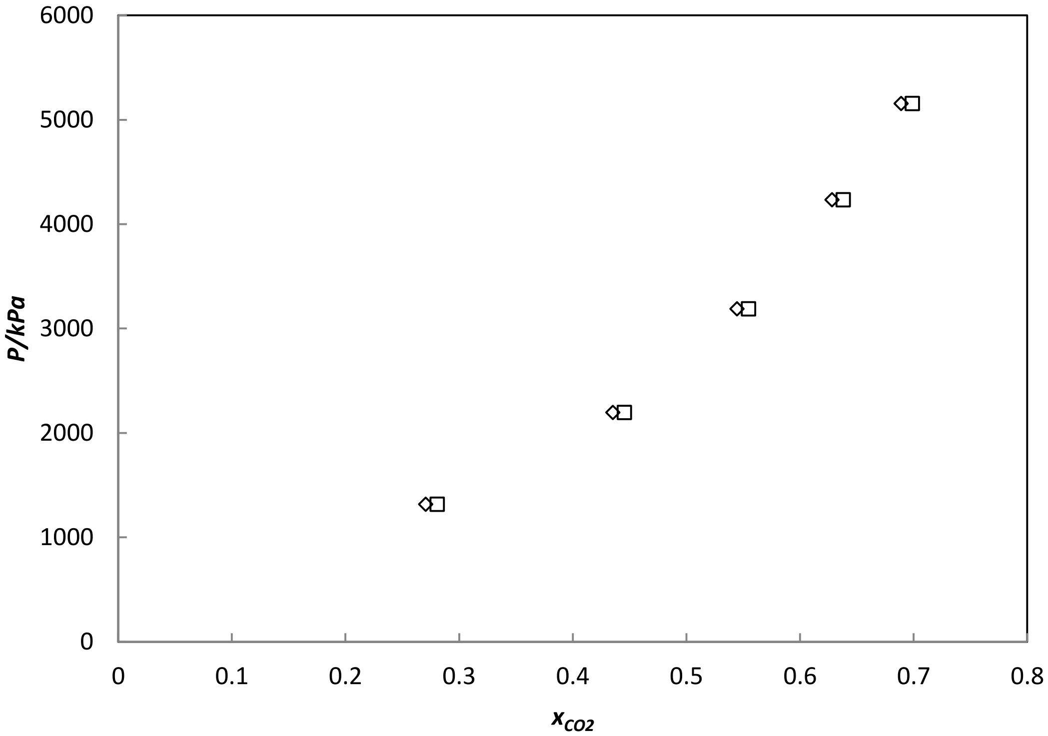

Figure 4.36. CO_2 solubility in pure [hmim][Tf_2N]. □, This work; ◊, values from Aki et. al. 2004.

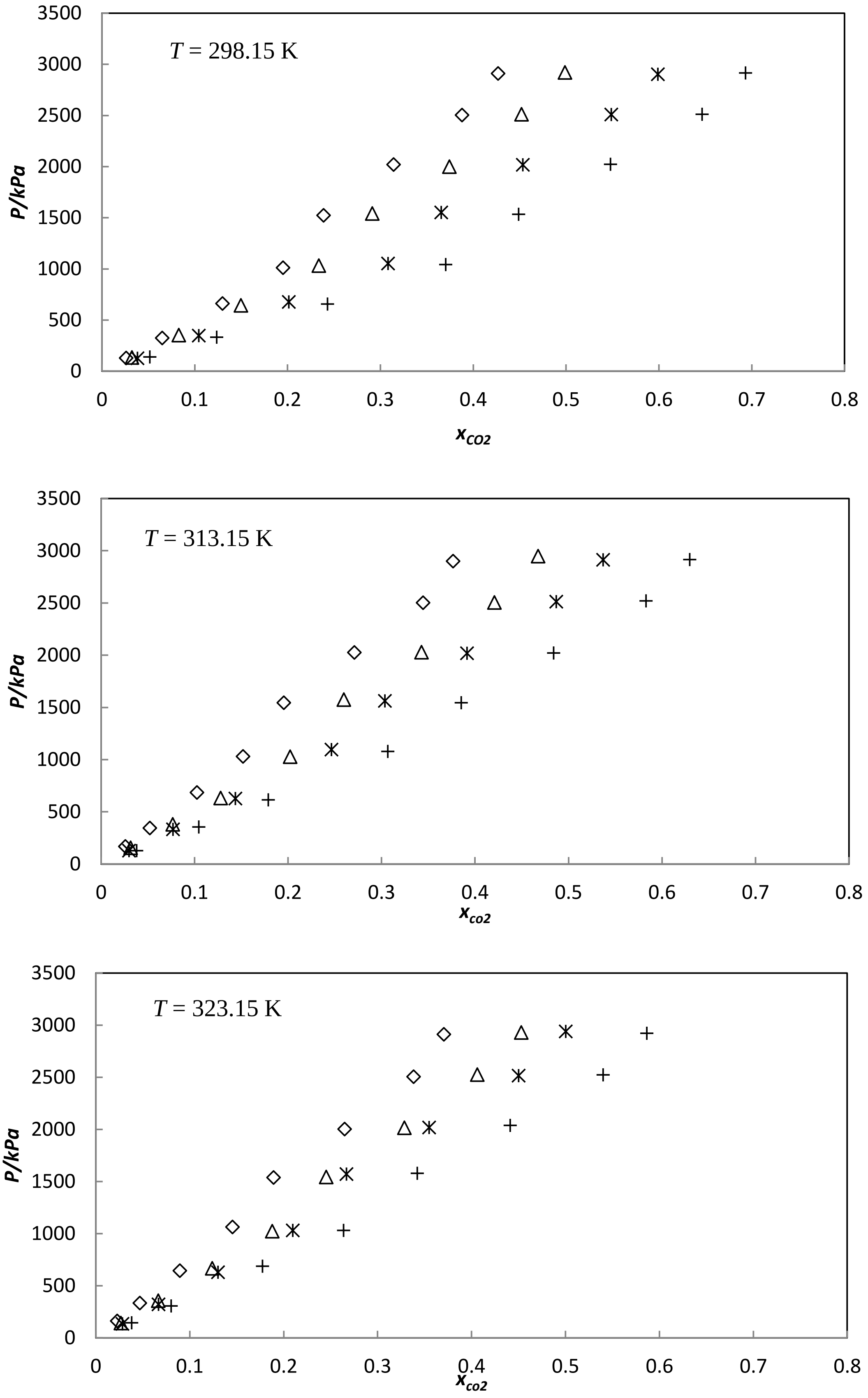

Figure 4.37. CO_2 solubility in the ionic liquids and amine: ◊, [hmim][BF_4]; Δ, MDEA; *, [hmim][Tf_2N]; +, [hmim][FAP].

solubility for the ILs studied in the present study has been discussed in the section 4.9. It was observed that the CO_2 solubility for all the pure solvents used in the present study decreased with increasing temperature (Figure 4.37). The pure liquids displayed lower values of CO_2 solubility at the fixed pressure conditions. This observed trend is also analogous to the one reported in the literature for the ILs and amines (Chakma and Meisen 1987; Aki et. al. 2004). Chen et. al. (2006) experimentally measured the CO_2 solubility in different imidazolium based ILs and observed that with increase in temperature the CO_2 solubility decreased in the ILs. Similar trends were also observed by many researchers (Blanchard et. al. 2001; Cadena et. al. 2004; Aki et. al. 2004), who reported the CO_2 solubility data in ILs. The decrease in CO_2 solubility with increase in temperature was also reported by many researchers who used aqueous solution of alkanolamines for the said purpose. Jou et. al. (1982) used aqueous solutions of MDEA to study the CO_2 solubility in these and concluded that with increase in temperature solubility decreased significantly. Chakma and Meisen (1987) reported the same trend that with increase in temperature CO_2 solubility decreased in the aqueous solutions of MDEA. The detailed discussion pertaining to the effect of temperature on CO_2 solubility in pure liquids as well as in the binary mixtures (solvents used in the present study) has been presented in section 4.8. The Henry's constants which are the function of temperature have been estimated; furthermore enthalpy and entropy changes in the solvents have also been evaluated and discussed. The CO_2 solubility increased linearly with increase in pressure, at the same condition of temperatures for all the pure solvents.

4.6.2. CO_2 solubility in the binary mixtures

The CO_2 solubility data for the binary mixtures of [hmim][BF_4]+MDEA, [hmim][Tf_2N]+MDEA and [hmim][FAP]+MDEA are listed in Tables C-2 to C-4 of the Appendix C. The mechanism of CO_2 solubility in the pure MDEA as well as its binary mixtures with ILs could be explained as physical solubility of CO_2. MDEA is a tertiary amine with no hydrogen atom attached to the nitrogen. The chemical reaction of CO_2 with MDEA occurs only when CO_2 dissolves itself in water to form a bicarbonate ion.

$$CO_2 + H_2O \rightleftharpoons HCO_3^- + H^+$$

The bicarbonate then undergoes an acid base reaction with amine to yield a chemical product. The overall reaction of CO_2 in the aqueous MDEA solution can be written as:

$$CO_2 + H_2O + R_2NCH_3 \rightleftharpoons HCO_3^- + R_2NHCH_3^+$$

Therefore in the absence of water the chemical reaction between MDEA and CO_2 cannot take place. Tertiary amines like *N*-methyldiethanolamine (MDEA) lack the N-H bond required to form the carbamate ion and therefore do not react directly with CO_2 and only physical absorption can take place in pure MDEA (Mohamadirad et. al. 2011). Versteeg and Swaaij (1988) studied the CO_2 absorption in the non aqueous solutions of MDEA and concluded that only physical absorption took place in the non aqueous solutions of MDEA. The ILs on the other hand also behave as physical solvents of CO_2 with no chemical reaction (Bara et. al. 2009). Therefore in the mixtures under study physical absorption is expected to take place. The CO_2 solubility in all the pure liquids as well as their binary mixtures increased linearly with increasing pressure which is a typical behavior of purely physical solubility (Kamps et. al. 2003). In this section each binary system has been discussed individually to understand the CO_2 solubility in these. The comparison among the pure liquids as well as their binary mixtures in terms of CO_2 has been explained for each binary system. The pure liquids and their respective binary mixtures have been analyzed in terms of CO_2 loadings. The binary mixtures used were having different concentrations of the IL to MDEA {molar ratio of IL to MDEA; (1:4), (1:1), (4:1)}.

[hmim][BF$_4$] + MDEA System

The Figure 4.38 shows the CO_2 solubility in the pure [hmim][BF_4], MDEA as well as in their binary mixtures at temperatures (298.15, 313.15, 323.15) K. It can be seen that among the pure liquids and binary mixtures, the binary mixture (1:4) shows the greatest and the binary mixture (4:1) shows the least CO_2 solubility. The solvents could be arranged in terms of CO_2 solubility as; (1:4)>MDEA>(1:1)>[hmim][BF_4]>(4:1). The similar trend was observed over the entire temperatures range. The binary mixture (1:4) showed 1.28 times higher CO_2 solubility in comparison to pure [hmim][BF_4]. However, with only 1.06 times higher CO_2 loadings in comparison to pure MDEA, the mixture (1:4) found a place quite closer to it (MDEA). The presence of less amount of IL in the mixtures resulted in enhanced CO_2 solubility. On the other hand, the presence of high concentration (4:1) of IL has badly affected the absorption. Ahmady et. al. (2010) reported the CO_2 absorption in the mixtures of [bmim][BF_4] with aqueous MDEA and noted a similar trend that in the mixtures slightly enhanced CO_2 absorption was observed when the concentration of IL was low, but for high concentrations of IL the mixtures suffered loss in solubility. It can be seen (Figure 4.38) that the CO_2 solubility in all the mixtures decreased with increase in temperature at a fixed pressure conditions and at the same time the CO_2 solubility increased with increase in pressure as expected.

[hmim][Tf_2N] + MDEA System

The CO_2 solubility data in the pure [hmim][Tf_2N], MDEA as well as their binary mixtures at temperatures (298.15, 313.15, 323.15) K is graphically illustrated in Figure 4.39 as a function of mole fraction of CO_2. It can be seen that among the pure liquids (MDEA, [hmim][Tf_2N]) and their binary mixtures, pure [hmim][Tf_2N] has the highest solubility over the entire range of temperature. The solvents could be arranged in terms of CO_2 solubility as [hmim][Tf_2N]>(4:1)>MDEA>(1:1)>(1:4). The similar trend was observed over the entire range of temperatures. The mixture (4:1) is quite closer to pure [hmim][Tf_2N] in terms of CO_2 loading with only 0.92 times lower values of absorption from it. On the other hand, the mixture (1:4) showed the least CO_2 solubility with 1.44 times lower value than pure [hmim][Tf_2N] and 1.15 times lower values than the pure MDEA. The mixtures (4:1) showed lower values of CO_2 solubility than pure IL. It means that the addition of even the small amount of MDEA in the pure IL has decreased its solubility. This is due to the fact that pure [hmim][Tf_2N] has higher CO_2 solubility than pure MDEA (Figure 4.37). When MDEA was added to it the contribution of [hmim][Tf_2N] towards CO_2 absorption was reduced and these could not work independently as MDEA molecules had suppressed their capabilities. Similarly the presence of small amount of [hmim][Tf_2N] resulted in the decrease in CO_2 solubility for pure MDEA. The capabilities of MDEA molecules were disturbed due to the presence of [hmim][Tf_2N] molecules. The CO_2 solubility in all the binary mixtures decreased with increase in temperature and increased with increase in pressures as expected.

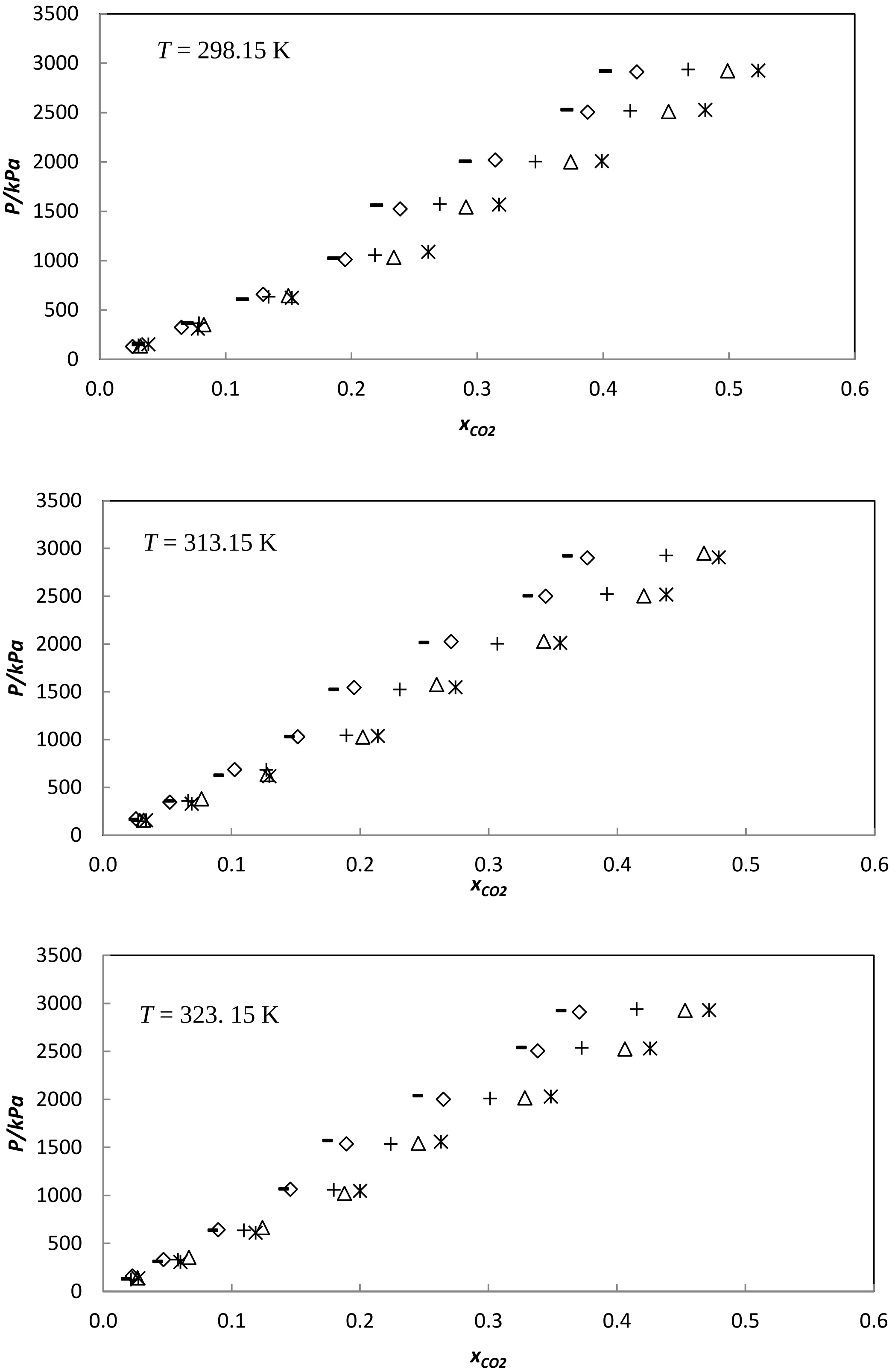

Figure 4.38. CO_2 solubility in pure [hmim][BF_4], MDEA and binary mixtures of [hmim][BF_4] + MDEA (with molar ratios 1:4, 1:1, 4:1 of the IL to MDEA): [hmim][BF_4] (◊), MDEA (Δ), {[hmim][BF_4]+MDEA (1:4)} (*), {[hmim][BF_4]+MDEA (1:1)} (+), {[hmim][BF_4]+MDEA (4:1)} (-).

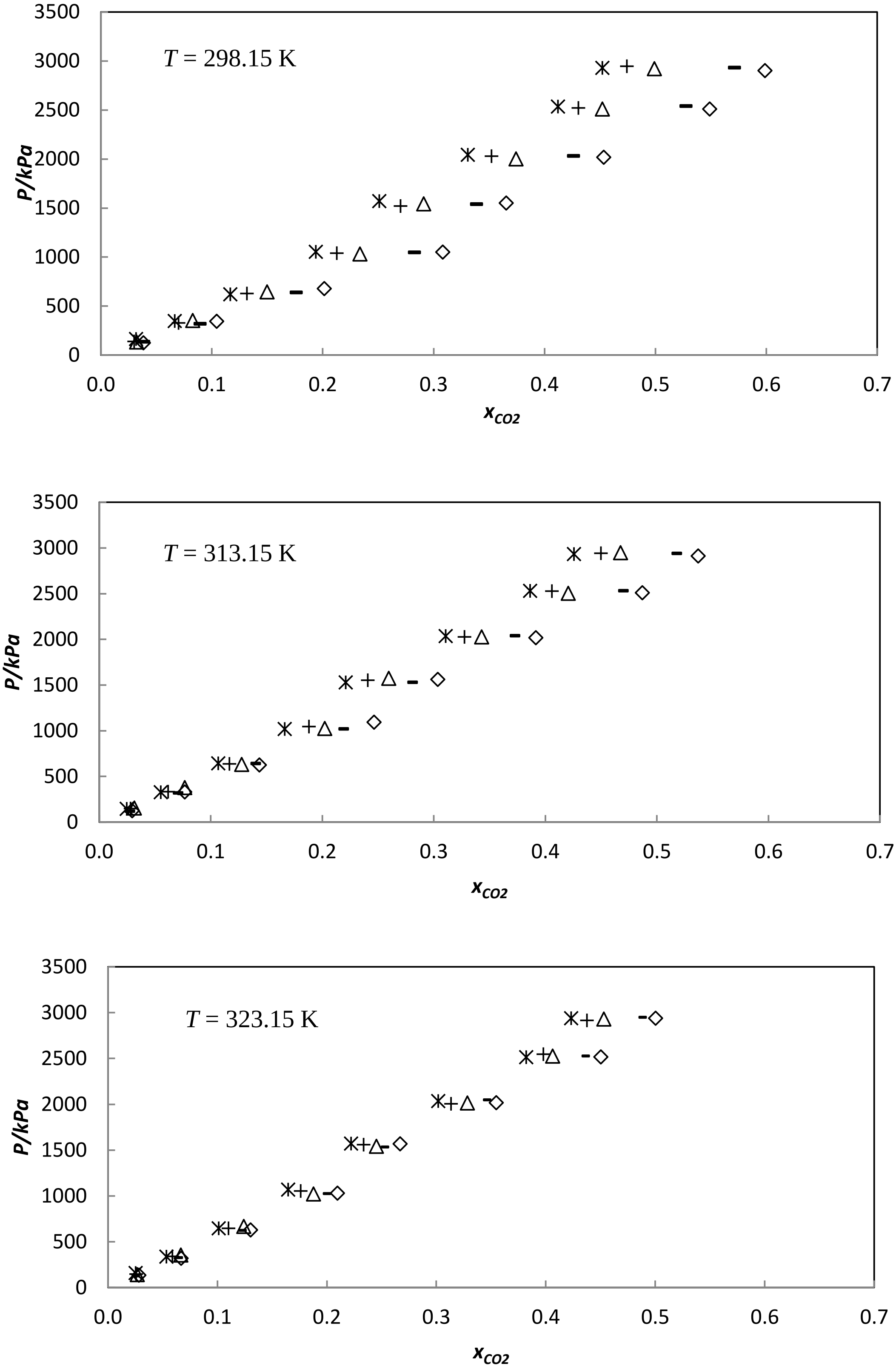

Figure 4.39. CO_2 solubility in pure [hmim][Tf_2N], MDEA and binary mixtures of [hmim][Tf_2N] + MDEA (with molar ratios 1:4, 1:1, 4:1 of the IL to MDEA) : [hmim][Tf_2N] (◊), MDEA (Δ), {[hmim][Tf_2N]+MDEA (1:4)} (*), {[hmim][Tf_2N]+MDEA (1:1)} (+), {[hmim][Tf_2N]+MDEA (4:1)} (-).

[hmim][FAP] + MDEA System

Among the pure liquids ([hmim][FAP], MDEA) and their binary mixtures, pure [hmim][FAP] has shown maximum solubility over the entire range of temperatures and pressures (Figure 4.40). The solvents could be arranged in terms of CO_2 loadings as; [hmim][FAP]>(4:1)>MDEA>(1:1)>(1:4). The pure [hmim][FAP] exhibited 1.35 times higher CO_2 loadings in comparison to pure MDEA. The mixture (4:1) showed only 1.10 times lower loadings than pure [hmim][FAP] and thereby succeeded to find a place closer to it. The mixture (1:4) showed very low (1.58 times) loadings than pure [hmim][FAP] and grabbed a position very far from the IL. However with only 1.18 times lower values than MDEA it found a position closer to it. The mixtures (4:1) has shown lower values of CO_2 absorption in contrast to pure [hmim][FAP]. The [hmim][FAP] molecules are larger in number in this mixture, whereas MDEA molecules are lesser in number. However, the MDEA molecules suppressed the capabilities of [hmim][FAP] molecules and thus resulted in lower absorption values than pure IL. The addition of even the small amount of MDEA in the IL has decreased its CO_2 capturing capability. The same trend was observed in the case of [hmim][Tf_2N] ionic liquid, wherein presence of small amount of MDEA in it decreased its CO_2 absorption.

In the previous section the comparisons among the pure solvents and their respective binary mixtures in terms of CO_2 solubility were discussed. In the next sections, the effect of concentrations, temperatures, pressures and anion on the CO_2 solubility in the solvents and mixtures used in the present study has been discussed in detail.

4.7. Effects of concentrations of MDEA

The effect of MDEA concentration in the IL + MDEA binary mixtures on the CO_2 loading is discussed in detail in the following sections. In order to have a better understanding three different molar ratios of the binary mixtures , where the MDEA concentration is less than ILs (4:1); equal to IL (1:1) and more than IL (4:1) are discussed separately.

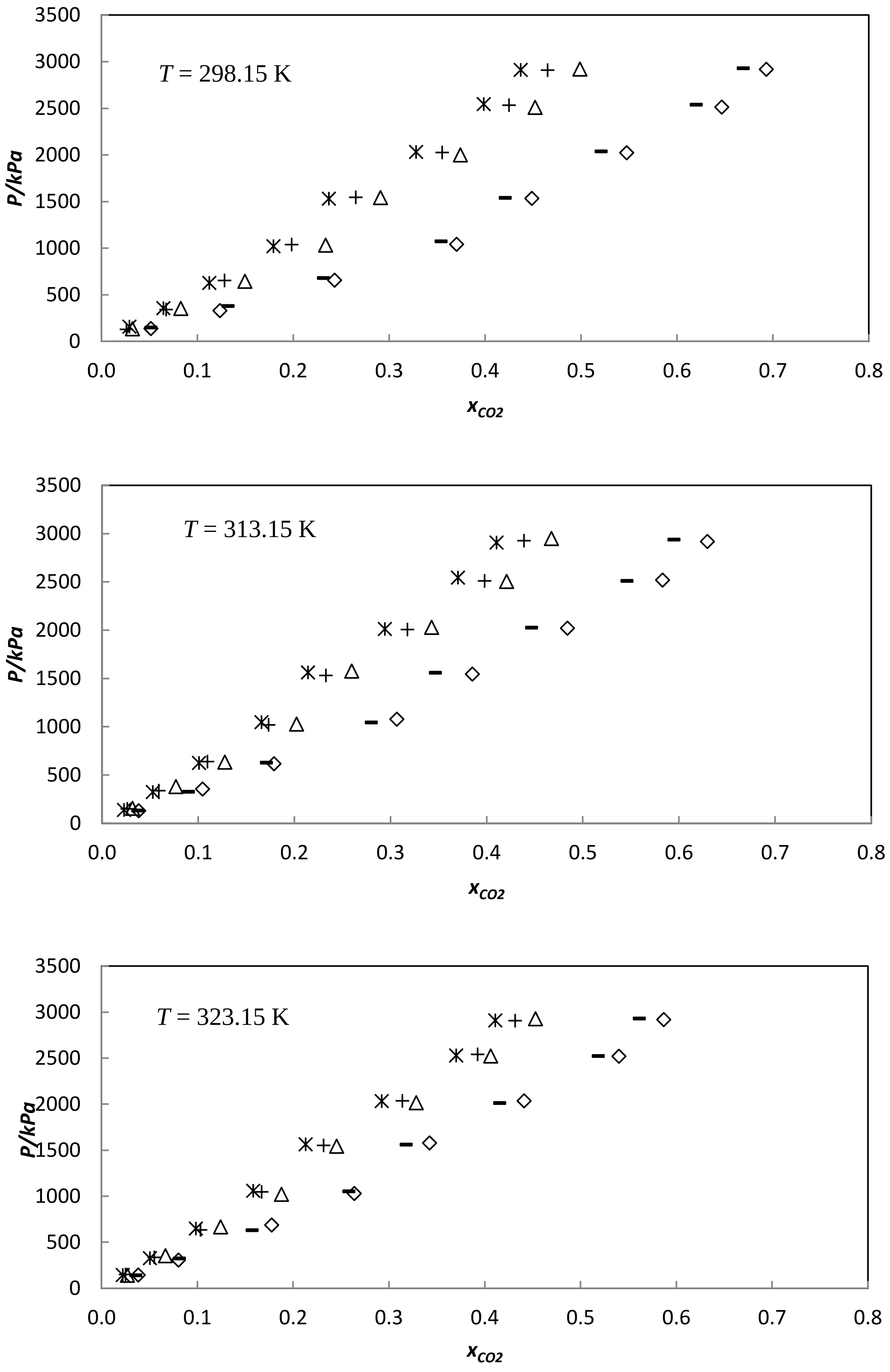

Figure 4.40. CO_2 solubility in pure [hmim][FAP], MDEA and binary mixtures of [hmim][FAP] + MDEA (with molar ratios 1:4, 1:1, 4:1 of the IL to MDEA): [hmim][FAP] (◊), MDEA (Δ), {[hmim][FAP]+MDEA (1:4)} (*), {[hmim][FAP]+MDEA (1:1)} (+), {[hmim][FAP]+MDEA (4:1)} (-).

4.7.1. MDEA concentration is less than ILs (Molar ratio (4:1) IL to MDEA)

The ([hmim][BF_4]+MDEA) binary mixture (4:1) shows lower CO_2 loading in comparison to pure IL (Figure 4.38). The IL suffered loss in CO_2 loading by the addition of small amount of MDEA in it. The same trend was observed at all temperatures. This means that the addition of MDEA (at this concentration) has not proven fruitful for the IL. The ([hmim][Tf_2N]+MDEA) binary mixture (4:1) also shows lower CO_2 absorption in comparison to pure IL over all temperatures (Figure 4.39). Again the IL suffered loss in CO_2 absorption when diluted with the slight amount of MDEA. The same trend was observed in the case of ([hmim][FAP]+MDEA binary mixture (4:1) over the entire temperature range (Figure 4.40). For all the systems under study it could be inferred that the addition of even the small amount of MDEA in the ILs has resulted in reduction of their CO_2 loading. The binary mixtures (4:1) of all the systems show solubility closer to their respective pure IL. This means that though the addition of MDEA has resulted in reduction of their CO_2 solubility even then the IL molecules are governing the absorption as these are quite higher in number in comparison to MDEA molecules. Therefore the addition of MDEA at this concentration though reduced the CO_2 loading but still was unable to completely suppress the capabilities of pure ILs.

4.7.2. MDEA concentration is equal to ILs (Molar ratio (1:1) IL to MDEA)

The ([hmim][BF_4]+MDEA) binary mixture (1:1) shows higher CO_2 loading in comparison to pure IL and the same trend was observed at all temperatures (Figure 4.38). The IL gained in terms of CO_2 loading by the addition of MDEA at this concentration. The mixture (1:1) shows solubility in between both the pure liquids. MDEA shows higher CO_2 loading than [hmim][BF_4] and the mixture (1:1) shows solubility closer to pure MDEA. It could be inferred that at this concentration MDEA molecules are dominating and governing the CO_2 solubility whereas [hmim][BF_4] playing the secondary role. This has resulted in enhanced CO_2 solubility for pure IL. The addition of MDEA in pure IL at this concentration has proved beneficial for the former. On the other hand, ([hmim][Tf_2N]+MDEA, [hmim][FAP]+MDEA) binary mixtures (1:1) show lower CO_2 loading as compared to respective pure ILs and the same trend was observed at all temperatures (Figure 4.39-4.40). Ionic liquids ([hmim][Tf_2N], [hmim][FAP]) show higher CO_2 loading than MDEA and the mixtures (1:1) show solubility closer to MDEA. Therefore it could be concluded that at this concentration again MDEA molecules are dominating the CO_2 loading. The binary mixtures (1:1) of all the systems show solubility closer to pure MDEA and almost similar among themselves over the entire range of temperatures (Figure 4.38-4.40). Therefore it could be concluded that at this concentration MDEA is governing the CO_2 loading by suppressing the capabilities of ILs.

4.7.3. MDEA concentration is higher than ILs (Molar ratio (1:4) IL to MDEA)

The ([hmim][BF_4]+MDEA) mixture (1:4) show higher CO_2 loading in comparison to pure IL and the same trend was observed over the entire temperature range (Figure 4.38). It has been discussed earlier that pure MDEA has higher CO_2 loading than [hmim][BF_4]. Therefore in this mixture where MDEA molecules are larger in number and [hmim][BF_4] molecules are fewer, former are dominating the CO_2 loading. The addition of MDEA at this concentration has enhanced the CO_2 loading of IL many folds. The mixture showed higher solubility even from the both pure liquids but closer to pure MDEA. This means that small amount of IL present in the mixture resulted in greater CO_2 solubility for pure MDEA. On the other hand, ([hmim][Tf_2N]+MDEA, [hmim][FAP]+MDEA) binary mixtures (1:4) show lower CO_2 solubility as compared to pure ILs and the same trend was observed at all temperatures (Figures 4.39-4.40). The addition of MDEA at this concentration has badly affected the CO_2 capture ability of pure ILs ([hmim][Tf_2N] and [hmim][FAP]). Furthermore the slightest amount of ILs in pure MDEA has also resulted in the reduction in CO_2 loading. The addition of MDEA at this concentration has proven fruitful for [hmim][BF_4] whereas for other ILs it did not proved beneficial at all. Based on the above results, it can be concluded that the ILs ([hmim][Tf_2N], [hmim][FAP]) suffered loss in CO_2 solubility by the addition of MDEA at all concentrations. Whereas IL ([hmim][BF_4]) gained in CO_2 absorption by the addition of MDEA at concentrations (1:1, 1:4). The experimental and computational reports on CO_2 gas absorption in ILs suggest that CO_2 takes up the free space from void cavities already available in the rigid and intricate topography of ILs when dissolves in these. ILs with [BF_4] anions have smaller cavities in comparison to the ILs with bigger anions ([Tf_2N], [FAP]) therefore could accommodate less CO_2 molecules which resulted in low CO_2 absorption

(Huang et. al. 2006). MDEA shows more CO_2 solubility than pure [hmim][BF_4] and less solubility than [hmim][Tf_2N] and [hmim][FAP]. Therefore the addition of MDEA in [hmim][BF_4] at higher concentrations resulted in enhanced CO_2 loading due to the presence of more cavities (MDEA part) for the adjustment of CO_2 molecules. For the case of [hmim][Tf_2N] and [hmim][FAP] the presence of MDEA reduced CO_2 solubility as the space available for CO_2 molecules to adjust was reduced (IL part).

The excess properties studies on the binary mixtures indicate the presence of dispersion forces between ionic liquid and MDEA molecules. From the excess molar volumes, viscosity deviations and refractive index deviation studies, the order of dispersion forces in the binary mixtures under study could be arranged as: ([hmim][FAP]+MDEA)>([hmim][Tf_2N]+MDEA)>([hmim][BF_4]+MDEA) (Figures 4.24-4.32). The mechanism of CO_2 absorption in imidazolium based ILs is based on the adjustment of CO_2 molecules in the void spaces present in the rigid topography of ILs (Huang et. al. 2006) and also on the arrangement of CO_2 molecules in the surrounding of ILs molecules in a tangent like configuration (Cadena et. al. 2004). On the other hand, it is well known that when excess molar volume values are positive and refractive and viscosity deviation values are negative for a binary system, the molecules present in the mixture adjust within themselves in such a manner that big molecules (like IL molecules in the cases of the binary mixtures under study) are surrounded by the smaller molecules (MDEA molecules) and adjusted thereof and remain intact due to the presence of dispersion forces (Fort and Moore 1966; Sovilj et. al. 2000; Deenadayalu et. al. 2008; Sinha 2010; Vural et. al. 2011; Bhatia et. al. 2011). Therefore in all the binary mixtures less CO_2 solubility were noticed in comparison to pure ILs as CO_2 molecules could not adjust themselves in the surrounding of the IL molecules, due to the presence of dispersion forces and MDEA molecules (which occupied the spaces where CO_2 molecules were supposed to adjust in a tangent like configuration). Only ([hmim][BF_4]+MDEA) mixtures at two concentrations (1:1), (1:4) displayed higher CO_2 loading than pure [hmim][BF_4]. The display of higher CO_2 solubility for these concentrations could be attributed to two reasons that, firstly the excess properties for this system displayed least values (among the other systems) thereby indicating that the dispersion forces were not as strong in this system as these were in the other systems, secondly pure MDEA have higher CO_2 solubility in comparison to pure [hmim][BF_4], which accounted for higher CO_2 solubility in the system at this concentration.

4.8 Effect of Temperatures and Pressures

The CO_2 solubility in the pure liquids as well as in their binary mixtures increased with increase in pressure (Figures 4.37-4.40). At higher CO_2 partial pressure, the solvents exhibited higher CO_2 loading as compared to that at lower pressure at the fixed temperature conditions. In all cases, at constant temperature when the pressure was raised the CO_2 loading increased linearly. On the other hand, the increase in temperature resulted in lesser CO_2 loadings, at the fixed pressure conditions. The effect of temperature on the CO_2 solubility was studied by conducting experiments at different temperatures T = (298.15, 313.15, 323.15) K. It was observed that with increase in temperature, the solubility of CO_2 in all solvents (pure as well as their binary mixtures) decreased. The CO_2 solubility in pure as well as their binary mixtures could alternatively be expressed as the Henry's constants which are dependent on temperature. The condition for the phase equilibrium is satisfied when the fugacities of the gas components have equal values in both phases at constant pressure and temperature as follows:

$$f_1^g = f_1^l \tag{4.6}$$

where f_1^g and f_1^l are the fugacities of CO_2 in gas and liquid phase respectively. Since the liquids used in the present study have negligible vapor pressure the fugacity of the gas in the gas liquid system is assumed to be equal to the pure gas. The fugacity of the pure gas is expressed as:

$$f_1^l(p,T) = p_{eq}\phi_1(p_{eq},T_{eq}) \tag{4.7}$$

where p_{eq} and T_{eq} are the pressure and temperature at equilibrium. The fugacity coefficients ϕ_1 were calculated by using PR EOS (Peng and Robinson 1976). Henry's constant is defined as (Prausnitz et. al. 1999):

$$K_H \cong \frac{\phi_1(p_{eq},T_{eq})p_{eq}}{x_{co2}} \tag{4.8}$$

The estimated Henry's constants for the pure as well as binary mixtures are listed in Table 4.3. Sample calculations for the estimation of Henry's constants with the help of Eq. (4.8) are listed in Table C-5 of Appendix C. A high value of Henry's constant indicates lower solubility and vice versa (Yunus et. al. 2012). The estimated Henry's constants for [hmim][FAP] and [hmim][Tf_2N] showed a fair agreement (< 2.5%) with the available literature (Muldoon et. al. 2007) values (Table 4.3). The minor differences could be attributed to the differences in water content and the presence of the impurities in the liquids. The temperature derivatives of the solubility are directly related either to the partial molar enthalpy (Δh_1) *or* the partial molar entropy (Δs_1) of the gas (1) in the liquid phase (2). If a solvent is non volatile the following equations can be applied to calculate enthalpy and entropy from the temperature dependency of Henry's constant (Prausnitz et. al. 1999).

Table 4.3. Estimated Henry's constants of the solvents

Solvents		K_H (MPa)		
Pure		T = 298.15 K	T = 313.15 K	T = 323.15 K
[hmim][BF_4]		4.93	6.50	7.01
[hmim][Tf_2N]		3.25 (3.16[a])	4.25	4.72
[hmim][FAP]		2.65 (2.52[a])	3.35	3.76
MDEA		4.16	4.85	5.25
Binary Mixtures	Molar Ratio (IL to MDEA)			
[hmim][BF_4] + MDEA	(1:4)	3.95	4.65	5.03
	(1:1)	4.57	5.26	5.66
	(4:1)	5.24	6.80	7.32
[hmim][Tf_2N] + MDEA	(1:4}	5.15	5.86	6.24
	(1:1)	4.63	5.32	5.73
	(4:1)	3.52	4.46	4.92
[hmim][FAP] + MDEA	(1:4)	5.41	6.03	6.42
	(1:1)	4.95	5.64	6.02
	(4:1)	2.85	3.56	3.93

[a] Values from Muldoon et. al. 2007

$$\Delta h_1 = R\left(\frac{\partial lnK_H}{\partial\left(\frac{1}{T}\right)}\right) \tag{4.9}$$

$$\Delta s_1 = -R\left(\frac{\partial lnK_H}{\partial lnT}\right) \tag{4.10}$$

The estimated values of enthalpy and entropy for the pure as well as solvents are listed in Table 4.4. The estimated values of enthalpies of dissolution of CO_2 are (-11.6, -11.2, -12.1) kJ/mol for [hmim][BF_4], [hmim][FAP] and [hmim][Tf_2N], respectively. These values are in fair agreement with the values reported for the said ILs in the open literature. Muldoon et. al. (2007) reported -12.1kJ/mol for [hmim][Tf_2N] whereas for other imidazolium based ILs the reported values were in the range of (-11.4 to -12.1) kJ/mol. The estimated values for [hmim][BF_4] and [hmim][Tf_2N] are also within the reported range. The estimated enthalpies for the pure solvents and their binary mixtures showed negative values indicating the exothermic nature of absorption. The enthalpy and entropy of gas dissolution are important parameters. The energy requirements for the conventional amine based CO_2 capture processes are quite high. This is attributed to the high energy associated with the regeneration of the solvent, to which the enthalpy of CO_2 absorption is the most important contributor. The importance of enthalpy is directly linked to the energy penalty that the CO_2 scrubber system imposes on the power plant. A solvent having high enthalpy means requiring more energy for absorption/desorption of CO_2 and vice versa. An amine solvent having higher value (large magnitude) of enthalpy (*e.g.* MEA = -80 kJ/mole) is also considered to have high affinity for CO_2 and as a consequence

Table 4.4. Estimated values of enthalpies and entropies of CO_2 dissolution in solvents.

Solvent		Δh_1 (kJ/mol)	Δs_1 (J/mol)
Pure			
[hmim][BF_4]		-11.6	-37.3
[hmim][FAP]		-11.2	-36.0
[hmim][Tf_2N]		-12.1	-36.7
MDEA		-13.5	-39.6
Binary Mixtures	Molar Ratio (IL to MDEA)		
[hmim][BF_4]+MDEA	(1:4)	-7.8	-25.2
	(1:1)	-6.9	-22.2
	(4:1)	-11.0	-35.4
[hmim][Tf_2N]+MDEA	(1:4)	-6.2	-20.0
	(1:1)	-6.9	-22.1
	(4:1)	-10.9	-35.1
[hmim][FAP]+MDEA	(1:4)	-5.5	-17.7
	(1:1)	-7.1	-22.8
	(4:1)	-10.4	-33.

requires more energy for absorption process (McCann et. al. 2011; Nierop et. al. 2011). Therefore solvents having less enthalpy values and showing high CO_2 loading are need of the hour. Ionic liquids usually exhibit half (and even less than that) enthalpy values in comparison to amine solvents. This means requiring quite less energy in comparison to amine solvents to process a given amount of CO_2 (Wappel et. al. 2010). The estimated enthalpy values for the ILs; [hmim][BF_4], [hmim][Tf_2N] and [hmim][FAP] are -11.6 kJ/mole, -12.1kJ/mole, -11.2kJ/mole respectively. The IL [hmim][Tf_2N] shows highest enthalpy value and therefore should exhibit highest CO_2 solubility according to the general principle (as applied to aqueous amine solvents *i.e.* high enthalpy value; high CO_2 loading) among the pure ILs. On the other hand, IL [hmim][FAP] shows the highest CO_2 solubility among pure ILs. Therefore it can be concluded that the high enthalpy value of an IL is not indicative of its high CO_2 uptake. Ramdin et. al. (2013) studied CO_2 solubility in different ILs and as part of it estimated the enthalpies of absorption for these ILs. They also observed that IL showing high enthalpy value did not show high CO_2 solubility. They concluded that it is not the enthalpy rather entropy which plays the major part for CO_2 solubility in ILs. The lower value of entropy indicates high solubility and vice versa. Entropy provides information about the ordering of CO_2 (or any gas which is being absorbed) molecules in the ILs. The lesser entropy indicates more disorder and hence more absorption. The order of CO_2 solubility in ILs ([FAP]>[Tf_2N]>[BF_4]) is consistent with their corresponding entropy values (Table 4.4). The experimental and computational reports on CO_2 in ILs suggest that CO_2 takes up the free space from void cavities already available in the rigid and intricate topography of ILs when dissolves in these. ILs with [BF_4] anions have smaller cavities in comparison to the ILs with bigger anions ([Tf_2N], [FAP]) therefore could accommodate less CO_2 molecules which resulted in low CO_2 absorption (Huang et. al. 2006). Therefore the entropic (free volume) effects govern the CO_2 solubility in ILs. Pure MDEA shows less enthalpy and less entropy values, which indicates that MDEA in its pure form is not an ideal medium for CO_2 absorption (as less enthalpy value for amines is indicative of their less affinity towards CO_2 absorption). The binary mixtures also showed less enthalpy and less entropy values than pure ILs. It indicates that the CO_2 absorption due to the entropic effect is dominant in these. However binary mixtures could not fully utilize entropic phenomena due to the presence of MDEA molecules which occupied valueable spaces around the ILs, thus hindering the CO_2 molecules to find space.

4.9 Effect of anion

4.9.1 Effect of anion in pure ILs

The CO_2 solubility in the pure ILs is greatly affected by the structure of the anion. The anion plays a vital role in the CO_2 solubility. In this study the ionic liquids used had ([hmim]) cation attached with different anions ([BF_4], [Tf_2N], [FAP]). The purpose was to study the effect of anion on CO_2 solubility in the pure ILs as well as their binary mixtures with MDEA. The CO_2 solubility in the pure ILs followed the order ([hmim][BF_4]<[hmim][Tf_2N]<[hmim][FAP]) (Figure 4.37). From the experimental results, the order of the CO_2 solubility follows the order of fluorination present in the anion and also on the molar mass of the anion. The [FAP] anion is analogous to [PF_6] anion, where the three fluorine atoms have been replaced with fluoroethyl group (Muldoon et. al. 2007). This replacement resulted in enhanced CO_2 solubility. The ILs with [Tf_2N] anion showed greater solubility in comparison with the IL with [BF_4] anion as it is more fluorinated than it. However the CO_2 solubility in IL with [Tf_2N] anion was lower than the IL with [FAP] anion as it was less fluorinated than it. Therefore it could be concluded that the fluorination of anion results in the enhanced CO_2 absorption. Based on his own experiments Muldoon et. al. (2007) concluded that the fluorination of anion resulted in enhanced CO_2 absorption. The more fluorinated anions like [FAP] showed higher CO_2 solubility in comparison to the less fluorinated anions like [Tf_2N].

4.9.2 Effect of anion on the CO_2 loading in binary mixtures

In the previous section the effect of anion on the CO_2 loading in the pure ILs has been discussed. In this section the effect of anion on the CO_2 solubility in the binary mixtures studied in the present has been discussed. Each molar ratio has been discussed individually for the better understanding.

Molar ratio (4:1) IL to MDEA

The comparisons of CO_2 solubility in the binary mixtures of ([hmim][Tf_2N]+MDEA), ([hmim][BF_4]+MDEA) and ([hmim][FAP]+MDEA) for molar ratio of (4:1) are illustrated in Figure 4.41. It can be seen that the binary mixture of ([hmim][FAP]+MDEA) showed the maximum solubility followed by the binary mixture ([hmim][Tf_2N]+MDEA) and ([hmim][BF_4]+MDEA). The mixture ([hmim][FAP]+MDEA) showed 1.25 times higher loadings than ([hmim][Tf_2N]+MDEA) mixtures and 1.78 times higher loadings than ([hmim][BF_4]+MDEA) mixture. The high solubility of [hmim][FAP]+MDEA mixture is due to the fact that pure [hmim][FAP] has high solubility in comparison to the other ILs (Figure 4.37). In the mixture (4:1) the IL molecules are in excess and hence these govern the CO_2 solubility. Based on the results it can be concluded that it is the anion, which dominates the CO_2 solubility in these mixtures ([FAP]>[Tf_2N]>[BF_4]). The results obtained using these mixtures at this concentration of MDEA (one mole MDEA mixed with four moles of pure IL) are analogous to the results obtained for the pure ILs. The presence of MDEA at this concentration in the mixtures was not able to diminish the pivotal role of anion in CO_2 solubility.

Molar ratio (1:1) IL to MDEA

The comparisons of CO_2 solubility in the binary mixtures of ([hmim][Tf_2N]+MDEA), ([hmim][BF_4]+MDEA) and ([hmim][FAP]+MDEA) for molar ratio (1:1) are illustrated in Figure 4.42. For the case of IL to MDEA molar ratio of (1:1) all binary mixtures exhibited almost similar CO_2 loadings except the system [hmim][BF_4] showing slightly higher CO_2 loadings than the other systems especially at T = 323.15 K (Figure 4.42). The moles of MDEA and the moles of the respective IL are same in number at this concentration. However it can be seen that the molecules of ILs are not controlling the CO_2 solubility in these mixtures. Because the results are not analogous to the one obtained for the pure ILs. On the other hand, it is clear that when MDEA is mixed with the ILs at this concentration it controls the CO_2 solubility because all the mixtures show CO_2 solubility quite closer the one shown by pure MDEA (Figure 4.38-4.40). Therefore it could be inferred that the additions of MDEA at this concentration in the ILs completely dominate the CO_2 solubility and thereby suppress the capabilities of the anions, which were controlling CO_2 solubility in the pure ILs and in the mixtures (4:1).

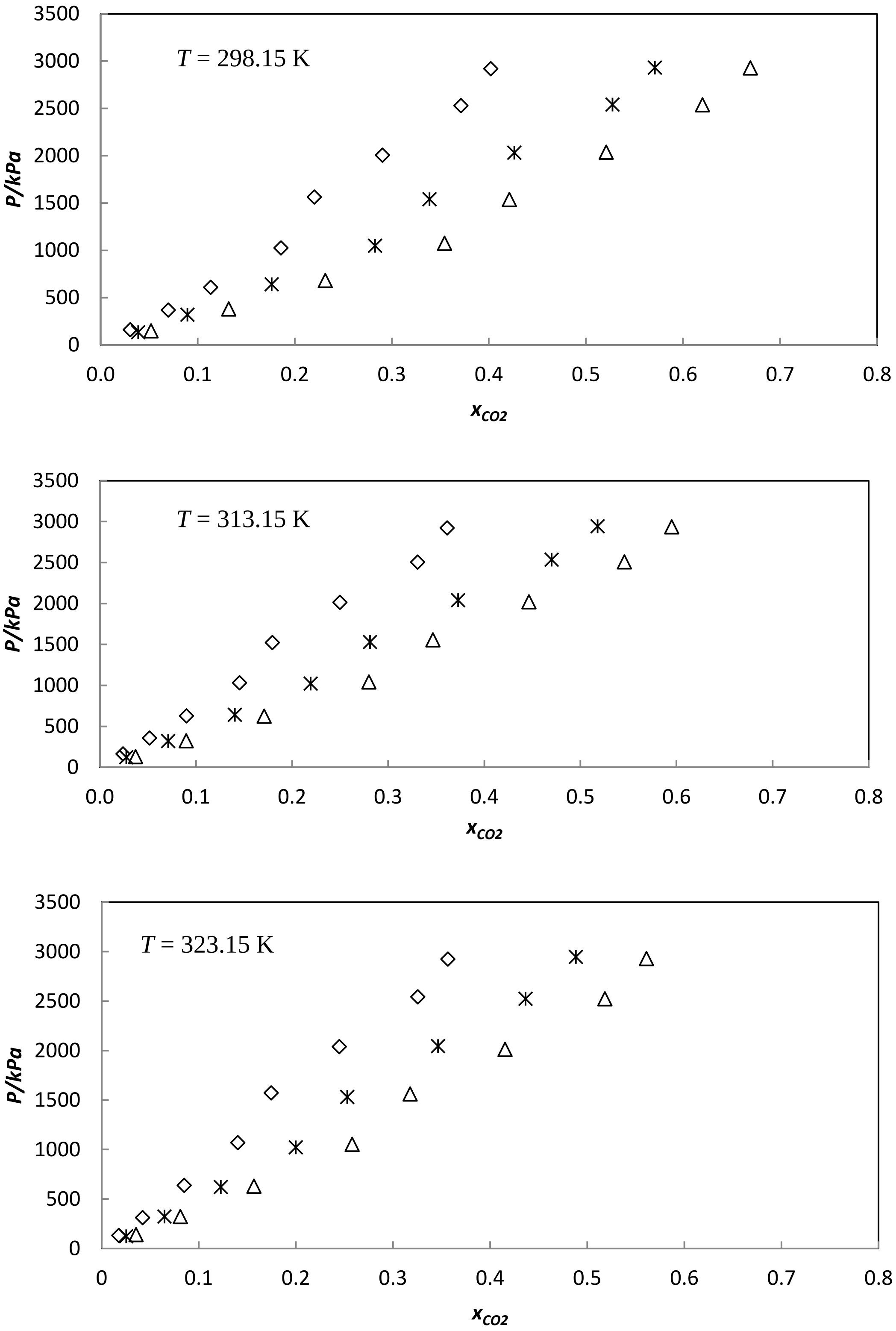

Figure 4.41. Comparison of CO_2 solubility in the binary mixtures of ([hmim][BF_4]+MDEA), ([hmim][Tf_2N]+MDEA) and ([hmim][FAP]+MDEA) for the molar ratio of the IL to MDEA (4:1): ([hmim][BF_4]+MDEA) (◊), ([hmim][FAP]+MDEA) (Δ), ([hmim][Tf_2N]+MDEA) (*).

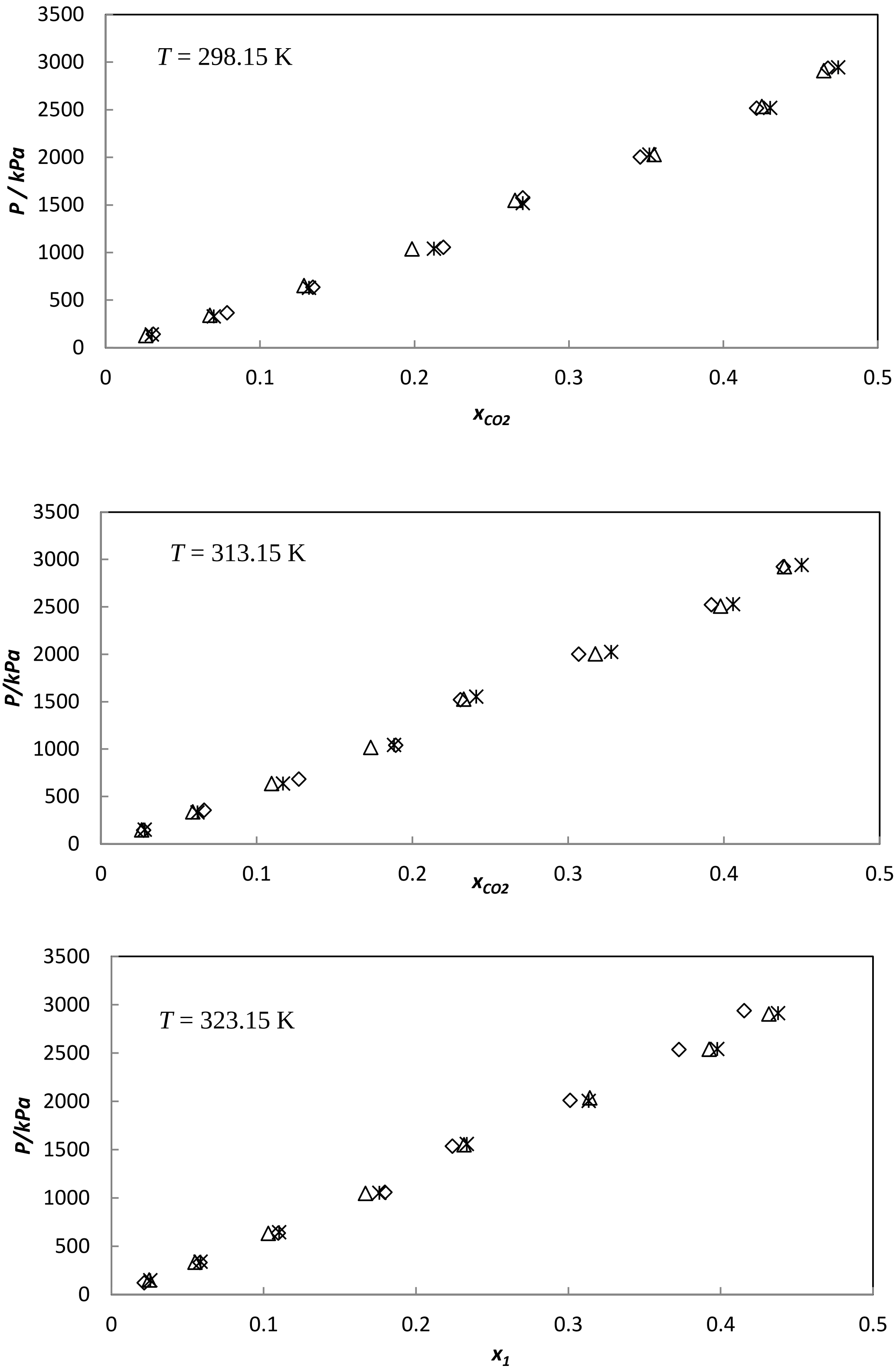

Figure 4.42. Comparison of CO_2 solubility in the binary mixtures of ([hmim][BF_4]+MDEA), ([hmim][Tf_2N]+MDEA) and ([hmim][FAP]+MDEA) for the molar ratio of the IL to MDEA (1:1). ([hmim][BF_4]+MDEA) (◊), ([hmim][FAP]+MDEA) (Δ), ([hmim][Tf_2N]+MDEA) (*).

Molar ratio (1:4) IL to MDEA

The binary mixture of [hmim][BF_4] with MDEA exhibits greater solubility than the other ([hmim][Tf_2N]+MDEA, [hmim][FAP]+MDEA) and the same trend was observed over the entire temperature range. The other binary mixtures exhibited lower CO_2 loadings with ([hmim][FAP]+MDEA) showing the least solubility (Figure 4.43). The binary mixtures of ([hmim][FAP]+MDEA, [hmim][Tf_2N]+MDEA) showed almost similar CO_2 loadings with ([hmim][Tf_2N]+MDEA) mixture showing slightly higher values. The high CO_2 solubility values for the binary mixture of [hmim][BF_4]+MDEA is due to the fact that pure MDEA has higher values of CO_2 solubility in comparison the pure [hmim][BF_4] (Figure 4.37), therefore the addition of MDEA in [hmim][BF_4] has enhanced its CO_2 absorption. On the other hand, the display of lower values of CO_2 absorption for the binary mixtures of [hmim][Tf_2N] and [hmim][FAP] is due to the fact that in pure state MDEA has lower values of absorption in comparison to these ILs. Therefore when they were diluted with MDEA (at this high concentration) they suffered loss, as the MDEA molecules are higher in number and they display lower values of absorption in comparison to the molecules of these pure ILs. The ILs with ([Tf_2N], [FAP]) anions has suffered badly due to the addition of MDEA. The IL with [BF_4] anion has gained in CO_2 solubility. The mixtures showed reverse trend of CO_2 solubility in contrast to pure ILs. The addition of MDEA at this concentration in the pure ILs has completely diminished the role of anions in CO_2 solubility. Based on the results it can be concluded that in the mixtures anions control the CO_2 solubility when the concentration of ILs is high (4:1), whereas in the equimolar (1:1) and (1:4) mixture the role of anions in CO_2 was suppressed completely due to the presence of MDEA molecules.

4.10. CO_2 solubility in some more Binary Mixtures and Aqueous IL amine mixtures

The CO_2 solubility in the binary mixtures ([hmim][BF_4]+MDEA, [hmim][Tf_2N]+MDEA, [hmim][FAP]+MDEA) was investigated. It was observed that the binary mixtures ([hmim][FAP]+MDEA, [hmim][Tf_2N]+MDEA) showed less absorption in comparison to pure ILs. Whereas binary mixtures of [hmim][BF_4] with

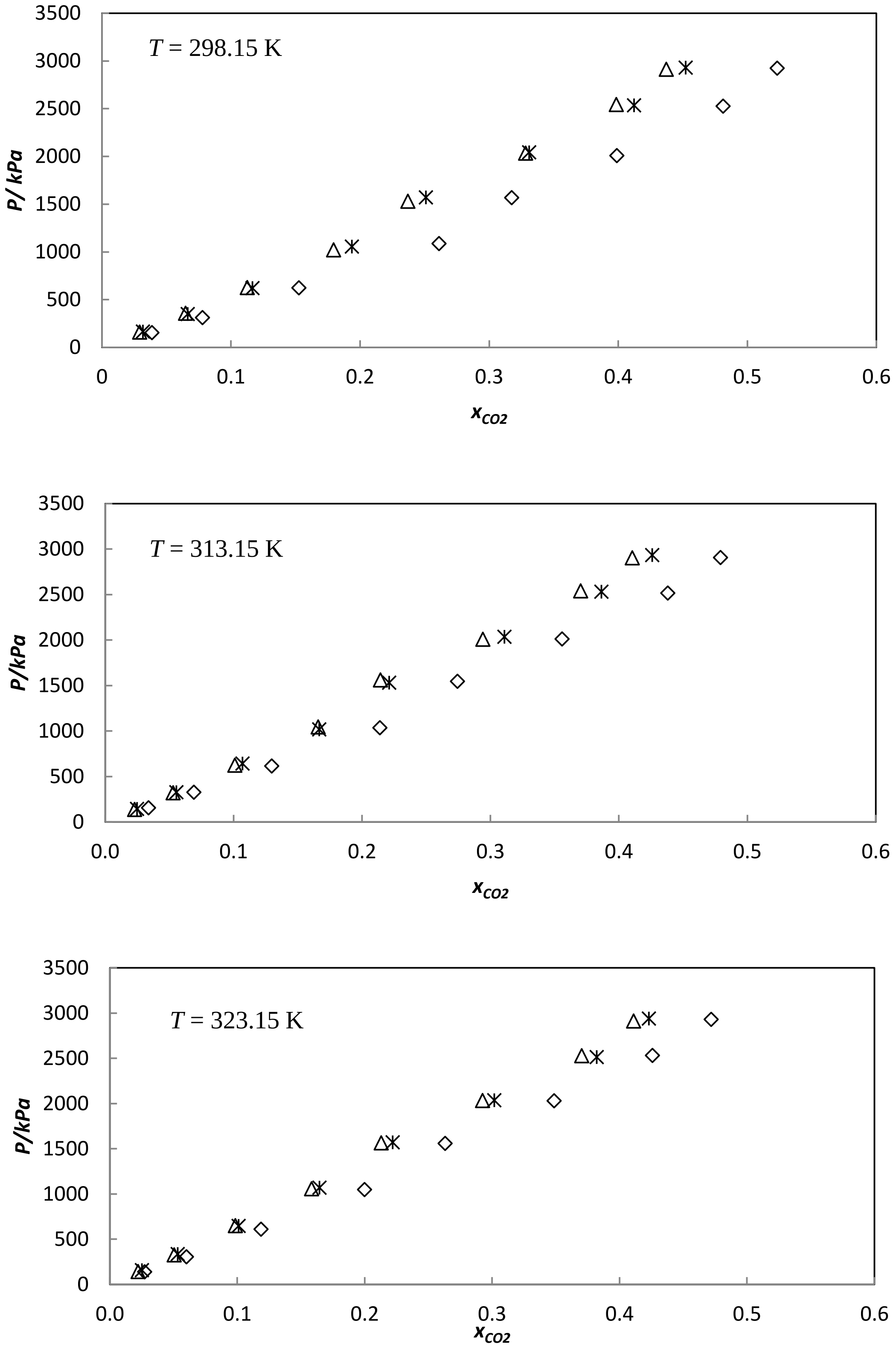

Figure 4.43. Comparison of CO_2 solubility in the binary mixtures of ([hmim][BF_4]+MDEA), ([hmim][Tf_2N]+MDEA) and ([hmim][FAP]+MDEA) for the molar ratio of the IL to MDEA (1:4): ([hmim][BF_4]+MDEA) (◊), ([hmim][FAP]+MDEA) (Δ), ([hmim][Tf_2N]+MDEA) (*).

MDEA showed only substantial increase in absorption in comparison to pure IL at some concentrations (1:4, 1:1). However it cannot be concluded that binary mixtures (MDEA+IL) always yield less CO_2 absorption or in some cases yield less pronounced increments in absorption. Therefore some more binary mixtures consisting of MDEA and ILs have been investigated as part of this present study. The ILs mixed with MDEA to form the binary mixtures were namely; 1-butyl-3-methylimidazolium tetrafluoroborate ([bmim][BF_4]), 1-butyl-3-methylimidazolium tris(pentafluoroethyl)trifluorophosphate ([bmim][FAP]), 1-butyl-3-methylimidazolium bis(trifluoromethylsulfonyl)imide ([bmim][Tf_2N]) and bis(2-hydroxyethyl)ammonium acetate ([bheaa]). These pure IL as well as their binary mixtures ([bmim][BF_4]+MDEA, [bmim][FAP]+MDEA, [bmim][Tf_2N]+MDEA, [bheaa]+MDEA) having (1:4, 1:1, 4:1) molar ratios (molar ratio of respective IL to MDEA) were studied in terms of CO_2 absorption. Furthermore some aqueous IL + amine mixtures were also investigated for CO_2 loadings. The IL used for in aqueous IL + amine mixtures were namely; 1-ethyl-3- methylimidazolium tris(pentafluoroethyl)trifluorophosphate ([emim][FAP]) and 1-ethyl-3-methylimidazolium bis(trifluoromethylsulfonyl)imide ([emim][Tf_2N]). The aqueous amine solvent mixed with these ILs was monoethanolamine (MEA) *or* diethanolamine (DEA). The compositions of aqueous IL + amine are listed in section 3.2.2 of Chapter 3. Each binary system is discussed below individually to investigate the CO_2 loading in it. The experimental solubility results for pure liquids, each binary system and aqueous IL + amine systems are listed in Tables C-6 to C-8 of Appendix C.

[bmim][FAP] + MDEA system

The comparison of CO_2 solubility in pure [bmim][FAP], MDEA and their binary mixtures is illustrated in Figure 4.44. It can be seen that the binary mixtures showed lower CO_2 absorption values in comparison to pure IL. This means that the addition of MDEA at all concentrations has not proven fruitful to the IL. The IL has suffered loss in terms of CO_2 absorption by the addition of MDEA at all concentration.

[bmim][Tf_2N] + MDEA system

The binary mixtures of [bmim][Tf_2N]+MDEA showed lower values of absorption in comparison to pure [bmim][Tf_2N] (Figure 4.44). The addition of MDEA at any concentration reduced the CO_2 absorption. The same results were obtained for the

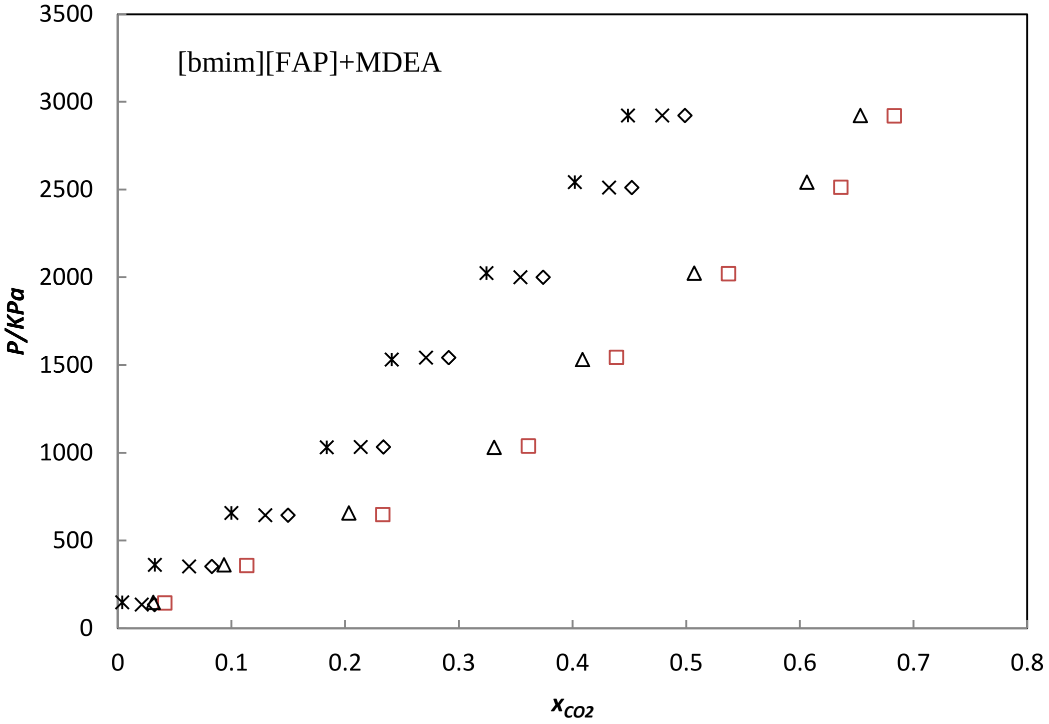

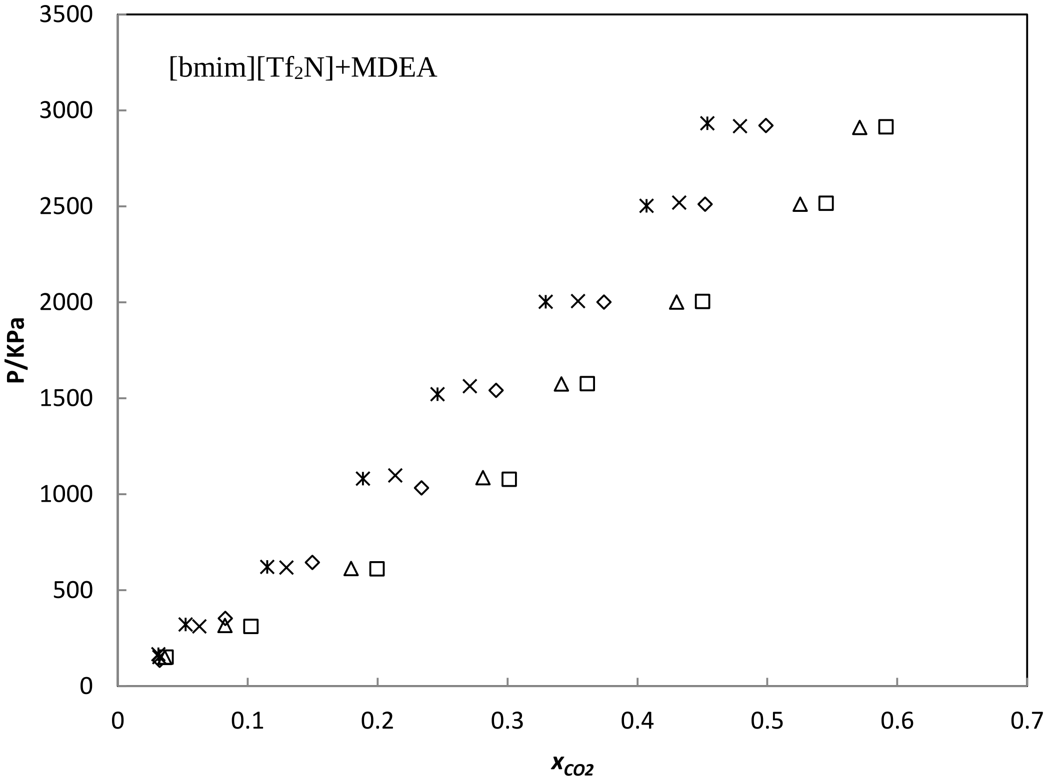

Figure 4.44: CO_2 solubility in pure IL, MDEA and binary mixtures of IL+MDEA (with molar ratios 1:4, 1:1, 4:1 of the IL to MDEA): IL (□), MDEA (◊), {IL+MDEA (1:4)} (*), {IL+MDEA (1:1)} (×), {IL+MDEA (4:1)} (Δ).

systems [hmim][Tf$_2$N]+MDEA, [hmim][FAP]+MDEA, [bmim][FAP]+MDEA. The systems in which the addition of MDEA reduces the CO_2 absorption consist of the IL which in its pure state exhibits more CO_2 absorption in comparison to MDEA. Therefore the addition of MDEA did not prove lucrative to the ILs with higher CO_2 loadings (in comparison to MDEA). The addition of MDEA suppressed their capabilities to effectively absorb CO_2.

[bmim][BF$_4$]+MDEA system

The binary mixtures of [bmim][BF$_4$]+MDEA having molar ratios (1:4, 1:1) showed substantially higher CO_2 loadings in comparison to pure IL (Figure 4.45). The CO_2 absorption in the molar ratios (1:4, 1:1) were quite closer to MDEA. MDEA in the pure form shows higher CO_2 loadings in comparison to [bmim][BF$_4$], therefore its addition to the IL enhanced absorption values. However the values were not appreciably high.

[bheaa]+MDEA system

The binary mixtures of [bheaa]+MDEA at concentrations 1:4, 1:1 displayed higher CO_2 absorption values in comparison to pure IL (Figure 4.45). Similar trends were noted in the systems [hmim][BF$_4$]+MDEA, [bmim][BF$_4$]+MDEA that binary mixtures having concentrations 1:4, 1:1 showed higher CO_2 absorption values in comparison to lean IL. MDEA in pure form has more CO_2 absorption in comparison to pure [bheaa] therefore the addition of it to the IL at concentrations 1:4, 1:1 enhanced absorption. At concentration 4:1 the binary mixture showed lesser values of absorption in comparison to pure IL.

Aqueous [emim][FAP] + MEA or DEA

The CO_2 absorption in the aqueous [emim][FAP] mixtures with MEA or DEA is illustrated in Figure 4.46. It can be seen the slightest amount of IL in the aqueous amine solvent decreased its solubility. The addition of IL to the aqueous amine solvent has not proven fruitful at all concentrations.

Aqueous [emim][Tf$_2$N] + MEA or DEA

The addition of IL [emim][Tf$_2$N] into the aqueous solution of MEA or DEA did not prove beneficial in terms of CO_2 solubility. The CO_2 capture ability of aqueous amine

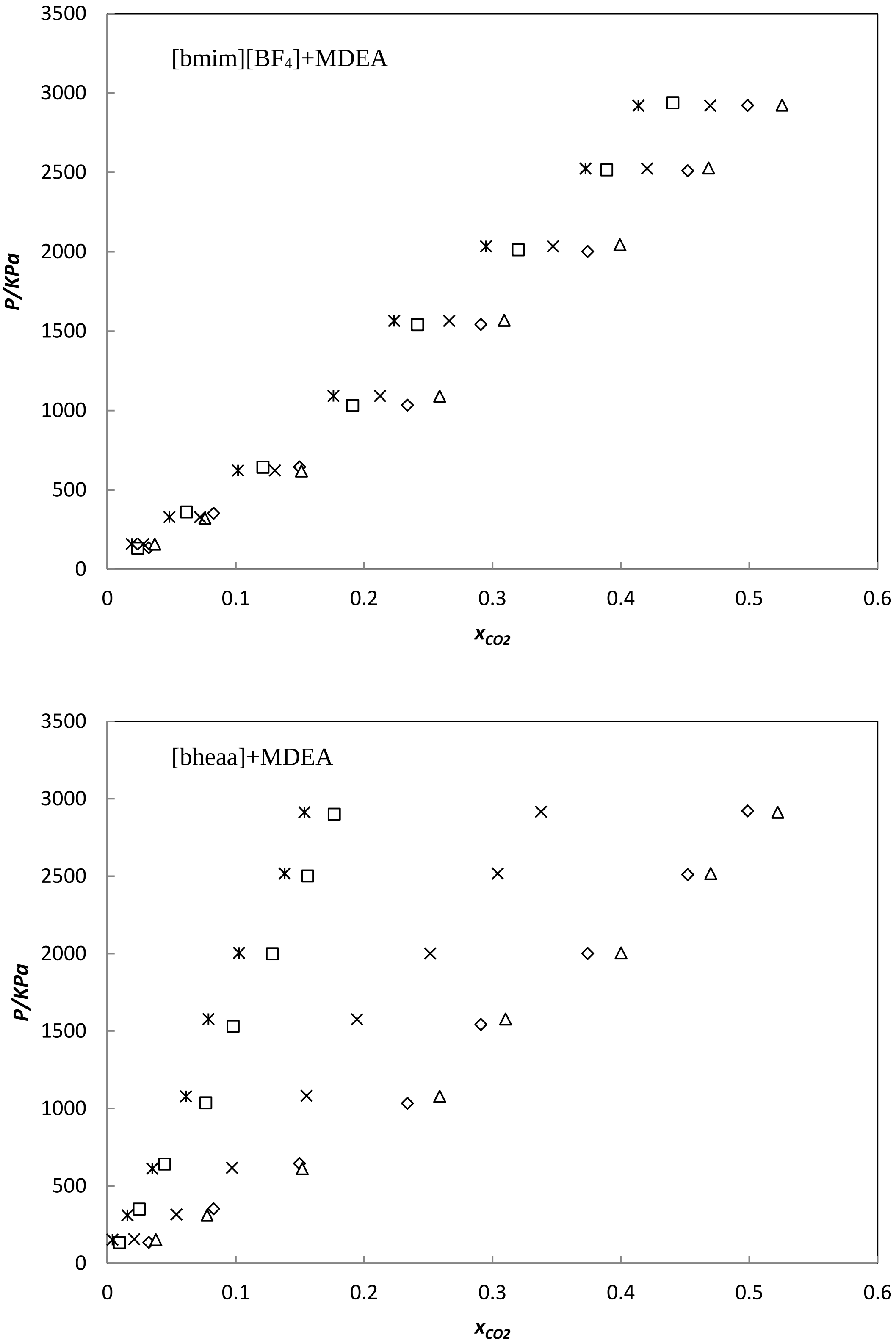

Figure 4.45: CO_2 solubility in pure IL, MDEA and binary mixtures of IL+MDEA (with molar ratios 1:4, 1:1, 4:1 of the IL to MDEA): IL (□), MDEA (◊), {IL+MDEA (1:4)} (Δ), {IL+MDEA (1:1)} (×), {IL+MDEA (4:1)} (*).

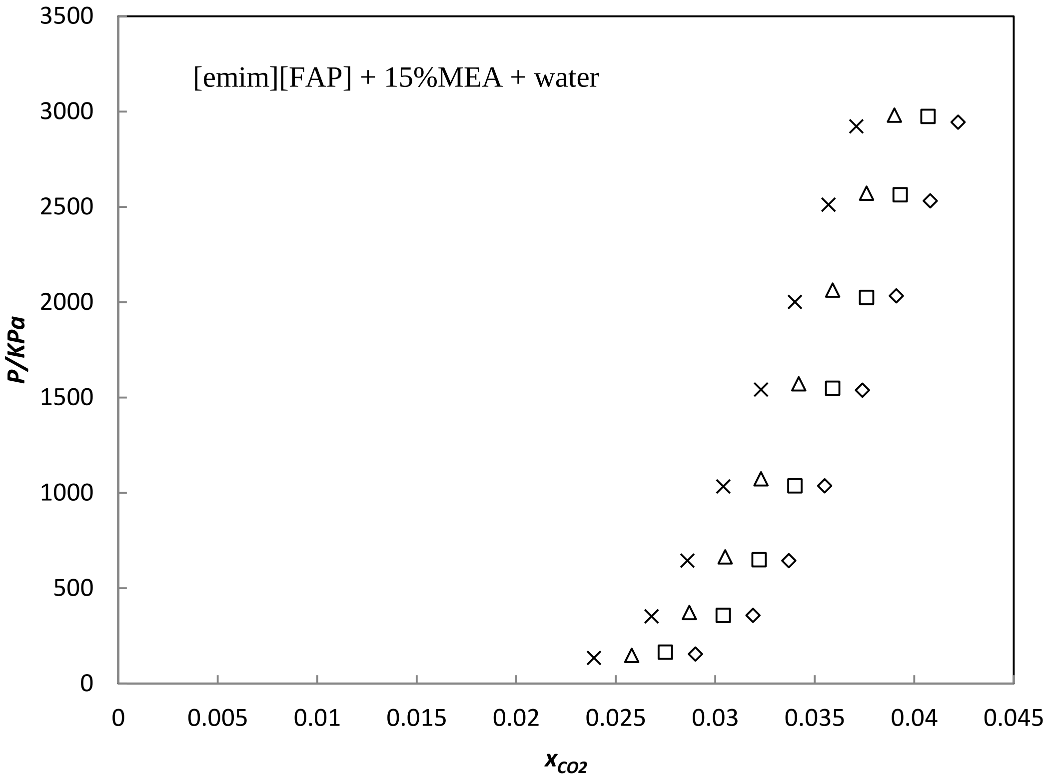

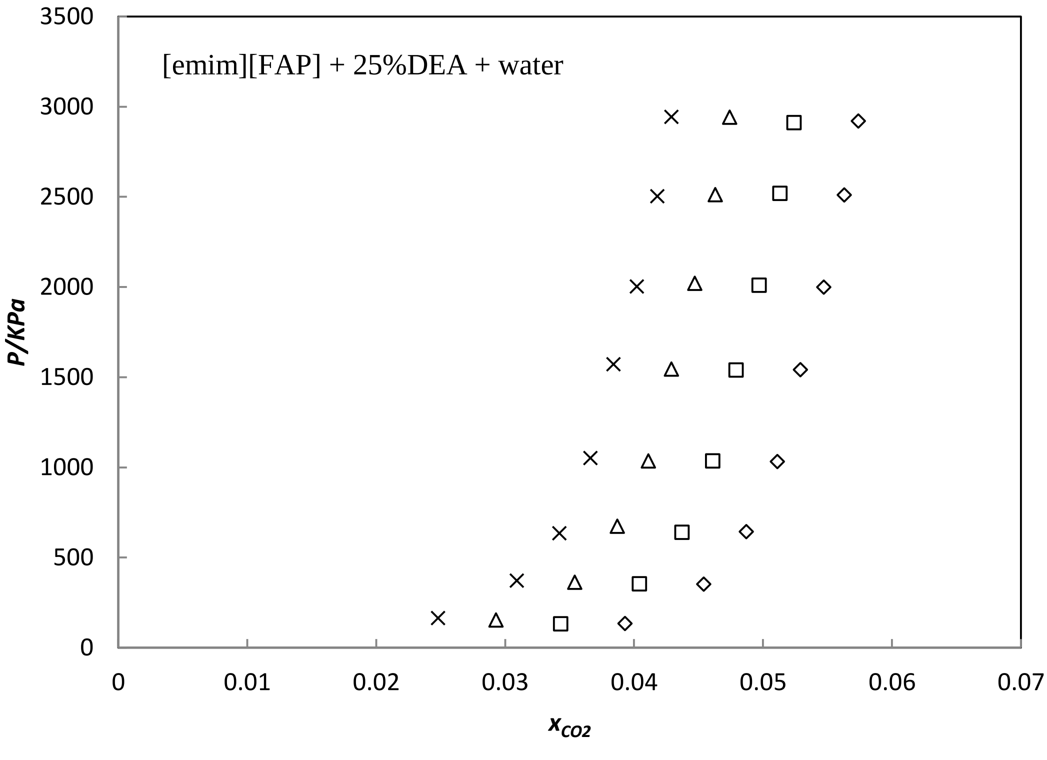

Figure 4.46: CO_2 solubility in aqueous IL + amine mixtures: Aqueous amine {15wt% MEA *or* 25wt% DEA} (◊), 5wt% [emim][FAP] (□), 10wt% [emim][FAP] (Δ), 15wt% [emim][FAP] (×).

solvent was reduced by the addition of even the slightest amount of IL in it (Figure 4.47). The addition of IL in the aqueous amine solvent solutions decreased their CO_2 solubility (Figures 4.46–4.47). This observed behaviour is in accordance to the one reported in the literature. Ahmady et. al. (2010) reported the similar trend that the addition of IL [bmim][BF_4] decreased the solubility of aqueous amine (MDEA) solvent. The presence of IL hindered in the chemical reaction between aqueous amine and CO_2, thus reduced its solubility. The CO_2 solubility decreased as the concentration of IL increased in the aqueous mixtures. This negative impact could be explained by the fact that the CO_2 loading capacity of aqueous MEA *or* DEA depend upon its concentration (pure MEA *or* DEA). The higher the concentration of amine in the aqueous solution lower is the absorption. Therefore the increase in concentration of IL in the solution increases the concentration of amine solvent in the aqueous solution. The IL concentration when increase reduces the water molecules (Aziz et. al. 2012). Sairi et. al. (2011) also observed the same behaviour that the addition of IL to the aqueous amine solvent reduced the CO_2 absorption of the former. The CO_2 absorption mechanism in primary or secondary amine has been explained in the section 1.1.3 of Chapter 1. Based on the experimental results obtained for CO_2 solubility in the binary (IL+MDEA) and ternary (aqueous IL+amine) mixtures it can be concluded that the CO_2 absorption generally decreases in these. Some binary mixtures exhibit enhanced CO_2 absorption, however the increments are not so much pronounced in comparison to the pure IL. The addition of IL to the aqueous amine solvents has not proven fruitful in general. The addition of IL to the aqueous amine solvent reduces the CO_2 absorption of the former by hindering the chemical reaction.

4.11. Thermodynamic Modelling

In an attempt to represent the experimental CO_2 solubility data, thermodynamic modeling was performed for the pure solvents as well as in the binary mixtures with the Peng Robinson (1976) and Soave-Redlich Kwong (1972) equations of state with the van der Waals (vdW) and Mathias-Klotz-Prausnitz (MK) mixing rules.

The Peng-Robinson equation of state is defined as:

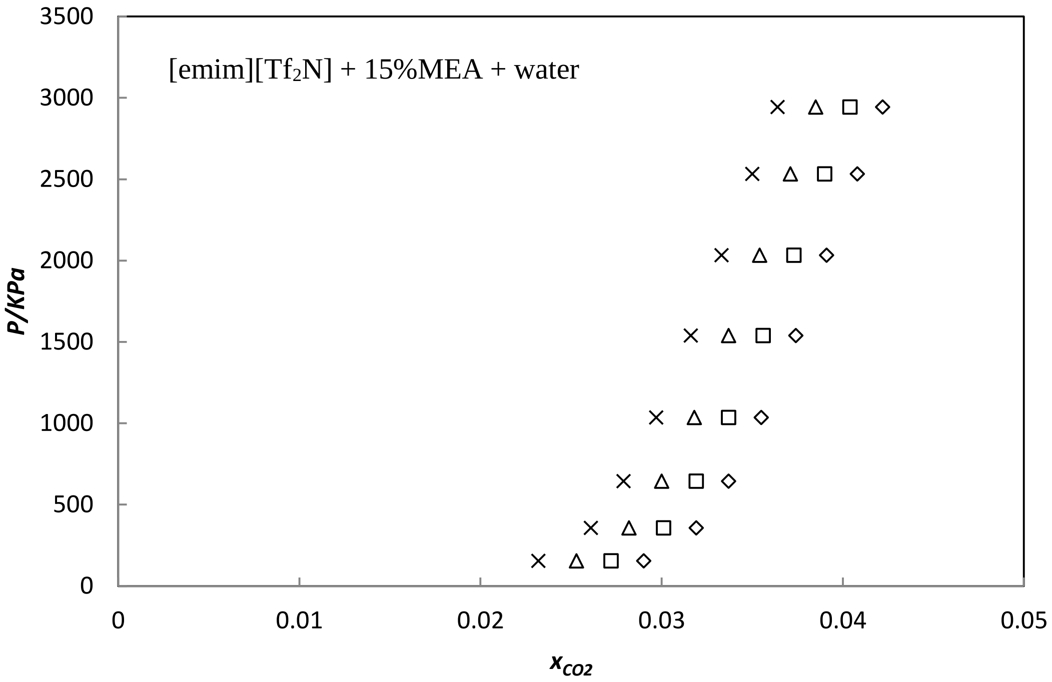

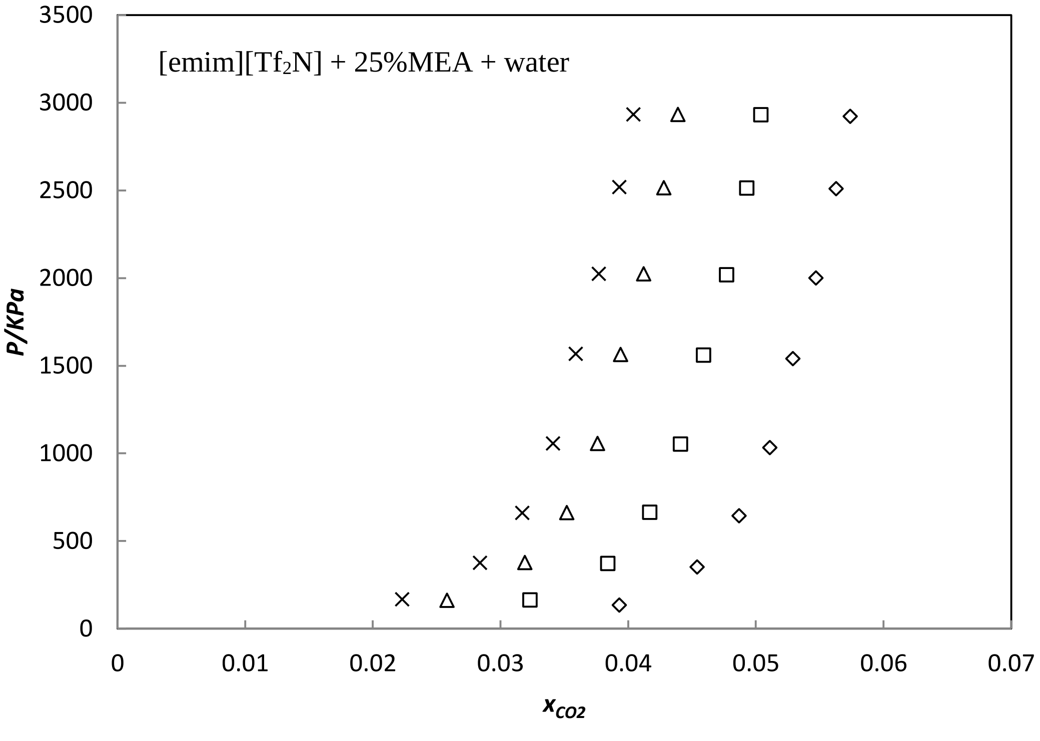

Figure 4.47: CO_2 solubility in aqueous IL + amine mixtures: Aqueous amine {15wt% MEA *or* 25wt% DEA} (◊), 5wt% [emim][Tf$_2$N] (□), 10wt% [emim][Tf$_2$N] (Δ), 15wt% [emim][Tf$_2$N] (×).

$$P = \frac{RT}{(v-b)} - \frac{a}{v(v+b)+b(v-b)} \tag{4.11}$$

where pure components parameters 'a_i' and 'b_i' are:

$$a_i = 0.457235\left(\frac{R^2T_{ci}^2}{P_{ci}}\right)\left[1+\left(0.37464+1.54226\omega_i-0.26992\omega_i^2\right)\left(1-\sqrt{\frac{T}{T_{ci}}}\right)\right]^2 \tag{4.12}$$

and

$$b_i = 0.077796\left(\frac{RT_{ci}}{P_{ci}}\right) \tag{4.13}$$

The Soave-Redlich-Kwong equation of state is represented by the following relation:

$$P = \frac{RT}{v-b} - \frac{a}{v^2-bv} \tag{4.14}$$

where

$$a_i = 0.42747\left(\frac{R^2T_{ci}^2}{P_{ci}}\right)\left[1+(0.48+1.57\omega_i-0.176\omega_i^2)\left(1-\sqrt{\frac{T}{T_{ci}}}\right)\right]^2 \tag{4.15}$$

and

$$b_i = 0.08664\left(\frac{RT_{ci}}{P_{ci}}\right) \tag{4.16}$$

In equations (4.12-4.13 and 4.15-4.16), T_{ci}, P_{ci} and ω are the critical temperature, critical pressure and acentric factor of the pure component 'i' respectively. These properties for the pure CO_2, MDEA, ([hmim][BF_4]), ([hmim][Tf_2N]) and ([hmim][FAP]) are listed in Table 4.5.

In Eqs. (4.11, 4.14) the parameters 'a' and 'b' have been obtained by using quadratic van der Waals and Mathias-Klotz-Prausnitz mixing rules. The conventional Van der Waals mixing rule is defined as:

$$a = \sum_{i=1}^{n}\sum_{j=1}^{n} x_i x_j a_{ij} \tag{4.17}$$

Table 4.5. Critical properties of the ionic liquids, MDEA and CO_2

Component	Formula	Molar Mass(g/mol)	T_c (K)	P_c (kpa)	ω
CO_2[a]	CO_2	44.01	304.25	7380	0.2280
MDEA[b]	$C_5H_{13}NO_2$	119.16	677.8	3876.1	1.2420
[hmim][BF_4][c]	$C_{10}H_{19}N_2BF_4$	254.08	690	1790	0.9625
[hmim][Tf_2N][c]	$C_{12}H_{19}N_3F_6S_2O_4$	447.42	1292.8	2390	0.3893
[hmim][FAP][d]	$C_{16}H_{19}F_{18}N_2P$	612.29	847.9	1393	0.1815

[a] Ren et. al. 2010, [b] Chunxi et. al. 2000, [c] Valderrama et. al. 2009, [d] Yokozeki et. al. 2008

Where

$$a_{ij} = \left(a_i a_j\right)^{\frac{1}{2}} \left(1 - k_{ij}\right) \tag{4.18}$$

with $k_{ij} = k_{ji}$,

and

$$b = \sum_{i=1}^{n} \sum_{j=1}^{n} x_i x_j b_{ij} \tag{4.19}$$

where

$$b_{ij} = \frac{1}{2} \left(b_i + b_j\right)\left(1 - l_{ij}\right) \tag{4.20}$$

with $l_{ij} = l_{ji}$

The mixing rule published by Mathias-Klotz-Prausnitz (1991) is represented by the following set of equations:

$$a = \sum_{i=1}^{n}\sum_{j=1}^{n} x_i x_j \sqrt{a_i a_j}\ \left(1 - k_{ij}\right) + \sum_{i=1}^{n} x_i \left(\sum_{j=1}^{n} x_j \left(\sqrt{a_i a_j}\ \lambda_{ij}\right)^{\frac{1}{3}}\right)^{3} \qquad (4.21)$$

with $k_{ij} = k_{ji}$, $\lambda_{ij} = -\lambda_{ji}$,

and

$$b = \sum_{i=1}^{n}\sum_{j=1}^{n} x_i x_j b_{ij} \qquad (4.22)$$

where

$$b_{ij} = \frac{1}{2}\left(b_i + b_j\right)\left(1 - l_{ij}\right) \qquad (4.23)$$

with $l_{ij} = l_{ji}$

In Eqs. (4.18, 4.20-4.21, 4.23), k_{ij}, l_{ij} and λ_{ij} are the binary interaction parameters. These binary interaction parameters were estimated by minimizing the optimization function (Eq. (4.24)) using simulated annealing method.

$$OF = \sum_{i=1}^{NOBS} \left(P_i^{exp} - P_i^{calc}\right)^2 \qquad (4.24)$$

where P_i^{calc} and P_i^{exp} are calculated and experimental pressure values, respectively, and *NOBS* is the number of experimental data points. The binary interaction parameters are listed in Tables 4.6 and 4.7. The experimental data and the one estimated with the help of Peng-Robinson and Soave-Redlich-Kwong equations of states with van der Waals and Mathias-Klotz-Prausnitz are listed in Tables 4.8-4.11 along with the rmsd values calculated by using the following relation:

$$rmsd = \sqrt{\sum_{i=1}^{n_{obs}} \frac{\left(P_i^{calc} - P_i^{exp}\right)^2}{n_{obs}}} \tag{4.25}$$

The experimental Henry’s constants (Table 4.3) for all pure solvents and binary mixtures and the one estimated with the values obtained from Peng Robinson and Soave Redlich Kwon EOS with Mathias-Klotz-Praustniz and van der Waals mixing rules are listed in Table C-9 to C-11 of Appendix C. and are compared in the Figures 4.48 to 4.51. It can be seen that the Peng-Robinson EOS with Mathias-Klotz-Praustniz mixing rules satisfactory correlate well the experimental data in comparison to the Peng-Robinson EOS with van der waals mixing rule and SRK EOS with van der Waal and Mathias-Klotz-Praustniz mixing rules. The SRK EOS with Mathias-Klotz-Prautniz mixing rule also correlated experimental data at par with Peng-Robinson EOS with Mathias-Klotz-Prautniz mixing rule, however the values of rmds were higher for all the systems under study as compared to PR-MK. Furthermore some deviations were observed especially at higher temperatures and pressures. Both equations of states (PR and SRK) with van der Waals mixing rules also yielded fair representation of the experimental results. However these results were not comparable to the one obtained with the help of these equations of states with Mathias-Klotz-Prautniz mixing rules. It could be concluded that Mathias-Klotz-Prautniz mixing rule gave better results than conventional van der Waals mixing rules. This is due to the fact that the Mathias-Klotz-Prautniz mixing rules possess the capability to offset the michelsen kistenmacher syndrome (Michelsen et. al. 1990). Michelsen kistenmacher indicated the problem of invariance, which occurred in the extension of binary results to calculate multicomponent systems accurately. Mathias et. al. (1991) provided and empirical modification which overcomes the problem of invariance indicated by Michelsen and Kistenmacher, and thereby enabled researchers to produce accurate correlation/estimation for the experimental results with a fair degree of reproducibility (Patel et. al. 1998).

Table 4.6: Binary interaction parameters for the binary systems.

	k_{12}	l_{12}	λ_{12}
T = 298.15 to 323.15 K			
System		PR-MK	
CO_2 (1) + [hmim][BF_4] (2)	0.042524	0.012131	0.053411
CO_2 (1) + [hmim][Tf_2N] (2)	0.033432	0.033423	0.046761
CO_2 (1) + [hmim][FAP] (2)	0.023241	0.023242	0.032115
CO_2 (1) + MDEA (2)	0.022311	0.025454	0.022321
		SRK-MK	
CO_2 (1) + [hmim][BF_4] (2)	0.032878	0.05526	0.034232
CO_2 (1) + [hmim][Tf_2N] (2)	0.053453	-0.042332	0.02211
CO_2 (1) + [hmim][FAP] (2)	0.053635	0.033432	0.03432
CO_2 (1) + MDEA (2)	0.053434	0.044321	0.02324
		PR-VdW	
CO_2 (1) + [hmim][BF_4] (2)	0.052315	0.055121	
CO_2 (1) + [hmim][Tf_2N] (2)	0.057128	0.060123	
CO_2 (1) + [hmim][FAP] (2)	0.049231	0.059901	
CO_2 (1) + MDEA (2)	0.063616	-0.013920	
		SRK-VdW	
CO_2 (1) + [hmim][BF_4] (2)	0.032423	0.023232	
CO_2 (1) + [hmim][Tf_2N] (2)	0.026262	0.024241	
CO_2 (1) + [hmim][FAP] (2)	0.066511	0.055432	
CO_2 (1) + MDEA (2)	0.045341	0.033411	

Table 4.7: Binary interaction parameters for the ternary systems.

System	$^{*}k_{12}$	$^{*}k_{13}$	k_{23}	$^{*}l_{12}$	$^{*}l_{13}$	l_{23}
CO_2(1)+[hmim][BF_4](2)+MDEA(3)	0.05231	0.06361	-0.1525	0.05512	-0.01392	-0.07563
CO_2(1)+[hmim][Tf_2N](2)+MDEA(3)	0.05712	0.06361	-0.1392	0.60123	-0.01392	-0.06594
CO_2(1)+[hmim][FAP](2)+MDEA(3)	0.04923	0.06361	-0.1498	0.05990	-0.01392	-0.09583

* values from Table 4.6.

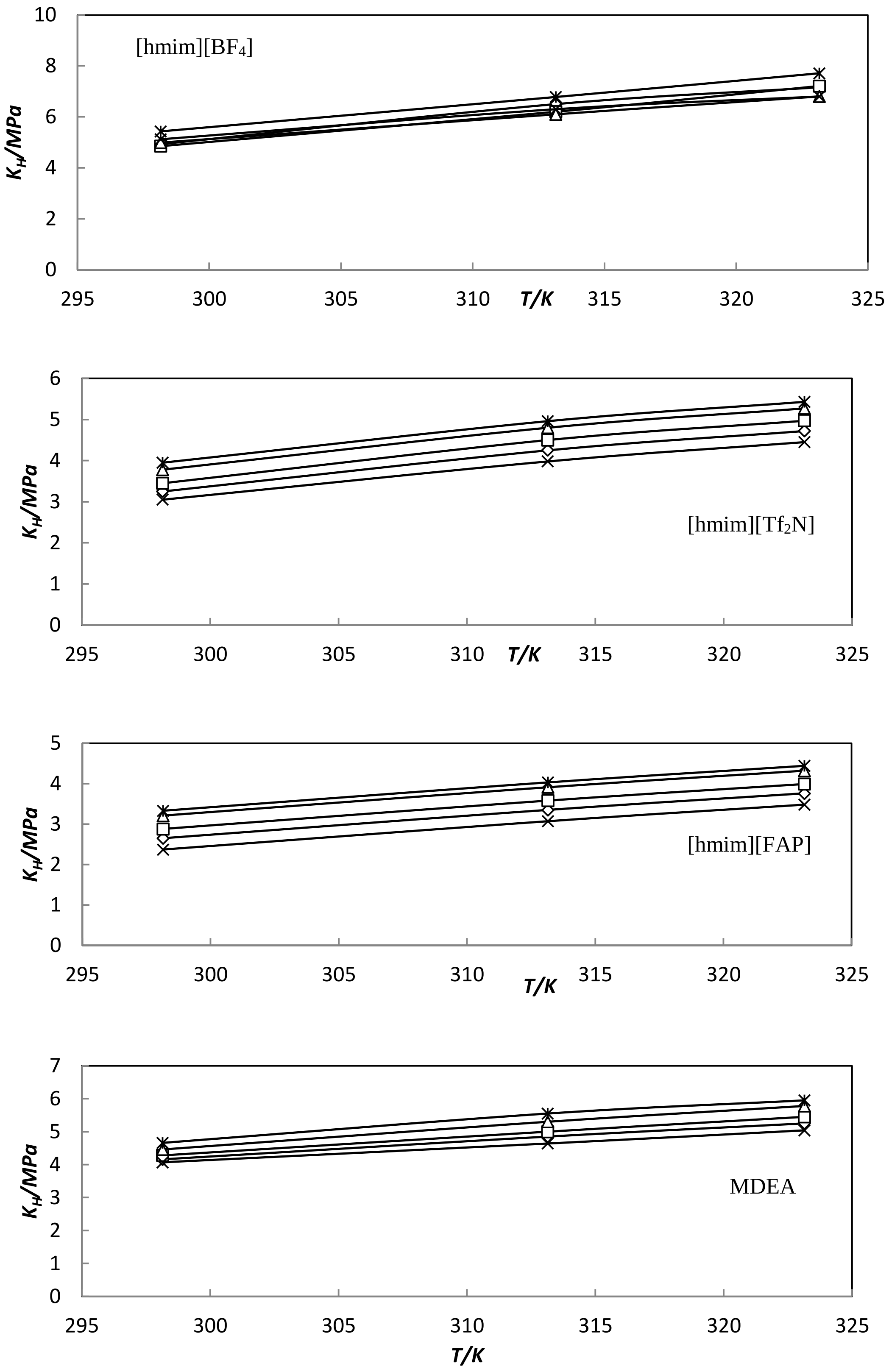

Figure 4.48. Comparison of the experimental Henry's constant with the calculated one for the pure solvents. Exp: (◊), Calc: PR-MK (□), PR-vdW (Δ), SRK-MK (×), SRK-vdW (*).

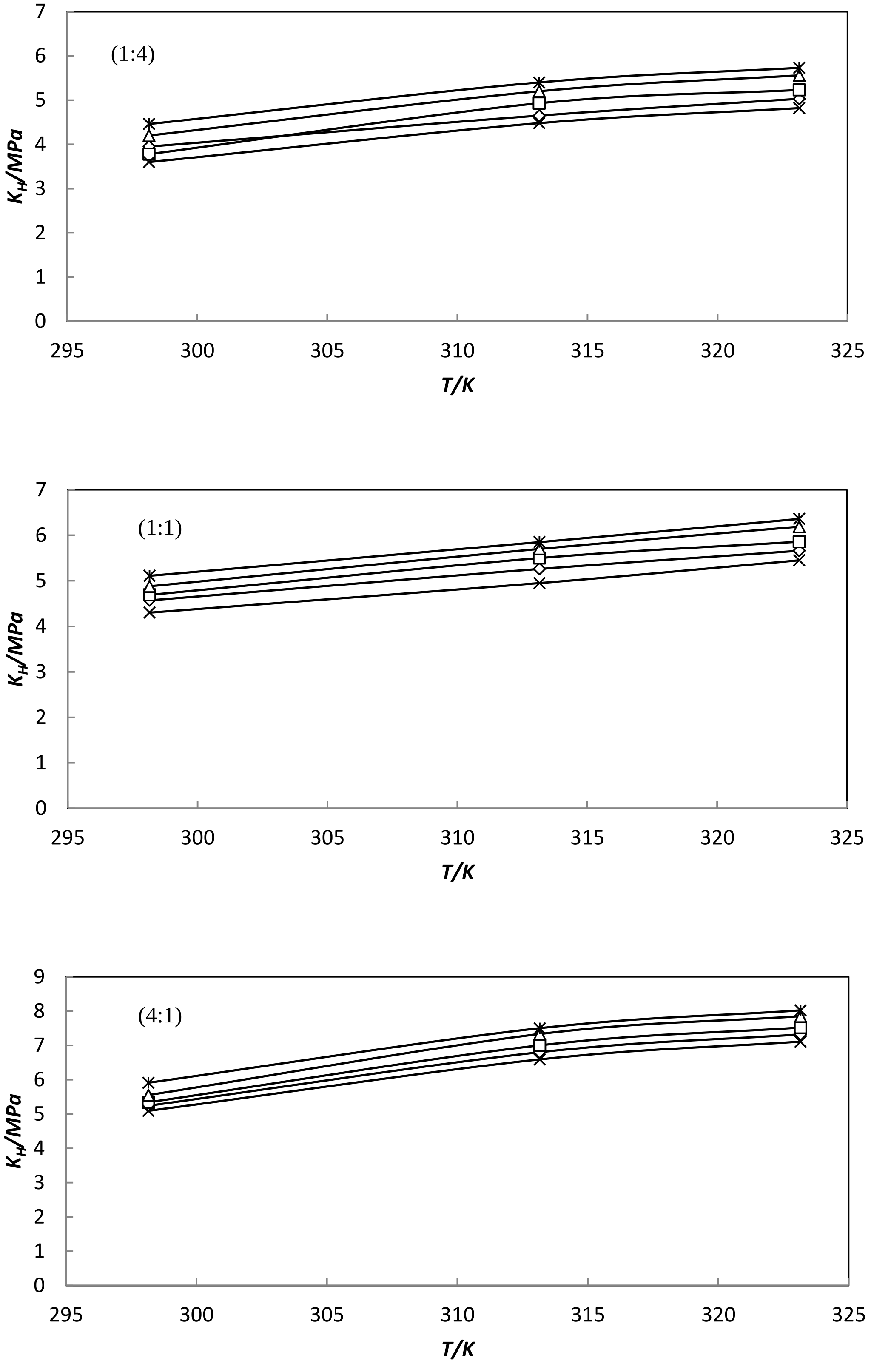

Figure 4.49. Comparison of the experimental Henry's constant with the calculated one for the [hmim][BF_4] + MDEA system. Exp: (◊), Calc: PR-MK (□), PR-vdW (Δ), SRK-MK (×), SRK-vdW (*).

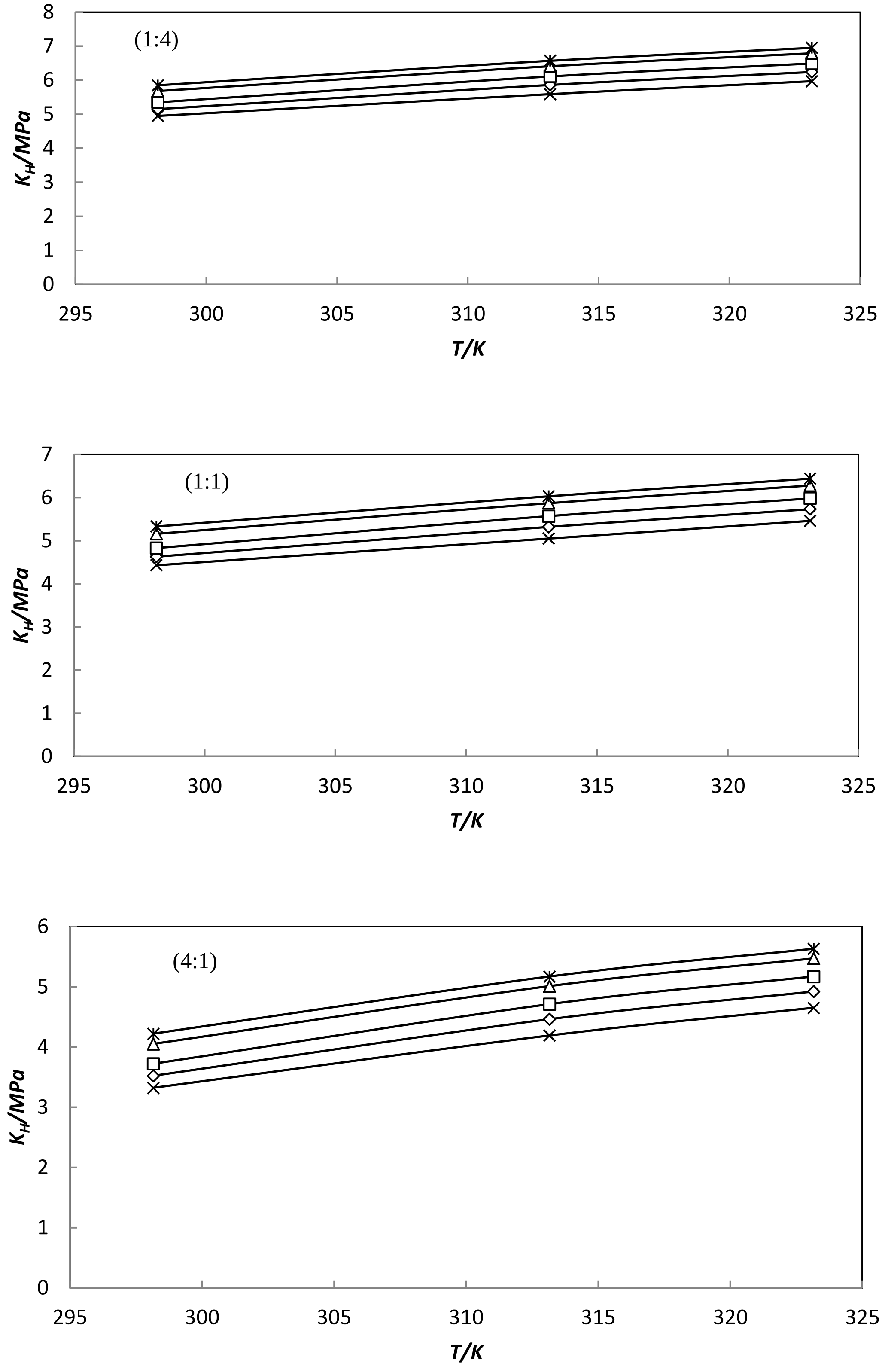

Figure 4.50. Comparison of the experimental Henry's constant with the calculated one for the [hmim][Tf_2N] + MDEA system. Exp: (◊), Calc: PR-MK (□), PR-vdW (Δ), SRK-MK (×), SRK-vdW (*).

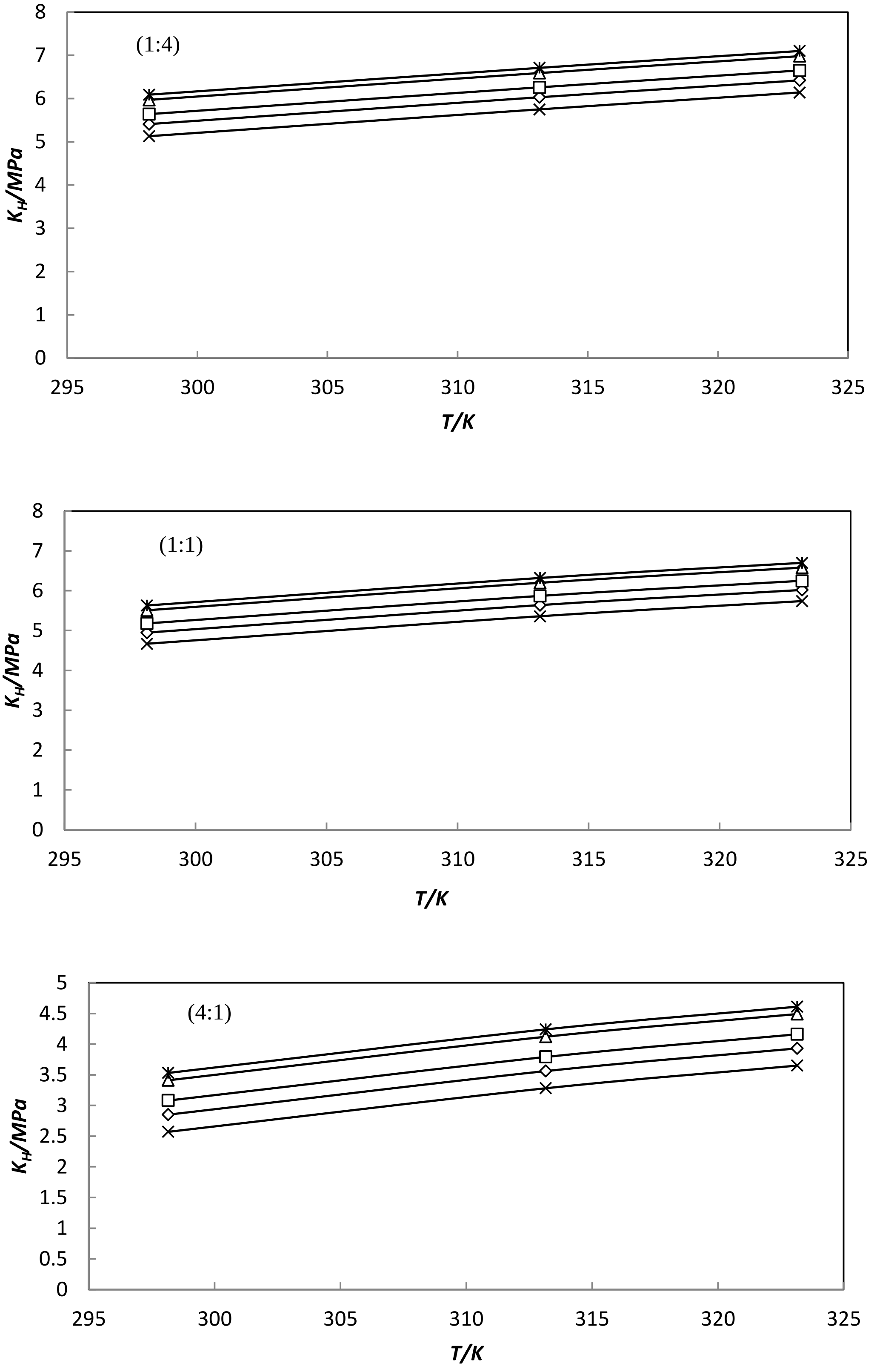

Figure 4.51. Comparison of the experimental Henry's constant with the calculated one for the [hmim][FAP] + MDEA system. Exp: (◊), Calc: PR-MK (□), PR-vdW (Δ), SRK-MK (×), SRK-vdW (*).

Table 4.8. The experimental and the estimated equilibrium pressures for the pure solvents.

CO_2 (1) + [hmim][BF_4] (2)																	
T = 298.15 K						***T = 313.15 K***						***T = 323.15 K***					
x_1	P/kPa	P_{calc} (PR-vdW)	P_{calc} (PR-MK)	P_{calc} (SRK-vdW)	P_{calc} (SRK-MK)	x_1	P/kPa	P_{calc} (PR-vdW)	P_{calc} (PR-MK)	P_{calc} (SRK-vdW)	P_{calc} (SRK-MK)	x_1	P/kPa	P_{calc} (PR-vdW)	P_{calc} (PR-MK)	P_{calc} (SRK-vdW)	P_{calc} (SRK-MK)
0.0261	130	115	128	120	122	0.0258	169	160	167	158	165	0.0227	160	158	162	160	161
0.0650	326	310	322	329	317	0.0521	344	334	342	332	344	0.0469	333	325	336	328	332
0.1300	661	640	658	632	656	0.1024	685	675	682	670	679	0.0893	642	625	645	629	641
0.1950	1012	990	1000	990	998	0.1517	1030	1020	1027	1015	1025	0.1456	1063	1050	1064	1055	1066
0.2387	1524	1510	1514	1443	1514	0.1953	1544	1535	1541	1532	1538	0.1892	1536	1525	1527	1527	1528
0.3142	2020	2000	2016	1985	2015	0.2708	2026	2000	2020	1998	2016	0.2647	2002	1990	1995	1993	1998
0.3878	2503	2500	2495	2433	2480	0.3444	2501	2470	2487	2465	2485	0.3383	2505	2490	2501	2489	2503
0.4267	2912	2900	2895	2992	2890	0.3766	2901	2860	2894	2855	2891	0.3705	2910	2870	2901	2876	2876
	rmsd	0.041	0.021	0.051	0.035			0.054	0.031	0.059	0.036			0.057	0.030	0.061	0.037
CO_2 (1) + [hmim][Tf_2N] (2)																	
0.0384	126	114	124	112	120	0.0297	127	120	125	118	123	0.0282	134	130	132	129	133
0.1045	347	335	340	332	335	0.0768	331	320	329	318	330	0.0668	319	308	316	306	317
0.2013	678	660	674	658	670	0.1437	627	615	625	613	622	0.1301	629	615	625	613	622
0.3082	1052	1035	1040	1032	1032	0.2464	1095	1080	1090	1075	1083	0.2096	1029	1015	1026	1025	1028
0.3654	1552	1540	1548	1537	1535	0.3035	1563	1550	1559	1552	1558	0.2668	1569	1556	1566	1556	1554
0.4533	2018	1970	2010	1973	1972	0.3914	2019	1989	2015	1991	1980	0.3547	2017	1980	2018	2011	2015
0.5488	2509	2460	2500	2462	2456	0.4869	2511	2470	2506	2463	2465	0.4502	2515	2480	2513	2512	2510
0.5988	2903	2850	2895	2843	2851	0.5369	2914	2870	2909	2863	2865	0.5002	2938	2900	2935	2931	2931
	rmsd	0.040	0.030	0.047	0.035			0.047	0.025	0.051	0.031			0.050	0.032	0.051	0.037
CO_2 (1) + [hmim][FAP] (2)																	
0.0518	139	130	137	129	132	0.0381	128	120	125	118	129	0.0381	144	133	142	130	146
0.1237	332	310	330	307	312	0.1044	354	340	349	335	358	0.0801	305	290	300	289	310
0.2431	658	640	655	637	643	0.1789	615	605	611	600	618	0.1773	686	670	680	666	673
0.3702	1042	1025	1038	1022	1028	0.3066	1077	1060	1065	1055	1073	0.2637	1030	1015	1026	1000	1025
0.4488	1535	1525	1532	1521	1529	0.3852	1544	1530	1540	1534	1547	0.3422	1578	1560	1570	1554	1577
0.5477	2023	1980	2025	1972	1988	0.4841	2021	2000	2018	1998	1994	0.4411	2036	1980	2032	1978	2038
0.6466	2512	2450	2515	2449	2455	0.5830	2519	2460	2508	2454	2446	0.5400	2522	2480	2515	2479	2521
0.6933	2917	2850	2920	2852	2855	0.6297	2916	2880	2910	2878	2887	0.5867	2920	2880	2914	2877	2901
	rmsd	0.041	0.037	0.046	0.039			0.056	0.031	0.057	0.037			0.048	0.031	0.051	0.038
CO_2 (1) + MDEA (2)																	
0.0322	135	125	133	126	123	0.0317	155	150	152	149	150	0.0267	142	146	144	143	140
0.0827	353	350	251	355	354	0.0767	379	385	372	382	370	0.0665	355	375	356	377	358
0.1498	645	655	642	643	641	0.1278	633	650	637	655	632	0.1240	666	686	669	683	662
0.2337	1033	1040	1028	1038	1027	0.2022	1027	1050	1036	1054	1032	0.1877	1021	1035	1024	1039	1026
0.2911	1542	1545	1538	1543	1543	0.2596	1575	1580	1577	1578	1572	0.2451	1542	1550	1544	1558	1543
0.3743	2001	1990	1998	1991	1986	0.3428	2029	1990	2033	1992	2031	0.3283	2015	1970	2018	1972	2000
0.4521	2511	2490	2501	2487	2487	0.4206	2504	2430	2511	2431	2508	0.4061	2525	2440	2528	2446	2522
0.4989	2922	2880	2912	2883	2883	0.4674	2949	2870	2943	2872	2876	0.4529	2928	2850	2926	2924	2926
	rmsd	0.057	0.029	0.060	0.035			0.058	0.031	0.060	0.033			0.041	0.030	0.043	0.035

Table 4.9. The experimental and the estimated equilibrium pressures for the [hmim][BF$_4$]+MDEA system.

CO_2 (1) + [hmim][BF_4] (2) + MDEA (3)																	
(1:4)						(1:1)						(4:1)					
x_1	P/kPa	P_{calc} (PR-vdW)	P_{calc} (PR-MK)	P_{calc} (SRK-vdW)	P_{calc} (SRK-MK)	x_1	P/kPa	P_{calc} (PR-vdW)	P_{calc} (PR-MK)	P_{calc} (SRK-vdW)	P_{calc} (SRK-MK)	x_1	P/kPa	P_{calc} (PR-vdW)	P_{calc} (PR-MK)	P_{calc} (SRK-vdW)	P_{calc} (SRK-MK)
T = 298.15 K																	
0.0387	154	150	155	148	157	0.0309	142	130	144	129	146	0.0305	162	170	166	169	157
0.0779	312	300	310	308	309	0.0788	367	355	369	352	366	0.0695	370	385	377	383	366
0.1527	624	610	620	618	625	0.1343	634	620	637	617	637	0.1133	610	625	614	624	605
0.2611	1088	1070	1086	1066	1065	0.2188	1055	1030	1057	1032	1051	0.1858	1025	1040	1027	1038	1022
0.3174	1567	1560	1566	1567	1557	0.2701	1574	1560	1572	1566	1562	0.2201	1564	1568	1568	1570	1566
0.3989	2009	1990	2000	1998	2006	0.3463	2004	1980	1999	1988	1992	0.2903	2007	2000	2010	1996	2013
0.4812	2527	2480	2520	2477	2521	0.4215	2517	2480	2504	2483	2481	0.3711	2530	2500	2533	2495	2537
0.5232	2924	2880	2919	2928	2922	0.4677	2936	2880	2926	2882	2881	0.4019	2921	2878	2917	2945	2927
	rmsd	0.080	0.040	0.082	0.045			0.09	0.035	0.101	0.043			0.077	0.042	0.089	0.044
T = 313.15 K																	
0.0336	157	151	153	150	155	0.0274	145	146	142	148	143	0.0242	166	160	163	158	162
0.0690	328	320	322	318	322	0.0663	356	345	352	360	358	0.0519	358	365	352	362	352
0.1296	617	605	612	603	610	0.1270	683	675	688	686	688	0.0901	629	637	620	633	632
0.2139	1037	1020	1033	1033	1033	0.1893	1043	1030	1037	1033	1047	0.1453	1032	1048	1026	1043	1034
0.2742	1547	1530	1544	1537	1555	0.2308	1523	1510	1520	1528	1533	0.1795	1526	1528	1520	1528	1527
0.3557	2012	1960	2008	1965	2016	0.3068	2003	1980	1999	1994	2008	0.2497	2016	2050	2019	2048	2011
0.4380	2516	2450	2506	2455	2510	0.3920	2523	2470	2534	2526	2527	0.3305	2506	2540	2510	2538	2500
0.4790	2906	2850	2895	2856	2894	0.4382	2926	2880	2929	2900	2920	0.3613	2923	2925	2925	2927	2917
	rmsd	0.076	0.044	0.087	0.049			0.066	0.034	0.076	0.043			0.063	0.021	0.071	0.032
T = 323.15 K																	
0.0273	137	132	130	133	127	0.0216	123	127	120	125	126	0.0179	132	128	130	128	126
0.0601	306	295	296	298	292	0.0582	332	330	327	328	336	0.0424	314	324	309	312	322
0.1186	611	600	603	602	607	0.1095	636	626	633	625	640	0.0853	639	649	630	633	644
0.1998	1047	1030	1044	1034	1043	0.1795	1059	1045	1055	1042	1065	0.1405	1070	1085	1066	1066	1082
0.2630	1560	1550	1555	1553	1557	0.2238	1538	1530	1532	1527	1540	0.1748	1573	1580	1570	1569	1576
0.3485	2031	1990	2028	1991	2029	0.3012	2011	1970	2007	1965	2015	0.2450	2041	2010	2038	2038	2004
0.4258	2532	2480	2524	2483	2524	0.3725	2538	2470	2543	2467	2540	0.3258	2543	2530	2544	2537	2533
0.4718	2931	2850	2920	2855	2927	0.4154	2941	2920	2947	2917	2944	0.3566	2927	2900	2922	2923	2934
	rmsd	0.067	0.043	0.069	0.048			0.076	0.032	0.066	0.035			0.065	0.023	0.069	0.034

Table 4.10. The experimental and the estimated equilibrium pressures for the [hmim][Tf$_2$N]+MDEA binary system.

CO_2 (1) + [hmim][Tf$_2$N] (2) + MDEA (3)																	
(1:4)						(1:1)						(4:1)					
x_1	P/kPa	P_{calc} (PR-vdW)	P_{calc} (PR-MK)	P_{calc} (SRK-vdW)	P_{calc} (SRK-MK)	x_1	P/kPa	P_{calc} (PR-vdW)	P_{calc} (PR-MK)	P_{calc} (SRK-vdW)	P_{calc} (SRK-MK)	x_1	P/kPa	P_{calc} (PR-vdW)	P_{calc} (PR-MK)	P_{calc} (SRK-vdW)	P_{calc} (SRK-MK)
***T* = 298.15 K**																	
0.0318	165	153	163	154	162	0.0301	140	136	138	138	139	0.0385	136	138	139	133	140
0.0666	349	359	345	362	345	0.0701	330	350	327	351	329	0.0894	320	330	323	332	326
0.1167	620	645	615	647	617	0.1317	630	650	625	652	626	0.1761	640	655	642	653	644
0.1937	1055	1086	1050	1089	1050	0.2127	1040	1060	1037	1066	1039	0.2827	1049	1066	1041	1062	1052
0.2511	1571	1580	1567	1588	1572	0.2701	1520	1530	1516	1533	1519	0.3387	1540	1560	1536	1559	1543
0.3309	2044	2040	2041	2043	2046	0.3521	2030	2040	2037	2044	2028	0.4261	2033	2040	2029	2039	2032
0.4122	2535	2540	2525	2544	2538	0.4304	2520	2540	2522	2542	2518	0.5274	2541	2560	2532	2557	2540
0.4522	2929	2935	2907	2934	2930	0.4743	2946	2960	2948	2962	2944	0.5711	2933	2960	2926	2958	2937
	rmsd	0.065	0.021	0.071	0.045			0.068	0.031	0.070	0.038			0.076	0.031	0.078	0.040
***T* = 313.15 K**																	
0.0247	146	140	144	139	145	0.0281	150	145	148	143	149	0.0276	124	134	122	133	120
0.0553	329	335	325	332	328	0.0620	334	340	332	325	330	0.0710	321	331	317	336	318
0.1069	643	663	641	660	640	0.1168	638	648	636	632	635	0.1404	644	654	640	657	641
0.1665	1020	1040	1016	1043	1015	0.1882	1046	1066	1043	1037	1040	0.2195	1023	1040	1017	1036	1028
0.2210	1531	1541	1526	1546	1543	0.2409	1553	1566	1543	1548	1550	0.2812	1532	1540	1522	1538	1539
0.3107	2038	1985	2031	1990	1989	0.3276	2027	2017	2020	2021	2017	0.3729	2042	2062	2034	2058	2066
0.3863	2531	2490	2533	2533	2499	0.4059	2528	2520	2526	2525	2517	0.4702	2536	2556	2530	2551	2557
0.4258	2934	2901	2927	2940	2915	0.4498	2943	2920	2938	2941	2932	0.5179	2944	2940	2942	2942	2944
	rmsd	0.067	0.032	0.070	0.041			0.071	0.034	0.077	0.044			0.072	0.034	0.075	0.041
***T* = 323.15 K**																	
0.0252	158	165	156	166	153	0.0256	147	140	144	143	149	0.0254	125	123	127	122	124
0.0532	336	356	330	359	339	0.0586	340	360	336	344	343	0.0648	324	334	327	332	330
0.1011	646	666	640	663	668	0.1101	647	667	641	644	649	0.1231	622	642	619	636	627
0.1645	1068	1088	1066	1085	1065	0.1760	1053	1073	1047	1057	1056	0.2001	1024	1044	1019	1038	1030
0.2219	1572	1582	1576	1578	1577	0.2334	1559	1570	1549	1555	1552	0.2531	1533	1550	1531	1548	1538
0.3017	2035	2020	2039	2013	2029	0.3134	2005	1980	1999	2001	1997	0.3465	2046	2034	2044	2031	2048
0.3820	2514	2480	2522	2477	2509	0.3977	2545	2520	2549	2543	2537	0.4366	2526	2510	2521	2508	2527
0.4230	2939	2920	2943	2917	2944	0.4376	2915	2870	2925	2900	2927	0.4885	2947	2935	2954	2921	2945
	rmsd	0.066	0.028	0.069	0.032			0.068	0.031	0.069	0.033			0.065	0.032	0.070	0.037

Table 4.11. The experimental and the estimated equilibrium pressures for the [hmim][FAP] +MDEA binary system.

CO_2 (1) + [hmim][FAP] (2) + MDEA (3)																	
(1:4)						(1:1)						(4:1)					
x_1	P/kPa	P_{calc} (PR-vdW)	P_{calc} (PR-MK)	P_{calc} (SRK-vdW)	P_{calc} (SRK-MK)	x_1	P/kPa	P_{calc} (PR-vdW)	P_{calc} (PR-MK)	P_{calc} (SRK-vdW)	P_{calc} (SRK-MZ)	x_1	P/kPa	P_{calc} (PR-vdW)	P_{calc} (PR-MK)	P_{calc} (SRK-vdW)	P_{calc} (SRK-MK)
***T* = 298.15 K**																	
0.0292	159	150	156	148	155	0.0260	129	122	119	122	127	0.0518	149	159	146	145	143
0.0648	357	377	360	372	351	0.0675	341	330	335	330	337	0.1320	381	395	373	376	376
0.1126	628	648	629	641	624	0.1285	654	640	647	641	655	0.2314	681	695	675	675	678
0.1795	1022	1048	1027	1044	1018	0.1985	1039	1015	1026	1025	1036	0.3543	1075	1090	1066	1067	1065
0.2371	1530	1550	1537	1547	1527	0.2651	1547	1530	1540	1542	1544	0.4210	1539	1550	1530	1528	1533
0.3282	2034	2040	2038	2038	2026	0.3552	2028	1990	2020	2022	2017	0.5209	2039	2059	2033	2033	2031
0.3985	2544	2560	2540	2551	2546	0.4250	2533	2500	2521	2522	2535	0.6201	2539	2559	2529	2531	2533
0.4372	2913	2950	2922	2943	2903	0.4651	2909	2900	2901	2919	2919	0.6692	2930	2940	2920	2932	2934
	rmsd	0.054	0.021	0.059	0.031			0.061	0.032	0.065	0.037			0.071	0.034	0.072	0.036
***T* = 313.15 K**																	
0.0227	138	135	136	130	126	0.0261	148	137	142	140	144	0.0373	133	140	127	143	128
0.0527	322	330	320	315	317	0.0590	338	330	330	333	335	0.0899	325	345	322	343	320
0.1009	625	645	619	620	622	0.1096	637	610	630	615	639	0.1709	626	646	622	644	622
0.1657	1045	1065	1034	1055	1040	0.1733	1019	990	1015	994	1023	0.2800	1044	1064	1038	1067	1036
0.2142	1561	1580	1554	1569	1566	0.2329	1529	1510	1520	1524	1526	0.3467	1558	1570	1550	1572	1547
0.2941	2010	2030	2007	2017	2013	0.3175	2006	2040	2000	2035	2000	0.4466	2024	2045	2019	2041	2021
0.3701	2542	2570	2537	2532	2543	0.3978	2508	2530	2495	2524	2501	0.5458	2510	2530	2501	2536	2500
0.4104	2905	2930	2887	2955	2925	0.4389	2925	2960	2914	2911	2922	0.5949	2937	2937	2931	2930	2911
	rmsd	0.057	0.021	0.058	0.032			0.065	0.033	0.066	0.037			0.065	0.030	0.069	0.033
***T* = 323.15 K**																	
0.0221	143	140	137	139	136	0.0249	151	145	148	143	149	0.0357	141	138	137	133	135
0.0503	327	347	322	340	325	0.0549	335	320	332	324	330	0.0811	323	333	319	335	318
0.0984	648	668	644	632	648	0.1031	635	615	630	618	628	0.1571	631	651	628	652	628
0.1582	1058	1080	1055	1050	1044	0.1669	1048	1020	1042	1024	1044	0.2581	1054	1065	1048	1061	1042
0.2128	1565	1575	1558	1567	1569	0.2316	1551	1532	1542	1538	1546	0.3179	1562	1575	1552	1578	1546
0.2924	2032	2050	2026	2037	2027	0.3140	2037	2030	2026	2037	2027	0.4155	2014	2030	2002	2027	2001
0.3702	2529	2560	2519	2532	2522	0.3925	2540	2545	2536	2543	2539	0.5184	2524	2550	2510	2548	2518
0.4109	2911	2955	2901	2922	2900	0.4316	2907	2900	2896	2906	2898	0.5612	2932	2930	2921	2926	2929
	rmsd	0.056	0.030	0.061	0.036			0.065	0.020	0.067	0.031			0.068	0.031	0.070	0.036

4.12 Solvent regeneration studies

4.12.1 Recycled pure liquids

The pure liquids; [hmim][BF_4], [hmim][Tf_2N], [hmim][FAP] and MDEA, which were once used for CO_2 solubility were regenerated and used again to investigate their potential applicability for recycling purpose. The pure liquids used in the present study for CO_2 absorption were collected after the measurements and placed in sealed containers. The recycling of pure liquids was carried out by desorbing CO_2 by the application of depressurization and vacuum (< 45 kPa).

The samples were kept for 24 hrs in the vacuum oven to ensure complete removal of CO_2. After that they were again used for CO_2 solubility. The CO_2 solubility data in the recycled pure liquids are listed in Table C-12 of the Appendix C. Figures 4.52 to 4.55 illustrate the comparison of CO_2 solubility in the pure liquids and recycled liquids. It can be seen from the figures that there is not much difference in CO_2 solubility in the pure liquids and recycled pure liquids. However at higher pressures some deviations were observed.

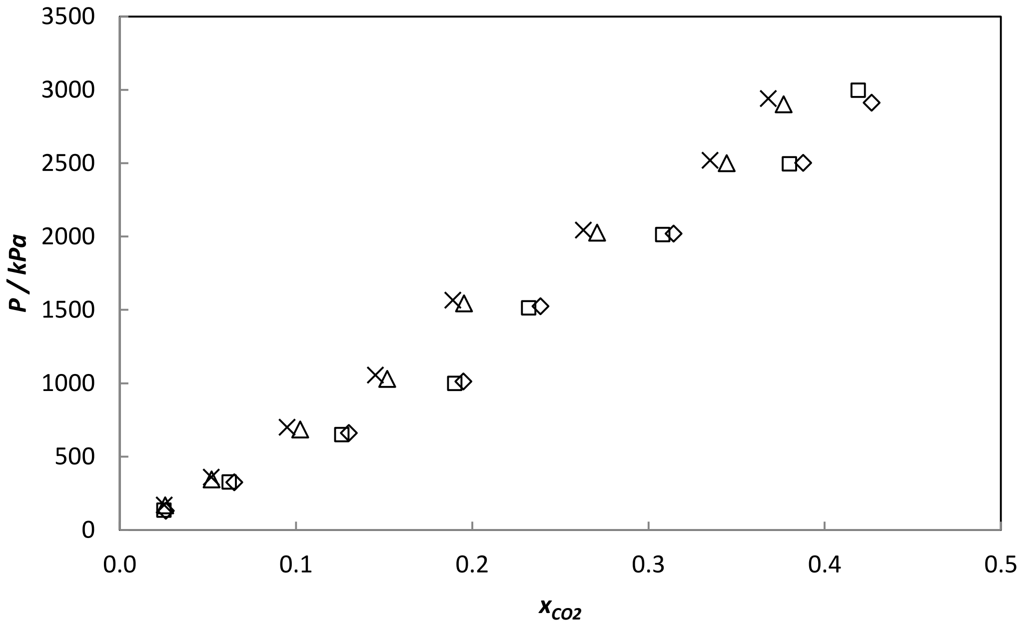

Figure 4.52. CO_2 solubility in the fresh and recycled IL ([hmim][BF_4]). For fresh IL: at T = 298.15 K (◊), T = 313.15 K (Δ). For recycled IL: at T = 298.15 K (□), T = 313.15 K (×).

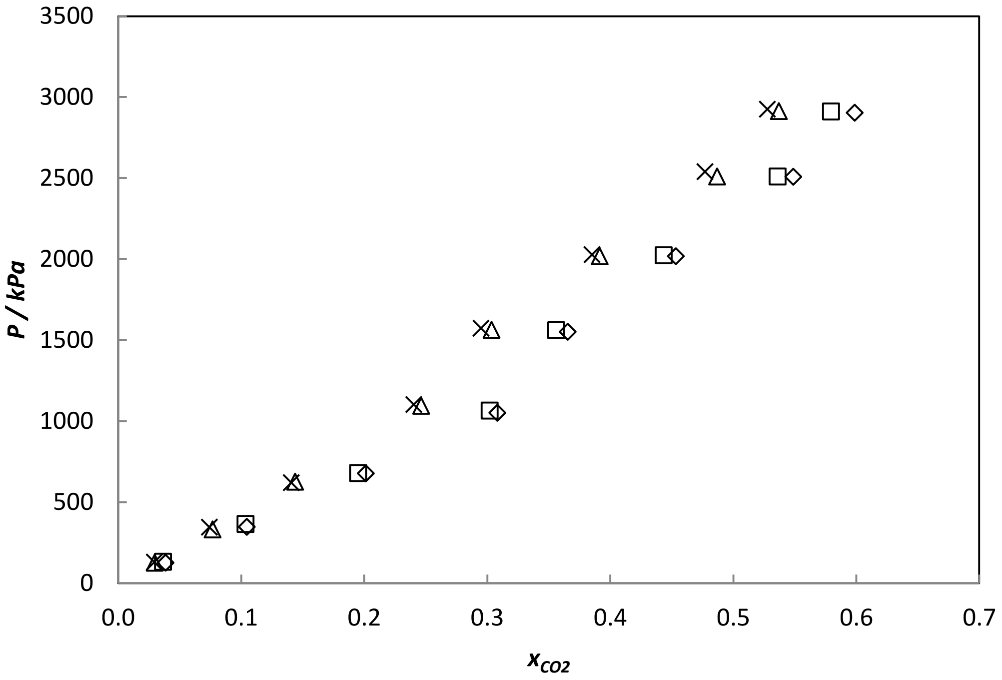

Figure 4.53. CO_2 solubility in the fresh and recycled IL ([hmim][Tf_2N]). For fresh IL: at T = 298.15 K (◊), T = 313.15 K (Δ). For recycled IL: at T = 298.15 K (□), T = 313.15 K (×).

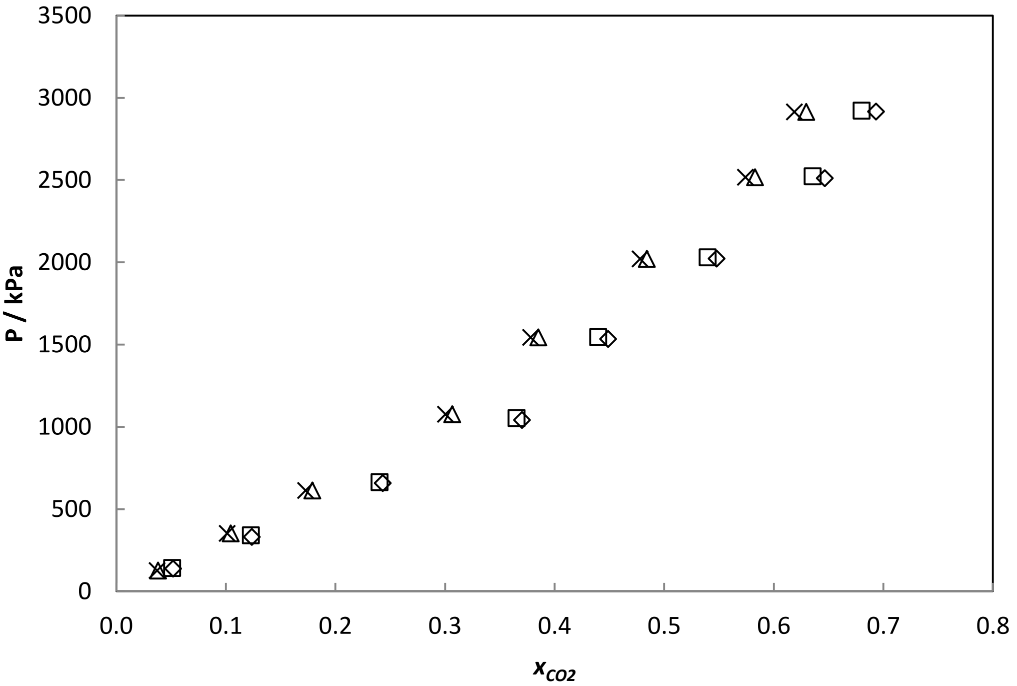

Figure 4.54. CO_2 solubility in the fresh and recycled IL ([hmim][FAP]). For fresh IL: at T = 298.15 K (◊), T = 313.15 K (Δ). For recycled IL: at T = 298.15 K (□), T = 313.15 K (×).

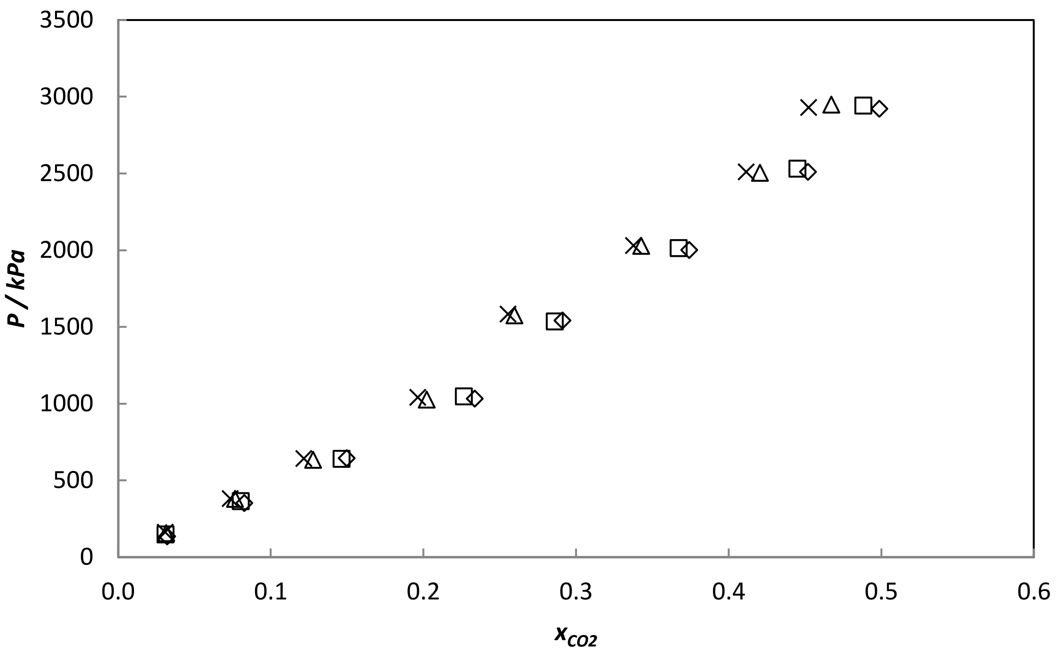

Figure 4.55. CO_2 solubility in the fresh and recycled MDEA. For fresh MDEA: at T = 298.15 K (◊), T = 313.15 K (Δ). For recycled MDEA: at T = 298.15 K (□), T = 313.15 K (×).

4.12.2 Recycled Binary Mixtures

The binary mixtures which showed a maximum CO_2 loading in comparison to other binary mixtures were selected and tested for recycling. These selected binary mixtures are listed in Table 4.12.

Table 4.12. List of binary mixtures used for recycling

Binary Mixture	Concentration
[hmim][BF_4] + MDEA	(1:4)
[hmim][Tf_2N] + MDEA	(4:1)
[hmim][FAP] + MDEA	(4:1)

The CO_2 solubility data in these recycled binary mixtures is listed in Table C-13 of the Appendix C. The comparison of CO_2 solubility between the fresh binary mixtures and recycled binary mixtures is plotted in Figure 4.56, 4.57 and 4.58 for ([hmim][BF_4]+MDEA), ([hmim][Tf_2N]+MDEA) and ([hmim][FAP]+MDEA) respectively. It can be seen from the figures that there is not much difference in terms of CO_2 solubility in the fresh and recycled binary mixtures. As was observed in the case of pure liquids minimum deviations were observed at high pressure for the binary mixtures also.

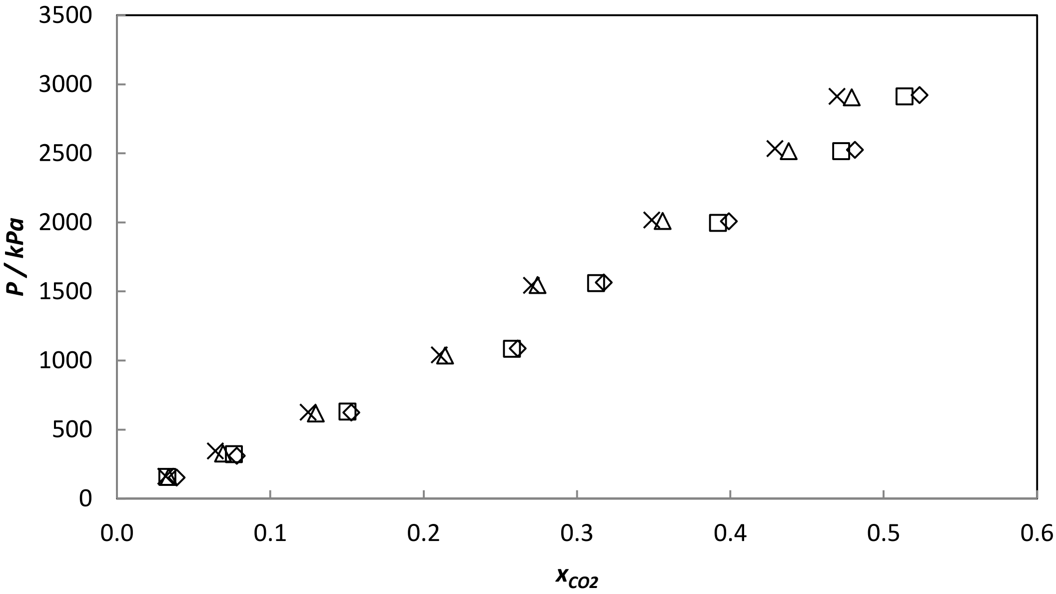

Figure 4.56. CO_2 solubility in the fresh and recycled binary mixture ([hmim][BF_4]+MDEA) (1:4). For fresh (1:4): at T = 298.15 K (◊), T = 313.15 K (Δ). For recycled (1:4): at T = 298.15 K (□), T = 313.15 K (×).

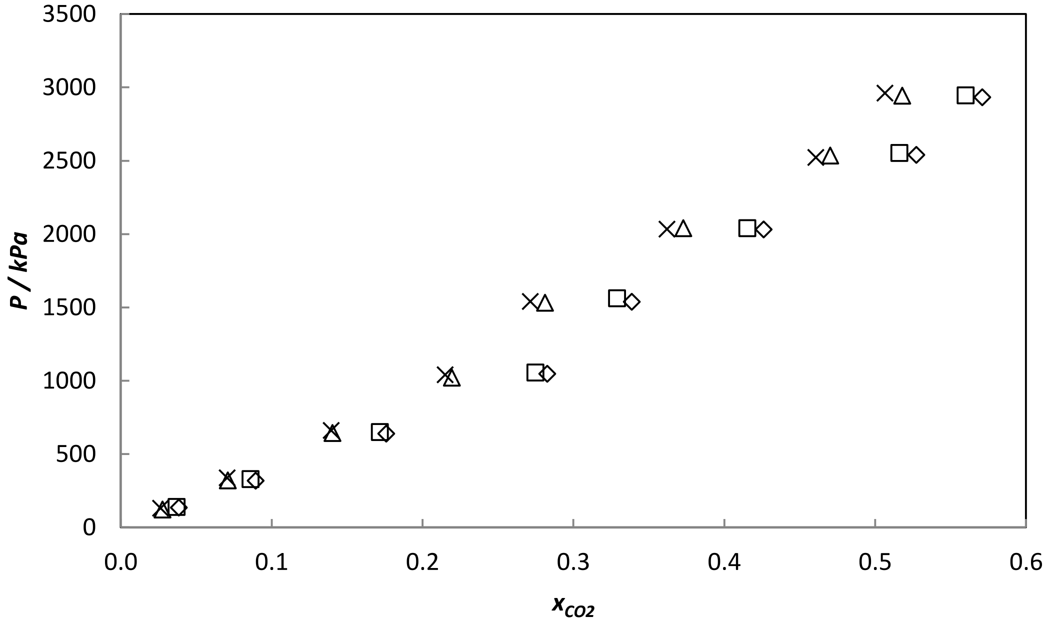

Figure 4.57. CO_2 solubility in the fresh and recycled binary mixture ([hmim][Tf_2N]+MDEA) (4:1). For fresh (1:4): at T = 298.15 K (◊), T = 313.15 K (Δ). For recycled (1:4): at T = 298.15 K (□), T = 313.15 K (×).

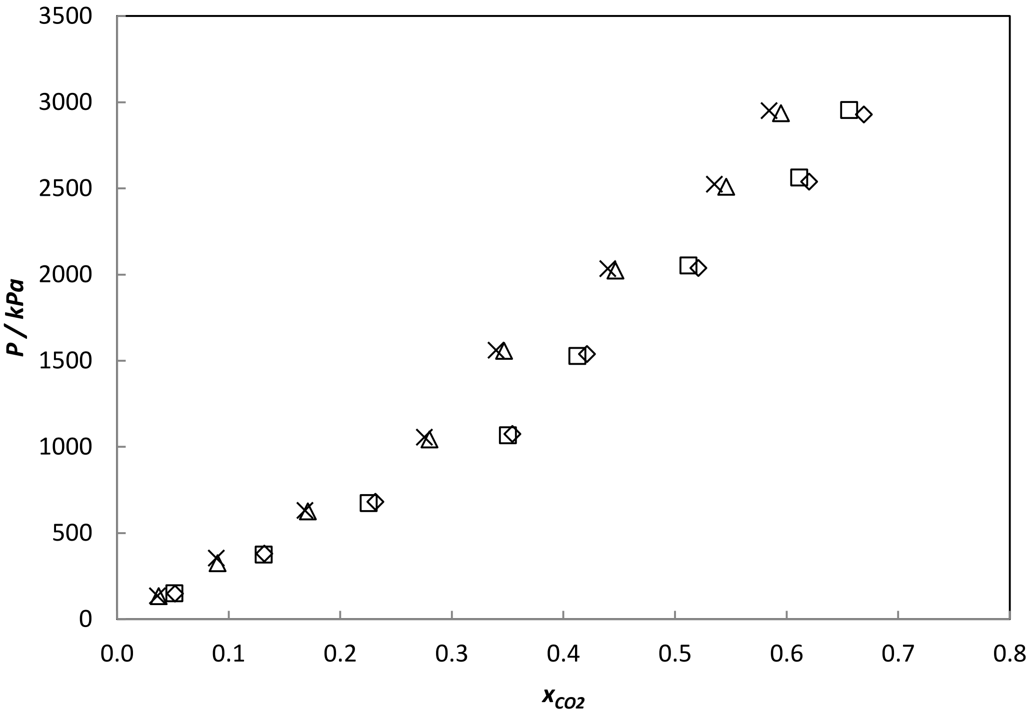

Figure 4.58. CO_2 solubility in the fresh and recycled binary mixture ([hmim][FAP]+MDEA) (4:1). For fresh (1:4): at $T = 298.15$ K (◊), $T = 313.15$ K (Δ). For recycled (1:4): at $T = 298.15$ K (□), $T = 313.15$ K (×).

4.13. Summary

The physical properties namely densities, viscosities, refractive indices of the pure ([hmim][BF_4], [hmim][Tf_2N], [hmim][FAP] and MDEA) as well as for the binary mixtures of IL with amine ([hmim][BF_4]+MDEA, [hmim][Tf_2N]+MDEA, [hmim][FAP]+MDEA) were measured at a temperature range of (298.15 to 323.15) over entire range of concentrations. The densities, viscosities and refractive indices were correlated as a function of concentration and temperatures simultaneously (for the case of binary mixtures) by using polynomial equation. The thermal stability (TGA) of the pure liquids as well as their binary mixtures (which were used for CO_2 solubility) was measured over a temperature range of (30 to 800 ^oC) at a heating rate of 10 $^oC.min^{-1}$. The excess (excess molar volumes) and deviation (viscosity and refractive index deviations) properties of the mixtures were deduced from the experimental data of densities, viscosities and refractive indices respectively. The pure liquids and the binary mixtures of IL with amine {having IL to MDEA molar ratios of (1:4), (1:1), (4:1)} were used for CO_2 solubility. The CO_2 solubility was measured at three different temperatures (298.15, 313.15, 323.15) K and at eight pressures (from 100 to ≤ 3000 kPa). The present results showed that among the pure solvents, the ionic liquid ([hmim][FAP]) showed the highest and pure MDEA showed the least CO_2 loadings. The same trend was observed over the entire temperature range. The IL ([hmim][FAP], [hmim][Tf_2N]) suffered loss in terms of CO_2 solubility by the addition of IL. The binary mixtures of IL ([hmim][BF_4]) with MDEA at two concentrations showed slightly higher CO_2 absorption values. The effects of concentration (for the case of binary mixtures only), temperature, pressure and anions have been discussed on the CO_2 solubility in the pure liquids as well as in the binary mixtures. It was observed that the CO_2 loadings decreased with increase in temperatures. The Henry's constants (which are function of temperature) were evaluated for the pure as well as for binary mixtures. The enthalpy and entropy changes (which provide an insight on the effect of temperature on the solubility and render information about the ordering of molecules of gas in solvent) were evaluated for the pure as well as for the binary mixtures. The experimental solubility data was correlated with the Peng Robinson (PR) and Soava Redlich Kwong (SRK) equation of state with the conventional quadratic van der waals and Mathias-Klotz-Praustniz mixing rule and . The estimated values showed a fair degree of agreement with the experimental data. The binary mixtures consisting of [bmim][BF_4]+MDEA, [bmim][Tf_2N]+MDEA, [bmim][FAP]+MDEA, [bheaa]+MDEA were also examined for CO_2 solubility. Furthermore aqueous IL solutions were also used for CO_2 solubility. The binary mixtures also yielded the same results that CO_2 solubility decreased in these and in some cases substantially increased. The aqueous IL mixtures showed that with the addition of IL in the aqueous amine solvent the CO_2 solubility decreased.

CHAPTER 5

CONCLUSIONS

5.0 Conclusions

In the present work, a fundamental and systematic investigation on the potential usage of hybrid mixtures (comprising of IL + amine) for CO_2 removal has been presented. Three imidazolium based ionic liquids namely 1-hexyl-3-methylimidazolium tetrafluoroborate ([hmim][BF_4]), 1-hexyl-3-methylimidazolium bis(trifluoromethylsulfonyl)imide ([hmim][Tf_2N]) and 1-hexyl-3-methylimidazolium tris(pentafluoroethyl)trifluorophosphate ([hmim][FAP]) were successfully mixed with *N*-methyldiethanolamine (MDEA) solvent. The basic physical properties of the pure solvents as well as for the binary mixtures were established and their application towards CO_2 solubility was analyzed experimentally. It was found that these binary mixtures have the potential to be used for CO_2 removal. The effects of concentrations, temperatures and pressures and anions on the CO_2 solubility were studied. The results indicated that the presence of MDEA in the ILs ([hmim][FAP] and [hmim][Tf_2N] at any concentration did not prove fruitful for them in terms of CO_2 solubility, where as the presence of MDEA in the IL ([hmim][BF_4]) at concentrations {(1:4), (1:1)} proved beneficial for it. The CO_2 loading increased linearly with increase in pressure. The temperature dependent parameters like Henry's constants and enthalpy and entropy were estimated to observe the behavior of the dissolved CO_2 in the solvents. The ILs with [Tf_2N] and [FAP] showed higher CO_2 solubility in comparison to the IL with [BF_4] anion, where as in the mixtures the anion failed to maintain their pivotal role in CO_2 solubility except at the concentration (4:1), where the concentration of IL was quite higher in comparison to MDEA. The experimental CO_2 solubility results were successfully correlated with the help of Peng Robinson and Soave-Redlich-

Kwong equations of state with conventional van der Waals and Mathias-Klotz-Prausnitz mixing rules, The Peng Robinson EOS with Mathias-Klotz-Prausnitz mixing rule yielded better results in comparison to Peng Robinson EOS with van der Waals and Soave-Redlich-Kwong EOS with Mathias-Klotz-Prausnitz mixing rules. Soave-Redlich-Kwong EOS with Mathias-Klotz-Prausnitz mixing also yielded fair results. The pure liquids and selected binary mixtures which were once used for CO_2 absorption were utilized again for CO_2 solubility to study their capability towards recycling. The recycled pure and binary mixtures showed almost similar results with the fresh solvents indicating their potential application towards recycling. The display of lower values of absorption in the binary mixtures ([hmim][FAP]+MDEA, [hmim][Tf_2N]+MDEA) in comparison to pure IL and substantially enhanced absorption values in some ([hmim][BF_4]+MDEA) mixtures led to probe more binary and even ternay mixtures for CO_2 absorption. It was done to done to investigate that whether the hybrid mixtures behave in the same manner (decreased or substantially increased absorption values) or show some highly pronounced absorption values in the mixtures. The binary mixtures of ILs namely: bis(2-hydroxyethyl)ammonium acetate ([bheaa]), 1-butyl-3-methylimidazolium tetrafluoroborate ([bmim][BF_4]), 1-butyl-3-methylimidazolium tris(pentafluoroethyl)trifluorophosphate ([bmim][FAP]), 1-butyl-3-methylimidazolium bis(trifluoromethylsulfonyl)imide ([bmim][Tf_2N]) with MDEA were used for CO_2 solubility. The aqueous IL solutions used for CO_2 solubility were comprised of the ILs: 1-ethyl-3-methylimidazolium tris(pentafluoroethyl)trifluorophosphate ([emim][FAP]), 1-ethyl-3-methylimidazolium bis(trifluoromethylsulfonyl)imide ([emim][Tf_2N]) with monoethanolamine (MEA) or diethanolamine (DEA). The same trends were observed for the case of binary mixtures that CO_2 solubility decreased and in some cases increased substantially. The binary mixtures of ILs ([bmim][FAP], [bmim][Tf_2N]) with MDEA showed lower values of solubility than pure ILs. Some binary mixtures of ILs ([bmim][BF_4], [bheaa]) with MDEA (1:4, 1:1) showed slightly higher values of solubility. The aqueous mixtures of ILs showed lower values of solubility than aqueous amine solutions. The addition of IL (at all concentrations) to aqueous amine solutions was not beneficial in terms of CO_2 solubility.

5.1. Recommendations

Based on the observations during the present study, the following recommendations are made for the future work in the field of solvents used for CO_2 removal:

1. To synthesize some task specific ionic liquids for CO_2 removal, as the hybrid solvents (IL+amine) did not yield the desired results.
2. The aqueous amine solvents be mixed with ILs, which do not hinder their reactivity.
3. The ILs be diluted with such organic solvents, which may reduce their viscosity but do not disturb their CO_2 absorption capability.

REFERENCES

Abbott, A.P. 2004. Application of Hole Theory to the Viscosity of Ionic and Molecular Liquids. *ChemPhysChem*, 5, 1242-1246.

Abbott, A.P. 2005. Model for the Conductivity of Ionic Liquids Based on an Infinite Dilution of Holes. *ChemPhysChem*, 6, 2502-2505.

Abbott, A.P., Capper G., Grey S. 2006. Design of Improved Deep Eutectic Solvents Using Hole Theory. *ChemPhysChem*, 7, 803-806.

Abu-Zahra, M.R.M., Feron, P.H.M., Jansens, P.J. Goetheer, E.L.V. 2009. New process concepts for CO_2 post-combustion capture process integrated with co-production of hydrogen. *International Journal of Hydrogen Energy*, 34, 3992-4004.

Ahmad, S., Carsten T., Berger, R., Butt, H.J., Endres, F. 2011. Surface polymerization of (3,4-ethylenedioxythiophene) probed by in situ scanning tunneling microscopy on Au(111) in ionic liquids. *Nanoscale*, 3, 251-257.

Ahmady, A., Hashim, M.A., Aroua, M.K. 2010. Experimental Investigation on the Solubility and Initial Rate of Absorption of CO_2 in Aqueous Mixtures of Methyldiethanolamine with the Ionic Liquid 1-Butyl-3-methylimidazolium Tetrafluoroborate. *Journal of Chemical and Engineering Data*, 55, 5733-5738.

Ahmady, A., Hashim, M.A., Aroua, M.K. 2011. Absorption of carbon dioxide in the aqueous mixtures of methyldiethanolamine with three types of imidazolium-based ionic liquids. *Fluid Phase Equilibria*, 309, 76-82.

Ahosseini, A., Scurto, A.M. 2008. Viscosity of Imidazolium-Based Ionic Liquids at Elevated Pressures: Cation and Anion Effects. *International Journal of Thermophysics*, 29, 1222-1243.

Ahosseini, A., Sensenich, B., Weatherley L.R., Scurto, A.M. 2010. Phase Equilibrium Volumetric, and Interfacial Properties of the Ionic Liquid, 1-Hexyl-3-methylimidazolium Bis(trifluoromethylsulfonyl)amide and 1-Octene. *Journal of Chemical and Engineering Data*, 55, 1611-1617.

Ahosseini, A., Weatherley, L.R., Scurto, A.M. 2011. Viscosity and Diffusivity for the Ionic Liquid 1-Hexyl-3-methylimidazolium Bis(trifluoromethylsulfonyl)amide with 1-Octene. *Journal of Chemical and Engineering Data*, 56, 3715-3721.

Aionicesei, E., Skerget, M., Knez, Z. 2008. Measurement of CO_2 solubility and diffusivity in poly(L-lactide) and poly(D,L-lactide-co-glycolide) by magnetic suspension balance. *Journal of Supercritical Fluids*, 47, 296-301.

Aki, S.N.V.K., Mellein, B.R., Saurer, E.M., Brennecke, J.F. 2004. High-Pressure Phase Behavior of Carbon Dioxide with Imidazolium-Based Ionic Liquids, *Journal of Physical Chemistry B,* 108, 20355-20365.

Al-Ghawas, H.A., Hagewiesche, D.P., Ruiz-Ibanez, G., Sandall, O.C. 1989. Physicochemical Properties Important for Carbon Dioxide Absorption in Aqueous Methyldiethanolamine, *Journal of Chemical and Engineering Data*, 34, 385-391.

Ally, M.R., Braustein, J., Baltus, R.E., Dai, S., DePaoli D.W., Simonson J.M. 2004. Irregular Ionic Lattice Model for Gas Solubilities in Ionic Liquids, *Industrial and Engineering Chemistry Research*, 43, 1296-1301.

Almantariotis, D., Stevanovic, S., Fandin, O., Pensado, A.S., Padua, A.A.H., Coxam, J.Y., Gomes, M.F.C. 2012. Absorption of Carbon Dioxide, Nitrous Oxide, Ethane and Nitrogen by 1-Alkyl-3-methylimidazolium ($C_n$mim, n = 2,4,6) Tris(pentafluoroethyl)trifluorophosphate Ionic Liquids (eFAP), *Journal of Physical Chemistry B*, 116, 7728-7738.

Almasi, M., Iloukhani, H. 2010, Densities, Viscosites, and Refractive Indices of Binary Mixtures of Methyl Ethyl Ketone + Pentanol Isomers at Different Temperatures, *Journal of Chemical and Engineering Data*, 55, 3918-3922.

Althuluth, M. Mota-Martinez, M.T., Kroon, M.C., Peters, C.J. 2012. Solubility of Carbon Dioxide in the Ionic Liquid 1-Ethyl-3-methylimidazolium Tris(pentafluoroethyl)trifluorophosphate. *Journal of Chemical and Engineering Data*, 57, 3422-3425.

Alvarez, E., Gomez-Diaz, D, Rubia, M.D.L., Navaza, J.M. 2006. Densities and Viscosities of Aqueous Ternary Mixtures of 2-(Methylamino)ethanol and 2-(Ethylamino)ethanol with Diethanolamine, Triethanolamine, N-Methyldiethanolamine, or 2-Amino-1-methyl-1-propanol from 298.15 to 323.15 K, *Journal of Chemical and Engineering Data*, 51, 955-962.

Alvarez, E., Cerdeira, F., Gomez-Diaz, D., Navaza, J.M. 2010. Density, Speed of Sound, Isentropic Compressibility, and Excess Volume of (Monoethanolamine + 2-Amino-2-methyl-1-propanol), (Monoethanolamine + Triethanolamine), and (Monoethanolamine + *N*-Methyldiethanolamine) at Temperatures from (293.15 to 323.15) K, *Journal of Chemical and Engineering Data*, 55, 994-999.

Alvis, R.S., Hatcher, N.A., Weiland, R.H. 2012, CO_2 Removal From Syngas Using Piperazine Activated MDEA and Potassium Dimethyl Glycinate, *presented at Nitrogen + Syngas, Athens, Greece.*

Amararene, F., Balz, P., Bouallou, C., Cadours, R., Lecomte, F., Mougin, P., Richon, D. 2003, Densities of Water + Diethanolamine + Methanol and Water + N-Methyldiethanolamine + Methanol at Temperatures Ranging from (283.15 to 353.15) K, *Jounal of Chemical and Engineering Data*, 48, 1565-1570.

Ambashta, R.D., Sillanpaa, M.E.T. 2012. Membrane purification in radioactive waste management a short review, *Journal of Environmental Radioactivity*, 105, 76-84.

Anthony, J.L., Maginn, E.J., Brennecke, J.F. 2002, Solubilities and Thermodynamic Properties of Gases in the Ionic Liquid 1-*n*-Butyl-3-methylimidazolium Hexafluorophosphate, *Journal of Physical Chemistry B*, 106, 7315-7320.

Arcis, H., Ballert-Busserolles, K., Rodier, L., Coxam, J.Y. 2011. Enthalpy of Solution of Carbon Dioxide in Aqueous Solutions of Monoethanolamine at Temperatures of 322.5 K and 372.9 K and Pressures up to 5 MPa. *Journal of Chemical and Engineering Data*, 56, 3351-3362.

Arshad, M.W. 2009. CO_2 Capture Using Ionic Liquids, M.Sc. thesis, Dept. of Chem. and BioChem. Eng. Technical Univ. of Denmark.

Austgen, D.M., Rochelle, G.T., Chen, C.C. 1991. Model of Vapor-Liquid Equilibria for Aqueous Acid Gas Alkanolamine Systems. 2. Representation of H_2S and CO2 Solubility in Aqueous MDEA and CO_2 Solubility in Aqueous Mixtures of MDEA with MEA *or* DEA, *Industrial and Engineering Chemistry Research*, 30, 543-555.

Azevedo, R.G.D., Esperanca, J.M.S.S., Szydlowski J., Visak, Z.P., Pires, P.F., Guedes, H.J.R., Rebelo, L.P.N. 2005. Thermophysical and thermodynamic properties of ionic liquids over and extended pressure range: [bmim][NTf_2] and [hmim][NTf_2]. *Journal of Chemical Thermodynamics*, 37, 888-899.

Aziz, N. Yusoff, R. Aroua, M.K. 2012. Absorption of CO_2 in aqueous mixtures of N-methyldiethanolamine and guanidinium tris(pentafluoroethyl)trifluorophosphate ionic liquid at high-pressure, *Fluid Phase Equilibria*, 322-323, 120-125.

Baek, J.I., Yoon, J.H., Eum, H.M. 2000. Physical and Thermodynamic Properties of Aqueous 2-Amino-2-Methyl-1, 3-Propanediol Solution. *International Journal of Thermophysics*, 21(5), 1175-1185.

Bald, A., Kinart, Z. 2011. Volumetric Properties of Some Aliphatic Mono and Dicarboxylic Acids in Water at 298.15 K. *Journal of Solution Chemistry*, 40, 1-16.

Baltus, R.E., Culbertson, B.H., Dai, S., Luo, H., DePaoli, D.W. 2004, Low-Pressure Solubility of Caron Dioxide in Room-Temperature Ionic Liquids Measured with a Quartz Crystal Microbalance, *Journal of Physical Chemistry B*, 108, 721-727.

Bandyopadhyay, A. 2011, Amine versus ammonia absorption of CO_2 as a measure of reducing GHG emission: a critical analysis. *Clean Technology and Environmental Policy*, 13, 269-294.

Bara, J.E., Carlisle, T.K., Gabriel, C.J., Camper, D., Finotello, A., Gin, D.L., Noble, R.D. 2009, Guide to CO_2 Separations in Imidazolium-Based Room-Temperature Ionic Liquids, *Industrial and Engineering Chemistry Research*, 48, 2739-2751.

Bates, E.D., Mayton, R.D., Ntai, I., Davis Jr. J.H. 2002. CO_2 Capture by a Task-Specific Ionic Liquid, *Journal of the American Chemical Society*, 124, 926-927.

Benamor, A., Aroua, M.K. 2005. Modeling of CO_2 solubility and carbamate concentration in DEA, MDEA and their mixtures using the Deshmukh-Mather model. *Fluid Phase Equilibria*, 231, 150-162.

Bernal-Garcia, J.M., Ramos-Estrada, M., Iglesias-Silva, G.A., Hall, K.R. 2003. Densities and Excess Molar Volumes of Aqueous Solutions of n-Methyldiethanolamine (MDEA) at Temperatures from (283.15 to 363.15) K, *Journal of Chemical and Engineering Data*, 48, 1442-1445.

Bernal-Garcia, J.M., Galicia-Luna, L.A., Hall, K.R., Ramos-Estrada, M., Iglesias-Silva, G.A. 2004. Viscosities for Aqueous Solutions of N-Methyldiethanolamine from 313.15 to 363.15 K. *Journal of Chemical and Engineering Data*, 49, 864-866.

Bhatia, S.C., Rani, R., Bhatia, R. 2011. Viscosities, densities, speeds of sound and refractive indices of binary mixtures of o-xylene, m-xylene, p-xylene, ethylbenzene and mesitylene with 1-decanol at 298.15 and 308.15 K. *Journal of Molecular Liquids*, 159, 132-141.

Bilyeu, B., Brostow, W., Menard, K.P. 2000. Epoxy thermosets and their applications. II. Thermal Analysis. *Journal of Materials Education*, 22(4-6), 108-130.

Blanchard, L.A., Gu, Z., Brennecke, J.F. 2001. High-Pressure Phase Behavior of Ionic Liquid/CO_2 Systems, *Journal of Physical Chemistry B*, 105, 2437-2444.

Borg, P.H., Majer, V., Gomes, M.F.C. 2003 Solubilites of Oxygen and Carbon Dioxide in Butyl Methyl Imidazolium Tetrafluoroborate as a Function of Temperature and at Pressures Close to Atmospheric Pressure. *Journal of Chemical and Engineering Data*, 48, 480-485.

Bosch, H., Versteeg, G.G., Versteeg, Van-Swaaij, W.P.M. 1990. Kinetics of the reaction of CO2 with the sterically hindered amine 2-Amino-2-methylpropanol at 298.15 K. *Chemical Engineering Science*, 45, 1167-1173.

Bottger, A., Ermatchkov, V., Maurer, G. 2009. Solubility of Carbon Dioxide in Aqueous Solutions of *N*-Methyldiethanolamine and Piperazine in the High Gas Loading Region. *Journal of Chemical and Engineering Data*, 54, 1905-1909.

Boumedine, R.S., Horstmann, S., Fischer, K., Provost, E., Furst, W., Gmehling, J. 2004. Experimental determination of carbon dioxide solubility data in aqueous alkanolamine solutions. *Fluid Phase Equilibria*, 218, 85-94.

Bredesen, R., Jordal, K., Bolland, O. 2004. High-temperature membranes in power generation with CO_2 capture. *Chemical Engineering and Processing*, 43, 1129-1158.

Brocos, P., Pineiro, A., Bravo, R., Amigo, A. 2003. Refractive indices, molar volumes and molar refractions of binary liquid mixtures: concepts and correlations. *Physical Chemistry Chemical Physics*, 5, 550-557.

Burr, B., Lyddon, L. 2000. A comparison of physical solvents for acid gas removal, *Bryan Research and Engineering*, 1-13.

Cadena, C., Anthony, J.L., Shah, J.K., Morrow, T.I., Brennecke, J.F., Maginn, E.J. 2004. Why is CO_2 So Soluble in Imidazolium-Based Ionic Liquids, *Journal of the American Chemical Society*, 126, 5300-5308.

Chakma, A., Meisen, A. 1987. Solubility of CO_2 in Aqueous Methyldiethanolamine and *N,N*-Bis(hydroxyethyl) piperazine solutions. *Industrial and Engineering Chemistry Research*, 26, 2461-2466.

Camper, D., Scovazzo, P., Koval, C., Noble, R. 2004. Gas Solubility in Room-Temperature Ionic Liquid. *Industrial and Engineering Chemistry Research*, 43, 3049-3054.

Camper, D., Bara, J.E., Gin, D.L., Noble, R.D. 2008. Room-Temperature Ionic Liquid-Amine Solutions: Tunable Solvents for Efficient and Reversible Capture of CO_2. *Industrial and Engineering Chemistry Research*, 47, 8496-8498.

Canongia-Lopes, J.N., Cordeiro, T.C., Espernaca, J.M.S.S., Guedes, H.J.R., Huq S., Rebelo, L.P.N., Seddon, K.R. 2005. Deviations from Ideality in Mixtures of Two Ionic Liquids Containing a Common Ion. *Journal of Physical Chemistry B*, 109, 3519-3525.

Carda-Broch, S., Berthod, A., Armstrong. D.W. 2003. Solvent Properties of the 1-butyl-3-methylimidazolium hexafluorophosphate ionic liquid. *Analytical and Bioanalytical Chemistry*, 375, 191-199.

Carvalho, P.J., Alvarez, V.H., Marrucho, I.M., Aznar, M., Continho, J.A.P. 2009. High pressure phase behaviour of carbon dioxide in 1-butyl-3-methylimidazolium bis(trifluoromethylsulfonyl)imide and 1-butyl-3-methylimidazolium dicyanamide ionic liquids. *Journal of Supercrical Fluids*, 50, 105-111.

Chen, S., Lei, Q., Fang, W. 2002. Density and Refractive Index at 298.15 K and Vapor – Liquid Equilibria at 101.3 kPa for Four Binary Systems of Methanol, *n*-Propanol, *n*-Butanol, or Isobutanol with *N*-Methylpiperazine. *Journal of Chemical and Engineering Data*, 47, 811-815.

Chen. Y. Zhang, S., Yuan, X., Zhang, Y., Zhang, X., Dai, W., Mori, R. 2006. Solubility of CO_2 in imidazolium-based tetrafluoroborate ionic liquids. *Thermochemica Acta*, 441, 42-44.

Chen, C.C., Evans, L.B. 1986. A local composition model for the excess Gibbs energy of aqueous electrolyte system. *American Institute of Chemical Engineers Journal*, 32, 444-454.

Cheung, O., Liu Q., Bacsik, Z., Hedin, N. 2012. Silicoaluminophosphates as CO_2 sorbents. *Microporous and Mesoporous Materials*, 156, 90-96.

Choi, W.J. Cho, K.C., Lee, S.S., Shim, J.G., Hwang, H.R., Park, S.W., Oh, K.J. 2007. Removal of carbon dioxide by absorption into blended amines: kinetics of absorption into aqueous AMP/HMDA, AMP/MDEA, and AMP/Piperazine Solutions. *Green Chemistry*, 9, 594-598.

Choi, W.J., Seo, J.B., Jang, S.Y., Jung, J.H., Oh, K.J. 2009 Removal Characteristics of CO_2 using aqueous MEA/AMP solutions in the absorption and regeneration process. *Journal of Environmental Sciences*, 21, 907-913.

Chowdhury, F.I., Akhtar, S., Saleh, M.A. 2010. Viscosities and excess viscosities of aqueous solutions of some diethanolamines. *Journal of Molecular Liquids*, 155, 1-7.

Chunxi, L., Furst, W. 2000, Representation of CO_2 and H_2S solubility in aqueous MDEA solutions using an electrolyte equation of state, *Chemical Engineering Science*, 55, 2975-2988.

Clara, R.A., Gomez-Marigliano, A.C., Morales, D., Solimo, H.N. 2010. Density, Viscosity, Vapor – Liquid Equilibrium, and Excess Molar Enthalpy of [Chloroform + Methyl tert Butyl Ether]. *Journal of Chemical and Engineering Data*, 55, 5862-5867.

Coats, A.W., Redfren J.P. 1953. Thermogravimetric Analysis: A Review. *Analyst*, 88, 906-924.

Corderi, S., Gonzalez, E.J., Calvar, N., Dominguez A. 2012. Application of [HMim][NTf_2], [HMim][TfO] and [BMim][TfO] ionic liquids on the extraction of toluene from alkanes: Effect of the anion and the alkyl chain length of the cation on the LLE. *Journal of Chemical Thermodynamics*, 53, 60-66.

Costantini, M., Toussaint, V.A., Shariati, A., Peters, C.J., Kikic I. 2005. High-Pressure Phase Behavior of Systems with Ionic Liquids: Part IV. Binary System Carbon Dioxide + 1-Hexyl-3-methylimidazolium Tetrafluoroborate. *Journal of Chemical and Engineering Data*, 50, 52-55.

Crosthwaite, J.M., Muldoon, M.J., Dixon, J.K. Anderson J.L., Brennecke, J.F. 2005. Phase transition and decomposition temperatures, heat capacities and viscosities of pyridinium ionic liquids. *Journal of Chemical Thermodynamics*, 37, 559-568.

Cullinane, J.T. 2005. Thermodynamics and Kinetics of Aqueous Piperazine with Potassium Carbonate for Carbon Dioxide Absorption. Ph.D. dissertation, Univ. of Texas at Austen, USA.

Cwiklinska, A., Kinart, C.M. 2011. Thermodynamic and physicochemical properties of binary mixtures of nitromethane with {2-methyoxyethanol + 2-butoxyethanol} systems at T = (293.15, 298.15, 303.15, 308.15, and 313.15) K. *Journal of Chemical Thermodynamics*, 43, 2011.

D’Alessandro, D.A., Smit, B., Long, J.R. 2010. Carbon Dioxide Capture: Prospects for New Materials. Angewandte Chemie International Edition, 49, 6058-6082.

Danckwerts, P.V. 1979. The reaction of Carbon Dioxide with Ethanolamines. *Chemical Engineering Science*, 34, 443-448.

Darman, N.H., Harun, A.R.B. 2006. Technical Challenges and Solutions on Natural Gas Development in Malaysia, *The petroleum Policy and Management (PPM) Project 4th Workshop of the China*, Beijing, 1-28.

David, J. 2000. Economic Evaluation of Leading Technology Options for Sequestration of Carbon Dioxide . M.S. thesis, Massachusetts Institute of Technology, USA

Dawodu, O.F., Meisen A. 1994. Solubility of Carbon Dioxide in Aqueous Mixtures of Alkanolamines. *Journal of Chemical and Engineering Data*, 39, 548-552.

Deenadayalu, N., Bhujrajh, P. 2008. Density, Speed of Sound, and Derived Thermodynamic Properties of Ionic Liquids $[EMIM]^+[BETI]^-$ or ($[EMIM]^+[CH3(OCH_2CH_2)_2OSO_3]^-$ + Methanol or + Acetone) at T = (298.15 or 303.15 or 313.15) K. *Journal of Chemical and Engineering Data*, 53, 1098-1102.

Deenadayalu, N., Bahadur, I., Hofman, T. 2010. Ternary excess molar volume of {methyltrioctylammonium bis(trifluoromethylsulfonyl)imide ethanol + methyl acetate, or ethyl acetate} systems at T = (298.15, 303.15, and 313.15) K. *Journal of Chemical Thermodynamics.* 42, 726-733.

Deetlefs, M., Seddon, K.R., Shahra, M. 2006. Neoteric optical media for refractive index determination of gems and minerals. *New Journal of Chemistry*, 30, 317-326.

Deng. Y., Husson, P., Jacquemin, J., Youngs, T.G.A. Kett, V.L., Hardcre, C., Costa Gomes, M.C. 2011. Volumetric properties and enthalpies of solution of alcohols C_kH_{2k}+1OH (k = 1,2,6) in 1-methyl-3-alkylimidazolium bis(trifluoromethylsulfonyl)imide {$[C_1C_n lm][NTf_2]$ n = 2,4,6,8, 10} ionic liquids. *Journal of Chemical Thermodynamics*, 43, 1708-1718.

Derks, P.W.J. 2006. Carbon Dioxide absorption in Piperazine activated *N*-methyldiethanolamine. Ph.D. dissertation, Univ. of Twente, Netherlands.

Derks, P.W.J. Hamborg, E.S., Hogendoorn, J.A., Niederer, J.P.M. Versteeg, G.F. 2008. Densities, Viscosities, and Liquid Diffusivities in Aqueous Piperazine and Aqueous (Piperazine + *N*-Methyldiethanolamine) Solutions. *Journal of Chemical and Engineering Data*, 53, 1179-1185.

Derks, P.W.J., Hogendoorn, J.A., Versteeg, G.F. 2010. Experimental and theoretical study of the solubility of carbon dioxide in aqueous blends of piperazine and *N*-Methyldiethanolamine. *Journal of Chemical Thermodynamics*, 42, 151-163.

Deshmukh, R.D., Mather, A.E. 1981. A Mathematical Model for Equilibrium Solubility of Hydrogen Sulfide and Carbon Dioxide in Aqueous Alkanolamine Solutions. *Chemical Engineering Science*, 36, 355-362.

Diguillo, R.M., Lee, R.J., Schaeffer, S.T., Brasher, L.L., Tela, A.S. 1992. Densities of Viscosities of the Ethanolamines, *Journal of Chemical and Engineering Data.* 37, 239-242.

Diwedi, A., Singh, M. 2007. Densities, viscosities, viscosity deviations and excess thermodynamic properties of binary mixtures of diethyl oxalate and dimethyl malonate with polar and non-polar solvents at 303.15 K. *Indian Journal of Chemistry*, 46, 789-794.

Doghaei, A.V., Rostami, A.A., Omrani, A. 2010. Densities, Viscosities, and Volumetric Properties of Binary Mixtures of 1,2-Propanediol + 1-Heptanol or 1-Hexanol and 1,2-Ethanediol + 2- Butanol or 2-Propanol at T = (298.15, 303.15, and 308.15) K. *Journal of Chemical and Engineering Data*, 55, 2894-2899.

Dresselhaus, M.S., Thomas, I.L. 2001. Alternative energy technologies. *Nature*, 414, 332-337.

Dzyuba, S.V., Bartsch, R.A. 2002. Influence of Structural Variations in 1-Alkyl(aralkyl)-3-Methylimidazolium Hexafluorophosphates and Bis(trifluoromethylsulfonyl)imides on Physical Properties of the Ionic Liquids. *ChemPhysChem*, 3, 161-166.

Ebune, G.E. 2008. Carbon Dioxide Capture from Power Plant Flue Gas using Regenerable Activated Carbon Powder Impregnated with Potassium Carbonate. M. S. Thesis, Youngstown State Univ. Ohio, USA.

Ermatchkov, V., Kamps, A.P.S., Maurer, G. 2006. Solubility of Carbon Dioxide in Aqueous Solutions of N-Methyldiethanolamine in the Low Gas Loading Region, *Industrial and Engineering Chemistry Research*, 45, 6081-6091.

Esperanca, J.M.S.S., Guedes, H.J.R., Guedes, Canongia-Lopes, J.N., Rebelo, L.P.N. 2008. Pressure – Density – Temperature (ρ-G-T) Surface of [C_6mim][NTf_2]. *Journal of Chemical and Engineering Data*, 53, 867-870.

Faiz, R., Al-Marzouqi, M. 2011. Insights on natural gas purification: Simultaneous absorption of CO_2 and H_2S using membrane contactors. *Separation and Purification Technology*, 76, 351-361.

Faridbod, F., Ganjali, M.R., Norouzi, P., Siavash R., Rashedi, H. Application of Room Temperature Ionic Liquids in Electrochemical Sensors and Biosensors. Ionic Liquids: Application and Perspectives. InTech, Europe, Crotia.

Feng, Z., Gang, F.C., Ting, W.Y., Tao, W.Y., Min, L.A., Bing, Z.Z. 2010. Absorption of CO_2 in the aqueous solutions of functionalized ionic liquids and MDEA. *Chemical Engineering Journal*, 160, 691-697.

Fitchett, B.D., Knepp, T.N., Conboy, J.C. 2004. 1-Alkyl-3-methylimidazolium Bis(perfluoroalkylsulfonyl)imide Water-Immiscible Ionic Liquids, The Effect of Water on Electrochemical and Physical Properties. *Journal of the Electrochemical Society*, 151(7), 219-225.

Fort, R.J., Moore, W.R. 1966. Viscosities of binary liquid mixtures. *Transactions of the Faraday Society*, 62, 1112-1119.

Fredlake, C.P., Crosthwaite, J.M., Hert, D.G., Aki, S.N.V.K., Brennecke, J.F. 2004. Thermophysical Properties of Imidazolium-Based Ionic Liquids. *Journal of Chemical and Engineering Data*, 49, 954-964.

Freire, M.G., Ventura, P.M., Santos, L.M.N.B.F. Marrucho, I.M., Coutinho, J.A.P. 2008. Evaluation of COSMO-RS for the prediction of LLE and VLE of water and ionic liquids binary systems. *Fluid Phase Equilibria*, 268, 74-84.

Fu, D., Sun, X., Pu. J., Zhao, S. 2006. Effect of Water Content on the Solubility of CO_2 in the Ionic Liquid [bmim][PF_6]. *Journal of Chemical and Engineering Data*, 51, 317-375.

Garcia-Abuin, A., Gomez-Diaz, D., Rubia, M.D.L., Navaza, J.M., Pacheco, R. 2009. Density, Speed of Sound, and Isentropic Compressibility of Triethanolamine (or N-Methyldiethanolamine) + Water + Ethanol Solutions from t = (15 to 50) ^{o}C. *Journal of Chemical and Engineering Data*, 54, 3114-3117.

Garcia-Miaja, G., Troncoso, J., Romani, L. 2009. Excess molar properties for binary systems of alkylimidazolium based ionic liquids + nitromethane. Experimental results and ERAS-model calculations. *Journal of Chemical and Engineering Data*, 41, 334-341.

Geng, Y., Chen, S., Wang, T.,Yu, D., Peng, C., Liu, H., Hu, Y. 2008. Density, viscosity and electrical conductivity of 1-butyl-3-methylimidazolium hexafluorophosphate + monoethanolamine and *N,N*-dimethylethanolamine. *Journal of Molecular Liquids*, 143, 100-108.

Gomez-Diaz, D., Rubia, M.D.L., Lopez, A.B., Navaza, J.M., Pacheco, R., Sanchez, S. 2012. Density, Speed of Sound, Refractive Index, and Viscosity of 1-Amino-2-Propanol {or Bis(2-hydroxypropyl)amine} + Triethanolamine + Water from

T = (288.15 to 333.15) K. *Journal of Chemical and Engineering Data*, 57, 1104-1111.

Gonzalez, E.J., Dominguez, A., Macedo, E.A. 2012. Excess properties of binary mixtures containing 1-hexyl-3-methylimidazolium bis(trifluoromethylsulfonyl)imide ionic liquid and polar organic compounds. *Journal of Chemical Thermodynamics*, 47, 300-311.

Gu. F., Fang, W. 2000. Density and Refractive Index at 298.15 K and Vapor – Liquid Equilibria at 101.3 kPa for Binary Mixtures of Water + *N*-Ethylpiperazine. *Journal of Chemical and Engineering Data*, 45, 288-291.

Guang Li, J., Hu, Y.F., Ling, S., Zhang, J.Z. 2011. Physicochemical Properties of [C_6mim][PF_6] and [C_6mim][$(C_3F_5)_3PF_3$] Ionic Liquids. *Journal of Chemical and Engineering Data*, 56, 3068-3072.

Gupta, M., Coyle, I., Thambimuthu, K. 2003. CO_2 Capture Technologies and Opportunities in Canada. *Ist Canadian CC&S Technology Roadmap Workshop,* Calgary, 1-36.

Gutkowski, K.I., Shariati, A., Peters, C.J. 2006. High-pressure phase behaviour of the binary liquid system 1-octyl-3-methylimidazolium tetrafluoroborate + carbon dioxide. *Journal of Supercritical Fluid*, 39, 187-191.

Han, J., Jin, J., Eimer, D.A., Melaaen, M.C. 2012. Density of Water (1) + Diethanolamine (2) + CO_2 (3) and Water (1) + *N*-Methyldiethanolamine (2) + CO_2 (3) from (298.15 to 423.15) K. *Journal of Chemical and Engineering Data*, 57, 1843-1850.

Han, X., Armstrong, D.W. 2007. Ionic Liquids in Separations. *Accounts of Chemical Research*, 40, 1079-1086.

Hawrylak, B., Burke, S.E., Palepu, R. 2000. Partial Molar and Excess Volumes and Adiabatic Compressibilities of Binary Mixtures of Ethanolamines with Water. *Journal of Solution Chemistry*, 29(6), 575-594.

Henni, A., Maham, Y., Tontiwachwuthikul, P., Chakma, A., Mather, A.E. 2000. Densities and Viscosities for Binary Mixtures of *N*-Methyldiethanolamine + Triethylene Glycol Monomethyl Ether from 25 ^oC to 70 ^oC and *N*-Methyldiethanolamine + Ethanol Mixtures at 40 ^oC. *Journal of Chemical and Engineering Data*, 45, 247-253.

Hernandez, J.A., Quintana, R.G., Guevara, F.M., Martinez, A.R., Trejo, A. 2001. Liquid Density of Aqueous Blended Alkanolamines and *N*-Methyldiethanolamine as a Function of Concentration and Temperature. *Journal of Chemical and Engineering Data*, 46, 861-867.

Hsu, C.H., Li, M.H. 1997. Densities of Aqueous Blended Amines. *Journal of Chemical and Engineering Data*, 42, 502-507.

Huang, J., Riisager, A., Wasserscheid, P., Fehrmann, R. 2006. Reversible physical absorption of SO_2 by ionic liquids. *Chemical Communications*, 01, 4027-2029.

Huddleston, J.G., Visser, A.E., Reichert, W.M., Willauer, H.D., Broker, G.A., Rogers, R.D. 2001. Characterization and comparison of hydrophilic and hydrophobic room temperature ionic liquids incorporating the imidazolium cation. *Green Chemistry*, 3, 156-164.

Hui, N., MinQiang, H., QuigQing, M., YuanHui, L., Dezhong, Y., Buxing, H. 2012. The physicochemical properties of some imidazolium-based ionic liquids and their binary mixtures. *Science China Chemistry*, 55(8), 1509-1518.

Huttenhuis, P.J.G., Agrawal, N.J., Hogendoorn, J.A., Versteeg, G.F. 2007. Gas solubility of H_2S and CO_2 in aqueous solutions of N-methyldiethanolamine, *Journal of Petroleum Science and Technology,* 55, 122-134.

Hwang, S., Park, YoonKook, Park, K. 2011. Measurement and prediction of phase behavior of 1-alkyl-3-methylimidazolium tetrafluoroborate and carbon dioxide: Effect of alkyl chain length in imidazolium cation. *Journal of Chemical Thermodynamics*, 43, 339-343.

Ignat'ev, N.V., Welz-Biermann, U., Kucheryna, A., Bissky, G., Willner, H. 2005. New ionic liquids with tris(perfluoroalkyl)trifluorophosphate (FAP) anions. *Journal of Fluorine Chemistry*, 126, 1150-1159.

Iloukhani, H., Rakhshi, M. 2009. Excess molar volumes, viscosities, and refractive indices for binary and ternary mixtures of {cyclohexanone (1) + *N,N*-dimethylacetamide (2) + *N,N*-diethylethanolamine (3)} at (298.15, 308.15, and 318.15) K. *Journal of Molecular Liquids*, 149, 86-95.

Isaacs, E.E., Otto, F.D., Mather, A.E. 1980. Solubility of Mixtures of H_2S and CO_2 in a Monoethanolamine Solution at Low Partial Pressures. *Journal of Chemical and Engineering Data*, 25, 118-120.

Islam, M.S., Yusoff, R., Ali, B.S. 2010. Degradation studies of amines and alkanolamines during CO_2 absorption and stripping system. *Engineering e Transaction*, 5, 97-109.

Ivanov, E.V., Kustov, A.V. 2010. Volumetric properties of (water + hexamethylphosphoric triamide) from (288.15 to 308.15) K. *Journal of Chemical Thermodynamics*, 42, 1087-1093.

Jacquemin, J., Gomes, M.F.C., Husson, P., Majer, V. 2006. Solubility of carbon dioxide, ethane, methane, oxygen, nitrogen, hydrogen, argon, and carbon monoxide in 1-butyl-3-methylimidazolium tetrafluoroborate between temperatures 283 K and 343 K and pressures close to atmospheric. *Journal of Chemical and Engineering Data*, 38, 490-502.

Jacquemin, J., Ge, R., Nancarrow, P., Rooney, D.W., Gomes, M.F.C., Padua, A.A.H., Hardacre, C. 2008. Prediction of Ionic Liquid Properties. I. Volumetric Properties as a Function of Temperature at 0.1 MPa. *Journal of Chemical and Engineering Data*, 53, 716-726.

Jane, I.S., Li, M.H. 1997. Solubilites of Mixtures of Carbon Dioxide and Hydrogen Sulfide in Water + Diethanolamine + 2-Amino-2-methyl-1-propanol. *Journal of Chemical and Engineering Data*, 42, 98-105.

Jones, J.H., Froning, H.R., Claytor Jr., E.E. 1959. Solubility of Acidic Gases in Aqueous Monoethanolamine. *Journal of Chemical and Engineering Data*, 4, 85-92.

Jou, F.Y., Mather, A.E., Otto, F.D. 1982. Solubility of H_2S and CO_2 in Aqueous Methyldiethanolamine Solutions. *Industrial and Engineering Chemistry Process Design and Development*, 21, 539-544.

Kamps, A.P.S., Tuma, D., Xia, J., Maurer, G. 2003. Solubility of CO_2 in the Ionic Liquid [bmim][PF_6]. *Journal of Chemical and Engineering Data*, 48, 746-749.

Kamps, A.P.S., Balaban, A., Jodecke, M., Kuranov, G., Smirnova, N.A., Maurer, G. 2001. Solubility of Single Gases Carbon Dioxde and Hydrogen Sulfide in Aqueous Solutions of *N*-Methyldiethanolamine at Temperatures from 313 to 393 K and Pressures up to 7.6 MPa: New Experimental Data and Model Extension. *Journal of Chemical and Engineering Data*, 40, 696-706.

Kanakubo, M., Umecky, T., Hiejima, Y., Aizawa, T., Nanjo, H., Kameda, Y. 2005. Solution Structures of 1-Butyl-3-methylimidazolium Hexafluorophosphate Ionic Liquid Saturated with CO_2: Experimental Evidence of Specific Anion-CO_2 Interaction. *Journal of Physical Chemistry B*, 109, 13847-13850.

Kandil, M.E., Marsh, K.N., Goodwin, R.H. 2007. Measurement of the Viscosity, Density, and Electrical Conductivity of 1-Hexyl-3-methylimidazolium Bis(trifluorosulfonyl)imide at Temperatures between (288 and 4330 K and Pressures below 50 MPa. *Journal of Chemical and Engineering Data*, 52, 2382-2387.

Kato, R., Krummen, M., Gmehling, J. 2004. Measurement and correlation of vapor – liquid equilibria and excess enthalpies of binary systems containing ionic liquids and hydrocarbons. *Fluid Phase Equilibria*, 224, 47-54.

Katritzky, A.R., Sild, S., Karelson, M. 1998. General Quantitative Strucutre – Property Relationship Treatment of the Refractive Index of Organic Compounds. *Chemical Information and Computer Science*, 38(5), 840-844.

Kavita, T., Atrri, P., Venkatesu, P. Devi, R.S.R. Hofman, T. 2012. Temperature dependence measurements and molecular interactions for ammonium ionic liquids with *N*-methyl-2-pyrrolidone. *Journal of Chemical Thermodynamics,* 54, 223-237.

Kennard, M.L., Meisen, A. 1984. Solubility of Carbon Dioxide in Aqueous Diethanolamine Solutions at Elevated Temperatures and Pressures. *Journal of Chemical and Engineering Data*, 29, 309-312.

Kent, R.L. Eisenberg, B. 1976. Better data for Amine Treating. *Hydrocarbon Processing*, 55(2), 87-90.

Kermanpour, F., Sharifi, T. 2012. Thermodynamic study of binary mixture of x_1 [C_6mim][BF_4] + x_2 1-propanol: Measurements and molecular modelling. *Thermochmica Acta*, 527, 211-218.

Kermanpour, F., Niakan, H.Z. 2012. Measurement and modelling the excess properties of binary mixtures of {[C_6mim][BF_4] + 3-amino-1-propanol} and {[C_6mim][BF_4] + isobutanol]}: Application of Priogogine-Flory Patterson theory. *Journal of Chemical Thermodynamics*, 48, 129-139.

Khupse, N.D., Kumar, A. Ionic Liquids: New Materials with wide applications. 2010. *Indian Journal of Chemistry,* 49A, 635-648.

Kijevcanin, M.L., Puric, I.M., Radovic, I.R., Djordjevic, B.D., Serbanovic, S.P. 2007. Densities and Excess Molar Volumes of the Binary 1-Propanol + Chloroform and 1-Propanol + Benzene and Ternary 1-Propanol + Chloroform + Benzene Mixtures at (288.15, 293.15, 298.15, 303.15, and 313.15) K. *Journal of Chemical and Engineering Data*, 52, 2067-2071.

Kim. S.T., Kang, J.W., Lee, J.S., Min, B.M. 2011. Analysis of the heat of reaction and regeneration in alkanolamine CO_2 system. *Korean Journal of Chemical Engineering*, 28(12), 2275-2281.

Kim, Y.S., Choi, W.Y., Jang, J.H., Yoo, K.P., Lee, C.S. 2005. Solubility measurement and prediction of carbon dioxide in ionic liquids. *Fluid Phase Equilibria*, 228-229, 439-445.

Kim. Y.S., Jang, J.H., Lim, B.D., Kang, J.W., Lee, C.S. 2007. Solubility of mixed gases containing carbon dioxide in ionic liquids: Measurement and predictions. *Fluid Phase Equilibria*, 256, 70-74.

Kim, J.S., Park, Y., Lee, H. 1996. Densities and Viscosities of the Water + Lithium Bromide + Ethanolamine System. *Journal of Chemical and Engineering Data*, 41, 678-680.

Klyamer, S.D., Kolesnikova, T.L., Rodin, Y. 1973. Equilibrium in Aqueous Solutions of Ethanolamines during the Simultaneous Absorption of Hydrogen Sulfide and Carbon Dioxide from Gases. *Gazov Promst*, 18, 44-48.

Ko, C.C., Chang, W.H., Li, M.H. 2008. Ternary diffusion coefficients of monoethanolamine and *N*-methyldiethanolamine in aqueous solutions. *Journal of the Chinese Institute of Chemical Engineers*, 39, 645-651.

Koo, K.K., Lee, H.R., Jeong, S., Oh, Y.S., Park, D.R., Baek, Y.S. 1998. Solubilities, Vapor Pressures, Densities, and Viscosities of the (Water + Lithium Bromide + Lithium Iodide + Lithium Chloride) System. *Journal of Chemical and Engineering Data*, 43, 722-725.

Kroon, M.C. Shariati, A., Costantini, M., Spronsen, J.V., Witkamp, G.J., Sheldon, R.A. Peters, C.J. 2005. High-Pressure Phase Behavior of Systems with Ionic Liquids: Part V. The Binary System. *Journal of Chemical and Engineering Data*, 50, 173-176.

Kroon M.C. Karakatsani, E.K., Economou, G., Witkamp, G.J., Peters, C.J. 2006. Modeling of Carbon Dioxide Solubility in Imidazolium-Based Ionic Liquids with the tPC-PSAFT Equation of State. *Journal of Physical Chemistry B.*, 110, 9262-9269.

Kumar, G., Mondal, T.K., Kundu, M. 2012. Solubility of CO_2 in Aqueous Blends of (Diethanolamine + 2-Amino-2-methyl-1-propanol) and (Diethanolamine + *N*-Methyldiethanolamine). *Journal of Chemical and Engineering Data*, 57, 670-680.

Kundu, M., Bandyopadhyay, S.S. 2006, Solubility of CO_2 in water + diethanolamine + N-methyldiethanolamine. *Fluid Phase Equilibria*, 248, 158-167.

Kuranov, G., Rumpf, B., Smirnova, N.A., Maurer, G. 1996. Solubility of Single Gases Carbon Dioxde and Hydrogen Sulfide in Aqueous Solutions of *N*-methyldiethanolamine in the Temperature Range 313-413 K at Pressures up to 5 MPa. *Industrial and Engineering Chemistry Research*, 35, 1959-1966.

Lachwa, J., Morgado, P., Esperanca, J.M.S.S., Guedes, H.J.R., Canongia-Lopes, J.N., Rebelo, L.P.N. 2006. Fluid-Phase Behavior of {1-Hexyl-3-methylimidazolium Bis(trifluoromethylsulfonyl)Imide, $[C_6mim][NTf_2]$, + C_2-C_8 *n*-Alcohol} Mixtures: Liquid-Liquid Equilibrium and Excess Volumes. *Journal of Chemical and Engineering Data*, 51, 2215-2221.

Lagalante, A.F., Spadi, M., Bruno, T.J. 2000. Kamlet-Taft Solvatochromic Parameters of Eight Alkanolamines. *Journal of Chemical and Engineering Data*, 45, 382-385.

Larriba, M., Garcia, S., Navarro, P., Garcia, J., Rodriguez, F. 2012. Physical Properties of N-Butylpyridinium Tetrafluoroborate and *N*-Butylpyridinium Bis(trifluoromethylsulfonyl)imide Binary Ionic Liquid Mixtures. *Journal of Chemical and Engineering Data*, 57, 1318-1325.

Lawson, J.D., Garst, A.W. 1976. Gas Sweetening Data: Equilibrium Solubility of Hydrogen Sulfide and Carbon Dioxide in Aqueous Monoethanolamine and Aqueous Diethanolamine Solutions. *Journal of Chemical and Engineering Data*, 21, 20-30.

Lee, S.H., Lee, S.B. 2005. The Hildebrand solubility parameters, cohesive energy densities and internal energies of 1-alkyl-3-methylimidazolium-based room temperature ionic liquid. *Chemical Communications*, 21, 3469-3471.

Lee, J.I., Otto, F.D. 1972. Solubility of Carbon Dioxide in Aqueous Diethanolamine Solutions at High Pressure. *Journal of Chemical and Engineering Data,* 17, 465-468.

Lee, S.B. 2005. Analysis of salvation in ionic liquids using a new linear salvation energy relationship. *Journal of Chemical Technology and Biotechnology*, 80, 133-137.

Lemoine, B., Li, Y.G., Cadours, R., Bouallou, C., Richon, D. 2000. Partial vapor pressure of CO_2 and H_2S over aqueous methyldiethanolamine solutions. *Fluid Phase Equilibria*, 172, 261-277.

Letcher, T.M., Reddy, P. 2004. Ternary liquid – liquid equilibria for mixtures of 1-hexyl-3-methylimidazolium (tetrafluoroborate or hexafluorophosphate) + ethanol + an alkene at T = 298.15 K. *Fluid Phase Equilibria*, 219, 107-112.

Letourneux, D. 2007. Absorption of Carbon Dioxide in Aqueous solutions of 2-amino-2-hydroxymethyl-1,3-propanediol," M.S. thesis, Univ. Laval, Quebic, Canada.

Li, X.X., Zhao, G., Liu, D.S., Cao, W.W. 2009. Excess Molar Volume and Viscosity Deviations for the Binary Mixtures of Diethylene Glycol Monobutyl Ether + Water from (293.15 to 333.15) K at Atmospheric Pressure. *Journal of Chemical and Engineering Data*, 54, 890-892.

Li, M.H., Lee, W.C. 1996. Solubility and Diffusivity of N_2O and CO_2 in (Diethanolamine + N-Methyldiethanolamine + Water) and in (Diethanolamine

+ 2-Amino-2-methyl-1-propanol + Water). *Journal of Chemical and Engineering Data*, 41, 551-556.

Li, M.H., Shen, K.P. 1992. Densities and Solubilities of Solutions of Carbon Dioxide in water + Monoethanolamine + *N*-Methyldiethanolamine. *Journal of Chemical and Engineering Data*, 37, 288-290.

Li, M.H., Lie, Y.C. 1994. Densities and Viscosities of Solution of Monoethanolamine + N-Methyldiethanolamine + Water and Monoethanolamine + 2-Amino-2-methyl-1-propanol + Water. *Journal of Chemical and Engineering Data,* 39, 444-447.

Liao, C.H., Li, M.H. 2002. Kinetics of absorption of carbon dioxide into aqueous solutions of monoethanolamine + *N*-methyldiethanolamine. *Chemical Engineering Science*, 57, 4569-4582.

Lin, C.Y., Soriano, A.N., Li, M.H. 2009. Kinetics study of carbon dioxide absorption into aqueous solutions containing *N*-methyldiethanolamine + diethanolamine. *Journal of the Taiwan Institute of Chemical Engineers*, 40, 403-412.

Liu, Y., Daum, P.H. 2008. Relationship of refractive index to mass density and self-consistency of mixing rules for multicomponent mixtures like ambient aerosol. *Journal of Aerosol Science*, 39, 974-986.

LNG, World Report. 2010.

Lukasik, R.B., Matkowska, D., Lukasik, E.B., Hofman, T. 2010. Isothermal vapour-liquid equilibria in the binary and ternary systems consisting of an ionic liquid, 1-propanol and CO_2. *Fluid Phase Equilibria,* 293, 168-174.

Ma’mun, S., Nilsen, R., Svendsen, H.F., Juliussen, O. 2005. Solubility of Carbon Dioxide in 30 mass % Monoethanolamine and 50 mass % Methyldiethanolamine. *Journal of Chemical and Engineering Data*, 50, 630-634.

Maham, Y., Lebrette, L., Mather, A.E. 2002. Viscosities and Excess Properties of Aqueous Solutions of Mono-and Diethylethanolamines at Temperatures between 298.15 and 353.15 K. *Journal of Chemical and Engineering Data*, 47, 550-553.

Maham, Y.M., Teng, T.T., Mather, A.E., Hepler, L.G. 1995. Volumetric properties of (water + diethanolamine) systems. *Canadian Journal of Chemistry,* 73, 1514-1519.

Mahmood, S.H. 2012. A Thermodynamic Investigation of the PVT, Solubility and Surface Tension of Polylactic Acid (PLA)/CO_2 Mixtures. Ph.D. dissertation, Univ. of Toronto, Canada.

Maiti, A. 2009. Theoretical Screening of Ionic Liquid Solvents for Carbon Capture. *ChemSusChem*, 2, 628-631.

Mandal, B.P. Bandyopadhyay, S.S. 2006. Absorption of carbon dioxide into aqueous blends of 2-amino-2-methyl-1-propanol and monoethanolamine. *Chemical Engineering Science*, 61, 5440-5447.

Mandal, B.P., Kundu, M., Bandyopadhyay, S.S. 2005. Physical Solubility and Diffusivity of N_2O and CO_2 into Aqueous Solutions of (2-Amino-2-methyl-1-propanol + Monoethanolamine). *Journal of Chemical and Engineering Data*, 50, 352-358.

Mandal, B.P., Kundu, M., Bandyopadhyay, S.S. 2003. Density and Viscosity of Aqueous Solutions of (*N*-Methyldiethanolamine + Monoethanolamine), (*N*-Methyldiethanolamine + Diethanolamine), (2-Amino-2-methyl-1-propanol + Monoethanolamine), and (2-Amino-2-methyl-1-propanol + Diethanolamine). *Journal of Chemical and Engineering Data*, 48, 703-707.

Marsh, K.N., Brennecke, J.F., Chirico, R.D., Frenkel, M., Heintz, A., Magee, J.W., Peters, C.J., Rebelo, L.P.N., Seddon, K.R. 2009. Thermodynamic and thermophysical properties of the reference ionic liquid: 1-hexyl-3-methylimidazolium bis(trifluoromethylsulfonyl)imide (including mixtures) Part 1. Experimental Methods and Results. *Pure and Applied Chemistry*, 81, 781-790.

Marsh, K.N., Boxall, J.A., Lichtenthaler, R. 2004. Room temperature ionic liquids and their mixtures – a review. *Fluid Phase Equilibria*, 219, 93-98.

Mathias, P.M., Klotz, H.C., Prausnitz, J.M. 1991. Equation-of-State mixing rules for multicomponent mixtures: the problem of invariance. *Fluid Phase Equilibria*, 67, 31-44.

Mathonat, C., Majer, V., Mather, A.E., Grolier, J.P.E. 1997. Enthalpies of absorption and solubility of CO_2 in aqueous solutions of methyldiethanolamine. *Fluid Phase Equilibria*, 140, 171-182.

Mathonat, C., Majer, V., Mather, A.E., Grolier, J.P.E. 1998. Use of Flow Calorimetry for Determing Enthalpies of Absorption and the Solubility of CO_2 in Aqueous Monoethanolamine Solutions. *Industrial and Engineering Chemistry Research*, 37, 4136-4141.

McCann, N., Maeder, M., Hasse, H. 2011. Production of overall enthalpy of CO_2 absorption in aqueous amine systems from experimentally determined reaction enthalpies. *Energy Procedia*, 4, 1542-1549.

Michelsen, M.L., Kistenmacher, H. 1990. On composition-dependent interaction coefficients. *Fluid Phase Equilibria*, 58, 229-230.

Mohamadirad, R., Hamlehdar, O., Boor, H., Monnavar, A.F., Rostami, S. 2011. Mixed Amines Application in Gas Sweetening Plants. *Chemical Engineering Transactions*, 24, 265-270.

Moore, S.K. Trainer, V.L., Mantua, Parker, M.S., Laws, E.A., Baker, L.C., Fleming, L.E. 2008. Impacts of climate variability and future climate change on harmful algal blooms and human health. *Journal of Environmental Health*, 7, 1-12.

Muhammad, A., Mutalib, M.I.A., Murugesan, T., Shafeeq A. 2008. Density and Excess Properties of Aqueous *N*-Methyldiethanolamine Solutions from (298.15 to 338.15) K. *Journal of Chemical and Engineering Data*, 53, 2217-2221.

Muhammad, A., Mutalib, M.I.A., Murugesan, T., Shafeeq, A. 2009. Thermophysical Properties of Aqueous Piperazine and Aqueous (N-Methyldiethanolamine + Piperazine) Solutions at Temperatures (298.15 to 338.15) K. *Journal of Chemical and Engineering Data*, 54, 2317-2321.

Muhammad, A., Mutalib, M.I.A., Wilfred, C.D., Murugesan, T., Shafeeq. A. 2008. Thermophysical properties of 1-hexyl-3-methylimidazolium based ionic liquids with tetrafluoroborate, hexafluorophosphate and bis(trifluoromethylsulfonyl)imide anions. *Journal Chemical Thermodynamics*, 40, 1433-1438.

Muhammad, A., Mutalib, M.I.A., Wilfred, C.D., Murugesan, T., Shafeeq, A. 2008a. Viscosity, Refractive Index, Surface Tension, and Thermal Decomposition of Aqueous *N*-Methyldiethanolamine Solutions from (298.15 to 338.15) K. *Journal of Chemical and Engineering Data*, 53, 2226-2229.

Muhammad, A. 2009. Thermophysical Properties and Solubility of CO_2/CH_4 in Aqueous Alkanolamine Solutions and Ionic Liquids," Ph.D. dissertation, Univ. Technology Petronas, Tronoh, Malaysia.

Mulodoon, M.J., Aki, S.N.V.K., Anderson, J.L., Dixon, J.K., Brennecke, J.F. 2007. Improving Carbon Dioxide Solubility in Ionic Liquid. *Journal of Physical Chemistry B.*, 111, 9001-9009.

Murshid, G., Shariff, A.M., Leong, L.K., Bustam, M.A. 2011. Thermo Physical Analysis of 2-Amino-2-methyl-1-propanol Solvent for Carbon Dioxide Removal. *Chemical Engineering Transactions*, 25, 45-50.

Nakata, M., Sakurai, M. 1987. Refractive index and excess volume for binary liquid mixtures. Part 1. Analysis of new and old data for binary mixtures. *Journal of the Chemical Society Faraday Transactions*, 83, 2449-2457.

Narayanaswamy, K., Rayer, A.V., Kadiwali, S., Henni, A. 2012. Volumetric properties, viscosities, refractive indices and surface tensions for (dimethylpropanolamine (DMA + water) mixtures from 298.15 K to 343.15 K. *Thermochemica Acta*, 543, 218-225.

Navarro, P., Larriba, M., Garcia, S., Rodriguez, F. 2012. Physical Properties of Binary and Ternary Mixtures of 2-Propanol, Water and 1-Butyl-3-methylimidazolium Tetrafluoroborate Ionic Liquid. *Journal of Chemical and Engineering Data*, 57, 1165-1173.

Navia, P. Troncoso, J., Romani, L. 2007. Excess Magnitudes for Ionic Liquid Binary Mixtures with a Common Ion. *Journal of Chemical and Engineering Data*, 52, 1369-1374.

Nierop, E.A.V., Hormoz, S., House, K.Z., Aziz, M.J. 2011. Effect of absorption enthalpy on temperature-swing CO2 separation process performance. *Energy Procedia*, 4, 1783-1790.

Ngo, H.L., LeCompte, K., Hargens, L., McEwen, A.B. 2000. Thermal properties of imidazolium ionic liquids. *Thermochemica Acta*, 357-358, 97-102.

Olajire, A.A. 2010. CO_2 capture and separation technologies for end-of-pipe applications – A review. *Energy*, 35, 2610-2628.

Orchille’s, A.V., Alfaro, V.G., Miguel, P.J., Vercher, E., Andreu, A.M. 2006. Volumetric properties of binary mixtures of ionic liquid 1-butyl-3-methylimidazolium octylsulfate with water or propanol in the temperature range of 278.15 K to 328.15. *Journal of Chemical Thermodynamics*, 38, 1124-1129.

Othmer, K. 2008. Separation Technology, John Wiley and Sons, 1, 1-2.

Pal, A., Gaba, R., Singh, T., Kumar, A. 2010. Excess thermodynamic properties of binary mixtures of ionic liquid (1-butyl-3-methylimidazolium hexafluorophosphate) with alkoxyalkanols at several temperatures. *Journal of Molecular Liquids*, 154, 41-46.

Park, J.Y., Soon, S.J., Lee, H., Yoon, J.H., Shim, J.G., Lee, J.K., Min, B.Y., Eum, H.M. 2002. Density, Viscosity, and Solubility of CO2 in Aqueous Solutions of 2-Amino-2-hydroxymethyl-1,3-propanediol. *Journal of Chemical and Engineering Data*, 47, 970-973.

Park, M.K., Sandall, O.C. 2001. Solubility of Carbon Dioxide and Nitrous Oxide in 50 mass % Methyldiethanolamine. *Journal of Chemical and Engineering Data*, 46, 166-168.

Partington, J.R. 1953. An Advanced Treatise on Physical Chemistry, Vol. 4, Longmans, Green: London.

Patel, N.C., Abovsky, V., Watanasiri, S. 1998. Mixing rules for van-der-Waals type equation of state based on thermodynamic perturbation theory. *Fluid Phase Equilibria*, 152, 219-223.

Paul, S. Mandal, B. 2006. Density and Viscosity of Aqueous Solutions of (N-Methyldiethanolamine + Piperazine) and (2-Amino-2-methyl-1-propanol + Piperazine) from (288 to 333) K. *Journal of Chemical and Engineering Data*, 51, 1808-1810.

Paul, S., Ghoshal, A.K., Mandal, B. 2009. Physicochemical Properties of Aqueous Solutions of 2-Amino-2-hydroxymethyl-1,3-propanediol. *Journal of Chemical and Engineering Data*, 54, 444-447.

Peng, D.Y., Robinson, D.B. 1976. A new two constant equation of state. *Industrial and Engineering Chemistry Fundamentals*, 15, 59-64.

Peralta, R.D., Infante, R., Cortez, G., Rodriguez, O., Wisniak, J. 2002. Volumetric Properties of Toluene with Ethyl Acrylate, Butyl Acrylate, Methyl Methacrylate, and Styrene at 25^{o}C. *Journal of Solution Chemistry*, 31, 175-186.

Pereiro, A.B., Legido, J.L., Rodriguez, A. 2007. Physical properties of ionic liquids based on 1-alkyl-3-methylimidazolium cation and hexafluorophosphate as anion and temperature dependence. *Journal of Chemical Thermodynamics*, 39, 1168-1175.

Plasynski, S.I., Litynski, J.T., Mellvried, H.G., Srivastava, R.D. 2009. Progress and New Developments in Carbon Capture and Storage. *Critical Reviews in Plant Sciences*, 28, 123-138.

Prausnitz, J.M., Lichtenthaler, R.N., Azevedo, E.G.D. 1999. Molecular Thermodynamics of Fluid Phase Equilibria," third ed. Prentice Hall, New Jersey.

Raeissa, S., Florusse, L., Peters, C.J. 2010. Scott van Konynenburg phase diagram of carbon dioxide + alkylimidazolium based ionic liquids. *Journal of Supercritical Fluids*, 55, 825-832.

Ramdin, M., Olasagasti, T.Z., Vlugt, T.J.H., Loos, T.W.D. 2013. High pressure solubility of CO_2 in non fluorinated phosphonium based ionic liquids. *Journal of Supercritical Fluids*, 82, 41-49.

Rao, A.B., Rubin, E.S. 2002. A Technical, Economic, and Environmental Assessment of Amine-Based CO2 Capture Technology for Power Plant Greenhouse Gas Control. *Environmental Science and Technology*, 36, 4467-4475.

Rayer, A.V., Kadiwali, S., Narayanaswamy, K., Henni, A. 2010. Volumetric Properties, Viscosities, and Refractive Indices for Aqueous 1-Amino-2-Propanol (Monoisopropanolamine (MIPA)) Solutions from (298.15 to 343.15) K. *Journal of Chemical and Engineering Data*, 55, 5562-5568.

Rayer, A.V., Henni, A., Tontiwachwuthikul, P. 2012. High-Pressure Solubility of Methan (CH_4) and Ethane (C_2H_6) in Mixed Polyethylene Glycol Ethers (Genosorb 1753) and Its Selectivity in Natural Gas Sweetening Operations. *Journal of Chemical and Engineering Data*, 57, 764-775.

Rebolledo-Libreros, M.E., Trejo, A. 2006. Density and Viscosity of Aqueous Blends of Three Alkanolamines: N-Methyldiethanolamine, Diethanolamine, and 2-Amino-2-methyl-1-propanol in the Range of (303 to 343) K. *Journal of Chemical and Engineering Data*, 51, 702-707.

Rebolledo-Libreros, M.E., Trejo, A. 2004. Gas Solubility of CO_2 in aqueous solutions of N-methyldiethanolamine and diethanolamine with 2-amino-2-methyl-1-propanol. *Fluid Phase Equilbria*, 218, 261-267.

Ren, W., Sensenich, B., Scurto, A.M. 2010. High – pressure phase equilibria of {carbon dioxide (CO_2) + n-alkylo-imidazolium bis(trifluormethylsulfonyl)amide} ionic liquids. *Journal of Chemical Thermodynamics*, 42, 305-311.

Rho, S.W., Yoo, K.P., Lee, J.S., Nam, S.C., Son, J.E., Min, B.M. 1997. Solubility of CO_2 in Aqueous Methyldiethanolamine Solutions. *Journal of Chemical and Engineering Data*, 42, 1161-1164.

Rilo, E., Vila, J., Pico, J., Garcia-Garabal, S., Segade, L., Varela, L.M., Cabeza, O. 2010. Electrical Conductivity and Viscosity of Aqueous Binary Mixtures of 1-Alkyl-3-methyl Imidazolium Tetrafluoroborate at Four Temperatures. *Journal of Chemical and Engineering Data*, 55, 639-644.

Rinker, E.B., Oelschlager, D.W., Colussi, A.T., Henry, K.R., Sandall, O.C. 1994. Viscosity, Density, and Surface Tension of Binary Mixtures of Water and N-Methyldiethanolamine and Water and Diethanolamine and Tertiary Mixtures of These Amines with Water over the Temperature Range 20-100 ^oC. *Journal of Chemical and Engineering Data*, 39, 392-395.

Rochelle, G.T. 2009. Amine Scrubbing for CO_2 capture. *Science Magazine*, 325, 1652-1654.

Rubin, E.S., Rao, 2002, A Technical, Economic and Environmental Assessment of Amine-based CO_2 capture technology for power plant green house gas.

Rufford, T.E., Smart, S., Watson, G.C.Y., Graham, B.F., Boxall, J. Diniz-da-Costa, J.C., May, E.F. 2012. The removal of CO_2 and N_2 from natural gas: A review of conventional and emerging process technologies. *Journal of Petroleum Science and Engineering*, 94-95, 123, 154.

Safarov, J., Hassel, E. 2010. Thermodynamic properties of 1-hexyl-3-methylimidazolium tetrafluoroborate. *Journal of Molecular Liquids*, 153, 153-158.

Saha, A.K., Bandyopadhyay, S.S., Biswas, A.J. 1993. Solubility and Diffusivity of N_2O and CO_2 in Aqueous 2-Amino-2-methyl-1-propanol. *Journal of Chemical and Engineering Data*, 38, 78-82.

Sairi, N.A., Yusoff, R., Alias, Y., Aroua, M.K. 2011. Solubilities of CO_2 in aqueous N-methyldiethnaolamine and guanidinium trifluoromethanesulfonate ionic liquid systems at elevated pressures. *Fluid Phase Equilibria*, 300, 89-94.

Samanta, A., Bandyopadhyay, S.S. 2011. Absorption of carbon dioxide into piperazine activated aqueous *N*-methyldiethanolamine. *Journal of Chemical and Engineering Data*, 171, 734-741.

Sanchez, L.G., Espel, J.R., Onink, F., Meindersma, G.W., Haan, A.B. 2009. Density, Viscosity, and Surface Tension of Synthesis Grade Imidazolium, Pyridinium, and Pyrrolidinium Based Room Temperature Ionic Liquids. *Journal of Chemical and Engineering Data*, 54, 2803-2812.

Sanchez, L.M.G., Meindersma, G.W., Haan, A.B.D. 2007. Solvent Properties of Functionalized Ionic Liquids for CO_2 Absorption. *Transaction International Chemical Engineering*, 85, 31-39.

Sanmamed, Y.A., Gonzalez-Salgado, D., Troncoso, J., Cerdeirina, C.A., Roman. 2007. Viscosity – induced errors in the density determination of room temperature ionic liquids using vibrating tube densitometry. *Fluid Phase Equilibria*, 252, 96-102.

Sanmamed, Y.A., Gonzalez-Salgado, D., Troncoso, J., Roman, L., Baylaucq, A., Boned, C. 2010. Experimental methodology for precise determination of density of RTILs as a function of temperature and pressure using vibrating tube densimeters. *Journal Chemical Thermodynamics*, 42, 553-563.

Santos, F.J.V. Nieto-de-Castro, C.A., Mota, P.J.F., Ribeiro, A.P.C. 2010. Electrical Conductivity and Viscosity of 1-Hexyl-3-methylimidazolium Bis(trifluorosulfonyl)imide, [C_6mim][(CF_3SO_2)$_2$N] (CAS-RN#382150-50-7). *International Journal of Thermophysics*, 31, 1869-1879.

Saravanakumar, K., Baskaran, R., Kubendran, T.R. 2011. Thermophysical Properties of Acetophenone with *N*,*N*-Dimethylethanolamine *or* *N*,*N*-Diethylethanolamine at Temperatures of (303.15, 313.15 and 323.15) K and Pressure of 0.1 MPa. *Journal of Solution Chemistry*, 40, 955-967.

Scholes, C.A., Stevens, G.W., Kentish, S.E. 2012. Membrane gas separation applications in natural gas processing. *Fuel*, 96, 15-28.

Scovazzo, P. Camper, D., Kieft, J., Poshusta, J., Koval, C., Noble, R., Regular Solution Theory and CO_2 Gas Solubility in Room-Temperature Ionic Liquids. *Industrial and Engineering Chemistry Research*, 43, 6855-6860.

Seddon, K.R., Stark, A., Torres, M.J. 2000. Influence of chloride, water, and organic solvents on the physical properties of ionic liquids. Pure and Applied Chemistry, *Pure and Applied Chemistry*, 72, 2275-2287.

Seoane, R.G., Gonzalez, E.J., Gonzalez, B. 2012. 1-Alkyl-3-methylimidazolium bis(trifluoromethylsulfonyl)imide ionic liquids as solvents in the separation of azeotropic mixtures. *Journal of Chemical Thermodynamics,* 53, 152-157.

Shariati, A., Peters, C.J. 2003. High-pressure phase behaviour of systems with ionic liquids: measurements and modelling of the binary system fluoroform + 1-ethyl-3-methylimidazolium hexafluorophosphate. *Journal of Supercritical Fluids*, 25, 109-117.

Shariati, A., Peters, C.J. 2005. High – pressure phase equilibria of systems with ionic liquids. *Journal of Supercritical Fluids,* 34, 171-176.

Shen, K.P., Li, M.H. 1992. Solubility of Carbon Dioxide in Aqueous Mixtures of Monoethanolamine with Methyldiethanolamine. *Journal of Chemical and Engineering Data*, 37, 96-100.

Shiflett, M.B., Yokozeki, A. 2005. Solubilities and Diffusivities of Carbon Dioxide in Ionic Liquids: [bmim][PF_6] and [bmim][BF_4]. *Industrial and Engineering Chemistry Research*, 44, 4453-4464.

Shiflett, M.B., Yokozeki, A. 2007. Solubility of CO_2 in Room Temperature Ionic Liquid [hmim][Tf_2N]. *Journal of Physical Chemistry B.*, 111, 2070-2074.

Shin, E.K., Lee, B.C., Lim, J.S. 2008. High-Pressure solubilities of carbon dioxide in ionic liquids: 1-Alkyl-3-methylimidazolium bis(trifluoromethylsulfonyl)imide. *Journal of Supercritical Fluids*, 45, 282-292.

Silkenbaumer, D., Rumpf, B., Lichtenthaler, R.N. 1998. Solubility of Carbon Dioxide in Aqueous Solutions of 2-Amino-2-methyl-1-propanol and N-Methyldiethanolamine and Their Mixtures in the Temperature Range from 313 to 353 K and Pressures up to 2.7 MPa. *Industrial and Engineering Chemistry Research*, 37, 3133-3141.

Simons, K. 2010. Membrane Technologies for CO_2 capture," Ph.D. dissertation, Univ. Of Twente, Netherlands.

Sinha, B. 2010. Excess molar volumes, viscosity deviations and speeds of sound for some alkoxyethanols and amines in cyclohexanone at 298.15 K. *Physics and Chemistry of Liquids*, 48, 183-198.

Smiljanic, J.D., Kijevcanin, M.L., Djordjevic, B.D., Grozdanic, D.K., Serbanovic, S.P. 2008. Densities and Excess Molar Volumes of the Ternary Mixture 2-Butanol + Chloroform + Benzene and Binary Mixtures 2-Butanol + Chloroform, or + Benzene over the Temperature Range (288.15 to 313.15) K. *Journal of Chemical and Engineering Data*, 53, 1965-1969.

Smith, G.J., Wilding, W.V., Oscarson, J.L., Rowley, R.L. 2003. Correlation of Liquid Viscosity at the normal boiling point. *presented at Fifteen Symposium on Thermophysical Properties, Boulder, Colorado, USA.*

Soave, G. 1972. Equilibrium Constants from a Modified Redlich-Kwong Equation of State. *Chemical Engineering Science*, 27, 1197-1203.

Song, J.H., Yoon, J.H., Lee, H., Lee, K.H. 1996. Solubility of Carbon Dioxide in Monoethanolamine + Ethylene Glycol + Water and Monoethanolamine + Poly(ethylene glycol) + Water. *Journal of Chemical and Engineering*, 41, 497-499.

Souckova, M., Klomfar, J., Patek, J. 2012. Temperature dependence of the surface tension and 0.1 MPa density for 1-C_n-3-methylimidazolium tris(pentafluoroethyl)trifluorophosphate with n = 2, 4, and 6. *Journal of Chemical Thermodynamics*, 48, 267-275.

Sovilj, M., Barjaktarovic, B. 2000. Excess Molar Volumes of Ternary Liquid Systems containing Aliphatic Alcohols at several temperatures. *Bulletin of the Chemists and Technologists of Macedonia*, 19, 73-78.

Speyer, D., Ermatchkov, V., Maurer, G. 2010. Solubility of Carbon Dioxide in Aqueous Solutions of *N*-Methyldiethanolamine and Piperazine in the Low Gas Loading Region. *Journal of Chemical and Engineering Data*, 55, 283-290.

Stoppa, A., Zech, O., Kunz, W., Buchner, R. 2010. The Conductivity of Imidazolium-Based Ionic Liquids from (-35 to 195) ^{o}C. A Variation of Cation's Alkyl Chain. *Journal of Chemical and Engineering Data*, 55, 1758-1773.

Tafat-Igoudjilene, O., Mostefai, L., Kaci, A.A. 2012. Excess molar volumes of (1-chlorobutane + heptane + 2-butanone or 2-pentanone) at (288.15, 303.15 and 313.15) K. Measurement and correlations. *Thermochemica Acta*, 540, 61-68.

Taguchi, R., Machida, H., Sato, Y., Smith Jr., R.L. 2009. High-Pressure Densities of 1-Alkyl-3-methylimidazolium Hexafluorophosphates and 1-Alkyl-3-methylimidazolium Tetrafluoroborates at Temperatures from (313 to 473) K and at Pressures up to 200 MPa. *Journal of Chemical and Engineering Data*, 54, 22-27.

Taib, M.M., Ziyada, A.K., Wilfred, C.D., Murugesan, T. 2011. Thermophysical properties of 1 – propyronitrile – hexylimidazolium bromide + methanol at temperatures (293.15 to 323.15) K. *Journal of Molecular Liquids*, 158, 101-104.

Taib, M.M., Ziyada, A.K., Wilfred, C.D., Murugesan, T. 2012. Volumetric Properties and Refractive Indices for Binary Mixtures of 1-propyronitrile-3-hexylimidazolium Bromide + Ethanol at Temperatures from 293.15 to 323.15 K. *Journal of Solution Chemistry*, 41, 100-111.

Taib, M.M., Murugesan, T. 2012. Solubilities of CO_2 in aqueous solutions of ionic liquids (ILs) and monoethanolamine (MEA) at pressure from 100 to 1600 kPa. *Chemical Engineering Journal*, 181-182, 56-62.

Tariq, M., Forte, P.A.S., Costa-Gomes, M.F., Canongia-Lopes, J.N., Rebelo, L.P.N. 2009. Densities and refractive indices of imidazolium and phosphonium-based ionic liquids: Effect of temperature, alkyl chain length, and anion. *Journal of Chemical Thermodynamics*, 41, 790-798.

Teng, T.T., Maham, Y., Hepler, L.G., Mather, A.E. 1994. Viscosities of Aqueous Solutions of *N*-Methyldiethanolamine and of Diethanolamine. *Journal of Chemical and Engineering Data*, 39, 290-293.

Thitakamol, B., Veawab, A., Aroonwilas, A. 2007. Environmental impacts of absorption-based CO_2 capture unit for post-combustion treatment of flue gas from coal-fired power plant. *International Journal of Greenhouse Gas Control*, 1, 318-342.

Tokuda , H., Hayamizu, K., Ishii, K., Susan, M.A.B.H., Watanabe, M. 2004. Physiochemical Properties and Structures of Room Temperature Ionic Liquids. 1. Variations of Anionic Species. *Journal of Physical Chemistry B.* 108(42), 16593-16600.

Tokuda, H., Hayamizu, K., Ishii, K., Susan, M.A.B.H., Watanabe, M. 2005. Physicochemical Properties and Structures of Room Temperature Ionic Liquids. 2. Variation of Alkyl Chain Lenght in Imidazolium Cation. *Journal of Physical Chemistry B.*, 109, 6103-6110.

Tokuda, H., Ishii, K., Susan, M.A.B.H., Tsuzuki, S., Hayamizu, K., Watanabe, M. 2006. Physicochemical Properties and Structures of Room-Temperature Ionic Liquids. 3. Variation of Cationic Strucutres. *Journal of Physical Chemistry B.*, 110, 2833-2839.

Tomida, D., Kenmochi, S., Tsukada, T., Qiao, K., Bao, Q., Yokoyama, C. 2012. Viscosity and Thermal Conductivity of 1-Hexyl-3-methylimidazolium Tetrafluoroborate and 1-Octyl-3-methylimidazolium Tetrafluoroborate at Pressures up to 20 MPa. *International Journal of Thermophysics*, 33, 959-969.

Tseng, Y.M., Thompson, A.R. 1964, Densities and Refractive Indices of Aqueous Monoethanolamine, Diethanolamine, Triethanolamine. *Journal of Chemical and Engineering Data*, 9, 264-267.

Tuinier, M.J., Annaland, M.V.S., Kramer, G.J., Kuipers, J.A.M. 2010. Cryogenic CO_2 capture using dynamically operated packed beds. *Chemical Engineering Science*, 65, 114-119.

Twu, P., Anderson, J.L., Stephens, T.W., Acree Jr., W.E., Abraham, M.H. 2012. Determination of the solubilising character of 1-methyloxyethyl-1-methylpiperidinium tris(pentafluoroethyl)trifluorophosphate based on the Abraham salvation parameter model. *European Chemical Bulletin*, 1(6), 212-222.

Vahidi, M., Matin, N.S., Goharrokhi, M., Jenab, M.H., Abdi, M.A., Najibi, Correlation of CO_2 solubility in N-methyldiethanolamine + piperazine aqueous solutions using extended Debye-Huckel model. *Journal of Chemical Thermodynamics*, 41, 1272-1278.

Vakili-Nezhaad, G., Vatani, M., Asghari, M., Ashour, I. 2012. Effect of temperature on the physical properties of 1-butyl-3-methylimidazolium based ionic liquids with thiocyanate and tetrafluorborate anions, and 1-hexyl-3-methylimidazolium with tetrafluoroborate and hexafluorophosphate anions. *Journal of Chemical Thermodynamics*, 54, 148-154.

Valderrama, J.O., Rojas, R.E. 2009. Critical Properties of Ionic Liquids. Revisited. *Industrial and Engineering Chemistry Research*, 48, 6890-6900.

Venkatachalam, S., Kandasamy, S. 2010. Prediction of Minimum Fluidization Velocity in Two-Phase and Three-Phase Fluidized Beds: Air/Newtonian and Non-Newtonian Liquids. *International Journal of Chemical Reactor Engineering*, 8, 1-16.

Vercher, E., Llopis, F.J., Gozalez-Alfaro, V., Martinez, A., 2010. Refractive Indices and Deviations in Refractive Indices for Binary Mixtures of 1-Ethyl-3-methylimidazolium Trifluoromethanesulfonate with Methanol, Ethanol, 1-Propanol, and 2-Propanol at Several Temperatures. *Journal of Chemical and Engineering Data*, 55, 1430-1433.

Versteeg, G.F., Swaaij, W.P.M.V. 1988. On the Kinetics between CO2 and alkanolamines both in aqueous and non aqueous solutions. II. Tertiary Amines. *Chemical Engineering Science*, 43, 587-591.

Vural, U.S., Muradoglu, V., Vural, S. 2011. Excess Molar Volumes and Refractive Index of Binary Mixtures of Glycerol + Methanol and Glycerol + Water at 298.15 K and 303.15 K. *Bulletin of Chemical Society of Ethopia*, 25(1), 111-118.

Wagner, M., Stanga, O., Schroer, W. 2004. The liquid – liquid coexistence of binary mixtures of the room temperature ionic liquid 1-methyl-3-hexylimidazolium tetrafluroborate with alcohols. *Physical Chemistry Chemical Physics*, 6, 4421-4431.

Wallace, J.S. 2005. Development of a Carbon Dioxide Continous Scrubber (CDOCS) System for Alkaline Fuel Cell," Ph.D. dissertation, Univ. Of Canterbuty, New Zealand.

Wang, Y.W., Xu, S., Otto, F.D., Mather, A.E. 1992, Solubility of N_2O in alkanolamines and in mixed solvents. *Chemical Engineering Journal*, 48, 31-40.

Wappel, D., Gronald, G., Kalb, R., Draxler, J. 2010. Ionic liquids for post-combustion CO_2 absorption. *International Journal of Greenhouse Gas Control*, 4, 486-494.

Wasserscheid, P., Welton, T. 2008. Ionic Liquids in Synthesis" vol. 1, 2nd Ed. Wiley VCH, Weinham, 71-72.

Weiland, R.W., Chakravarty, T., Mather, A.E. 1993. Solubility of carbon dioxide and hydrogen sulphide in aqueous alkanolamine. *Industrial and Engineering Chemistry Research*, 32(7), 1419-1430.

Weiland, R.W., Dingman, J.C., Cronin, D.B., Browning, G.J. 1998. Density and Viscosity of Some Partially Carbonated Aqueous Alkanolamine Solutions and Their Blends. *Journal of Chemical and Engineering Data*, 43, 378-382.

Welsh, L.M., Davis, R.A. 1995, Density and Viscosity of Aqueous Blends of N-Methyldiethanolamine and 2-Amino-2-methyl-1-propanol. *Journal of Chemical and Engineering Data*, 40, 257-259.

Widegren, J.A., Magee, J.W. 2007. Density, Viscosity, Speed of Sound, and Electrolytic Conductivity for the Ionic Liquid 1-Hexyl-3-methylimidazolium Bis(trifluoromethylsulfonyl)imide and Its Mixtures with Water. *Journal of Chemical and Engineering Data*, 52, 2331-2338.

Wisnaik, J., Peralta, R.D., Infante, R., Cortez, G., Lopez, R.G. 2005. Densities, isobaric thermal compressibilities and derived thermodynamic properties of the binary systems of cyclohexane with allyl methacrylate, butyl methacrylate, methacrylic acid, and vinyl acetate at t = (298.15 and 308.15) K. *Thermochemica Acta*, 437, 1-6.

Wu, T.Y., Chen, B.K., Hao, L., Lin, K.F., Sun, I.W. 2011. Thermophysical properties of a room temperature ionic liquid (1-methyl-3-pentyl-imidazolium hexafluorophosphate) with poly(ethylene glycol). *Journal of the Taiwan Institute of Chemical Engineers*, 42, 914-921.

Wu. T.Y., Sun, I.W. Gung, S.R., Lin, M.W., Chen, B.K., Wang, H.P., Su, S.G. 2011a. Effects of cations and anions on transport properties in tetrafluoroborate based ionic liquids. *Journal of Taiwan Institute of Chemical Engineers*, 42, 513-522.

Wu, T.Y., Chen, B.K. Hao, L. Kuo, C.W., Sun, I.W. 2012. Thermophysical properties of binary mixtures {1-methyl-3-pentylimidazolium tetrafluoroborate + polyethylene glycol methyl ether}. *Journal of the Taiwan Institute of Chemical Engineers*, 43, 313-321.

Wu, S. Bergins, C., Kikkawa, H., Kobayashi, H., Kawasaki, T. 2010. Techology options for clean coal power generation with CO_2 capture. World Energy Congress, Canada.

ION solution is a commercial solvent comprised of IL+amine for CO_2 removal: Available online: www.ion-engineering.com (accessed June 2013).

Xiao, Y., Low, B.T., Hosseini, S.S., Chung, T.S., Paul, D.R. 2009. The strategies of molecular architecture and modification of polyimide-based membranes for

CO_2 removal from natural gas-A review. *Progress in Polymer Science*, 34, 561-580.

Xu, S., Otto, F.D., Mather, A.E. 1991. Physical Properties of Aqueous AMP Solutions. *Journal of Chemical and Engineering Data*, 36, 71-75.

Xu, G.W., Zhang, C.F., Qin, S.J., Gao, W.H., Liu, H.B. 1998. Gas – Liquid Equilibrium in a CO_2-MDEA-H_2O System and the Effect of Piperazine on It. *Industrial and Engineering Chemistry Research*, 37, 1473-1477.

Xu, G., Li, L., Yang, Y., Tian, L., Liu, T., Zhang, K. 2012. A novel CO_2 cryogenic liquefaction and separation system. *Energy*, 42, 522-529.

Yao, C., Pitner, W.R., Anderson, J.L. 2009. Ionic Liquids Containing the Tris(pentafluoroethyl)trifluorophosphate Anion: a New Class of Highly Selective and Ultra Hydrophobic Solvents for the Extraction of Polycyclic Aromatic Hydrocarbons Using Single Drop Microextraction. Analytical Chemistry, 81, 5054-5063.

Yasmin, M., Gupta, M., Density, Viscosity, Velocity and Refractive Index of Binary Mixtures of Poly(Ethylene Glycol) 200 with Ethanolamine, m-Cresol and Aniline at 298.15 K. *Journal of Solution Chemistry*, 40, 1458-1472.

Yazdizadeh, M., Rahmani, F., Forghani, A.A. 2011. Thermodynamic modelling of CO_2 solubility in ionic liquid ([Cn-mim][Tf2N]; n = 2,4,6,8) with using Wong-Sandler mixing rule, Peng-Robinson equation of state (EOS) and differential evolution (DE) method. *Korean Journal of Chemical Engineering*, 28(1), 246-251.

Yeh, J.T., Pennline, H.W. 2004. Absorption and Regeneration Studies for CO_2 capture by Aqueous Ammonia. *presented at the Third Annual Conference on Carbon Capture and Sequestration, Alexandria*, 1-12.

Yokozeki, A. Shiflett, M.B., Junk, C.P., Grieco, L.M., Foo, T. 2008. Physical and Chemical Absorptions of Carbon Dioxide in Room-Temperature Ionic Liquids. Journal of Physical Chemistry B., 112, 16654-16663.

Yoon, S.J., Lee, H.S., Lee, H., Baek, J.I., Yoon, J.H., Eum, H.M. 2002. Densitites, Viscosities, and Surface Tensions of Aqueous 2-Amino-2-ethyl-1,3-propanediol Solutions. *Journal of Chemical and Engineering Data*, 47, 30-32.

Yu, G., Zhao, D., Wen, L., Yang, S., Chen, X. 2012. Viscosity of Ionic Liquids: Database, Observation, and Quantitative Structure-Property Relationship Analysis. *American Institute of Chemical Engineers Journal*, 58, 2885-2899.

Yu, Z., Gao, H., Wang, H., Chen, L. 2012. Thermodynamic Properties of Binary Mixtures of Amino Acid Ionic Liquids [Bmim][Glu] or [Bmim][Gly] with Methanol at T = 298.15 to 333.15 K. *Journal of Solution Chemistry*, 41, 173-186.

Yunus, N.M., Mutalib, M.I.A., Man, Z., Bustam, M.A., Murugesan, T. 2012. Solubility of CO_2 in pyridinium based ionic liquids. *Chemical Engineering Journal*, 189-190, 94-100.

Zhang, X., Zhang, C.F., Liu, Y. 2002. 41, Kinetics of Absorption of CO_2 into Aqueous Solution of MDEA Blended with DEA. *Industrial and Engineering Chemistry Research*, 41, 1135-1141.

Zhu, A., Wang, J., Liu, R. 2011. A volumetric and viscosity study for the binary mixtures of 1-hexyl-3-methylimidazolium tetrafluoroborate with some molecular solvents. *Journal of Chemical Thermodynamics*, 43, 796-799.

Zoghi, A.T., Feyzi, F., Zarrinpashneh, S. 2012. Experimental investigation on the effect of addition of amine activators to aqueous solutions of *N*-methyldiethanolamine on the rate of carbon dioxide absorption. *International Journal of Greenhouse Gas Control*, 7, 12-19.

PUBLICATIONS

Journal Publications

[1] Majid Majeed Akbar, Thanabalan Murugesan, "Thermophysical properties for the binary mixtures of 1-hexyl-3-methylimidazolium bis(trifluoromethylsulfonyl) imide [hmim][Tf2N] + N-methyldiethanolamine (MDEA) at temperatures (303.15 to 323.15) K," *J. Mol. Liq.* vol. 169, pp. 95-101, 2012.

[2] Majid Majeed Akbar, Thanabalan Murugesan, "Thermophysical properties of 1-hexyl-3-methylimidazolium tetrafluoroborate [hmim][BF_4] + *N*-methyldiethanolamine (MDEA) at temperature (303.15 to 323.15) K," *J. Mol. Liq.* vol. 177, pp. 54-59, 2013.

[3] Majid Majeed Akbar, Khashayar Nasifar, Thanabalan Murugesan, "Solubilities of CO_2 in the binary mixtures of *N*-methyldiethanolamine (MDEA) with three types of imidazolium based ionic liquids," *Fluid Phase Equilib.* (under review)

[4] Majid Majeed Akbar, Thanabalan Murugesan, "Thermophysical properties for the binary mixtures of 1-hexyl-3-methylimidazolium tris(pentafluoroethyl)trifluorophosphate [hmim][FAP] + N-methyldiethanolamine (MDEA) at temperatures (303.15 to 328.15) K," *J. Mol. Liq.* (under review)

Conference

[1] Majid Majeed Akbar, Thanabalan Murugesan, "Experimental Viscosites of the binary mixtures of 1-hexyl-3-methylimidazolium tris(pentafluoroethyl)trifluorophosphate with *N*-methyldiethanolamine," *Procd. World Eng. Sci. and Tech. Congress ESTCON 2012, Kuala Lumpur, Malaysia.*

APPENDICES

APPENDIX A

Section 1A: Experimental Densities of the pure liquids as well as for the binary systems Tables A-1 to A-3

Table A-1: Experimental densities of the system ([hmim][BF_4] (1) + MDEA (2)) at temperatures from (298.15 to 323.15) K.

	ρ / g.cm^{-3}					
	T = 298.15	T = 303.15	T = 308.15	T = 313.15	T = 318.15	T = 323.15
x_1						
0	1.03700	1.03356	1.03001	1.02640	1.02275	1.01901
0.1176	1.05825	1.05486	1.05120	1.04738	1.04345	1.03942
0.2072	1.07157	1.06830	1.06450	1.06072	1.05665	1.05258
0.3065	1.08427	1.08106	1.07730	1.07344	1.06950	1.06547
0.4064	1.09556	1.09223	1.08842	1.08463	1.08080	1.07683
0.5051	1.10526	1.10193	1.09816	1.09438	1.09064	1.08676
0.6084	1.11418	1.11094	1.10720	1.10351	1.09980	1.09598
0.7091	1.12192	1.11893	1.11526	1.11160	1.10790	1.10409
0.8080	1.12961	1.12656	1.12289	1.11931	1.11573	1.11187
0.9030	1.13673	1.13346	1.12993	1.12638	1.12291	1.11932
1	1.14426	1.14082	1.13738	1.13395	1.13052	1.12711

Table A-2: Experimental densities for the system ([hmim][Tf_2N](1) + MDEA (2)) at temperatures from (298.15 to 323.15) K.

	ρ /g.cm^{-3}					
	T = 298.15	T = 303.15	T = 308.15	T = 313.15	T = 318.15	T = 323.15
x_1						
0.0000	1.03700	1.03356	1.03001	1.02640	1.02275	1.01901
0.1010	1.11678	1.11274	1.10866	1.10457	1.10048	1.09639
0.1990	1.17335	1.16914	1.16486	1.16057	1.15628	1.15199
0.2951	1.21575	1.21141	1.20703	1.20259	1.19822	1.19378
0.3925	1.24970	1.24526	1.24081	1.23634	1.23186	1.22734
0.5012	1.28010	1.27560	1.27106	1.26653	1.26200	1.25741
0.6001	1.30261	1.29802	1.29342	1.28882	1.28426	1.27964
0.7023	1.32182	1.31725	1.31264	1.30804	1.30346	1.29886
0.8101	1.34129	1.33667	1.33207	1.32748	1.32291	1.31834
0.9011	1.35621	1.35162	1.34702	1.34244	1.33788	1.33332
1.0000	1.36917	1.36457	1.35999	1.35542	1.35087	1.34631

Table A-3: Experimental densities for the system ([hmim][FAP] (1) + MDEA (2)) at temperatures (298.15 to 323.15) K.

	ρ / g.cm^{-3}					
x_1	T = 298.15	T = 303.15	T = 308.15	T = 313.15	T = 318.15	T = 323.15
0	1.03700	1.03356	1.03001	1.02640	1.02275	1.01901
0.1007	1.17647	1.17216	1.16778	1.16350	1.15911	1.15490
0.1989	1.26715	1.26254	1.25784	1.25312	1.24850	1.24385
0.2995	1.33465	1.32985	1.32488	1.31997	1.31509	1.31013
0.4026	1.38718	1.38206	1.37690	1.37174	1.36664	1.36144
0.5001	1.42608	1.42079	1.41548	1.41018	1.40487	1.39954
0.5999	1.45860	1.45323	1.44785	1.44248	1.43709	1.43167
0.7039	1.48810	1.48264	1.47719	1.47175	1.46631	1.46086
0.8003	1.51105	1.50555	1.50004	1.49452	1.48901	1.48349
0.8993	1.53130	1.52580	1.52032	1.51485	1.50938	1.50395
1	1.54960	1.54416	1.53869	1.53327	1.52785	1.52249

Section 2A: Experimental Viscosities of the pure liquids as well as for the binary systems Tables A-4 to A-6

Table A-4: Experimental viscosity (η) of the system ([hmim][BF$_4$] (1) + MDEA (2)) at temperatures from (298.15 to 323.15) K.

	η / mPa.s.					
x_1	T = 298.15	T = 303.15	T = 308.15	T = 313.15	T = 318.15	T = 323.15
0	77.80	57.50	44.21	35.00	27.51	22.00
0.1176	81.01	60.12	46.50	36.84	28.93	23.26
0.2072	83.52	62.20	48.33	38.32	30.08	24.27
0.3065	86.36	64.61	50.46	40.03	31.41	25.46
0.4064	89.28	67.14	52.72	41.84	32.82	26.71
0.5051	92.23	69.76	55.06	43.73	34.28	28.03
0.6084	95.39	72.63	57.65	45.82	35.90	29.49
0.7091	98.53	75.58	60.32	47.98	37.57	31.01
0.8080	101.68	78.62	63.10	50.23	39.31	32.59
0.9030	104.78	81.69	65.93	52.51	41.08	34.22
1	108.00	85.03	69.02	55.00	43.01	36.00

Table A-5: Experimental viscosity of the system ([hmim][Tf_2N] (1) + MDEA (2)) at temperatures (298.15 to 323.15) K.

	η / *mPa.s.*					
	T = 298.15	T = 303.15	T = 308.15	T = 313.15	T = 318.15	T = 323.15
x_1						
0	77.80	57.50	44.21	35.00	27.51	22.00
0.1010	77.20	57.58	44.81	35.61	28.21	22.63
0.1990	76.62	57.66	45.40	36.22	28.91	23.26
0.2951	76.06	57.74	45.98	36.81	29.60	23.88
0.3925	75.49	57.81	46.58	37.43	30.31	24.52
0.5012	74.86	57.90	47.24	38.12	31.11	25.26
0.6001	74.28	57.98	47.86	38.75	31.86	25.93
0.7023	73.70	58.06	48.50	39.42	32.64	26.65
0.8101	73.08	58.15	49.18	40.13	33.48	27.41
0.9011	72.56	58.22	49.76	40.74	34.21	28.07
1	72.00	58.30	50.40	41.40	35.00	28.80

Table A-6: Experimental viscosity (η) of the system ([hmim][FAP] (1) + MDEA (2)) at temperatures (298.15 to 323.15) K.

	η / *mPa.s.*					
	T = 298.15	T = 303.15	T = 308.15	T = 313.15	T = 318.15	T = 323.15
x_1						
0	77.80	57.50	44.21	35.00	27.51	22.00
0.1007	78.83	58.60	45.23	35.81	28.24	22.62
0.1989	79.84	59.68	46.23	36.61	28.97	23.25
0.2995	80.88	60.80	47.28	37.45	29.73	23.91
0.4026	81.96	61.97	48.37	38.33	30.54	24.61
0.5001	82.99	63.09	49.41	39.18	31.32	25.29
0.5999	84.05	64.24	50.50	40.07	32.13	26.01
0.7039	85.17	65.46	51.65	41.01	33.00	26.78
0.8003	86.21	66.61	52.73	41.90	33.83	27.51
0.8993	87.29	67.80	53.85	42.83	34.70	28.29
1	88.40	69.02	55.01	43.80	35.60	29.10

Section 3A: Experimental Refractive index values for the pure as well as for the binary systems Table A-7 to A-9

Table A- 7: Experimental refractive index (n_D) of the system ([hmim][BF$_4$] (1) + MDEA (2)) at temperatures (298.15 to 323.15) K.

	n_D					
	T = 298.15	T = 303.15	T = 308.15	T = 313.15	T = 318.15	T = 323.15
x_1						
0	1.46730	1.46528	1.46320	1.46105	1.45897	1.45695
0.1176	1.46129	1.45949	1.45765	1.45575	1.45390	1.45210
0.2072	1.45659	1.45490	1.45316	1.45138	1.44962	1.44793
0.3065	1.45172	1.45015	1.44854	1.44690	1.44526	1.44369
0.4064	1.44744	1.44595	1.44440	1.44284	1.44127	1.43979
0.5051	1.44376	1.44232	1.44084	1.43934	1.43782	1.43638
0.6084	1.44036	1.43896	1.43753	1.43609	1.43462	1.43322
0.7091	1.43740	1.43605	1.43466	1.43327	1.43183	1.43047
0.8080	1.43481	1.43348	1.43213	1.43078	1.42937	1.42804
0.9030	1.43254	1.43126	1.42995	1.42866	1.42729	1.42601
1	1.43042	1.42918	1.42791	1.42666	1.42533	1.42409

Table A- 8: Experimental refractive index (n_D) of the system ([hmim][Tf$_2$N] (1) + MDEA (2)) at temperatures (298.15 to 323.15) K.

	n_D					
	T = 298.15	T = 303.15	T = 308.15	T = 313.15	T = 318.15	T = 323.15
x_1						
0	1.46730	1.46528	1.46320	1.46105	1.45897	1.45695
0.1010	1.45970	1.45808	1.45635	1.45465	1.45294	1.45093
0.1990	1.45276	1.45120	1.44966	1.44810	1.44652	1.44471
0.2951	1.44762	1.44610	1.44450	1.44296	1.44140	1.43972
0.3925	1.44352	1.44198	1.44048	1.43891	1.43741	1.43570
0.5012	1.44053	1.43910	1.43755	1.43599	1.43453	1.43295
0.6001	1.43805	1.43674	1.43526	1.43371	1.43227	1.43069
0.7023	1.43603	1.43454	1.43298	1.43164	1.43030	1.42880
0.8101	1.43440	1.43291	1.43142	1.42991	1.42843	1.42689
0.9011	1.43325	1.43176	1.43031	1.42882	1.42737	1.42582
1	1.43234	1.43089	1.42940	1.42796	1.42650	1.42494

Table A- 9: Experimental refractive index (n_D) of the system ([hmim][FAP] (1) + MDEA (2)) at temperatures (298.15 to 323.15) K.

	n_D					
x_1	T = 298.15	T = 303.15	T = 308.15	T = 313.15	T = 318.15	T = 323.15
0	1.46730	1.46528	1.46320	1.46105	1.45897	1.45695
0.1007	1.44411	1.44235	1.44052	1.43865	1.43679	1.43499
0.1989	1.42775	1.42644	1.42485	1.42322	1.42161	1.42005
0.2995	1.41681	1.41508	1.41354	1.41197	1.41042	1.40890
0.4026	1.40853	1.40683	1.40536	1.40387	1.40241	1.40095
0.5001	1.40225	1.40086	1.39948	1.39808	1.39671	1.39534
0.5999	1.39784	1.39602	1.39467	1.39330	1.39197	1.39063
0.7039	1.39343	1.39197	1.39061	1.38924	1.38792	1.38657
0.8003	1.39030	1.38891	1.38756	1.38620	1.38489	1.38355
0.8993	1.38774	1.38636	1.38500	1.38363	1.38231	1.38095
1	1.38567	1.38433	1.38298	1.38162	1.38032	1.37897

Section 4A:Thermograms for the binary mixtures Figure A-1 to A-9

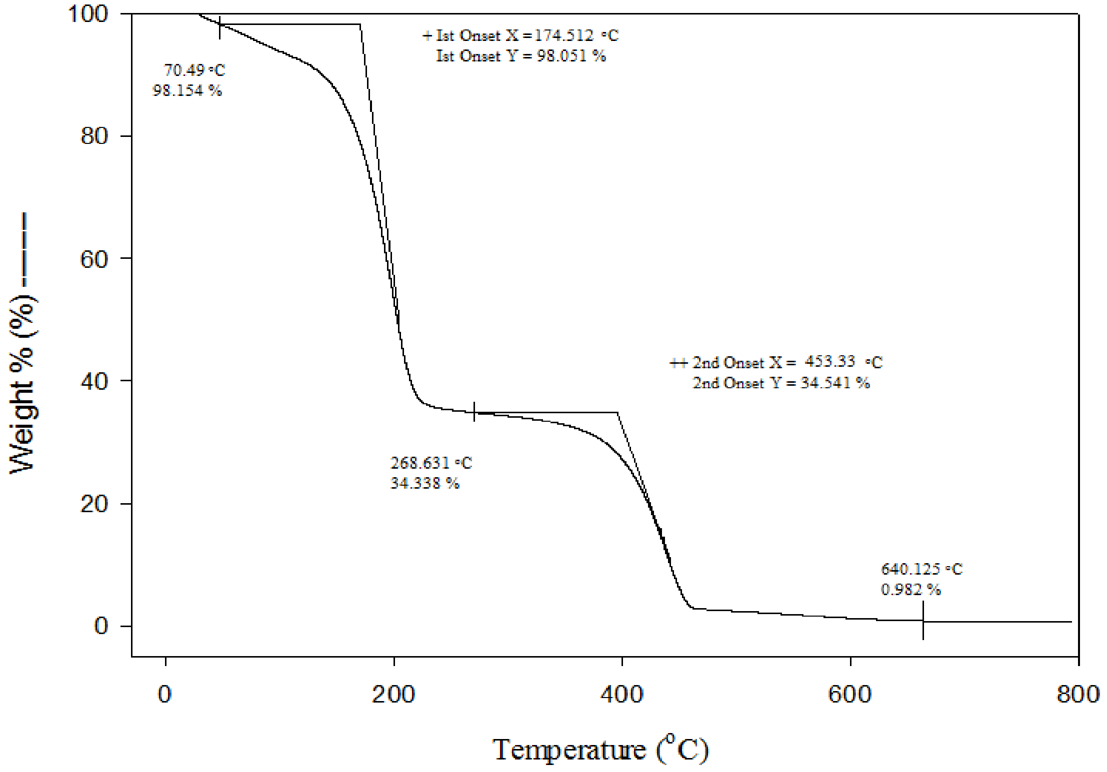

Figure A-1: Plot of Thermal decomposition for the binary mixtures of ([hmim][BF$_4$]+MDEA having IL to MDEA molar ratio of (1:4) at the heating rate of 10 °C/min.

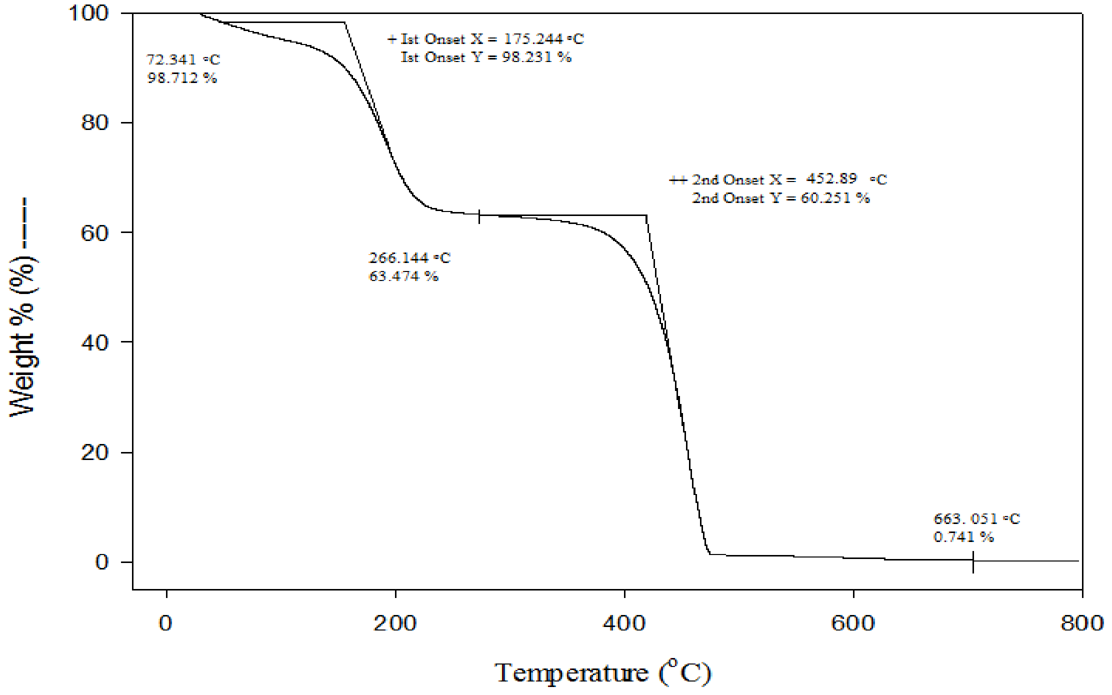

Figure A-2: Plot of Thermal decomposition for the binary mixtures of ([hmim][BF$_4$]+MDEA having IL to MDEA molar ratio of (1:1) at the heating rate of 10 °C/min.

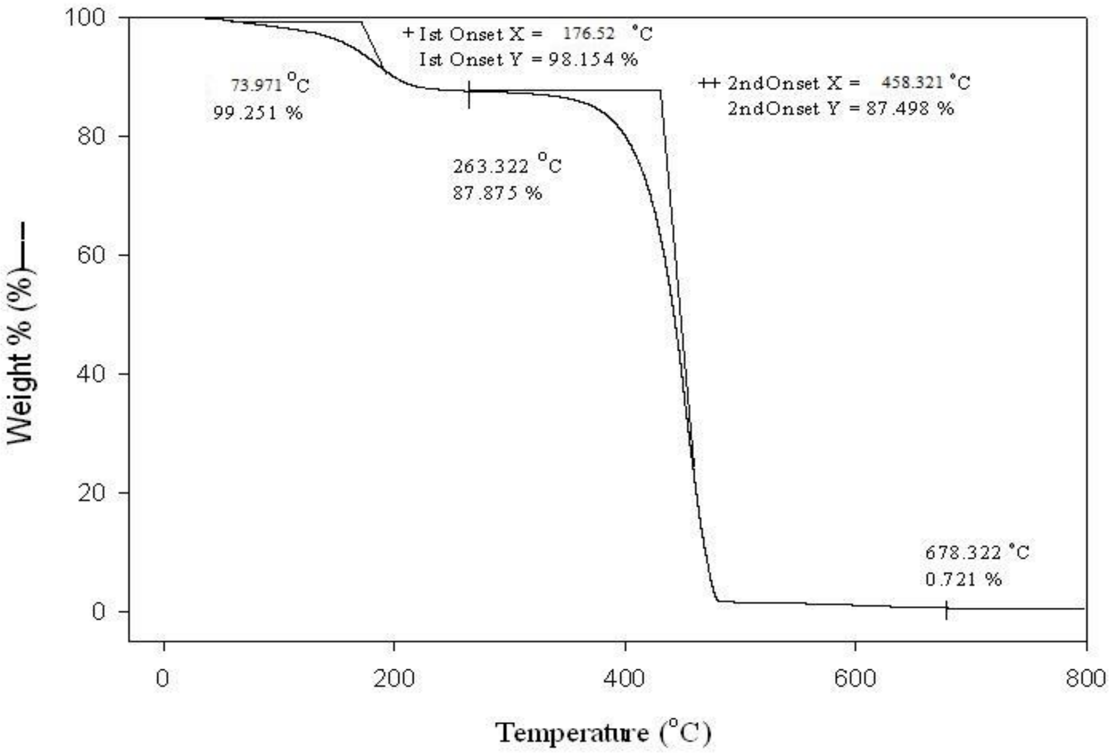

Figure A-3: Plot of Thermal decomposition for the binary mixtures of ([hmim][BF_4]+MDEA having IL to MDEA molar ratio of (4:1) at the heating rate of 10 °C/min.

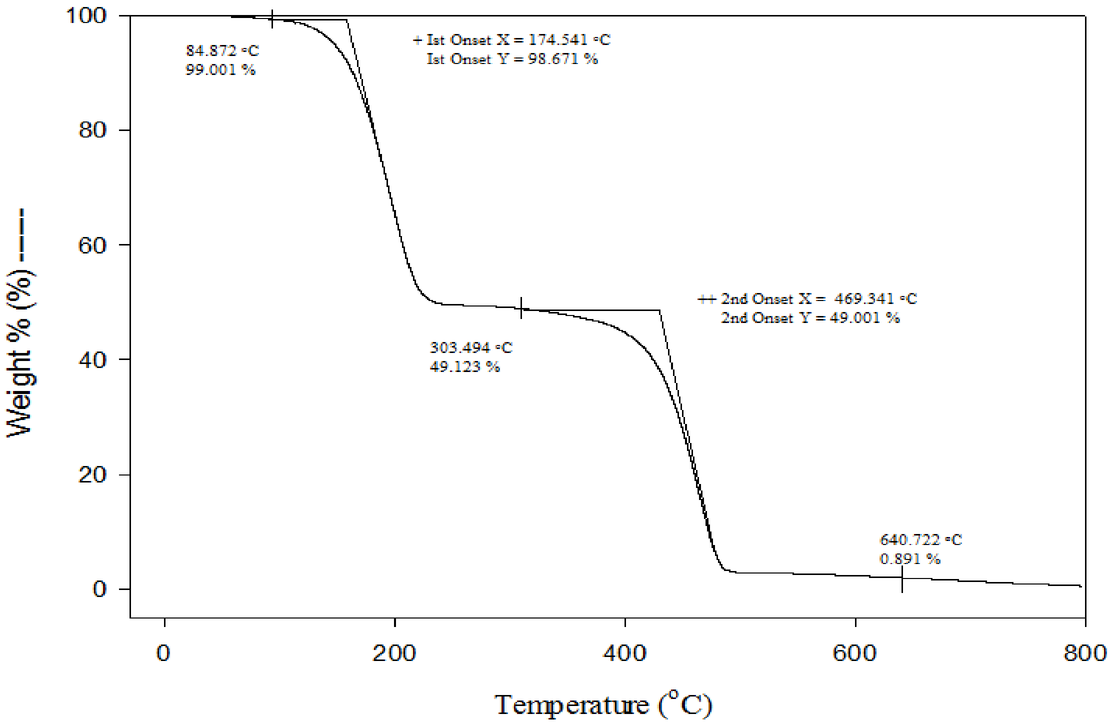

Figure A-4: Plot of Thermal decomposition for the binary mixtures of ([hmim][Tf_2N]+MDEA having IL to MDEA molar ratio of (1:4) at the heating rate of 10 °C/min.

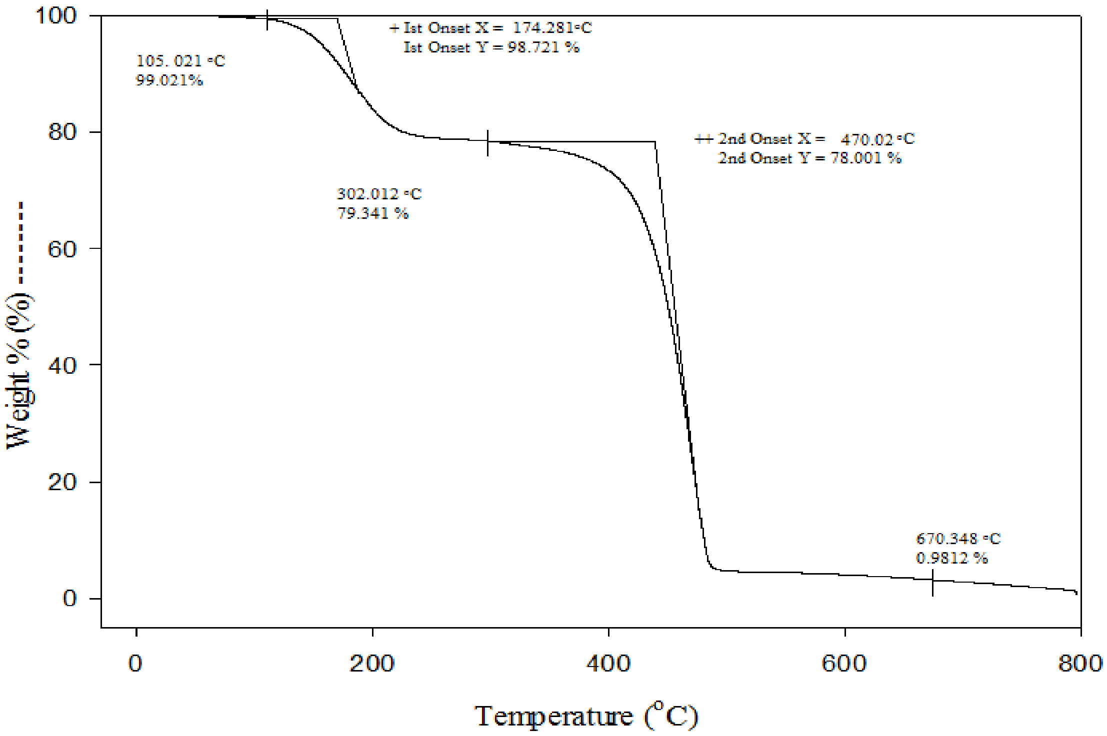

Figure A-5: Plot of Thermal decomposition for the binary mixtures of ([hmim][Tf$_2$N]+MDEA having IL to MDEA molar ratio of (1:1) at the heating rate of 10 °C/min.

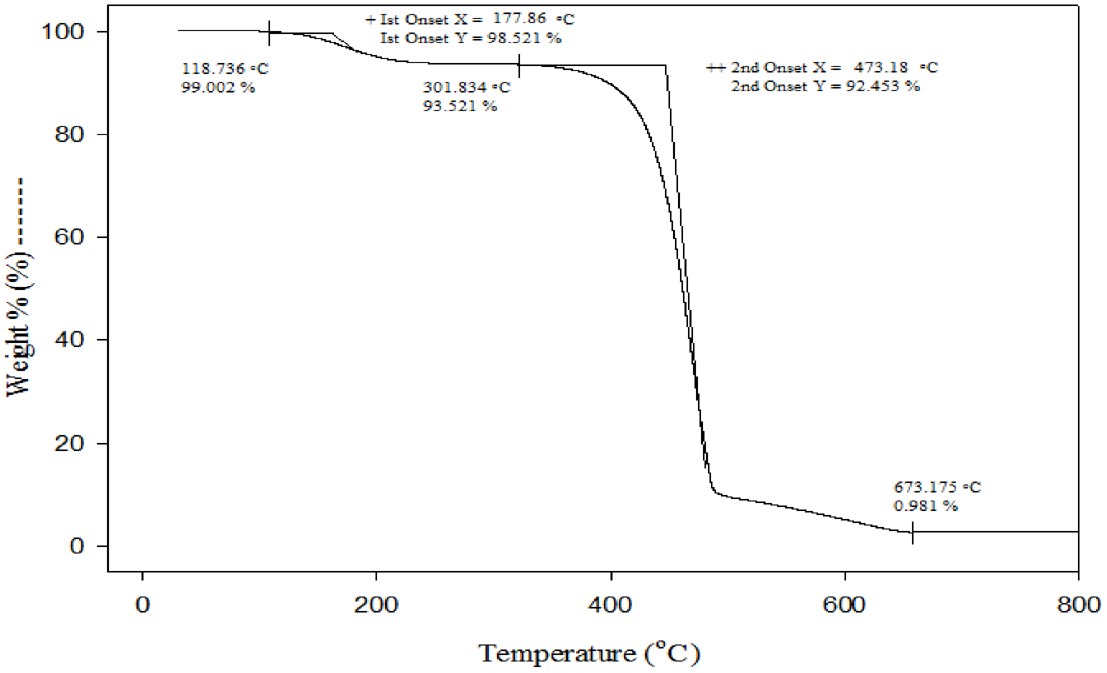

Figure A-6: Plot of Thermal decomposition for the binary mixtures of ([hmim][Tf$_2$N]+MDEA having IL to MDEA molar ratio of (4:1) at the heating rate of 10 °C/min.

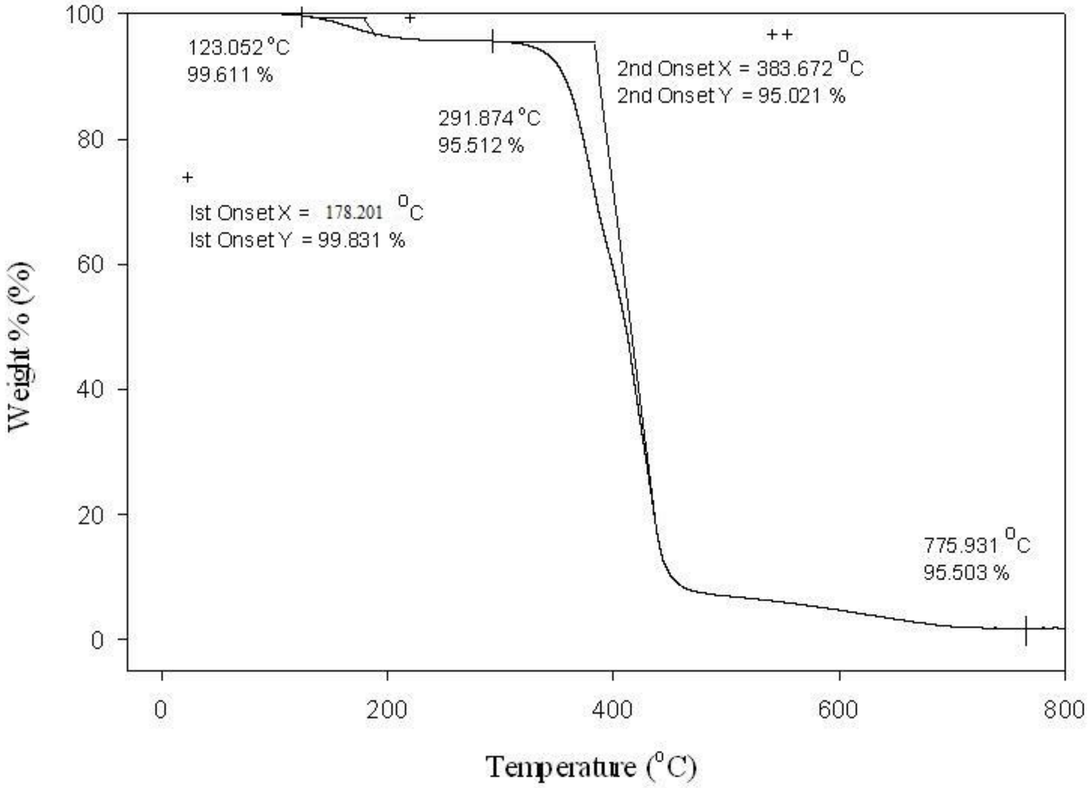

Figure A-7: Plot of Thermal decomposition for the binary mixtures of ([hmim][FAP]+MDEA having IL to MDEA molar ratio of (1:4) at the heating rate of 10 °C/min.

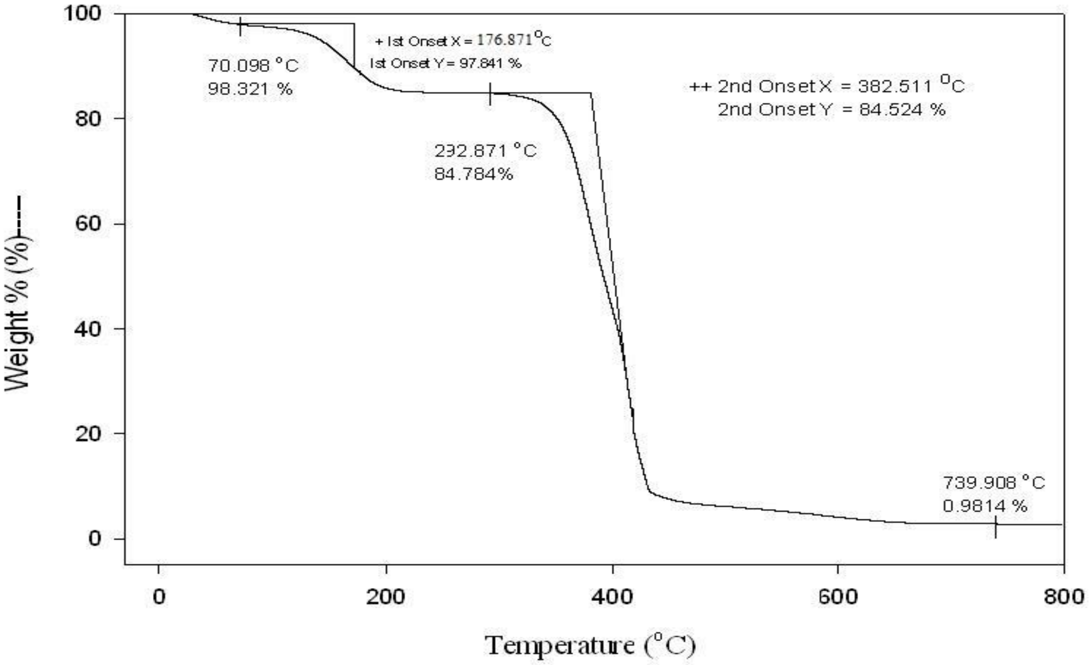

Figure A-8: Plot of Thermal decomposition for the binary mixtures of ([hmim][FAP]+MDEA having IL to MDEA molar ratio of (1:1) at the heating rate of 10 °C/min.

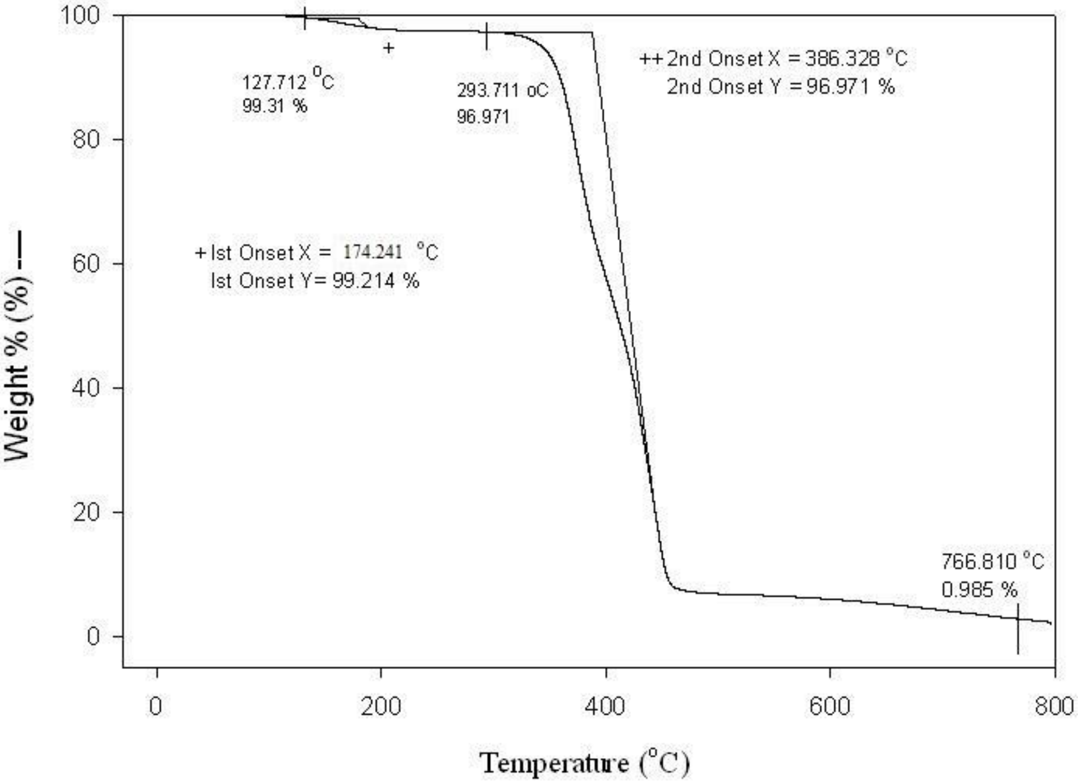

Figure A-9: Plot of Thermal decomposition for the binary mixtures of ([hmim][FAP]+MDEA having IL to MDEA molar ratio of (4:1) at the heating rate of 10 ^{o}C/min.

Section 5A: **Sample Calculations with the help of Eq. 4.1**

$$\rho/g.cm^{-3}\ \boldsymbol{or}\ \eta/mPa.s\ \boldsymbol{or}\ n_D\ = \sum_{i=0}^{2}\left[A_i x^i + B_i x^i (T/K) + C_i x^i (T/K)^2\right]$$

expanding the right hand side of the equation yields

$$\begin{aligned}&\rho/g.cm^{-3}\ \boldsymbol{or}\ \eta/mPa.s\ \boldsymbol{or}\ n_D \\ &\qquad = A_o + B_o(T) + C_o(T^2) + A_1 x + B_1 x(T) + C_1 x(T^2) \\ &\qquad + A_2(x^2) + B_2(x^2)T + C_2(x^2)T^2\end{aligned}$$

The values of constants are:

A_0 = 0.92934, A_1 = 0.30869, A_2 = -0.03118, B_0 = 0.00142742, B_1 = -9.9415×10^{-4}, B_2= -2.3108×10^{-4}, C_0 = -3.5198×10^{-6}, C_1 = 1.5712×10^{-6}, C_2 = 5.2526×10^{-7} for the system [hmim][BF_4] + MDEA for the density values. Substituting the values on the right hand side of the Eq. for x = 0.1176 and T = 298.15 K. The value of the density estimated is 1.05818. Similarly for the remaining mole fractions and for temperatures (T = 298.15 to 323.15 K) the values of the density can be estimated. In the same manner the values of the viscosity and refractive indices can also be estimated by using their respective constants mentioned in Table 4.1.

APPENDIX B

Experimental Excess Molar Volumes for the Binary Systems Tables B-1 to B-3

Table B-1: Calculated excess molar volumes (V^E) of the ([hmim][BF_4](1) + MDEA (2) system at temperatures (298.15 to 323.15) K.

	V^E / $cm^3.mol^{-1}$					
	T = 298.15	*T* = 303.15	*T* = 308.15	*T* = 313.15	*T* = 318.15	*T* = 323.15
x_1						
0	0.0000	0.0000	0.0000	0.0000	0.0000	0.0000
0.1176	0.0644	0.0802	0.0960	0.1258	0.1658	0.2102
0.2072	0.1311	0.1604	0.1973	0.2270	0.2919	0.3505
0.3065	0.2200	0.2606	0.2967	0.3428	0.3981	0.4610
0.4064	0.3027	0.3506	0.3986	0.4405	0.4868	0.5503
0.5051	0.3837	0.4303	0.4768	0.5227	0.5613	0.6203
0.6084	0.4560	0.5000	0.5464	0.5830	0.6225	0.6798
0.7091	0.4926	0.5311	0.5695	0.6054	0.6484	0.7105
0.8080	0.4200	0.4508	0.4921	0.5169	0.5424	0.6206
0.9030	0.3034	0.3206	0.3379	0.3593	0.3666	0.3998
1	0.0000	0.0000	0.0000	0.0000	0.0000	0.0000

Table B-2: Calculated excess molar volumes (V^E) of the ([hmim][Tf_2N](1) + MDEA (2) system at temperatures (298.15 to 323.15) K.

	V^E / $cm^3.mol^{-1}$					
	T = 298.15	*T* = 303.15	*T* = 308.15	*T* = 313.15	*T* = 318.15	*T* = 323.15
x_1						
0.0000	0.0000	0.0000	0.0000	0.0000	0.0000	0.0000
0.1010	0.0810	0.1211	0.1561	0.1870	0.2147	0.2333
0.1990	0.1570	0.1976	0.2394	0.2781	0.3148	0.3432
0.2951	0.2601	0.3021	0.3432	0.3899	0.4248	0.4629
0.3925	0.3805	0.4234	0.4628	0.5029	0.5443	0.5857
0.5012	0.5113	0.5502	0.5967	0.6323	0.6724	0.7174
0.6001	0.6612	0.7210	0.7705	0.8122	0.8513	0.8953
0.7023	0.8508	0.8811	0.9197	0.9564	0.9916	1.0266
0.8101	0.5925	0.6172	0.6424	0.6668	0.6901	0.7096
0.9011	0.1397	0.1482	0.1624	0.1736	0.1843	0.1919
1.0000	0.0000	0.0000	0.0000	0.0000	0.0000	0.0000

Table B-3: Calculated excess molar volumes (V^E) of the ([hmim][FAP](1) + MDEA (2) system at temperatures (298.15 to 323.15) K.

	V^E / $cm^3.mol^{-1}$					
	T = 298.15	T = 303.15	T = 308.15	T = 313.15	T = 318.15	T = 323.15
x_1						
0.0000	0.0000	0.0000	0.0000	0.0000	0.0000	0.0000
0.1007	0.3693	0.4126	0.4535	0.4777	0.5120	0.5163
0.1989	0.7988	0.8414	0.8856	0.9304	0.9583	0.9856
0.2995	1.1082	1.1446	1.1969	1.2398	1.2754	1.3216
0.4026	1.2961	1.3564	1.4129	1.4715	1.5179	1.5823
0.5001	1.4431	1.5109	1.5731	1.6374	1.7022	1.7744
0.5999	1.5000	1.5629	1.6194	1.6798	1.7432	1.8189
0.7039	1.1799	1.2413	1.2917	1.3478	1.4033	1.4699
0.8003	0.8676	0.9202	0.9663	1.0245	1.0802	1.1497
0.8993	0.5107	0.5454	0.5669	0.5972	0.6275	0.6615
1.0000	0.0000	0.0000	0.0000	0.0000	0.0000	0.0000

Experimental viscosity deviation values for the binary systems Table B-4 to B-6

Table B-4: Calculated viscosity deviations ($\Delta\eta$) of the ([hmim][BF_4](1) + MDEA (2)) system at temperatures (298.15 to 323.15) K.

	$\Delta\eta$ / mPa.s.					
	T = 298.15	T = 303.15	T = 308.15	T = 313.15	T = 318.15	T = 323.15
x_1						
0.0000	0.0000	0.0000	0.0000	0.0000	0.0000	0.0000
0.1176	-0.3372	-0.6175	-0.6277	-0.5120	-0.4028	-0.3864
0.2072	-0.5355	-1.0042	-1.0206	-0.8240	-0.6416	-0.6308
0.3065	-0.6955	-1.3279	-1.3543	-1.1000	-0.8508	-0.8310
0.4064	-0.7922	-1.5482	-1.5728	-1.2880	-0.9892	-0.9796
0.5051	-0.8239	-1.6454	-1.6815	-1.3720	-1.0591	-1.0414
0.6084	-0.7882	-1.6193	-1.6544	-1.3480	-1.0402	-1.0276
0.7091	-0.6849	-1.4415	-1.4828	-1.2020	-0.9310	-0.9174
0.8080	-0.5169	-1.1242	-1.1565	-0.9300	-0.7240	-0.7220
0.9030	-0.2929	-0.6696	-0.6834	-0.5500	-0.4265	-0.4220
1.0000	0.0000	0.0000	0.0000	0.0000	0.0000	0.0000

Table B-5: Calculated viscosity deviations ($\Delta\eta$) of the ([hmim][Tf$_2$N](1) + MDEA (2)) system at temperatures (298.15 to 323.15) K.

	$\Delta\eta$ / *mPa.s.*					
	T = 298.15	T = 303.15	T = 308.15	T = 313.15	T = 318.15	T = 323.15
x_1						
0.0000	0.0000	0.0000	0.0000	0.0000	0.0000	0.0000
0.1010	-0.0136	-0.0153	-0.0244	-0.0323	-0.0540	-0.0547
0.1990	-0.0239	-0.0269	-0.0429	-0.0568	-0.0950	-0.0963
0.2951	-0.0312	-0.0350	-0.0563	-0.0742	-0.1242	-0.1260
0.3925	-0.0357	-0.0401	-0.0649	-0.0852	-0.1428	-0.1449
0.5012	-0.0374	-0.0420	-0.0680	-0.0895	-0.1501	-0.1524
0.6001	-0.0359	-0.0403	-0.0652	-0.0861	-0.1445	-0.1467
0.7023	-0.0313	-0.0351	-0.0570	-0.0751	-0.1262	-0.1282
0.8101	-0.0230	-0.0258	-0.0418	-0.0554	-0.0931	-0.0947
0.9011	-0.0133	-0.0149	-0.0242	-0.0321	-0.0541	-0.0550
1.0000	0.0000	0.0000	0.0000	0.0000	0.0000	0.0000

Table B-6: Calculated viscosity deviations ($\Delta\eta$) of the ([hmim][FAP](1) + MDEA (2)) system at temperatures (298.15 to 323.15) K.

	$\Delta\eta$ / *mPa.s.*					
	T = 298.15	T = 303.15	T = 308.15	T = 313.15	T = 318.15	T = 323.15
x_1						
0.0000	0.0000	0.0000	0.0000	0.0000	0.0000	0.0000
0.1007	-0.0406	-0.0629	-0.0705	-0.0781	-0.0856	-0.0932
0.1989	-0.0716	-0.1110	-0.1243	-0.1377	-0.1511	-0.1644
0.2995	-0.0944	-0.1464	-0.1641	-0.1818	-0.1995	-0.2172
0.4026	-0.1084	-0.1682	-0.1886	-0.2090	-0.2295	-0.2499
0.5001	-0.1128	-0.1752	-0.1965	-0.2179	-0.2392	-0.2605
0.5999	-0.1084	-0.1685	-0.1891	-0.2097	-0.2303	-0.2509
0.7039	-0.0943	-0.1467	-0.1647	-0.1827	-0.2006	-0.2186
0.8003	-0.0724	-0.1127	-0.1266	-0.1404	-0.1543	-0.1682
0.8993	-0.0411	-0.0640	-0.0719	-0.0798	-0.0877	-0.0956
1.0000	0.0000	0.0000	0.0000	0.0000	0.0000	0.0000

Experimental refractive index deviation values for the binary systems Tables B-7 to B-9

Table B-7: Calculated refractive index deviations (*Δn_D*) of the ([hmim][BF_4](1) + MDEA (2)) system at temperatures (298.15 to 323.15) K.

	Δn_D					
x_1	T = 298.15	T = 303.15	T = 308.15	T = 313.15	T = 318.15	T = 323.15
0.0000	0.0000	0.0000	0.0000	0.0000	0.0000	0.0000
0.1176	-0.0017	-0.0015	-0.0014	-0.0013	-0.0011	-0.0010
0.2072	-0.0031	-0.0029	-0.0027	-0.0025	-0.0024	-0.0022
0.3065	-0.0043	-0.0041	-0.0038	-0.0036	-0.0034	-0.0032
0.4064	-0.0049	-0.0047	-0.0045	-0.0042	-0.0040	-0.0038
0.5051	-0.0049	-0.0047	-0.0045	-0.0043	-0.0042	-0.0040
0.6084	-0.0045	-0.0044	-0.0042	-0.0040	-0.0039	-0.0037
0.7091	-0.0037	-0.0036	-0.0035	-0.0034	-0.0033	-0.0032
0.8080	-0.0027	-0.0026	-0.0026	-0.0025	-0.0024	-0.0024
0.9030	-0.0015	-0.0014	-0.0014	-0.0013	-0.0013	-0.0013
1.0000	0.0000	0.0000	0.0000	0.0000	0.0000	0.0000

Table B-8: Calculated refractive index deviaitons (*Δn_D*) of the ([hmim][Tf_2N](1) + MDEA (2)) system at temperatures (298.15 to 323.15) K.

	Δn_D					
x_1	T = 298.15	T = 303.15	T = 308.15	T = 313.15	T = 318.15	T = 323.15
0.0000	0.0000	0.0000	0.0000	0.0000	0.0000	0.0000
0.1010	-0.0060	-0.0059	-0.0059	-0.0059	-0.0059	-0.0059
0.1990	-0.0095	-0.0094	-0.0092	-0.0090	-0.0090	-0.0089
0.2951	-0.0110	-0.0109	-0.0108	-0.0107	-0.0106	-0.0105
0.3925	-0.0115	-0.0114	-0.0113	-0.0112	-0.0111	-0.0110
0.5012	-0.0104	-0.0103	-0.0102	-0.0101	-0.0100	-0.0099
0.6001	-0.0092	-0.0090	-0.0089	-0.0088	-0.0087	-0.0086
0.7023	-0.0074	-0.0074	-0.0074	-0.0072	-0.0070	-0.0068
0.8101	-0.0050	-0.0050	-0.0050	-0.0050	-0.0049	-0.0049
0.9011	-0.0028	-0.0028	-0.0027	-0.0027	-0.0027	-0.0027
1.0000	0.0000	0.0000	0.0000	0.0000	0.0000	0.0000

Table B-9: Calculated refractive index deviations (Δn_D) of the ([hmim][FAP](1) + MDEA (2)) system at temperatures (298.15 to 323.15) K.

	Δn_D					
x_1	T = 298.15	T = 303.15	T = 308.15	T = 313.15	T = 318.15	T = 323.15
0.0000	0.0000	0.0000	0.0000	0.0000	0.0000	0.0000
0.1007	-0.0150	-0.0148	-0.0146	-0.0144	-0.0143	-0.0141
0.1989	-0.0233	-0.0227	-0.0224	-0.0220	-0.0217	-0.0214
0.2995	-0.0260	-0.0257	-0.0253	-0.0250	-0.0247	-0.0244
0.4026	-0.0261	-0.0258	-0.0255	-0.0252	-0.0249	-0.0246
0.5001	-0.0242	-0.0239	-0.0236	-0.0233	-0.0229	-0.0226
0.5999	-0.0205	-0.0203	-0.0201	-0.0199	-0.0197	-0.0195
0.7039	-0.0164	-0.0163	-0.0161	-0.0159	-0.0157	-0.0155
0.8003	-0.0117	-0.0116	-0.0114	-0.0113	-0.0111	-0.0110
0.8993	-0.0062	-0.0061	-0.0061	-0.0060	-0.0059	-0.0059
1.0000	0.0000	0.0000	0.0000	0.0000	0.0000	0.0000

APPENDIX C

CO_2 solubility in the pure liquids as well as in the binary systems Table C-1 to C-4

Table C-1: CO_2 solubility in pure solvents at T =(298.15, 313.15, 323.15) K.

CO_2 (1) + [hmim][BF_4] (2)					
T = 298.15 K		T = 313.15 K		T = 323.15 K	
P (kPa)	x_1	P (kPa)	x_1	P (kPa)	x_1
130	0.0261	169	0.0258	160	0.0227
326	0.0650	344	0.0521	333	0.0469
661	0.1300	685	0.1024	642	0.0893
1012	0.1950	1030	0.1517	1063	0.1456
1524	0.2387	1544	0.1953	1536	0.1892
2020	0.3142	2026	0.2708	2002	0.2647
2503	0.3878	2501	0.3444	2505	0.3383
2912	0.4267	2901	0.3766	2910	0.3705
CO_2 (1) + [hmim][Tf_2N] (2)					
126	0.0384	127	0.0297	134	0.0282
347	0.1045	331	0.0768	319	0.0668
678	0.2013	627	0.1437	629	0.1301
1052	0.3082	1095	0.2464	1029	0.2096
1552	0.3654	1563	0.3035	1569	0.2668
2018	0.4533	2019	0.3914	2017	0.3547
2509	0.5488	2511	0.4869	2515	0.4502
2903	0.5988	2914	0.5369	2938	0.5002
CO_2 (1) + [hmim][FAP] (2)					
139	0.0518	128	0.0381	144	0.0381
332	0.1237	354	0.1044	305	0.0801
658	0.2431	615	0.1789	686	0.1773
1042	0.3702	1077	0.3066	1030	0.2637
1535	0.4488	1544	0.3852	1578	0.3422
2023	0.5477	2021	0.4841	2036	0.4411
2512	0.6466	2519	0.5830	2522	0.5400
2917	0.6933	2916	0.6297	2920	0.5867
CO_2 (1) + MDEA (2)					
135	0.0322	155	0.0317	142	0.0267
353	0.0827	379	0.0767	355	0.0665
645	0.1498	633	0.1278	666	0.1240
1033	0.2337	1027	0.2022	1021	0.1877
1542	0.2911	1575	0.2596	1542	0.2451
2001	0.3743	2029	0.3428	2015	0.3283
2511	0.4521	2504	0.4206	2525	0.4061
2922	0.4989	2949	0.4674	2928	0.4529

Table C-2: CO_2 solubility in [hmim][BF_4] + MDEA binary mixtures with IL to MDEA molar ratios {(1:4), (1:1), (4:1)} at T = (298.15, 313.15, 323.15) K.

CO_2 (1) + [hmim][BF_4] (2) + MDEA								
	(1:4)			(1:1)			(4:1)	
P (kPa)	x_1	x_2	P (kPa)	x_1	x_2	P (kPa)	x_1	x_2
T = 298.15 K								
154	0.0387	0.1923	142	0.0309	0.4849	162	0.0305	0.7756
312	0.0779	0.1844	367	0.0788	0.4609	370	0.0695	0.7444
624	0.1527	0.1695	634	0.1343	0.4331	610	0.1133	0.7094
1088	0.2611	0.1478	1055	0.2188	0.3910	1025	0.1858	0.6514
1567	0.3174	0.1365	1574	0.2701	0.3654	1564	0.2201	0.6240
2009	0.3989	0.1202	2004	0.3463	0.3272	2007	0.2903	0.5678
2527	0.4812	0.1038	2517	0.4215	0.2896	2530	0.3711	0.5032
2924	0.5232	0.0954	2936	0.4677	0.2665	2921	0.4019	0.4785
T = 313.15 K								
157	0.0336	0.1933	145	0.0274	0.4866	166	0.0242	0.7807
328	0.0690	0.1862	356	0.0663	0.4673	358	0.0519	0.7586
617	0.1296	0.1741	683	0.1270	0.4370	629	0.0901	0.7280
1037	0.2139	0.1572	1043	0.1893	0.4058	1032	0.1453	0.6839
1547	0.2742	0.1452	1523	0.2308	0.3851	1526	0.1795	0.6564
2012	0.3557	0.1289	2003	0.3068	0.3470	2016	0.2497	0.6003
2516	0.4380	0.1124	2523	0.3920	0.3044	2506	0.3305	0.5356
2906	0.4790	0.1042	2926	0.4382	0.2812	2923	0.3613	0.5110
T = 323.15 K								
137	0.0273	0.1945	123	0.0216	0.4897	132	0.0179	0.7858
306	0.0601	0.1880	332	0.0582	0.4715	314	0.0424	0.7662
611	0.1186	0.1763	636	0.1095	0.4457	639	0.0853	0.7318
1047	0.1998	0.1600	1059	0.1795	0.4114	1070	0.1405	0.6877
1560	0.2630	0.1474	1538	0.2238	0.3886	1573	0.1748	0.6602
2031	0.3485	0.1303	2011	0.3012	0.3500	2041	0.2450	0.6041
2532	0.4258	0.1148	2538	0.3725	0.3143	2543	0.3258	0.5394
2931	0.4718	0.1056	2941	0.4154	0.2926	2927	0.3566	0.5148

Table C-3: CO$_2$ solubility in [hmim][Tf$_2$N] + MDEA binary mixtures with IL to MDEA molar ratios {(1:4), (1:1), (4:1)} at T = (298.15, 313.15, 323.15) K.

CO$_2$ (1) + [hmim][Tf$_2$N] (2) + MDEA								
	(1:4)			(1:1)			(4:1)	
				T = 298.15 K				
P (kPa)	x_1	x_2	P (kPa)	x_1	x_2	P (kPa)	x_1	x_2
165	0.0318	0.1937	140	0.0301	0.4853	136	0.0385	0.7693
349	0.0666	0.1867	330	0.0701	0.4657	320	0.0894	0.7286
620	0.1167	0.1767	630	0.1317	0.4347	640	0.1761	0.6592
1055	0.1937	0.1613	1040	0.2127	0.3941	1049	0.2827	0.5739
1571	0.2511	0.1498	1520	0.2701	0.3653	1540	0.3387	0.5291
2044	0.3309	0.1353	2030	0.3521	0.3243	2033	0.4261	0.4592
2535	0.4122	0.1176	2520	0.4304	0.2852	2541	0.5274	0.3781
2929	0.4522	0.1096	2946	0.4743	0.2633	2933	0.5711	0.3432
				T = 313.15 K				
146	0.0247	0.1951	150	0.0281	0.4872	124	0.0276	0.7780
329	0.0553	0.1890	334	0.0620	0.4695	321	0.0710	0.7433
643	0.1069	0.1786	638	0.1168	0.4421	644	0.1404	0.6878
1020	0.1665	0.1667	1046	0.1882	0.4079	1023	0.2195	0.6247
1531	0.2210	0.1558	1553	0.2409	0.3812	1532	0.2812	0.5751
2038	0.3107	0.1379	2027	0.3276	0.3369	2042	0.3729	0.5018
2531	0.3863	0.1228	2528	0.4059	0.2979	2536	0.4702	0.4240
2934	0.4258	0.1149	2943	0.4498	0.2759	2944	0.5179	0.3858
				T = 323.15 K				
158	0.0252	0.1950	147	0.0256	0.4878	125	0.0254	0.7798
336	0.0532	0.1894	340	0.0586	0.4714	324	0.0648	0.7482
646	0.1011	0.1798	647	0.1101	0.4457	622	0.1231	0.7016
1068	0.1645	0.1671	1053	0.1760	0.4127	1024	0.2001	0.6401
1572	0.2219	0.1557	1559	0.2334	0.3840	1533	0.2531	0.5976
2035	0.3017	0.1397	2005	0.3134	0.3439	2046	0.3465	0.5229
2514	0.3820	0.1236	2545	0.3977	0.3017	2526	0.4366	0.4508
2939	0.4230	0.1154	2915	0.4376	0.2817	2947	0.4885	0.4092

Table C-4: CO_2 solubility in [hmim][FAP] + MDEA binary mixtures with IL to MDEA molar ratios {(1:4), (1:1), (4:1)} at T = (298.15, 313.15, 323.15) K.

CO$_2$ (1) + [hmim][FAP] (2) + MDEA								
	(1:4)			(1:1)			(4:1)	
P (kPa)	x_1	x_2	P (kPa)	x_1	x_2	P (kPa)	x_1	x_2
				T = 298.15 K				
159	0.0292	0.1942	129	0.0260	0.4876	149	0.0518	0.7587
357	0.0648	0.1871	341	0.0675	0.4668	381	0.1320	0.6945
628	0.1126	0.1775	654	0.1285	0.4366	681	0.2314	0.6150
1022	0.1795	0.1641	1039	0.1985	0.4015	1075	0.3543	0.5167
1530	0.2371	0.1526	1547	0.2651	0.3681	1539	0.4210	0.4633
2034	0.3282	0.1344	2028	0.3552	0.3230	2039	0.5209	0.3833
2544	0.3985	0.1203	2533	0.4250	0.2880	2539	0.6201	0.3040
2913	0.4372	0.1126	2909	0.4651	0.2679	2930	0.6692	0.2647
				T = 313.15 K				
138	0.0227	0.1955	148	0.0261	0.4879	133	0.0373	0.7704
322	0.0527	0.1895	338	0.0590	0.4713	325	0.0899	0.7281
625	0.1009	0.1798	637	0.1096	0.4459	626	0.1709	0.6633
1045	0.1657	0.1669	1019	0.1733	0.4141	1044	0.2800	0.5761
1561	0.2142	0.1572	1529	0.2329	0.3842	1558	0.3467	0.5227
2010	0.2941	0.1412	2006	0.3175	0.3419	2024	0.4466	0.4428
2542	0.3701	0.1260	2508	0.3978	0.3016	2510	0.5458	0.3634
2905	0.4104	0.1179	2925	0.4389	0.2811	2937	0.5949	0.3242
				T = 323.15 K				
143	0.0221	0.7823	151	0.0249	0.4884	141	0.0357	0.1926
327	0.0503	0.7597	335	0.0549	0.4733	323	0.0811	0.1837
648	0.0984	0.7213	635	0.1031	0.4492	631	0.1571	0.1685
1058	0.1582	0.6734	1048	0.1669	0.4173	1054	0.2581	0.1483
1565	0.2128	0.6298	1551	0.2316	0.3849	1562	0.3179	0.1364
2032	0.2924	0.5661	2037	0.3140	0.3436	2014	0.4155	0.1168
2529	0.3702	0.5038	2540	0.3925	0.3043	2524	0.5184	0.0962
2911	0.4109	0.4713	2907	0.4316	0.2847	2932	0.5612	0.0876

Sample Calculations for the estimation of experimental Henry's constants

The Henry's constants were estimated by using eq. (4.8) as:

$$K_H = \frac{\phi_1 \times P/KPa}{x_{CO2}}$$

where ϕ_1 is the fugacity coefficient of CO_2 gas and P is the equilibrium pressure, x_{CO2} is the mole fraction of CO_2 dissoved. The fugucaity coefficients were estimated by using the Peng Robinson EOS as:

$$ln\,\phi = \left(\frac{PV}{RT} - 1\right) - ln\left\{\frac{P(V-b)}{RT}\right\} + \frac{a}{2.828bRT}\,ln\left(\frac{V+2.414b}{V-0.414b}\right)$$

where P is pressure, R is universal gas constant and a and b are the Peng Robinson EOS parameters (defined in section 4.10 of chapter 4). A computer written by ChemSof was used to estimate the values of ϕ.

The sample calculations for the estimation of Henry's constant in pure [hmim][BF$_4$] are listed below:

Table C-5: Sample calculations for the estimation of Henry's Constants

P/KPa	ϕ_1	x_{CO2}	$P\phi_1$	H/Kpa = $P\phi_1$ / x_{CO2}	H/Mpa
130	0.9908	0.02610	128.807	4935.145	4.931
326	0.9840	0.06500	320.784	4935.116	4.932
661	0.9706	0.13000	641.568	4935.127	4.932
1012	0.9509	0.19500	962.352	4935.138	4.933
1524	0.9029	0.23870	1178.018	4935.118	4.934
2020	0.8676	0.31420	1550.621	4935.128	4.936
2503	0.7949	0.38780	1913.847	4935.121	4.937
2912	0.7531	0.42670	2105.824	4935.122	4.938

Table C-6: CO_2 solubility in the ILs [bmim][BF_4], [bmim][FAP], [bmim][Tf_2N] and [bheaa] at T = 298.15 K.

CO_2 (1)+[bmim][BF_4](2)		CO_2(1)+[bmim][FAP](2)	
P (kPa)	x_1	P (kPa)	x_1
133	0.0237	145	0.0414
361	0.0617	358	0.1135
642	0.1211	648	0.2332
1032	0.1911	1038	0.3612
1540	0.2415	1544	0.4387
2012	0.3201	2021	0.5372
2516	0.3889	2513	0.6361
2939	0.4405	2921	0.6832

CO_2(1)+[bmim][Tf_2N](2)		CO_2(1)+[bheaa](2)	
P(kPa)	x_1	P (kPa)	x_1
152	0.0371	133	0.0095
311	0.1025	350	0.0248
611	0.1995	641	0.0446
1078	0.3012	1037	0.0766
1577	0.3614	1531	0.0980
2005	0.4501	1999	0.1285
2517	0.5452	2501	0.1561
2914	0.5912	2901	0.1768

Table C-7: CO_2 solubility in the binary mixtures [bmim][BF$_4$]+MDEA, [bmim][Tf$_2$N]+MDEA, [bmim][FAP]+MDEA, [bheaa]+MDEA at T = 298.15 K.

CO_2(1)+[bmim][BF$_4$](2)+MDEA(3)					
(1:4)		(1:1)		(4:1)	
P(kPa)	x_1	P(kPa)	x_1	P(kPa)	x_1
158	0.0369	160	0.028	160	0.019
321	0.076	328	0.0722	328	0.0484
619	0.1511	622	0.1304	622	0.1017
1090	0.2588	1091	0.2124	1091	0.176
1568	0.3092	1565	0.2663	1565	0.2234
2045	0.3993	2035	0.3472	2035	0.2951
2527	0.4684	2524	0.4205	2524	0.3726
2924	0.5256	2921	0.4697	2921	0.4138
CO_2(1)+[bmim][Tf$_2$N](2)+MDEA(3)					
166	0.0312	151	0.0321	150	0.0361
321	0.0523	312	0.0627	317	0.0825
622	0.1152	619	0.1298	614	0.1795
1082	0.1887	1099	0.2137	1086	0.2812
1521	0.2461	1564	0.2711	1575	0.3414
2003	0.3293	2006	0.3543	2001	0.4301
2503	0.4071	2519	0.4321	2512	0.5252
2933	0.4539	2918	0.4789	2911	0.5712
CO_2(1)+[bmim][FAP](2)+MDEA(3)					
148	0.0041	135	0.021	148	0.0311
362	0.0327	353	0.0627	362	0.0935
657	0.0998	645	0.1298	657	0.2032
1032	0.1837	1033	0.2137	1032	0.3312
1532	0.2411	1542	0.2711	1532	0.4087
2024	0.3243	2001	0.3543	2024	0.5072
2543	0.4021	2511	0.4321	2543	0.6061
2923	0.4489	2922	0.4789	2923	0.6532
CO_2(1)+[bheaa](2)+MDEA(3)					
152	0.0377	156	0.0209	152	0.0035
311	0.0776	315	0.0538	311	0.0155
611	0.1519	617	0.0972	611	0.0351
1078	0.2592	1082	0.1552	1078	0.0613
1577	0.3103	1576	0.1946	1577	0.0788
2005	0.4001	2002	0.2514	2005	0.1027
2517	0.4702	2518	0.3041	2517	0.1381
2914	0.5222	2916	0.3379	2914	0.1535

Table C-8: The experimental CO_2 solubility data in the aqueous IL solutions at T=298.15 K.

[emim][FAP]+MEA+Water							
15% aq. MEA		5% IL		10% IL		15% IL	
P(kPa)	x_{CO2}	P(kPa)	x_{CO2}	P(kPa)	x_{CO2}	P(kPa)	x_{CO2}
155	0.0290	165	0.0275	147	0.0258	135	0.0239
357	0.0319	357	0.0304	373	0.0287	353	0.0268
645	0.0337	649	0.0322	665	0.0305	645	0.0286
1036	0.0355	1037	0.034	1073	0.0323	1033	0.0304
1539	0.0374	1549	0.0359	1572	0.0342	1542	0.0323
2033	0.0391	2025	0.0376	2063	0.0359	2001	0.034
2532	0.0408	2564	0.0393	2572	0.0376	2511	0.0357
2944	0.0422	2974	0.0407	2981	0.039	2922	0.0371
[emim][FAP]+DEA+Water							
25% aq. DEA		5% IL		10% IL		15% IL	
135	0.0393	133	0.0343	157	0.0293	165	0.0248
353	0.0454	355	0.0404	363	0.0354	373	0.0309
645	0.0487	641	0.0437	675	0.0387	635	0.0342
1033	0.0511	1037	0.0461	1036	0.0411	1053	0.0366
1542	0.0529	1540	0.0479	1545	0.0429	1572	0.0384
2001	0.0547	2011	0.0497	2021	0.0447	2003	0.0402
2511	0.0563	2521	0.0513	2513	0.0463	2504	0.0418
2922	0.0574	2912	0.0524	2943	0.0474	2945	0.0429
[emim][Tf_2N]+MEA+Water							
15% aq. MEA		5% IL		10% IL		15% IL	
158	0.0290	159	0.0272	151	0.0253	150	0.0232
356	0.0319	362	0.0301	356	0.0282	354	0.0261
642	0.0337	635	0.0319	642	0.03	643	0.0279
1031	0.0355	1076	0.0337	1033	0.0318	1031	0.0297
1536	0.0374	1509	0.0356	1538	0.0337	1537	0.0316
2032	0.0391	2083	0.0373	2032	0.0354	2038	0.0333
2530	0.0408	2562	0.039	2542	0.0371	2537	0.035
2942	0.0422	2965	0.0404	2932	0.0385	2940	0.0364
[emim][Tf_2N]+DEA+Water							
25% aq. DEA		5% IL		10% IL		15% IL	
135	0.0393	165	0.0323	163	0.0258	168	0.0223
353	0.0454	373	0.0384	378	0.0319	377	0.0284
645	0.0487	665	0.0417	663	0.0352	662	0.0317
1033	0.0511	1053	0.0441	1058	0.0376	1058	0.0341
1542	0.0529	1562	0.0459	1564	0.0394	1568	0.0359
2001	0.0547	2020	0.0477	2024	0.0412	2025	0.0377
2511	0.0563	2514	0.0493	2516	0.0428	2519	0.0393
2922	0.0574	2932	0.0504	2933	0.0439	2934	0.0404

Experimental and Estimated Henry's constants for the pure solvents as well as for the binary systems Tables C-5 to C-7

Table C-9: Experimental and estimated Henry's constants for the system [hmim][BF_4] + MDEA

	H (Mpa)				
Solvent	H_{exp}	$H_{PR\text{-}MK}$	$H_{PR\text{-}VdW}$	$H_{SRK\text{-}MK}$	$H_{SRK\text{-}VdW}$
			T = 298.15 K		
[hmim][BF_4]	4.93	4.85	4.99	5.12	5.43
MDEA	4.16	4.28	4.46	4.07	4.66
[hmim][BF_4] + MDEA					
(1:4)	3.95	3.78	4.2	4.33	4.46
(1:1)	4.57	4.69	4.88	4.67	5.11
(4:1)	5.24	5.34	5.55	5.71	5.91
			T = 313.15 K		
[hmim][BF_4]	6.5	6.2	6.1	6.3	6.78
MDEA	4.85	5	5.3	4.64	5.55
[hmim][BF_4] + MDEA					
(1:4)	4.65	4.93	5.2	4.48	5.4
(1:1)	5.26	5.5	5.8	4.9	5.85
(4:1)	6.8	7	7.33	6.59	7.5
			T = 323.15 K		
[hmim][BF_4]	7.01	7.21	7.54	6.8	7.71
MDEA	5.25	5.45	5.78	5.04	5.95
[hmim][BF_4] + MDEA					
(1:4)	5.03	5.23	5.56	4.82	5.73
(1:1)	5.66	5.86	6.19	5.45	6.36
(4:1)	7.32	7.52	7.85	7.11	8.02

Table C-10: Experimental and estimated Henry's constants for the system [hmim][Tf_2N] + MDEA

	H (Mpa)				
Solvent	H_{exp}	$H_{PR\text{-}MK}$	$H_{PR\text{-}VdW}$	$H_{SRK\text{-}MK}$	$H_{SRK\text{-}VdW}$
			T = 298.15 K		
[hmim][Tf_2N]	3.25	3.45	3.78	3.05	3.95
MDEA	4.16	4.28	4.46	4.07	4.66
[hmim][Tf_2N] + MDEA					
(1:4)	5.15	5.35	5.68	4.95	5.85
(1:1)	4.63	4.83	5.16	4.43	5.33
(4:1)	3.52	3.72	4.05	3.32	4.22
			T = 313.15 K		
[hmim][Tf_2N]	4.25	4.5	4.8	3.98	4.96
MDEA	4.85	5	5.3	4.64	5.55
[hmim][Tf_2N] + MDEA					
(1:4)	5.86	6.11	6.41	5.59	6.57
(1:1)	5.32	5.57	5.87	5.05	6.03
(4:1)	4.46	4.71	5.01	4.19	5.17
			T = 323.15 K		
[hmim][Tf_2N]	4.72	4.97	5.27	4.45	5.43
MDEA	5.25	5.45	5.78	5.04	5.95
[hmim][Tf_2N] + MDEA					
(1:4)	6.24	6.49	6.79	5.97	6.95
(1:1)	5.73	5.98	6.28	5.46	6.44
(4:1)	4.92	5.17	5.47	4.65	5.63

Table C-11: Experimental and estimated Henry's constants for the system [hmim][Tf$_2$N] + MDEA

	H (Mpa)				
Solvent	H_{exp}	$H_{PR\text{-}MK}$	$H_{PR\text{-}VdW}$	$H_{SRK\text{-}MK}$	$H_{SRK\text{-}VdW}$
			T = 298.15 K		
[hmim][FAP]	2.65	2.88	3.21	2.37	3.33
MDEA	4.16	4.28	4.46	4.07	4.66
[hmim][FAP] + MDEA					
(1:4)	5.41	5.64	5.97	5.13	6.09
(1:1)	4.95	5.18	5.51	4.67	5.63
(4:1)	2.85	3.08	3.41	2.57	3.53
			T = 313.15 K		
[hmim][FAP]	3.35	3.58	3.91	3.07	4.03
MDEA	4.85	5	5.3	4.64	5.55
[hmim][FAP] + MDEA					
(1:4)	6.03	6.26	6.59	5.75	6.71
(1:1)	5.64	5.87	6.2	5.36	6.32
(4:1)	3.56	3.79	4.12	3.28	4.24
			T = 323.15 K		
[hmim][FAP]	3.76	3.99	4.32	3.48	4.44
MDEA	5.25	5.45	5.78	5.04	5.95
[hmim][FAP] + MDEA					
(1:4)	6.42	6.65	6.98	6.14	7.1
(1:1)	6.02	6.25	6.58	5.74	6.7
(4:1)	3.93	4.16	4.49	3.65	4.61

CO_2 solubility in the recycled pure as well as in the binary systems Tables C-12 to C-13

Table C-12: Comparison of CO_2 Solubility in the Fresh and Recycled Pure Liquids at T = (298.15, 313.15) K.

CO_2 (1) + [hmim][BF_4] (2)							
T = 298.15 K				T = 313.15 K			
Fresh		*Recycled*		*Fresh*		*Recycled*	
P (kPa)	x_1	P (kPa)	x_1	P (kPa)	x_1	P (kPa)	x_1
130	0.0261	135	0.0250	169	0.0258	170	0.0252
326	0.0650	328	0.0620	344	0.0521	360	0.0519
661	0.1300	650	0.1260	685	0.1024	700	0.0950
1012	0.1950	999	0.1900	1030	0.1517	1056	0.1450
1524	0.2387	1515	0.2320	1544	0.1953	1566	0.1890
2020	0.3142	2014	0.3080	2026	0.2708	2045	0.2630
2503	0.3878	2495	0.3800	2501	0.3444	2520	0.3350
2912	0.4267	2998	0.4190	2901	0.3766	2940	0.3680
CO_2 (1) + [hmim][Tf_2N] (2)							
126	0.0384	132	0.0364	127	0.0297	130	0.0294
347	0.1045	365	0.1035	331	0.0768	345	0.0741
678	0.2013	680	0.1950	627	0.1437	621	0.1407
1052	0.3082	1065	0.3020	1095	0.2464	1102	0.2404
1552	0.3654	1561	0.3560	1563	0.3035	1574	0.2950
2018	0.4533	2024	0.4433	2019	0.3914	2028	0.3852
2509	0.5488	2510	0.5360	2511	0.4869	2541	0.4770
2903	0.5988	2912	0.5794	2914	0.5369	2925	0.5278
CO_2 (1) + [hmim][FAP] (2)							
139	0.0518	142	0.0509	128	0.0381	128	0.0371
332	0.1237	341	0.1227	354	0.1044	354	0.1013
658	0.2431	665	0.2401	615	0.1789	615	0.1728
1042	0.3702	1054	0.3652	1077	0.3066	1077	0.3004
1535	0.4488	1547	0.4398	1544	0.3852	1544	0.3781
2023	0.5477	2031	0.5397	2021	0.4841	2021	0.4781
2512	0.6466	2524	0.6356	2519	0.5830	2519	0.5741
2917	0.6933	2924	0.6801	2916	0.6297	2916	0.6187
CO_2 (1) + MDEA (2)							
135	0.0322	147	0.0312	155	0.0317	162	0.0310
353	0.0827	365	0.0805	379	0.0767	382	0.0735
645	0.1498	641	0.1464	633	0.1278	643	0.1218
1033	0.2337	1047	0.2267	1027	0.2022	1042	0.1964
1542	0.2911	1535	0.2861	1575	0.2596	1583	0.2556
2001	0.3743	2014	0.3673	2029	0.3428	2031	0.3378
2511	0.4521	2532	0.4451	2504	0.4206	2511	0.4116
2922	0.4989	2942	0.4884	2949	0.4674	2931	0.4524

Table C-13: CO_2 solubility in the selected binary mixtures of ILs with MDEA at T = (298.15, 313.15) K.

([hmim][BF_4] + MDEA) (1:4)							
T = 298.15 K				T = 313.15 K			
Fresh		*Recycled*		*Fresh*		*Recycled*	
P (kPa)	x_{CO2}	P (kPa)	x_{CO2}	P (kPa)	x_{CO2}	P (kPa)	x_{CO2}
154	0.0387	158	0.0327	157	0.0336	162	0.0316
312	0.0779	322	0.0761	328	0.0690	347	0.0641
624	0.1527	632	0.1501	617	0.1296	627	0.1246
1088	0.2611	1085	0.2575	1037	0.2139	1041	0.2100
1567	0.3174	1561	0.3124	1547	0.2742	1544	0.2701
2009	0.3989	1998	0.3919	2012	0.3557	2018	0.3487
2527	0.4812	2517	0.4721	2516	0.4380	2535	0.4289
2924	0.5232	2914	0.5135	2906	0.4790	2914	0.4695
([hmim][Tf_2N] + MDEA) (4:1)							
136	0.0385	140	0.0371	124	0.0276	132	0.0264
320	0.0894	331	0.0861	321	0.0710	340	0.0706
640	0.1761	651	0.1718	644	0.1404	661	0.1394
1049	0.2827	1057	0.2749	1023	0.2195	1042	0.2151
1540	0.3387	1564	0.3289	1532	0.2812	1541	0.2714
2033	0.4261	2041	0.4154	2042	0.3729	2035	0.3621
2541	0.5274	2554	0.5161	2536	0.4702	2524	0.4607
2933	0.5711	2947	0.5601	2944	0.5179	2961	0.5065
([hmim][FAP] + MDEA) (4:1)							
149	0.0518	151	0.0512	133	0.0373	135	0.0361
381	0.1320	375	0.1314	325	0.0899	354	0.0889
681	0.2314	674	0.2254	626	0.1709	631	0.1684
1075	0.3543	1067	0.3501	1044	0.2800	1057	0.2754
1539	0.4210	1528	0.4124	1558	0.3467	1562	0.3397
2039	0.5209	2054	0.5119	2024	0.4466	2034	0.4396
2539	0.6201	2564	0.6112	2510	0.5458	2524	0.5354
2930	0.6692	2955	0.6560	2937	0.5949	2951	0.5842

Pressure drop of CO_2 during absorption in the pure as well as in the binary solvents Figures C-1 to C-6

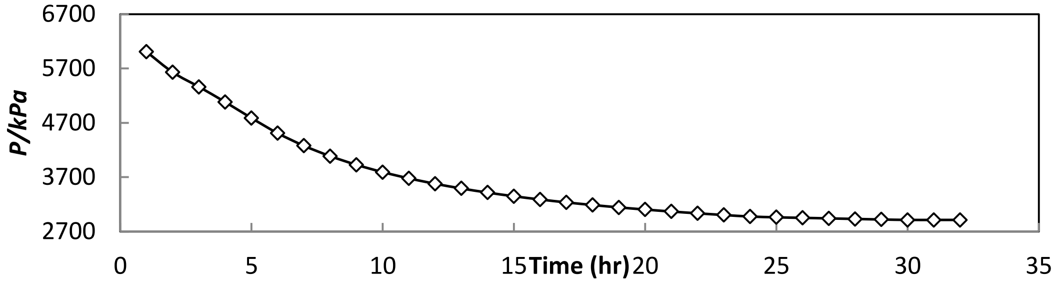

Figure C-1: Pressure drop vs time during the absorption of CO_2 in [hmim][BF_4] at T = 298.15 K.

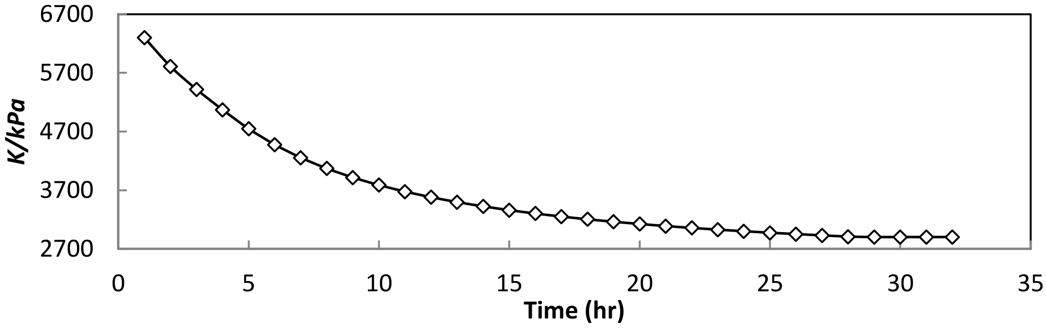

Figure C-2: Pressure drop vs time during the absorption of CO_2 in [hmim][Tf_2N] at T = 298.15 K.

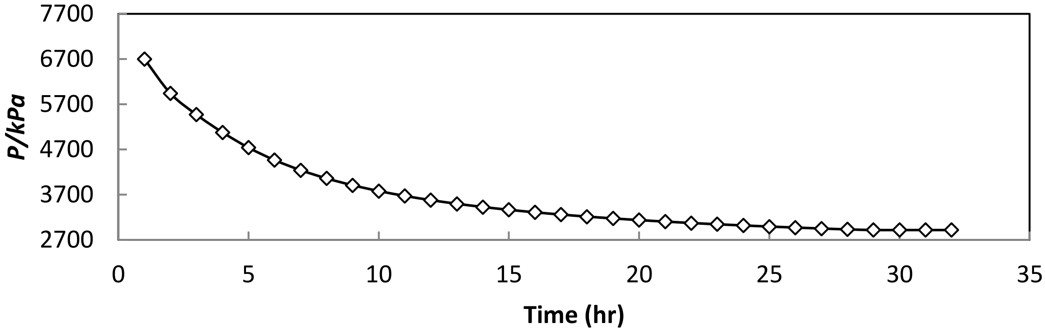

Figure C-3: Pressure drop vs time during the absorption of CO_2 in [hmim][FAP] at T = 298.15 K.

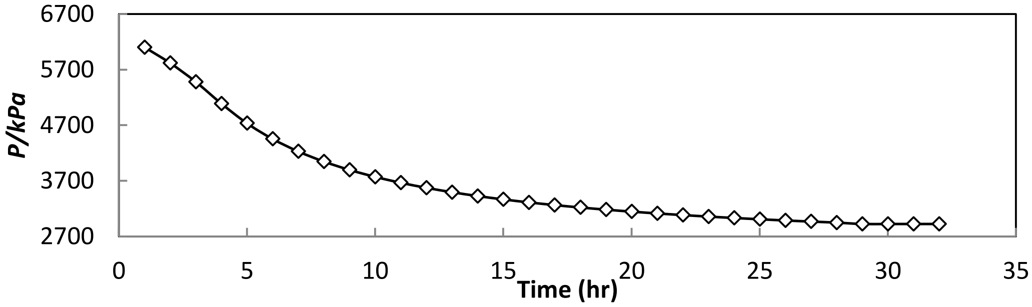

Figure C-4: Pressure drop vs time during the absorption of CO_2 in MDEA at T = 298.15 K.

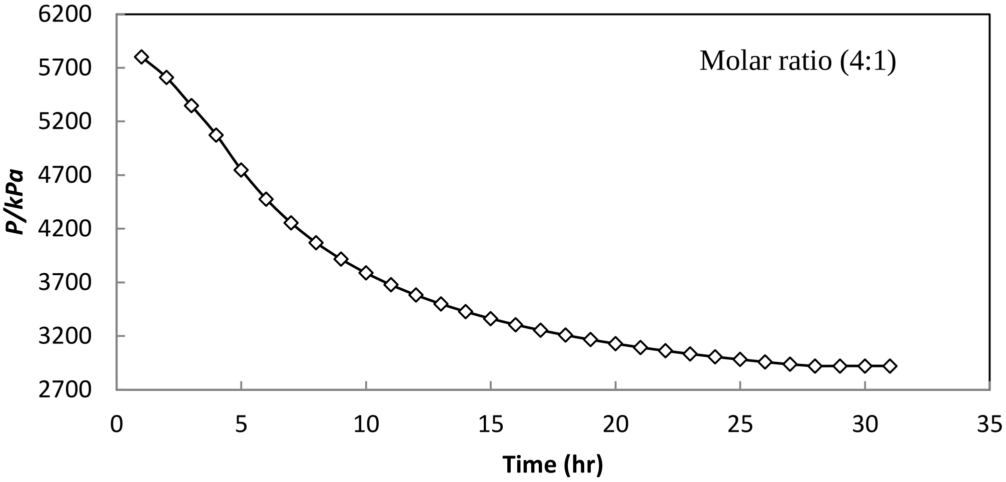

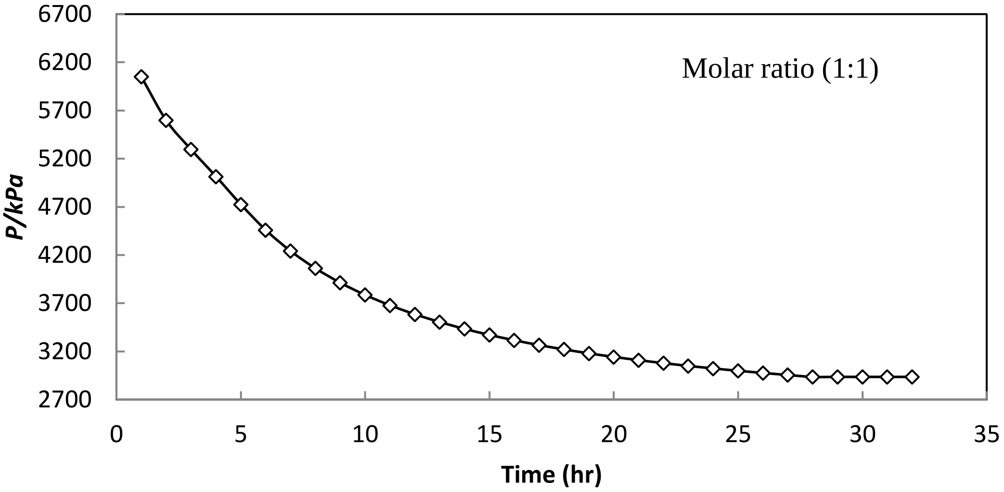

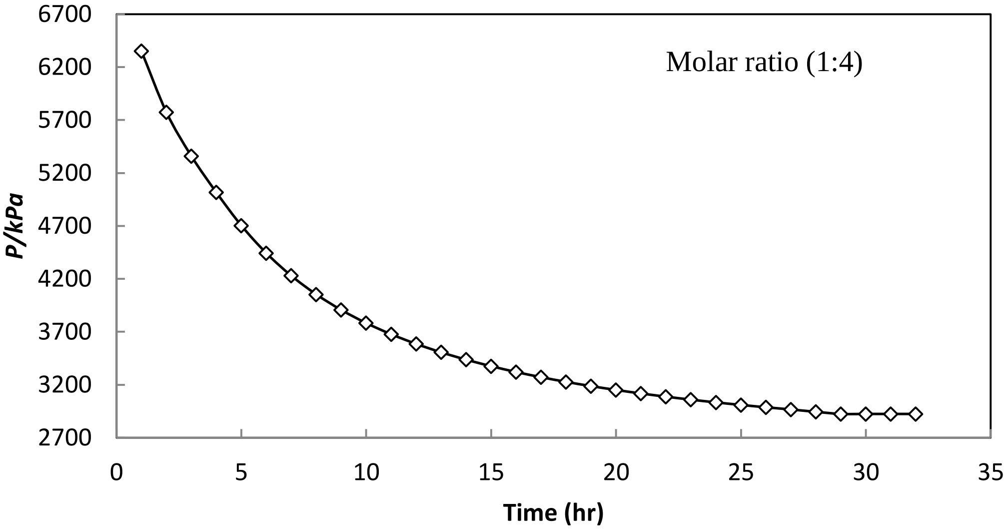

Figure C-5: Pressure drop vs time during the absorption of CO_2 in the binary mixtures of [hmim][BF_4] + MDEA at T = 298.15 K.

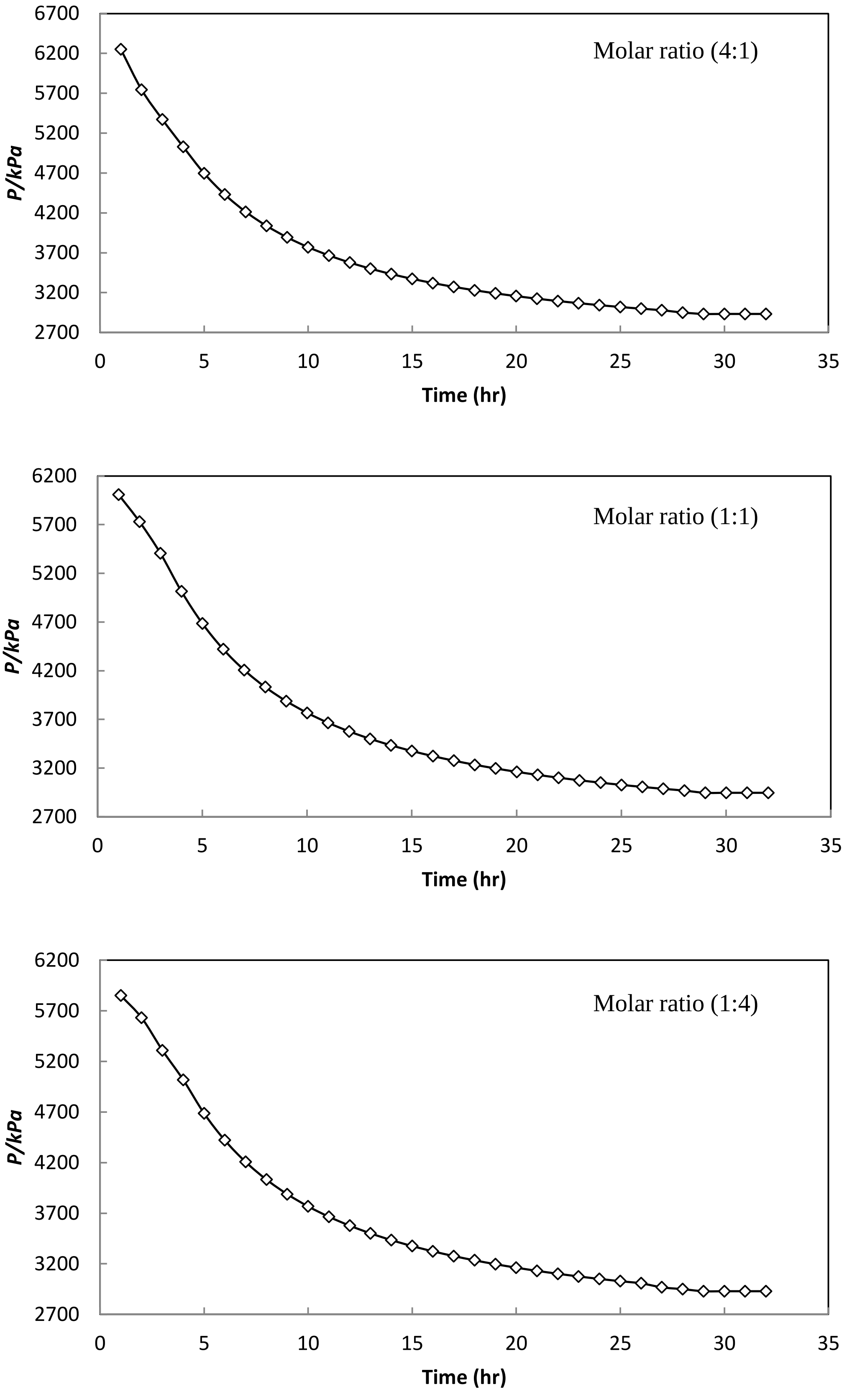

Figure C-6: Pressure drop vs time during the absorption of CO_2 in the binary mixtures of [hmim][Tf_2N] + MDEA at T = 298.15 K.

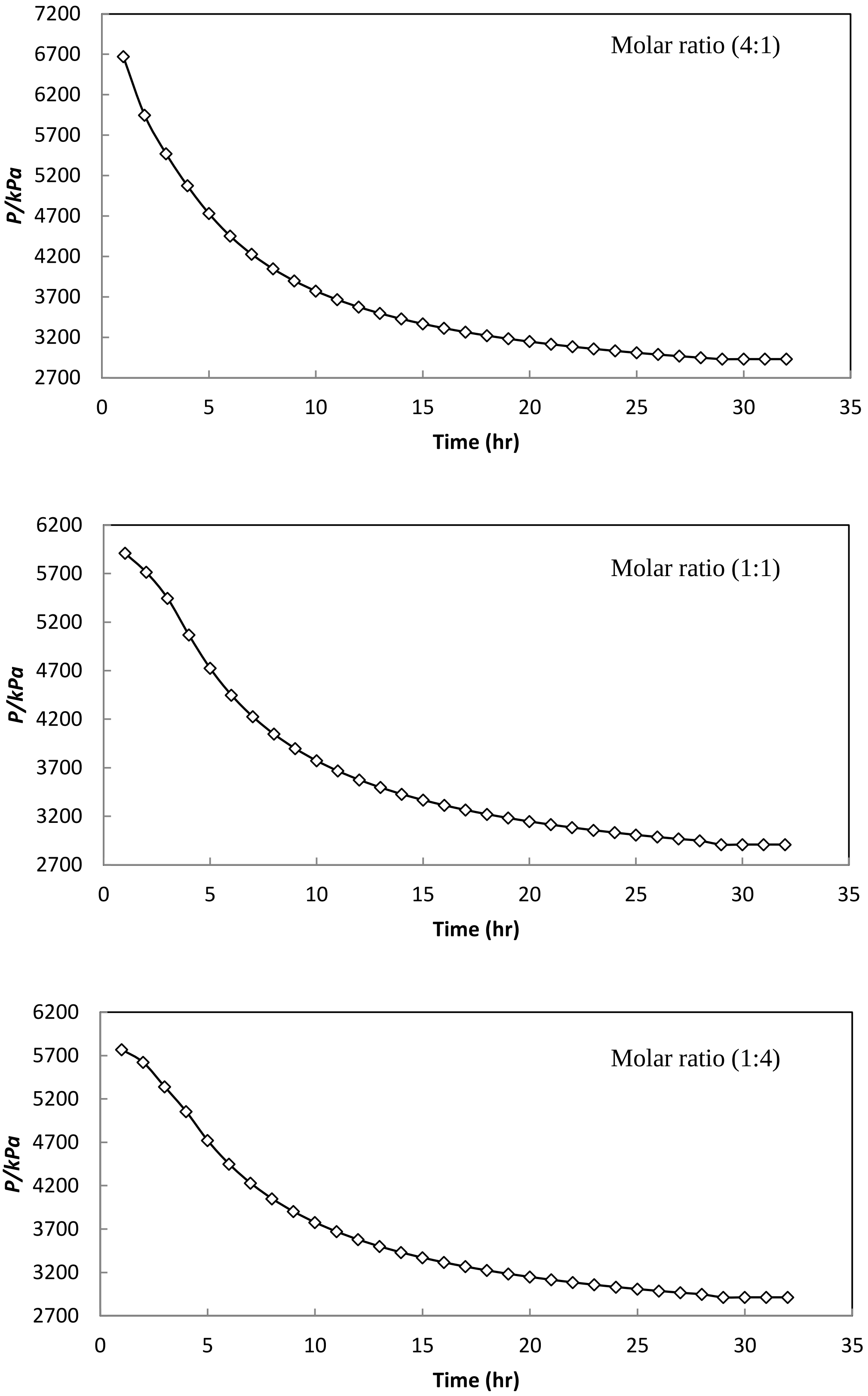

Figure C-7: Pressure drop vs time during the absorption of CO_2 in the binary mixtures of [hmim][FAP] + MDEA at T = 298.15 K.